THE OP27 CELL LINE AS A MODEL SYSTEM TO STUDY THE EFFECTS OF FGF-2 IN OLFACTORY NEURONAL DEVELOPMENT

Aubrey Themba Shoko

A thesis submitted for the Degree of

DOCTOR OF PHILOSOPHY

Department of Molecular and Cell Biology

University of Cape Town

July 2004

ABSTRACT

Due to its unique capacity to regenerate continously, the olfactory neuroepithelium serves as an excellent model system for investigating the molecular and cellular mechanisms involved in neurogenesis. The OP27 cell line (generated by infecting embryonic mouse olfactory placodes with a retrovirus carrying the temperature-sensitive alleles of the SV40 large T antigen) was used as an *in vitro* system to test the effects of fibroblast growth factor-2 (FGF-2) in directing olfactory neurogenesis. The OP27 cells proliferate under the control of the retrovirus at the permissive temperature (33°C). When shifted to the non-permissive temperature (39°C) the SV40 large T antigen is inactivated and the cells stop dividing, thereby allowing one to study the effects of growth factors on these cells. Although FGF-2 also plays an important role in regulating the proliferation of neural progenitors, the main focus in this study was its effect on neuronal differentiation.

When shifted to 39°C in the presence of FGF-2, OP27 cells proceed through one round of cell division and then give rise to a subpopulation of differentiating cells. These cells have a bipolar morphology, characteristic of olfactory receptor neurons (ORNs) and their number increases with time. A combination of RT-PCR assays, western blots and immunocytochemistry showed that these cells express various markers which are characteristic of their differentiation into ORN-like cells. These include GAP-43 and NCAM which are up-regulated, neurotrophin receptors and components of the olfactory chemosensory signalling system.

Although each ORN is hypothesized to select only one of the possible 1000 olfactory receptor (OR) genes for expression, a series of RT-PCR and restriction enzyme digest assays revealed that differentiating OP27 cells are not committed to express a single OR gene. Instead, a small OR gene repertoire was selected for expression as OP27 cells differentiate. It was also discovered that each time

OP27 cells are induced to differentiate, new OR genes are selected for expression. Furthermore, the OR genes identified in differentiating OP27 cells are localized on different chromosomes.

In addition to analysing the expression of marker and OR genes, the possible role of FGF-2 in regulating the expression of the proneural basic helix-loop-helix transcription (bHLH) factors Mash-1, Ngn-1 and NeuroD was investigated in OP27 cells. These proteins are sequentially expressed during mouse olfactory placode development, with Mash-1 appearing first in apical and basal progenitor cells, Ngn-1 transiently expressed in mitotically active basal cells and NeuroD in the last cell division and at the beginning of differentiation of the postmitotic neurons. The Notch signalling cascade, on the other hand, inhibits neuronal differentiation through the activation of Hes-1 and Hes-5, both bHLH genes that repress expression of Mash-1 and Ngn-1. At 33°C the OP27 cells express high mRNA levels of the *Notch-1* receptor and low levels of *Delta-1* (its ligand), *Hes-1* and *Ngn-1*. Both *Mash-1* and *NeuroD* mRNAs are not detected at 33°C. When shifted to 39°C and treated with FGF-2, OP27 cells up-regulate transcript levels of *Hes-1* and *Delta-1*. *Hes-1* is up-regulated before changes in morphology are noticed. This suggests that neuronal differentiation is delayed through the activation of *Hes-1*. On the other hand, *Delta-1* is up-regulated later and this is concomittant with the change in morphology of a subpopulation of OP27 cells. Ngn-1 is expressed in differentiating OP27 cells for a limited period of time only, after which it disappears. *NeuroD*, which is expressed downstream of *Ngn-1* in the olfactory neuronal lineage *in vivo*, was transiently expressed in OP27 cells, downstream and overlapping both *Ngn-1* and *Delta-1* expression. These results indicate that FGF-2 interacts with the Notch signalling cascade in controlling neuronal differentiation in the olfactory neuroepithelium.

Having examined the expression profiles of genes known to be associated with neuronal differentiation, the differential display technique was used to search for uncharacterised genes differentially expressed

in FGF-2 induced OP27 cells. Identification of these genes would allow for better understanding of the regulatory mechanisms involved in neuronal differentiation. This search resulted in the identification of 16 FGF-2 regulated gene transcripts, 15 of which were elevated and one that was transiently down-regulated. Among those characterized are genes that have been previously identified and implicated in neurogenesis but shown for the first time in this thesis to respond to FGF-2. A second group of transcripts identified in this study includes previously named genes whose functions are unknown. A third group represents novel genes that have not been identified previously. Bioinformatic analysis of genes in the latter group reveales protein motifs known to be necessary for functions. For example, one gene contains a scaffold attachment factor box that binds to genomic scarffold attachment regions to organize chromatin and regulate gene expression. A second novel gene with a high homology to GCN5-related N-acetyl transferases was predicted to contain a nuclear localization signal that may target the protein product of this gene to the nucleus to N-acetylate nuclear proteins. It is hoped that the genes identified in this study will shed light on the regulatory mechanisms that control neuronal development.

ACKNOWLEDGEMENTS

I would like to thank my supervisor, Assoc. Prof. Nicola Illing, for all her guidance, mentoring and expert advice throughout my project. I also appreciated all the wonderful opportunities over the years.

A special thank you is extended to the members of the lab: Mrs Faezah Davids for excellent technical assistance, organization and teaching me tissue culture. Dr Helen Collett for her time in reading parts of the thesis, for very helpful comments and for her constant interest in how I was doing during the writing-up. Keke Tloti, Zac McDonald, Inonge Mulako, Arthur Shen and Nicholas Bredenkamp for all their assistance, support and everyday life in the lab.

All my fellow students, past and present (Linda Mtwisha), in the Department of Molecular and Cell Biology for friendship and a nice atmosphere to work in.

Dr Kate Storey for giving me the opportunity to work in her group at the Department of Human Anatomy, Oxford University during the year long tenure in the UK. Sincere gratitude also go to the lab members who made me feel very welcome and were always helpful: Dr Anne Goriely, Dr Jennifer Brown, Dr Julie Adam, Dr Ruth Diez del Corral, and Dorette Breitkreuz.

Dr Jane Roskams for giving the opportunity to work in her group at the CMMT, University of British Columbia in 2001 and for all the help with western blots, immunocytochemistry and helpful discussions. Warm thanks also go to the lab members Erin, Edmund, Cath, Lisa, Jenny, Lindsey and Kathryn for a welcoming atmosphere. I enjoyed the time spent in their lab. Thank you Dr Roskams for the financial support in 2002.

My warmest thanks to my mother, Miss Christina Shoko for her constant support. I also appreciate the support from my twin-sister, Miss Thembisa Shoko and brother, Andile.

I would like to extend my sincere gratitude to the John Sainsbury Scholarship/ Linbury Trust for financially supporting my PhD studies and for the opportunity to spend the year in the United Kingdom.

TABLE OF CONTENTS

List of Figures

Chapter 1

Chapter 3

Chapter 4

Chapter 5

Chapter 6

List of Tables

Chapter 1

Chapter 2

Chapter 3

Chapter 4

Chapter 6

Chapter 1

INTRODUCTION

---

1. NEUROGENESIS

Neurogenesis, the generation of distinct classes of neurons in the germinal neuroepithelium (the ventricular zone) of the vertebrate neural tube occurs through a series of well co-ordinated and regulated steps. Self-renewing neural stem cells give rise to lineage restricted committed neuronal progenitors which in turn proliferate, migrate and exit the cell cycle to differentiate into neurons. A number of signalling molecules, both extrinsic (e.g the fibroblast growth factors, bone morphogenetic proteins, etc) and intrinsic (e.g basic helix-loop-helix transcription factors) have been shown to possibly interact to regulate these events (Edlund and Jessel, 1999). Several findings have implicated fibroblast growth factor-2 (FGF-2) as one of the key signalling molecules that regulate neurogenesis by controlling proliferation, lineage commitment, differentiation and survival of these progenitors. I will review current literature on the effects of FGF-2 on these neural developmental processes. Another signalling pathway that has been shown to be involved in the decision of whether the cell remains in the proliferative mode, or whether it progresses along the differentiation pathway to a different fate (e.g neurons or glia) is that activated by the cell-membrane anchored *Notch*. *Notch* influences the fate of the progenitor cells by regulating the expression of the basic helix-loop-helix (bHLH) transcription factors which are expressed transiently and sequentially by neuronal progenitor cells and their progeny as neurogenesis proceeds.

1.1 CELLULAR STAGES OF NEUROGENESIS

Knowledge of sequence of events involved in neurogenesis has been derived mainly from studies using the developing cerebral cortex as a model system, and these events seem to be well conserved in other parts of the central nervous system. The cerebral cortex is derived from the dorsal telencephalic neuroepithelium, which is also known as the pseudostratified ventricular epithelium (PVE) or the ventricular zone (VZ) (Vaccarino *et al.*, 1999). The PVE/VZ contains actively proliferating multipotent progenitor cells that give rise to the cortical neurons and glia. Cortical neurons are generated through a highly regulated series of events which are characterized by neuroblast proliferation, fate determination, migration and terminal differentiation. Before neurogenesis begins, the progenitor cells go through a number of symmetrical divisions to expand the progenitor pool as both daughter cells re-enter the cell cycle. When neurogenesis begins at E13 in the rat cortex, the VZ is characterized by assymetrical divisions of some of the progenitor cells. During this stage, some of the daughter cells re-enter the cell cycle whereas others become post-mitotic and start migrating away from the VZ along radial glial fibers through the intermediate zone and into the cortical plate where they will differentiate and form the six layers of the cortex (Fig 1.1). This period of neurogenesis continues through to E19 and is followed by generation of glial cells. Glial progenitor cells are also generated in the VZ and these migrate to the subventricular zone (SVZ) where they continue to proliferate and generate astrocytes and oligodendrocytes during postnatal development.

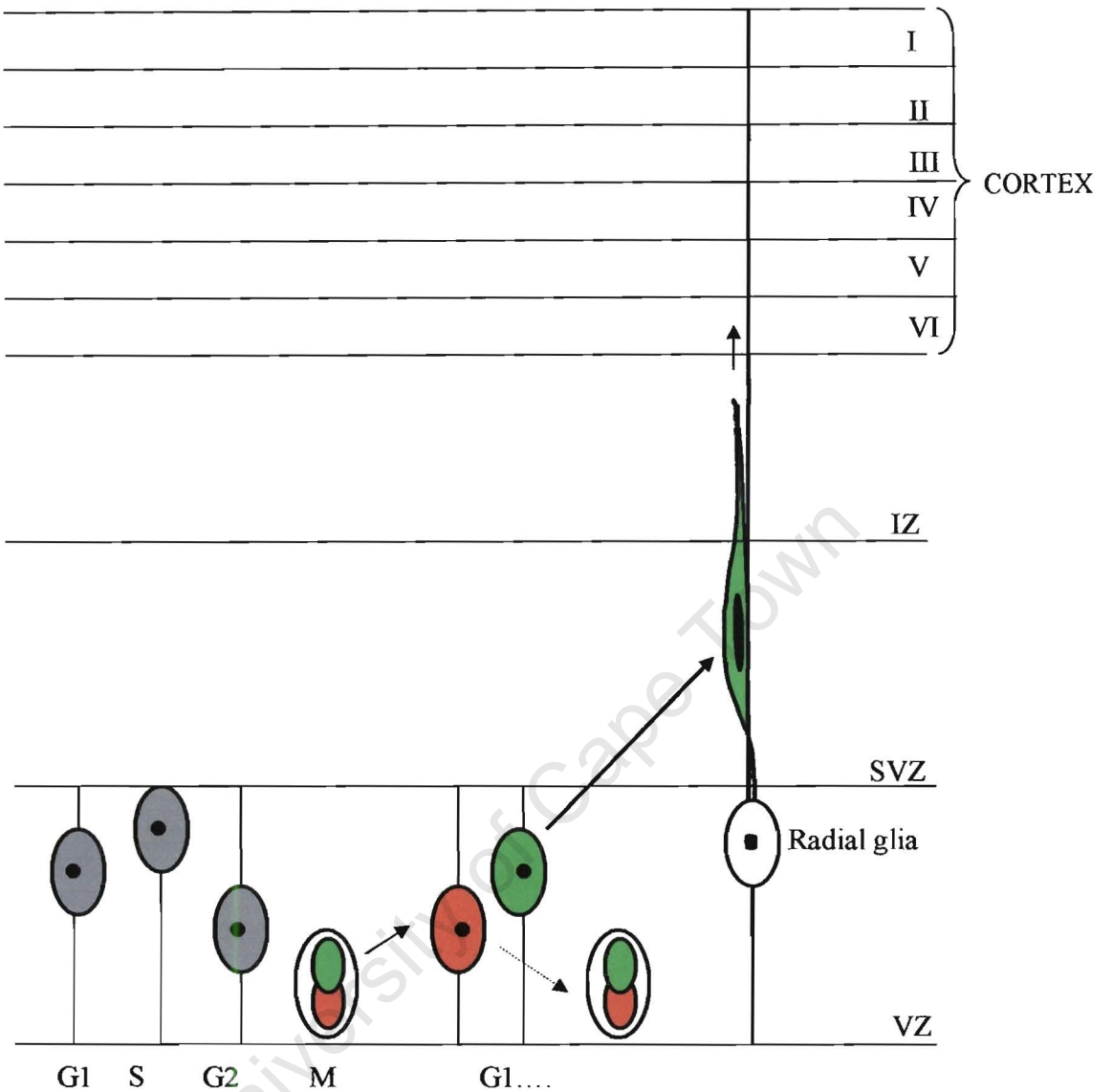

Figure 1.1 Model of the development of the embryonic cerebral cortex. The successive stages of the cell cycle are shown in the VZ and via asymmetric division one daughter cell (shown in red) re-enters the cell cycle while the other (in green) leaves the cell cycle and migrates out of the VZ along the radial glia into the cortical plate where it will differentiate. VZ, ventricular zone; SVZ, sub ventricular zone; IZ, intermediate zone; I-VI; six layers of the cerebral cortex.

The fate of the multipotent cortical progenitor cells has been studied by using lineage tracing in which cells are marked with either retroviruses which express β-galactosidase or dye injection and their developmental potentials monitored by examining the number, morphology and fate of daughter cells. Multipotential neural stem cells give rise to the progenitor cells which are capable of dividing a limited number times before giving rise to a progeny that generates either neurons (neuronal precursor cell) or

oligodendrocytes and astrocytes (glial precursor cells) but not both (Figure 1.2). The neuronal precursor cells frequently undergo one or more rounds of cell divisions before differentiating into neuronal cells.

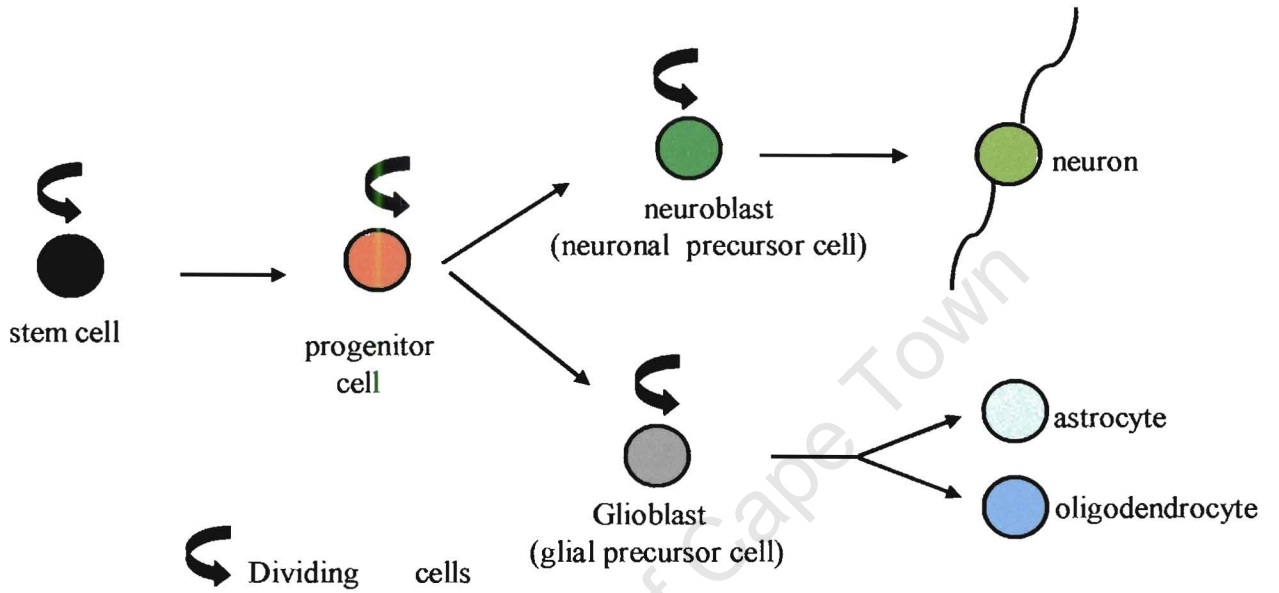

Figure 1.2 The sequential differentiation of the different neural cell types from neural stem cells. One stem cell which is capable of self-renewal gives rise to progenitor cells that have limited self-renewal. These then generate the neural precursors, neuroblasts and glioblasts that ultimately give rise to the postmitotic neurons and glia (astrocytes and oligodendrocytes), respectively.

1.2. FGF-2 AS AN EXTRINSIC REGULATOR OF NEURAL DEVELOPMENT

1.2.1 FGF-2: PROTEIN STRUCTURE

FGF-2 is a member of the large heparin-binding FGF family of signalling proteins involved in many biological processes during development. The family currently has 22 members (Ford-Perris *et al.*, 2001) that have been identified by oncogene assays, expression cloning, or low-stringency hybridizations to other FGFs. Members have different amino- and carboxy- termini but share a

conserved 120 amino acid core region with 30-60% amino acid homology. They have been implicated in the developmental processes such as induction, patterning, mitosis and differentiation, survival and migration of a variety of cell types (Ornitz and Itoh, 2001, Ford-Perris *et al.*, 2001).

FGF-2 is synthesized as five different forms of the protein from a single mRNA species. These forms differ in their amino terminus as a result of multiple translational initiation sites (Arnaud *et al.*, 1999). An ATG codon, found in a proper context to start translation, initiates the translation of a 155 amino acid protein (molecular weight, MW 18 kDa) while various in-frame CTG codons (coding for Leu) upstream of the ATG, initiate translation of proteins with 22, 22.5, 24 and 34 kDa. The higher MW FGF-2 proteins have a nuclear localization signal (NLS) that directs them to the nucleus, while the smaller 18KDa isoform lacks a NLS, and is localized in the cytosol.

1.2.2 FGF-2 EXPRESSION PATTERNS IN THE DEVELOPING BRAIN

FGF-2 is generally expressed throughout the developing nervous system into adulthood in both neuronal and non-neuronal cells. Expression studies in embryos show the mRNA is present in the rat telencephalon as early as E9.5 and around E10.5 in the mouse neural tube (Kalyani *et al.*, 1999). FGF-2 protein levels peak during the earliest stages of neurogenesis in the mouse VZ which gives rise to the cerebral cortex but gets down-regulated during mid-neurogenesis and disappears when this process is complete (Vaccarino *et al.*, 1999; Raballo *et al.* 2000). Levels of the FGF-2 protein are highest in the anterior brain regions, particularly the ventricular (VZ) and the subventricular zones (SVZ) (regions where neural progenitors are generated) compared to the caudal regions including the spinal cord (Dono *et al.* 1998).

1.2.3 MECHANISM OF ACTION OF FGF-2: THE FGF RECEPTORS

Two classes of FGF receptors have been identified: the low-affinity and the high-affinity receptors.

1.2.3.1 Heparan sulphate proteoglycans (HSPGs)

Heparin sulphate proteoglycans (HSPGs) which are present on cell surface and in the extracellular matrix carry carbohydrate side chains. They form low-affinity, high capacity binding sites for FGFs. The essential role of HSPGs in FGF binding has been demonstrated by a number of experiments (Yayon *et al.*, 1991; Bernard *et al.*, 1991). It was found that FGFR-1 could not bind FGF in cells that were not capable of producing heparan sulfates and could only do so once heparin was present (Yayon *et al.*, 1991), thus suggesting that an interaction with the low-affinity receptor was a pre-requisite in activating the high-affinity receptors. FGF-1 and FGF-2 could only support proliferation of cells transfected with FGFR-1 once heparin was present in the culture medium (Bernard *et al.*, 1991). Both biochemical and X-Ray crystallography data have suggested that HSPGs interact with both FGF ligands and FGFRs to form active ternary signalling complexes. Different models have been proposed for this interaction. It is possible that heparin and other heparan sulphates possibly modify the structure of the FGF ligand so it can be able to bind and activate the high affinity- receptor (Yayon *et al.*, 1991).

HSPGs have been shown to play important roles in regulating the biological activity of FGF ligands in a variety of cellular processes. They enhance the neurite outgrowth of PC12 cells mediated by FGF-1 and FGF-2 (Damon *et al.*, 1988). FGF-2 induced proliferation of neural precursor cells isolated from rat E14 mesencephalon was found to be specifically potentiated by heparin (Caldwell and Svendsen, 1998).

HSPGs regulate these events in a ligand and FGFR specific manner. In the immortalized E10 mouse neuroepithelium 2.3D cell line different HSPG forms were found to enhance the activity of FGF-2 in their proliferation whereas the neuronal differentiation of these cells was potentiated by activating FGF-1 (Nurcombe *et al.*, 1993). In these cells, HSPGs were shown to preferentially bind FGFR-1 instead of FGFR-3 in potentiating the mitotic effects of FGF-2 (Brickman *et al.*, 1995). Lastly, HSPGs also regulate FGF actions in a developmental stage-specific manner. It is however not clear what effects this have on the function on the HSPGs (Allen and Rapraeger, 2003).

1.2.3.2 FGF tyrosine kinase receptors

Fibroblast growth factor receptors (FGFR-) represent the high-affinity, low capacity binding sites for FGF ligands. They are responsible for intracellular signal transduction and for mediating biological response of the cells to the FGFs. There are currently 4 FGF receptor genes that have been cloned and a number of variants exist as a result of alternative splicing. The 4 receptors differ in structure, ligand binding properties, and their patterns of expression.

1.2.3.2.1 Structure and diversity of FGFR-s

All FGFR-s share a common primary structure (Figure 1.3). They contain a ~20 amino acid terminal hydrophobic signal peptide; either 2 or 3 extracellular immunoglobulin (Ig)- like domains (I-III); a string of acidic amino acid residues between the first two Ig domains (known as the acid box), a hydrophobic transmembrane (TM) domain, the juxtamembrane (JM) domain between the TM and the catalytic tyrosine kinase (TK) domain which is split by 14 amino acid residues. The highest degree of homology between the 4 receptors is found in the TK domain (75-92%) whereas the IgI domain shows

significantly less similarity (19-40%) (Johnson and Williams, 1993). The IgIII doman is essential for high-affinity binding of FGF ligands.

Alternative mRNA splicing of the two exons that code for the C-terminal half of IgIII domain of FGFR-s 1 to 3 gives rise to distinct functional receptor variants, FGFR-1 IIIb; FGFR-1 IIIc; FGFR-2 IIIb; FGFR-2 IIIc, FGFR-3 IIIb; and FGFR-3 IIIc resulting in differences in ligand binding affinities (see Table 1.1). FGFR-4 has never been shown to have alternative splicing in this region. Additional isoforms of FGFR-1 and FGFR-2 exist as a result of alternative splicing of IgI. FGFR-1α and FGFR-2α isoforms contain all 3 Ig loops; FGFR-1β and FGFR-2β are missing IgI and FGFR-1γ lacks IgI and instead has a 144 bp insert in that region. FGFR-$2\beta_2$ isoforms are identical to FGFR2-β_1 except that they lack the acid box as well (Bansal *et al.*, 1996). Since the IgI is not essential for ligand binding, the FGFR-α and FGFR-β do not show any significant difference in ligand binding (Xu *et al.*, 1999).

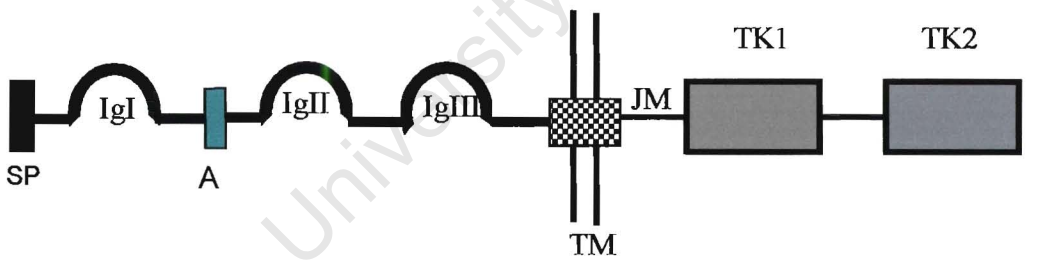

Figure 1.3 Schematic representation of FGFR-1-4. SP, signal peptide; IgI, IgII, IgIII, Ig-like domains; A, acid box; TM, transmembrane domain; JM, juxtamembrane; TK1 and TK2, tyrosine kinase domains.

The interaction between the ligands and their receptors has been studied *in vitro* using a mitogenic cell assay in which the BaF3 cell line was engineered to express the different splicing variants (Ornitz *et al.*, 1996, Xu *et al.*, 2000). This assay has shown that the seven receptor isoforms have distinct and overlapping binding specificities (summarized in Table 1.1).

1.2.4 Expression patterns of FGF receptors in the brain

Differential, tissue-specific expression of the different FGFR-s has been studied using either RT-PCR, northern blot, RNase protection assays or in situ hybridizations. All the receptors with the exception of FGFR-4 have been detected in CNS neural cells. These cells were found to predominantly express the IIIc isoforms of FGFR-1, FGFR-2, and FGFR-3 as early as E10.5 (Bansal *et al.*, 1996; Qian *et al.*, 1997; Hajihosseini and Dickson, 1999). FGFR-1 and FGFR-2 are expressed by both neuronal and glial precursor cells while the FGFR-3 is mainly expressed in glial cells (Bansal *et al.*, 1996; Kalyani *et al.*, 1999). In the developing cerebral cortex, mRNA transcripts for both FGFR-1 IIIc and FGFR-2 IIIc were found in both the VZ and SVZ regions whereas mainly the FGFR-2 IIIc was still present in the cortex which contains differentiated neuronal cells (Dono *et al.*, 1998).

Table 1.1 The relative specificity of FGFR- and FGF ligand interactions.

	FGF RECEPTORS						
	FGFR-1		FGFR-2		FGFR-3		FGFR-4
	IIIb	IIIc	IIIb	IIIc	IIIb	IIIc	
FGF-1	+++	+++	+++	+++	+++	+++	+++
FGF-2	++	+++	-	++	-	+++	+++
FGF-3	+	-	++	-	-	-	-
FGF-4	+	+++	+	+++	-	++	+++
FGF-5	-	++	-	+	-	+	-
FGF-6	-	++	-	++	-	-	+++
FGF-7	-	-	+++	-	-	-	-
FGF-8	-	-	-	+	-	++	++
FGF-9	-	+	-	+++	++	+++	+++
FGF-10	-	-	+++	-	-	-	-
FGF-17	-	-	-	++	-	+++	+++
FGF-18	-	-	-	-	-	+	+++

The interaction between FGFR- and the FGF ligands has been determined in a mitogenic assay using BaF3 cells expressing the various FGFR- isoforms. FGF-1 was found to maximally activate all the FGFR- isoforms. Mitogenic activities of the other FGF ligands were expressed relative (%) to that of FGF-1. +++, 75-100%; ++, 40-75%; +, 10-40%; -, <10%. +++ and ++ represent potential interactions between the receptor and ligand. The interactions between the receptors and FGFs 11-16, and 19-23 are currently unknown. Data based on Ornitz *et al.*, 1996; Szebenyi and Fallon, 1999; Xu *et al.*, 2000; and Ford-Perriss *et al.*, 2001.

1.2.5 FGF Receptor activation and intracellular signalling cascades

Activation of FGF receptors by their ligands is known to induce receptor dimerization and stimulation of tyrosine kinase activity. Both homodimers between receptors of the same type and/or heterodimers between different types, can be formed (Bellot *et al.*, 1991). Once activated the receptor kinases phosphorylate each other on their cytoplasmic C-terminal tails and initiate dowstream signalling pathways. The key components of these intracellular signalling pathways that have been shown to be activated by FGF signalling include the Ras/Raf/mitogen activated protein kinase (MAPK) pathway; phospholipase C-γ (PLC-γ), Src and phosphoinositol 3' kinase (PI3-kinase) pathways (Fig 1.4).

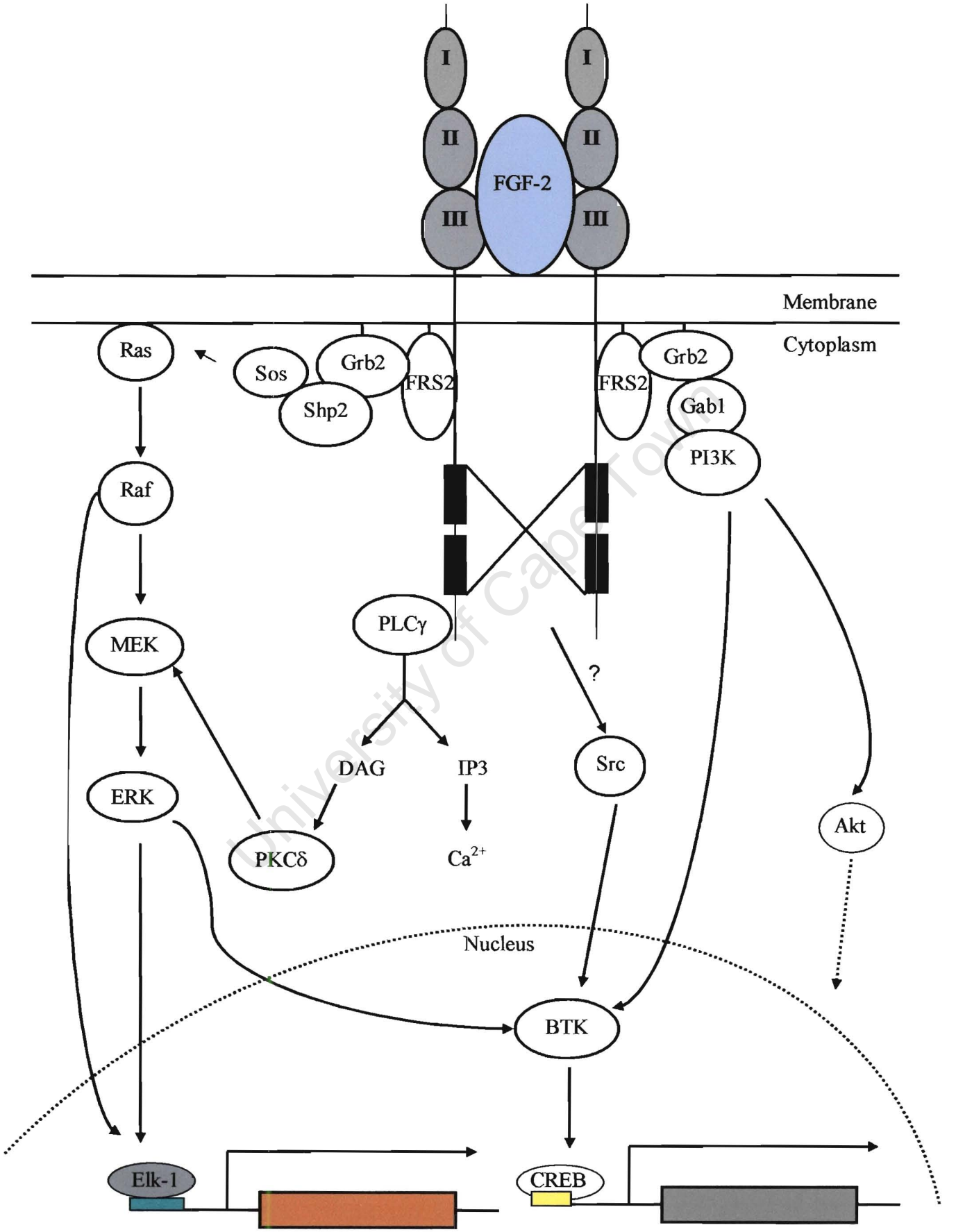

Figure 1.4 FGF-mediated signal transduction pathways. Binding of FGF to FGFR is followed by FGFR- dimerization and the activation of their intracellular protein tyrosine kinase domains (■). This results in FGFR autophosphorylation and the initiation of both cytoplasmic and nuclear signalling cascades. Each pathway will eventually result in specific effects, e.g gene transcription that may cause either the cell to proliferate, differentiate and/or survive. The cascades that are mediated by FGF include the Ras/MAPK, PLCγ, Src, and PI3K pathways. Components of these cascades translocate to the nucleus to activate transcription factors.

The FGFRs are linked to the signalling cascades via interactions with various scarffold and adapter proteins. For example, the scaffold protein FRS2 has been shown to link FGFR-1 activation to the Ras/MAPK signalling pathway (Kouhara *et al.*, 1997). FRS2 interacts with the juxtamembrane domain of FGFR-1, becomes phosphorylated and consequently binds the adapter protein Grb2 which recruits Sos, a guanine nucleotide exchange factor that activates the G protein Ras. Activated Ras directly interacts and activates Raf which in turn phosphorylates and activates MEK. The MAP kinase (MAPK) ERK (extracellular signal regulated kinase) is the target for phosphorylation and activation by MEK. ERK gets translocated to the nucleus and activates transcription factors like Elk-1 and cAMP response element binding protein CREB (Chung *et al.*, 1998; Yang *et al.*, 2004)(Fig. 1.4).

PLC-γ becomes activated by directly interacting with a phosphorylated tyrosine residue at the C-terminus of FGFR-1. When activated, PLC-γ generates inositol-1,4,5-triphosphate (IP_3) and diacylglycerol (DAG) by hydrolysing phosphatidylinositol (PIP2). IP3 induces Ca2+ release from intracellular stores whereas DAG activates protein kinase C (PKC). PKCδ has been shown to mediate MAPK activation by phosphorylating MEK upon FGF-2 stimulation (Corbit *et al.*,1999) (Fig. 1.4).

The Src pathway has not been completely characterized. It is not clear what proteins, if any, act upstream of Src following FGFR1 activation (Powers *et al.*, 2000). However, Bruton's tyrosine kinase (BTK) has recently been shown to be activated downstream of Src. Following activation, BTK

phosphorylates and activates the transcription factor CREB to induce neuronal differentiation (Yang *et al.*, 2004) (Fig. 1.4).

The PI3K pathway is, like the MAPK cascade, linked to FGFR activation via the protein FRS2. PI3K is recruited to FGFR via the interaction of the adapter protein Gab1 with the Grb2-FRS2 complex (Hadari *et al.*, 2001). Activation of this pathway has been implicated in the regulation of cell proliferation, neuronal differentiation and cell survival. The sequential activation of BTK and CREB downstream of PI3K has been shown to be required to induce neuronal differentiation (Yang *et al.*, 2004). On the other hand, the serine-threonine kinase Akt has been shown to act downstream of PI3K to promote cell survival by suppressing the apoptotic function of components of intrinsic cell death machinery in different cell types, including cerebellar granule cells and immortalized hippocampal cells (Brunet *et al.*, 1999; Eves *et al.*, 1998)

FGF-2 has been shown to have multiple effects on neural cells, ranging from stimulation of cell proliferation to the regulation of differentiation and cell survival.

1.2.6 EFFECTS OF FGF-2 ON NEURAL PROGENITORS

Effects of FGF-2 on neural cells have been demonstrated both *in vitro* using primary cell cultures and cell lines and *in vivo* with *Fgf-2* knock-out mutant mice and the micro-injection of either recombinant FGF-2 or FGF-2 neutralizing antibodies in the telencephalic ventricles.

1.2.6.1 In vitro effects of FGF-2 on primary cell cultures from different regions of the brain

Using primary tissue culture assays it has been shown that FGF-2 was mitogenic for progenitor cells from various regions of the developing nervous system. When E10 telencephalic and mesencephalic neuroepithelial cells were stimulated with low concentrations of FGF-2 (<0.5ng/ml) *in vitro*, about 50% of the cells incorporated [3H]-thymidine compared to 3% in control cultures. It was also shown that at higher FGF-2 concentrations (>0.5ng/ml), the cells differentiated to neuronal cells first and glial cells appearing later (Murphy *et al.* 1990). Similarly, FGF2 increased proliferation of multipotential progenitors from the embryonic mouse cerebrum, ultimately giving rise to both neurons and glia (Kilpatrick and Bartlett, 1995). These results suggested that FGF-2 was not only important for proliferation of these cells but may be important for influencing their differentiation as well.

Three groups studying the neuronal development in the cortex and hippocampus have reported opposing effects of FGF-2 and neurotrophin 3 (NT-3), a neurotrophin, on neural progenitor cells (Ghosh and Greenberg, 1995; Vicario-Abejón *et al.*, 1995; Lukaszewicz *et al.*, 2002). It was found that FGF-2 increased proliferation of E16 hippocampal progenitors and maintained the expression of the intermediate filament nestin in these cells. In contrast, NT-3 induced neuronal differentiation of the progenitor cells. FGF-2 was also able to induce neuronal differentiation but when added together with NT-3 to cultured cells ,the effect was not additive suggesting that the same progenitor population was responding to both. It was therefore concluded that in these cultures there were two populations of cells, one responding to FGF2 by proliferating and the other by differentiating to neuronal cells (Vicario-Abejón *et al.*, 1995).

Similarly, the study conducted by Ghosh and Greenberg (1995) showed that FGF-2 increased the number of cortical progenitor cells that incorporated BrdU thus expanding the precursor population. It would seem that cell-cell contacts are required in these cultures for FGF-2 to be able to promote proliferation. Only cells in clusters and not dissociated single cells were induced to divide by the administration of FGF-2. Over time the proliferating cells withdrew from the cell-cycle and differentiated into neurons first and glia later on. NT-3 on the other hand was shown to regulate neuronal differentiation only.

Lukaszewicz *et al.* (2002) examined *in vitro* the influence of both FGF-2 and NT-3 on cell-cycle parameters using mouse cortical precursor cells. FGF-2 increased expression levels of positive cell-cycle regulators while NT-3 reduced their expression and instead up-regulated expression of negative regulators with the resultant withdrawal from the cell-cycle. A second finding from this study was that FGF-2 shortened the cell-cycle by ~20-30% with respect to control cultures, thus increasing the speed of proliferation in progenitors. This is in agreement with another *in vitro* study where FGF-2 was shown to reduce the population doubling time of a cell line derived from multipotent human neuroectodermal precursors (Derrington *et al.*, 1998).

Lastly, Qian and co-workers have shown *in vitro* that FGF-2 influences the differentiation of primary cultures of cortical progenitor cells into neuronal or glial lineages in a dose-dependent manner. Low concentrations were required for neuronal differentiation while oligondendrocytes were induced by higher levels of the growth factor (Qian *et al.*, 1997).

1.2.6.2 In vivo studies of the effects of FGF-2 on cerebral cortex

The effects of FGF-2 on neuronal development *in vivo* have been studied by several groups and their findings are summarized in Table 1.2. *Fgf-2* knock-out mice are viable, have normal organogenesis but display defects in the cerebral cortex (Ortega *et al.*, 1998; Dono *et al.*, 1998; Vaccarino *et al.*, 1999; Raballo *et al.*, 2000; Korada *et al.*, 2002).

These studies have shown that the absence of the gene causes defects in the developing cortex and not the basal ganglia which are derived from the ventral telencephalon (Ortega *et al.*, 1998; Korada *et al.*, 2002). Mutant mice were characterized by significant reduction of proliferating progenitor cells in the dorsal VZ , which will give rise to the cerebral cortex (Vaccarino *et al.*, 1999; Raballo *et al.*, 2000). This leads to decreased neurogenesis of the glutamatergic pyramidal neurons in the anterior regions of the cortex (Korada *et al.*, 2002). The number of neurons within the developing basal ganglia or hippocampus were not affected by the missing *Fgf-2*. This suggests that the absence of *Fgf-2* was either compensated for by other signalling molecule or it was not critical for the developing basal telencephalon (Raballo *et al.*, 2000; Korada *et al.*, 2002). However, Tao and co-workers have shown that injecting recombinant FGF-2 *in vivo* led to a 50% increase in [3H] thymidine incorporation in granule cell precursors in the hippocampus and this could be negated by injecting with FGF-2 neutralising antibodies (Tao *et al.*, 1997).

In agreement with the *Fgf-2* knock-out studies, injection of recombinant FGF-2 into lateral ventricles of adult rat caused expansion of the SVZ by increasing the number of progenitors that incorporated BrdU. This had a stimulatory effect on the generation of olfactory bulb neurons (Kuhn *et al.*, 1997). These studies demonstrate that FGF-2 stimulates cell proliferation in the cerebral cortex, resulting in an

increased number of neural progenitor cells and a subsequent increase in neurons during cortical development.

Table 1.2 A summary of the effects of FGF-2 on neuronal development *in vivo*.

Reference	Type of experiment	Affected region (s)	Effect
Dono *et al.*, 1998	*Fgf-2* knock-out	Cerebral cortex Hippocampus Spinal cord	Proliferation of neuronal progenitors normal Fraction of neuronal progenitors fail to reach target in cerebral cortex Thickness of cerebral cortex reduced by 10% Compressed differentiating cortical layers Very few differentiated large pyramidal neurons Reduced paravalbumin-positive neurons in adult cortical layers Ectopic paravalbumin-positive neurons in hippocampus Reduced neuron number in spinal-cord
Korada *et al.*, 2002	*Fgf-2* knock-out	Cerebral cortex	40% reduction in cortical glutamatergic pyramidal neurons Decreased number and size of neuronal population in anterior cortex layers Cortical cell migration and aggregation into specific layers not affected No significant difference in hippocampal pyramidal and granule cell layers
Kuhn *et al.*, 1997	Infusion of recombinant FGF-2 into lateral ventricless of adult rat	SVZ Hippocampus Olfactory bulb (OB)	Expansion of the SVZ and increase in the number of $BrdU^+$progenitor cells Stimulatory effect on generation of OB neurons Proliferation and differentiation of hippocampus progenitors not affected Number of glia cells not altered
Ortega *et al.*, 1998	*Fgf-2* knock-out	Cerebral cortex	Reduction in neuronal density in most layers of motor-cortex No neuronal defects in striatum and hippocampus
Raballo *et al.*, 2000	*Fgf-2* knock-out	Cerebral cortex	60% decrease in the total number of $BrdU^+$ cells in dorsal PVE 50% reduction in neuronal number in the cortical plate. Development of basal telencephalon not affected
Tao *et al.*, 1997	Peripheral injection of recombinant FGF-2	Hippocampus	50% increase in [^{3}H] thymidine incorporation in granule cell precursors
Wagner *et al.*, 1999	Injection of FGF-2 neutralizing antibody	Cerebellum Hippocampus	53% reduction in cerebellar granule precursor mitosis 60% reduction in DNA synthesis
Vaccarino *et al.*, 1999a	Micro-injection of recombinant FGF-2 at E15.5	Cerebral ventricles	Increase in cortical volume and total cell volume 70% increase in cortical plate neurons No significant increase in glial cell numbers
	Injection at E20.5		Significant increase in glial cells when injected at E20.5 Total number of neurons not affected
	Fgf-2 knock-out		Total cell population in adult $^{-/-}$ mice half that in wild-type Mutant mice showed reduced BrdU labeling at E11.5 No change in length of cell cycle General decrease in neurons

In their study also using *Fgf-2* mutant mice, Dono *et al.* (1998) showed that FGF-2 is essential for migration and differentiation of specific neocortical neurons (Table 1.2). A fraction of progenitor cells failed to reach their targets in the cerebral cortex and very few differentiated large pyramidal neurons were observed. In contrast to other knock-out studies, this group found that proliferation was not affected in these mutants since there was no difference in [3H]thymidine incorporation when compared with the wild type animals. In addition to the effects observed in cortex, there was also neuronal deficit in the spinal cord and both cortical neuron and glial numbers were low (Dono *et al* 1998), suggesting FGF-2 was required for the development of these structures.

It has been suggested by *in vivo* studies that FGF-2 may regulate the timing of neuronal differentiation, after proliferating progenitor cells have exited the cell cycle. Expression of both FGF-2 and FGFR-1 is down-regulated during mid-neurogenesis and disappears towards the end of this process, possibly to allow differentiation to take place (Vaccarino *et al.*, 1999a; Raballo *et al.*, 2000; Lukaszewicz *et al.*, 2002). Secondly, the effects of FGF-2 on neuron and glial differentiation *in vivo* were also found to be critically dependent on the stage of corticogenesis. When recombinant FGF-2 was injected at E15.5 when the earliest neurons are generated in the cortex, the number of neurons increased by 70% and there was no significant increase in glial cell numbers. When injected at E20.5, the time when neurogenesis has ended and glial progenitor cells are still actively dividing in the SVZ, a large increase in the total number of glial cells was observed (Table 1.2, Vaccarino *et al.*, 1999).

1.2.6.3 *In vitro* effects of FGF-2 on cell lines

Cell lines have been used as *in vitro* model systems to study the effects of FGF-2 on neuronal development. The rat pheochromocytoma cell line, PC12 is the best characterized model system to date (Vaudry *et al.*, 2002). When treated with FGF-2, PC12 cells extend neurites and differentiate into a sympathetic neuron-like phenotype (Hadari *et al.*, 1998; Skaper *et al.*, 2000). Another cell line, H19-7, derived from E17 rat hippocampal cells has also been used as a model system for both neuronal differentiation and cell survival induced by FGF-2. H19-7 cells were immortalized with the temperature sensitive SV40 large T antigen (Eves *et al.*, 1992). When treated with FGF-2 at 39°C the non-permissive temperature at which the large T antigen is inactivated, H19-7 cells extend neurites, differentiate and express neuronal markers (Kuo *et al.*, 1996). Both these cell lines have also been very useful for dissecting out the signalling transduction pathways involved in neuronal differentiation induced by FGF signals. Several pathways have been implicated. Sustained activation of the MAPK pathway was required for the neurite extension and differentiation of PC12 cells in response to FGF-2. This was mediated by the recruitment of the protein tyrosine phosphatase Shp2 by FRS2 into a complex with Grb2, and Sos (Fig 1.4). Expression of a mutant FRS2 with a reduced association with Shp2 in PC12 cells allowed a transient but not sustained activation of ERK. This resulted in a decreased neurite outgrowth induced by FGF (Hadari *et al.*, 1998). FGF-2 has been found to activate both MAPK-dependent and –independent pathways during neuronal differentiation of H19-7 cells (Kuo *et al.*, 1996; Kuo *et al.*, 1997; Chung *et al.*, 1998; Corbit *et al.*, 1999). PKCδ which likely acts downstream of PLC-γ, was shown to mediate FGF-2 induced neuronal differentiation of H19-7 cells by activating the MAPK pathway at the level of MEK (Corbit *et al.*, 1999) (Fig. 1.4). The Src kinase was activated in response to FGF-2 and its activation was found necessary for neuronal differentiation of

H19-7 cells (Kuo *et al.*, 1997). The three signalling pathways (MAPK, Src and PI3K) were shown to stimulate CREB phosphorylation and the subsequent CRE (cAMP response element) mediated gene activation in H19-7 cells in response to FGF-2. CREB phosphorylation and activation in these cells was mediated by the protein BTK (Sung *et al.*, 2001; Yang *et al.*, 2004) (Fig. 1.4). In addition to activating CREB, PI3K was found to activate its target Akt to inhibit apoptosis in differentiating H19-7 cells (Eves *et al.*, 1998). It is clear therefore that FGF-2 has multiple effects on neural progenitor cells and that several signalling pathways are activated to mediate these effects.

1.2.6.4 Identity of FGFRs that transmit FGF-2 signals during neurogenesis

The FGFRs that mediate FGF-2 actions during neurogenesis have not been well characterized. This is mainly because FGFR knock-out mice die early (Deng *et al.*, 1994). However, FGFR-1 is likely to be the receptor that may mediate FGF-2 signals. Signalling through the FGFR-1 was found critical for the proliferation of FGF-2 dependent neural stem cells *in vitro* (Tropepe *et al.*, 1999). Although the immortalized E10 mouse neuroepithelium 2.3D cell line expresses both FGFR-1 and FGFR-3, the mitogenic effect of FGF-2 was found to be transduced exclusively by FGFR-1 (Brickman *et al.*, 1995). Additionally, a study of chimeric mice has shown that FGFR-1 is critical for neural tube development (Deng *et al.*, 1997). It is not clear though which FGFR-1 isoform is required for these activities. Thus the generation of FGFR isoform-specific knock-outs would help in the understanding of FGF-FGFR function during neurogenesis.

1.3. INTRINSIC MOLECULES REGULATING NEUROGENESIS

1.3.1 Basic helix-loop-helix transcription factors

Neurogenesis in vertebrates involves sequential activation of transcription factors of the large family of evolutionary conserved basic helix-loop-helix (bHLH) family that regulate both determination and differentiation of neural progenitor cells. These are vertebrate homologues of the bHLH genes *achaete-scute* complex and *atonal* originally identified in *Drosophila*. The relationship between the various neural bHLH transcription factors is summarized in the phylogenetic tree shown in Fig.1.5.

The proneurogenic members of this family include the mammalian *achaete-scute* homolog 1 (Mash1), Neurogenin1, 2 and 3 (Ngn1, Ngn2, Ngn3) which are involved in the specification of neural precursor populations, and the mammalian *atonal* homologs Math1, Math2, Math3, and NeuroD which are required for the terminal differentiation into neurons (Kageyama *et al.*, 1997). These transcription factors display tissue-specific expression patterns in both the CNS and the PNS. They form hetero-dimers with the ubiquitously expressed bHLH proteins E2-2, HEB, E12 and E47 and bind to E box (CANNTG) containing promoter sequences via their basic domains to activate transcription of tissue-specifc target genes to promotes neurogenesis. Involvement of the bHLH proteins in neurogenesis has been studied by looking at their patterns of expression during nervous system development, the phenotype of tissues following targeted disruption of the gene (loss-of-function) in mice and also ectopic expression in *Xenopus* embryos (gain-of-function).

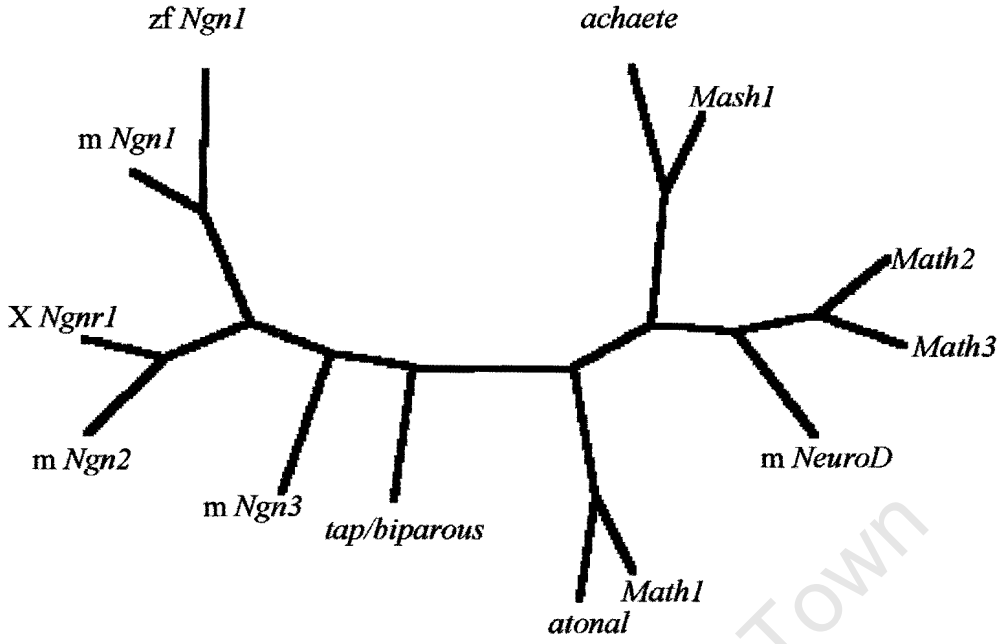

Figure 1.5 A radial phylogenetic tree of the various neural bHLH transcription factors. Full-length sequences of mouse (m), *Xenopus* (X), zebrafish (zf) and *Drosophila* (*achaete*, *tap/biparous*) orthologues were aligned using the Clustal W software (Thompson *et al.*, 1994). The tree was constructed using the PhyloDraw drawing tool (Choi *et al.*, 2000). GenBank accession numbers: zebrafish *Ngn1*, AF017301; *atonal*, L36646; mouse *neuroD*, U28068; *Xenopus Ngnr-1*, U67778; *Ngn2*, Y07621; *Ngn3*, Y09167; *Ngn1*; Y09166; *Math3*, D85845; *Math2*, D44480, *Math1*, D43694; *tap/biparous*, AF022883; *Mash1*, NM_008553; *achaete*, NM_057476.

1.3.1.1 Mash1

In situ hybridization, northern hybridizations and immunocytochemical studies have shown that *Mash1* is transiently expressed during development of neural precursor cells in both the CNS and PNS. In the CNS *Mash1* transcripts were found in the ventral telencephalon of E13.5 rat forebrain, including the ventral thalamus, hypothalamus, and the ganglionic eminence but not in the dorsal telencephalon (Casarosa *et al.*, 1999; Torri *et al.*, 1999; Schuurmans and Guillemot 2002). A northern blot analysis using mouse embryos revealed that *Mash1* transcripts are present as early as E8.5 and levels increase until E17.5 (Guillemot and Joyner, 1993). Cells expressing *Mash1* in the PNS are represented by autonomic (but not sensory) neuronal progenitors and precursors in the olfactory epithelium (Guillemot and Joyner, 1993; Kageyama *et al.*, 1997).

Targeted gene disruption studies have been conducted to obtain insights into the functions of *Mash1* in neurogenesis. Mutant mice display a severe loss of neuronal populations in the OE and the autonomic nervous system, suggesting that Mash1 plays a critical role in the neuronal lineages in the PNS (Guillemot *et al.*, 1993). Consistent with this, forced expression of the Mash1 protein in neural crest stem cells led to neuronal differentiation (Lo *et al.*, 1997). In the CNS *Mash1* mutant mice fail to generate committed neuronal precursors in ventral forebrain and there was a deficit of neurons in the mantle zone (Casarosa *et al.*, 1999; Torii *et al.*, 1999). Loss of the neuronal progenitor cell population suggests that Mash1 has a determinative function in these cells.

1.3.1.2 Ngn1 and Ngn2

The Ngn1 and Ngn2 transcription factors represent a subfamily of bHLH factors which are closely related to the *Drosophila tap/biparous* gene and distantly to *atonal* (Guillemot, 1999; Hassan and Bellen, 2000) (Fig. 1.5). Like *Mash1, Ngn1* and *Ngn2* are expressed specifically at early stages of neurogenesis. The transcripts are found in sensory neuronal precursors of the neural crest (Perez *et al*, 1999). In the CNS both are expressed by neuroepithelial precursor cells in the cortical VZ during early neurogenesis (Sun *et al.*, 2001). Knock-out mice show defects in neural tissues and a lack of sensory neurons in both dorsal root and cranial ganglia (Ma *et al.*, 1996). Expression of downstream bHLH genes like *neuroD* and *Math-3* was also negatively affected by these mutations. On the other hand, ectopic expression of *Xenopus* neurogenin related-1 (Xngnr-1) in *Xenopus* embryos induced ectopic primary neurogenesis and the expression of *neuroD*, thus demonstrating a proneural function of this protein (Lee *et al.*, 1995). In chick, forced expression of Ngn1 was shown to induce a neuronal identity even in cells not fated to be neuronal (the mesoderm) (Perez *et al.*, 1999).

1.3.1.3 NeuroD

NeuroD is thought to positively regulate neuronal development at the level of post-mitotic differentiation. *In situ* hybridization in mice did not reveal any expression in cells of the VZ. Instead, expression was detected in subpopulations of fully differentiated neurons, including the hippocampus, dentate gyrus, and pyramidal neurons of the cerebral cortex (Schwab *et al.*, 1998; Lee *et al.*, 2000). Ectopic expression in *Xenopus* embryonic neural ectoderm cells resulted in premature neuronal differentiation and inhibition of the alternative epidermal fate (Lee *et al.*, 1995). NeuroD also inhibited the formation of glia in the retina (Morrow *et al.* 1999). A severe neurological phenotype results in knock-out mutant due to a failure of cerebellar and hippocampal granule cells to differentiate (Miyata *et al.*, 1999).

1.3.2 Cascades of proneural bHLH transcription factors in neuronal differentiation

bHLH transcription factors are known to function in well co-ordinated cascades to control determination, commitment, proliferation and differentiation of progenitor cells. These cascades have been revealed by ectopic expression, loss-of-function experiments and patterns of expressions of the bHLH proteins. They have been observed in a few neuronal developmental contexts, including primary neurogenesis in *Xenopus* (Ma *et al.*, 1996; Dubois *et al.*, 1998; Pozzoli *et al.*, 2001), sensory neuron lineage in the PNS (reviewed by Anderson, 1999), the developing telencephalon (reviewed by Schuurmans and Guillemot, 2002) and in the OE neurogenesis [see Chapter 5, (Cau *et al.*, 1997; 2000; 2002]. In primary neurogenesis and in the sensory lineage the bHLH have been shown to interact with members of the repeat HLH (rHLH) superfamily, particularly the Early B cell factor/olfactory transcription factor (EBF/OLF) subfamily (Dubois *et al.*, 1998; Anderson, 1999; Pozzoli *et al.*, 2001).

To date, 3 mouse genes have been cloned, namely *ebf1/OE-1*; *ebf2/OE-3*; and *ebf3/OE-2* and these share at least 75% overall identity. Orthologs of the *ebf2/OE-3* and *ebf3/OE-2* have been identified in *Xenopus* as *Xcoe2/Xebf2* and *Xebf3*, respectively.

In primary neurogenesis, X-ngnr-1 has been proposed to have a determinative function. It is expressed before the formation of the primary neurons in the neural plate. Overexpression of *Xngnr-1* results in ectopic neuronal differentiation in nonneural ectoderm and also results in ectopic expression of *XneuroD* (Ma *et al.*, 1996). Although *XneuroD* can also induce ectopic neuron formation when overexpressed (Lee *et al.*, 1995), it cannot reciprocate the ectopic expression of *Xngnr-1* (Ma *et al.*, 1996). This therefore suggests that both *XNgnr-1* and X*neuroD* function in a unidirectional cascade with *XNgnr-1* operating upstream of X*neuroD*. The expression of the rHLH factor *Xcoe2/Xebf2* has been shown to represent an intermedate step, functioning downstream of *XNgnr-1* and upstream of X*neuroD* to control primary neurogenesis (Dubois *et al.*, 1998). Overexpressed *Xngnr-1* results in ectopic *Xcoe2* mRNA and *Xcoe2* can in turn induce ectopic expression of *Xngnr-1* in a positive feedback loop and of the later gene X*neuroD* (Dubois *et al.*, 1998). *Xcoe2/Xebf2* has therefore been suggested to maintain the expression of the earlier gene *Xngnr-1* thus enforcing the commitment of progenitors to the neuronal fate and also promoting the neuronal differentiation. The homolog of *Xcoe2/Xebf2, Xebf3* has recently been shown to be expressed during primary neurogenesis, but downstream of *XneuroD* (Pozzoli *et al.*, 2001). Overexpression of *XneuroD* leads to ectopic expression of *Xebf3*, but *Xebf3* cannot induce *XneuroD* in turn. Instead, overexpression of *Xebf3* causes ectopic expression of the neuronal specific markers NCAM, N-tubulin, and neurofilament (Pozzoli *et al.*, 2001). These results would therefore define the following cascade during *Xenopus* primary neurogenesis: Xngnr-1→Xcoe2/Xebf2→ XneuroD→Xebf3 (Fig 1.6).

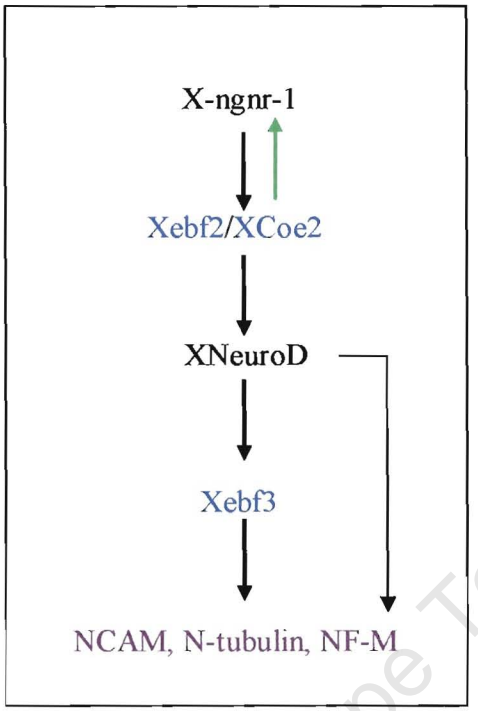

Figure 1.6 Model of transcriptional cascades implicated in different neuronal development. In primary neurogenesis during *Xenopus* development the expression of X-ngnr-1 induces neuronal differentiation by activating Xebf2/Xcoe2 which in turn induces the expression of XneuroD. Xebf2/Xcoe2 can also cause expression of Xngnr-1 in a positive feedback loop (shown by the green arrow) thus maintaining its expression. Downstream of XneuroD is the Xebf3 protein which promotes neuronal differentiation by activating the expression of neuronal specific markers NCAM, N-tubulin and neurofilament. Overexpression of NeuroD can also induce expression of neuronal markers.

1.3.3 Involvement of proneural bHLH transcription factors in neuronal versus glial fate determination

It has come to light through recent data that in addition to positively promoting neuronal differentiation, proneural bHLH factors actively inhibit gliogenesis and thus regulate the timing of glial differentiation. Analysis of mice deficient for proneural bHLH transcription factors *Mash1* and *Math3* has shown increased glial differentiation and severely reduced neurogenesis in the tectum, hindbrain and retina. In these mutants, cells that normally give rise to neurons become astrocytes (Tomita *et al.*, 2000). Likewise, premature generation of astrocytes at the expense of neurons during cortical

development was in observed in embryonic mice with a double mutation of the *Mash1* and *Ngn2* genes (Nieto *et al.*, 2001). Ectopic glial differentiation in these mutant mice indicate that the proneural factors may actively inhibit glial differentiation.

In an important experiment Sun *et al.* (2001) described a mechanism by which proneural bHLH transcription factors actively regulate gliogenesis. Astrocytic differentiation is initiated when signalling molecule CNTF/LIF binds and activates the receptor associated tyrosine kinase Jak1, followed by phosphorylation of transcription factors STAT1 and STAT3. The two transcription factors then dimerize and get translocated to the nucleus where they cooperate with Smads signalling molecules via the coactivator proteins p300/CBP to activate glial specific gene expression from STAT binding elements in glial promoters (Figure 1.7). It was found that Ngn1 prevented binding to STAT elements by sequestering the p300/CBP-Smad complex away from glial promoters and re-directing it to neuron-specific promoters. Additionally, it was found that Ngn1 prevented the phosphorylation of the STAT transcription factors by an unknown mechanism (Sun *et al.*, 2001). These results imply that proneural factors may determine the timing of both neuro- and gliogenesis. However, it is currently unknown whether other proteins use the same mechanism. These studies suggest that the proneural bHLH transcription factors not only determine neuronal fate via transcriptional up-regulation of neuron-specific target genes e.g *NeuroD*, but may also actively inhibit glial differentiation by reducing their response to extrinsic signalling molecules, such as BMP and/or CNTF.

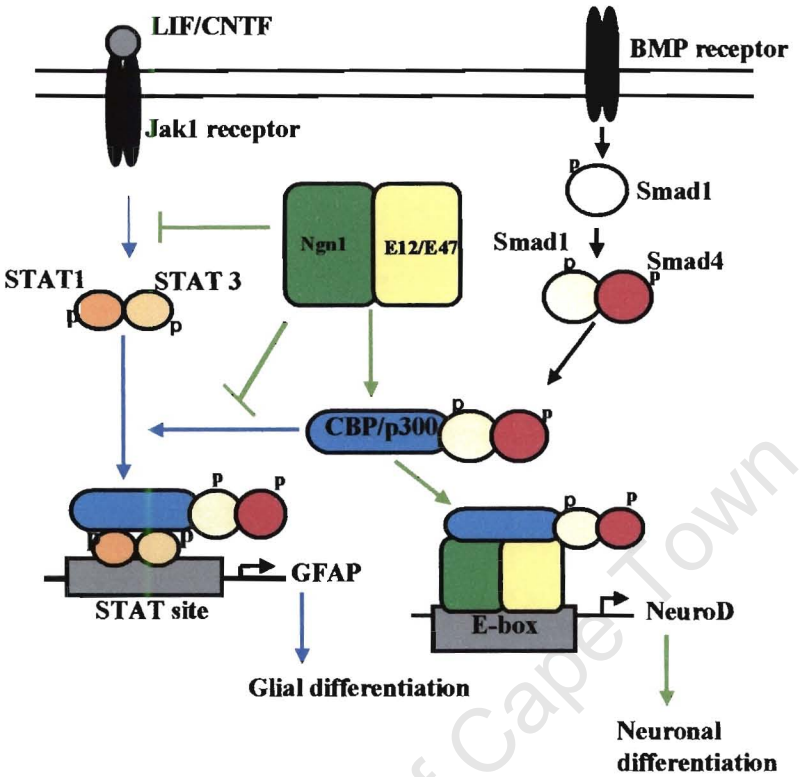

Figure 1.7 Mechanisms by which Ngn1 promotes neuronal differentiation (green arrows) while inhibiting glial differentiation (blue arrows). Ngn1 inhibits activation of STAT1/3 transcription factors and sequesters the CBP/p300-Smad transcriptional co-activator complex and re-directs it towards E-box containing promoter sequences to activate transcription of neuronal-specific genes e.g. NeuroD to promote neuronal differentiation.

1. 4. LATERAL INHIBITION

Lateral inhibition is a process by which one cell out of a cluster of cells with the potential to differentiate into neuronal cells (the proneural cluster), is selected to be a neuronal progenitor cell, while the rest are inhibited from acquiring the same fate (Figure 1.8A). This process is mediated by the genes encoding for the single-transmembrane receptor Notch and its ligand Delta, also a single-transmembrane protein. At first, all cells in the proneural cluster are capable of becoming neuronal progenitor cells and express equivalent levels of both Notch and Delta. An imbalance occurs and one

cell expresses higher levels of *Delta* than its neighbours, leading to an increase in Notch signalling in the adjacent cells thus inhibiting their differentiation along the same pathway (Fig 1.8B).

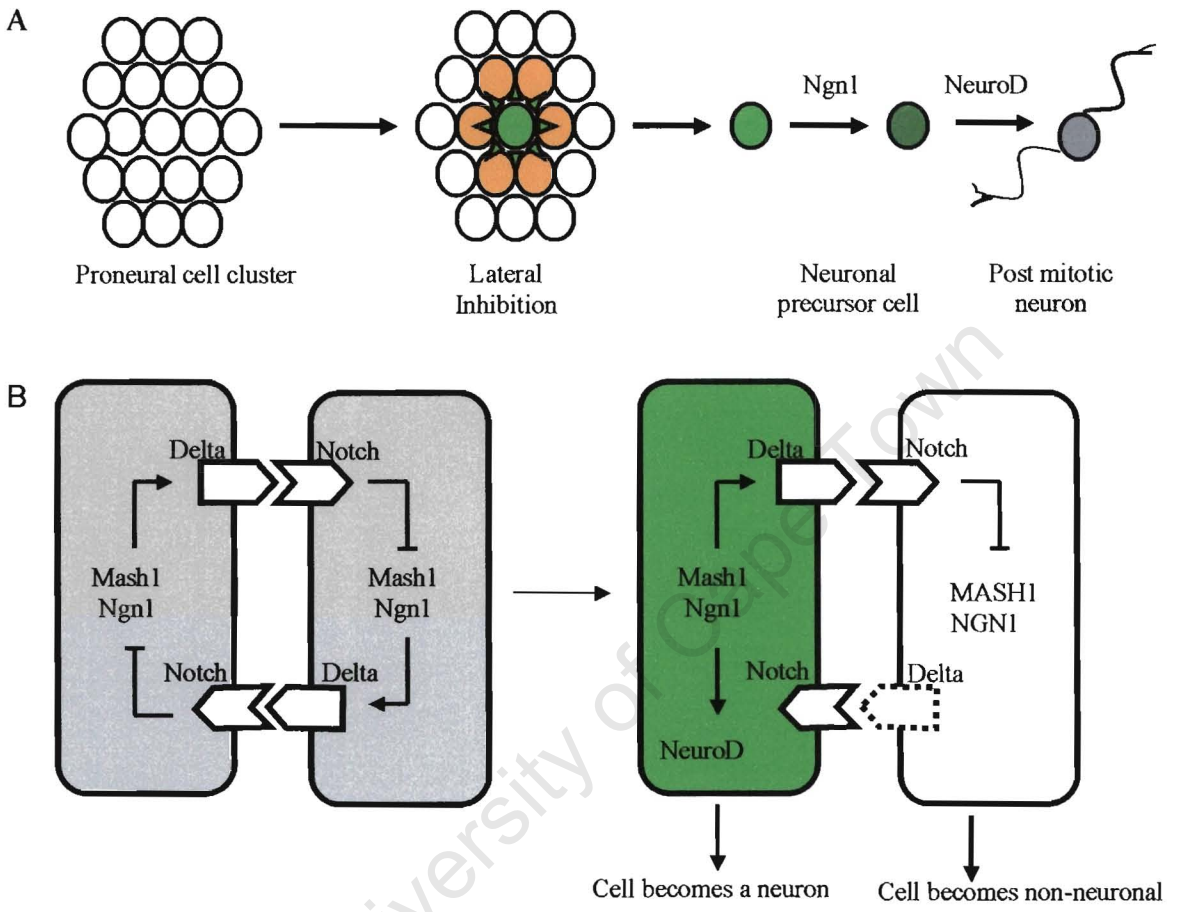

Figure 1.8 The process of lateral inhibition and its molecular components. (A) Each cell in the proneural cluster has the potential to become a neuron but only one cell is selected (shown in green) to become a neuroblast and inhibits its neighbouring cells from becoming neurons. (B) Two cells in contact are shown. At first, both cells express equivalent levels of Notch and Delta. Soon, the prospective neuron expresses higher levels of the ligand, Delta and activates Notch signalling in the other cell. The expression of proneural genes is turned off in this cell and as a result this cell is inhibited from acquiring a neuronal identity. On the other hand, the prospective neuron does not receive Notch signalling and the proneural genes (Mash1 and Ngn1) are expressed at high levels, leading to expression of NeuroD and neuronal differentiation.

Binding of Delta to Notch leads to activation of the Notch signalling pathway which is initiated by the proteolytic cleavage of the intracellular domain (ICD) of Notch, by the cytoplasmic protease *Presenilin* 1 (PS1). The ICD is then translocated to the nucleus where it forms a complex with the transcriptional cofactor CSL to activate transcription of target genes, Hes1 and Hes5 which down-regulate the

expression of the proneural bHLH proteins (Mash1, Ngn1, Math1) that are required for neuronal differentiation (Jarriault *et al.*, 1998) (Figure 1.9). The components of the Notch signalling pathway have been identified in mouse, *Drosophila*, and *Caenorhabditis elegans* and the names vary according to the species (Justice and Jan, 2002). These are summarized in Table 1.3.

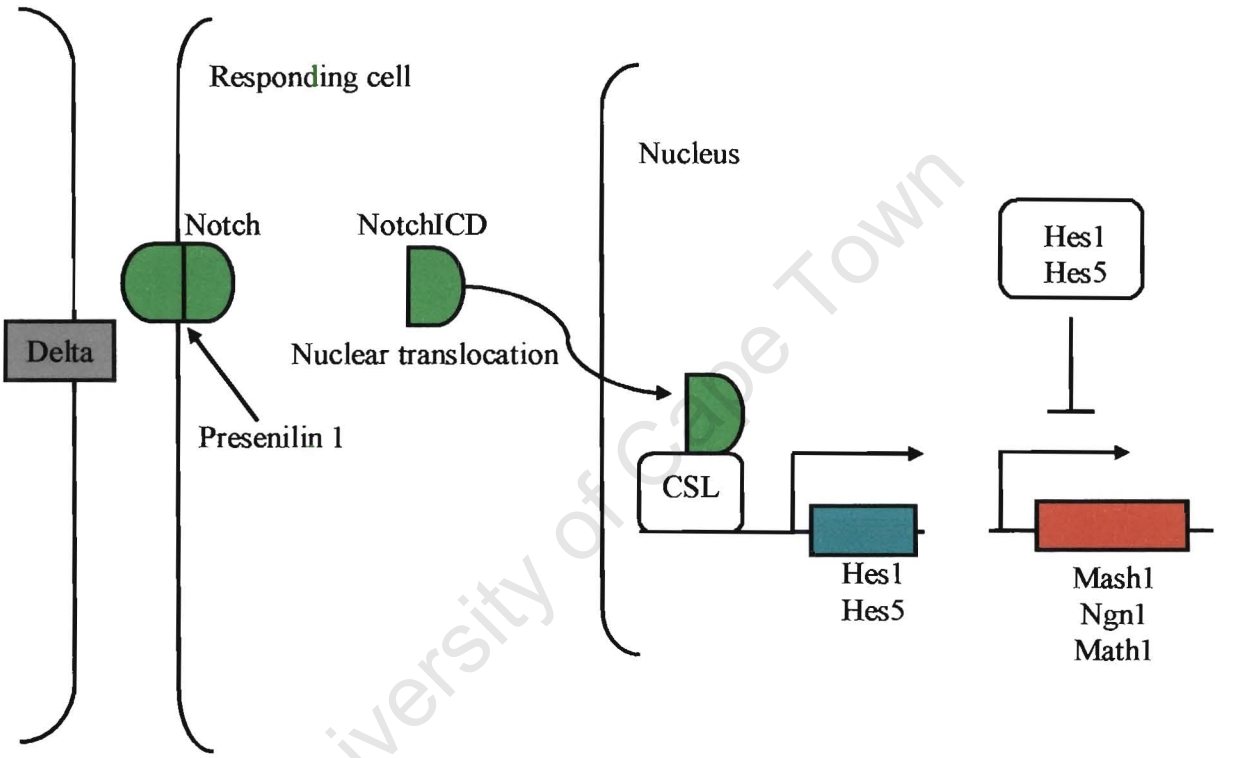

Figure 1.9 The Notch-Delta signalling pathway. The ligand Delta interacts with the receptor Notch via their extracellular regions. The intracellular domain (ICD) of Notch is cleaved by Presenilin 1 and translocates to the nucleus where it complexes with the CSL transcriptional co-activator. They then bind to regulatory sequences of Hes1/Hes5 to activate their transcription. HES1/HES5 then inhibit the transcription of the proneural bHLH proteins (Mash1, Ngn1 etc).

1.4.1 Role of *Notch-Delta* signalling

The role of *Notch* signalling in the generation of the various cell types in the vertebrate nervous system has been addressed using both gain-of-function studies and mutant analyses of the various components of the pathway. Historically, *Notch* was thought to maintain the progenitor pool by keeping the cells in

an undifferentiated state, but recently has been found to also influence neural cell fate decisions in both the CNS and PNS.

Table 1.3 The orthologues of the components of Notch signalling pathway. Shown in brackets are the number of orthologous genes found in each species (Justice and Jan, 2002).

Components of the pathway	***Drosophila***	**Mouse**	***C. elegans***	**Consensus**
Receptor	*Notch (1)*	*Notch (4)*	*Lin-12 (2)*	*Notch*
Ligand	*Delta, Serrate*	*Delta-like-1, Jagged (3)*	*Lag-2 (1)*	*DSL*
Protease for cleavege of Notch	*dPs (2)*	*Presenilin (2)*	*Sel-12*	*Presenilin*
Nuclear transcriptional cofactor	*Suppressor of hairless Su(H)*	*CBF-1/RBPJκ*	*Lag-1*	*CSL*
Target gene	*Enhancer of split*	*Hes (7)*	*Lin-22*	*Hes*

The role of *Notch* in maintaining the multipotent progenitor cell population has been shown by studying mutants that were homozygous for *Hes1*, *Notch1*, *RBP-Jκ* or *PS1* genes (Nakamura *et al.*, 2000; Hitoshi *et al.*, 2002). E10.5 *Hes1*$^{-/-}$ mice displayed a severe depletion in the number of progenitor cells compared to wild-type animals. It was found that their self-renewal capacity was disrupted, and the *Hes1*$^{-/-}$ progenitors went through only one round of cell division before giving rise to postmitotic neurons (Nakamura *et al.*, 2000). Similarly, *Notch1*$^{-/-}$, *RBP-Jκ*$^{-/-}$ and *PS1*$^{-/-}$ mutants showed depleted neural stem cells in the brains and excess neuronal and glial differentiation (Hitoshi *et al.*, 2002). Although neural stem cells could be generated in the absence of these genes, it was found that the mutant progenitors were unable to produce secondary progenitors, suggesting that they could not self-renew to maintain their population. Introduction of a constitutively active form of *Notch* could rescue the self-renewal ability of the progenitors, suggesting *Notch* was critical for self-renewal of neural stem cells. Taken together, these studies suggest that *Notch* signalling was not required for the

generation of the neural stem cells but rather critical for their maintance and inhibition of the differentiation pathway to both neuronal and glial cells (Hitoshi *et al.*, 2002). Consistent with the idea of maintaining neural stem cells, gain-of-function experiments as shown by overexpression of constitutively active forms of *Notch* and *Delta* in neural precursor cells prevented them from undergoing neuronal differentiation, instead maintaining a neuroepithelial progenitor morphology (Appel *et al.*, 2001).

On the other hand, Notch signalling may control the neuronal/glial fate switch of neural stem cells in both the CNS and PNS (Gaiano *et al.*, 2000; Morrison *et al.*, 2000; Tanigaki *et al.*, 2001; Grandbarbe *et al.*, 2003). Recent gain-of-function experiments in vertebrates have shown that Notch directly and instructively induces astrocytic differentiation and inhibits both the neuronal and oliogodendrocyte lineage pathways. Overexpression of the constitutively active *Notch* ICD in E9.5 telencepahalic progenitors (before the onset of neurogenesis) forced the cells to adopt a radial glial identity (Gaiano *et al.*, 2000). Radial glia are a specialized cell type with glial characteristics and are generated before or at the same time as neurons unlike other glial cells that are normally generated postnataly after neurogenesis (Gaiano *et al.* 2000). These cells act as scaffolds along which newborn neurons migrate to the cortex (Fig. 1.1). In a similar study using E14.5 dorsal telencephalic progenitors (during mid-neurogenesis), activated Notch enhanced expression of glial markers at the expense of neuronal specific markers (Chambers *et al.*, 2001).

When adult hippocampus-derived progenitor cells were stably transfected with the retrovirus carrying the Notch ICD, the cells were transformed into an astrocytic morphology and began to express GFAP. This was accompanied by down-regulation of markers specific for both neurons and oligodendrocytes,

suggesting Notch was actively instructing astrocytic differentiation while inhibiting the alternative fates (Tanigaki *et al.*, 2001). Similarly, when chick PNS neural crest cells were electroporated with recombinant retroviral vectors carrying the *Notch* ICD, or when exposed to a soluble form of the Notch ligand Delta, an increase in the generation of the glial Schwann cells was observed (Morrison *et al.*, 2000).

In vitro experiments conducted by Grandbarbe *et al.* (2003) have provided a model by which Notch activation may control the generation of both neurons and glia from neural stem cells. It would seem that Notch acts at two stages during this process (Fig. 1.10). Firstly, it promotes the switch from neuronal to glial fate by inhibiting the uncommitted neural progenitor cell from differentiating into a neuronal precursor, instead allowing it to become a glial precursor that has the ability to form both astrocytes and oligodendrocytes. Secondly, Notch acts on both committed neuronal and glial precursors to control their terminal differentiation pathways. A consequence of Notch activation at the stage is that the differentiation of both neurons and oligodendrocytes is inhibited and that of astrocytes promoted.

1.4.2 MECHANISM OF NOTCH ACTIVITY

As in *Drosophila*, inhibition of neurogenesis by Notch signalling in vertebrates is mediated by the direct induction of target transcriptional repressors. Hes1 is the best characterized antagonistic regulator of neuronal differentiation, downstream of Notch activation (Ohtsuka *et al.*, 1999). The phenotypes of both gain- and loss-of-function in *Xenopus* and mice, respectively, are consistent with its inhibitory function in neurogenesis. *Hes1* homozygous mice mutants are characterized by the loss of progenitor population and the concomittant premature expression of the neuronal markers MAP2 and

neurofilament in the telencephalon and mesencephalon (Ohtsuka *et al.*, 1999; Nakamura *et al.*, 2000). When expressed ectopically, *Hes1* was found to represses neuronal differentiation of neural cells in the ventricular zone of the telencephalon (Ohtsuka *et al.*, 2001). Taken together these studies suggest that Hes1 is required to maintain progenitor cells in an undifferentiated state by inhibiting neurogenesis.

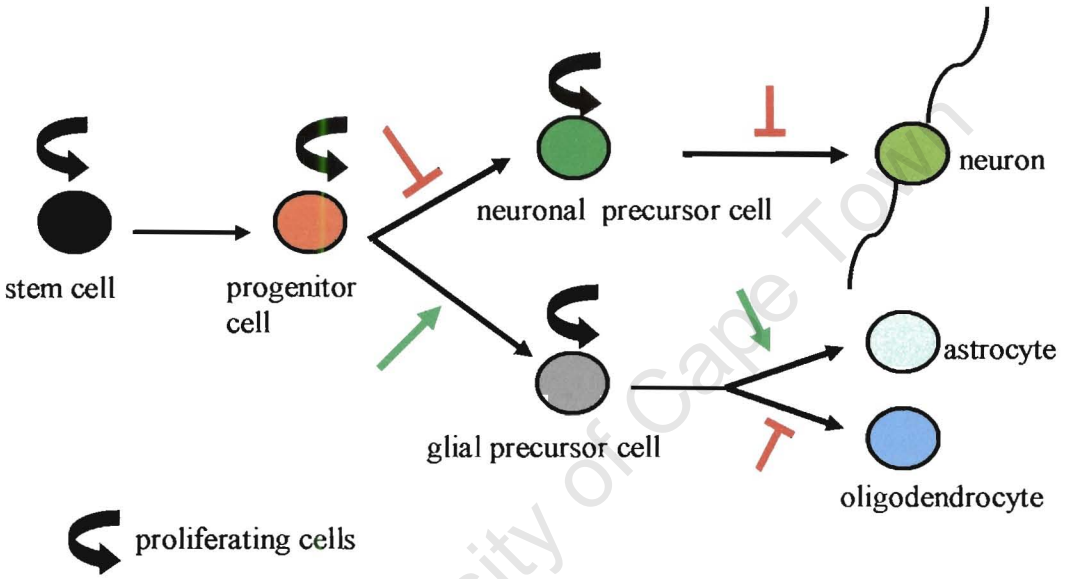

Figure 1.10 Model for the role of Notch in controlling both the neuronal/glial switch and terminal differentiation of neuro-glial cell types of the nervous system. Notch first inhibits the specification of neuronal fate while promoting that of glia. During terminal differentiation Notch also inhibits the differentiation of both neurons and oligodendrocytes while promoting that of astrocytes. The inhibitory effects of Notch are shown in red while the stimulatory effects are shown by green arrows.

Hes proteins are characterized by the presence of two distinct functional domains (for dimerization and for DNA binding) that are essential for their transcriptional repressor activity. The basic DNA binding domain contains a proline residue that decreases affinity for the E-box, instead prefering the represssor specific DNA site known as the N-box which is defined by the nucleotide sequence CACNAG. The second functional domain, represented by the 4 amino acid sequence motif WRPW (Trp-Arg-Pro-Trp) at the C-terminus recruits the non-DNA binding transcriptional co-repressor *Groucho* (Gro) in

Drosophila or the mammalian *Transducin-like Enhancer of Split* (TLE) to mediate active transcriptional repression (Castella *et al.*, 1999; Nuthall *et al.*, 2002). In this complex Hes1 functions as a DNA binding protein while Gro/TLE provides a transcription repressor function (Fig. 1.11A). Foxg1/BF-1, a winged-helix transcription factor that has been shown to maintain cell proliferation of neural progenitor cells of the telencephalon and inhibit neuronal differentiation (Xuan *et al.*, 1995) has recently been shown to interact with Hes1 and Gro/TLE to repress transcription in transfected cells (Yao *et al.*, 2001). Hes1 can also achieve its repressive action in a non-DNA-binding fashion by titrating the proneural transcription factors away from the E-box binding site. This mode of repression is achieved by Hes1 interfering with the complex between the ubiquitously expressed bHLH proteins E12 or E47 and the proneural proteins (Fig 1.11B).

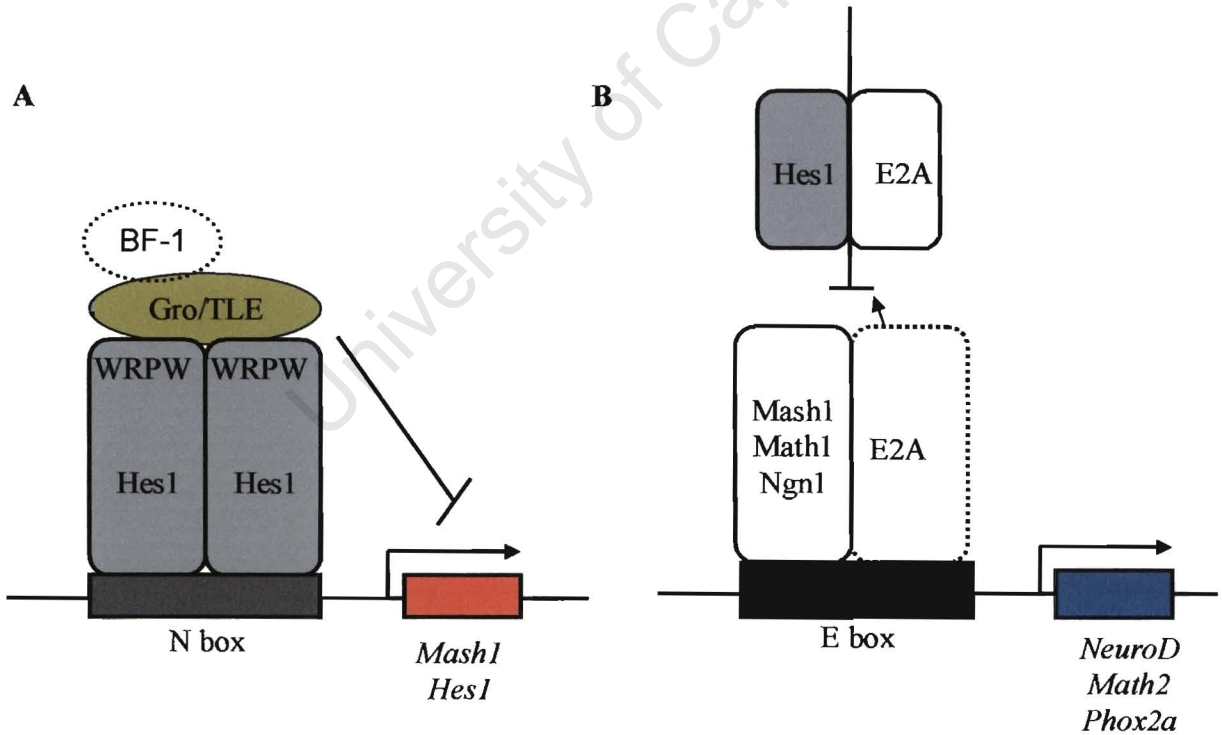

Figure 1.11 Two ways in which Hes1 can repress transcription of proneural bHLH transcription factors. (A) Hes1 represses the transcription of target genes (e.g Mash1) by recruiting the Gro/TLE co-repressor (and possibly BF-1) and by binding to the N-box. Hes1 may also repress its own transcription in a negative autoregulatory loop. (B) Hes1 may also inhibit the transcription of positive bHLH proteins by titrating the ubiquitous E-proteins away from promoter sequences that contain the E-box consensus sequences. As a consequence, activation of gene expression to promote neuronal differentiation is inhibited.

Genetic studies of nervous system development have shown that the neuronal commitment bHLH proteins Mash1 and Ngn1 are targets of the Notch-Hes signalling pathway (Chitnis and Kintner, 1996; Blader *et al.*, 1997; Chen *et al.*, 1997; de la Pompa *et al.*, 1997; Castella *et al.*, 1999; Cornell and Eisen, 2002; Sriuranpong *et al.*, 2002). Overexpression of Hes1 was shown to reduce expression of the human homolog of Mas-1 (Hash-1) by binding directly to the N-box in its promoter (Chen *et al.* 1997; Sriuranpong *et al.*, 2002). This is consistent with *Mash1* mRNA up-regulation in various brain regions of *Notch1* knock-out mutants (de la Pompa *et al.*, 1997).

In an *in vitro* approach using E17 hippocampal cell cultures expressing exogenous Mash1, Hes1 was found inhibit the differentiation of these cells (Castella *et al.*, 1999). It was postulated that Hes1 prevented transcriptional activation initiated by Mash1 by titrating its heterodimer partner E2A away from the E-box sequences present in Mash1 target genes (Castella *et al.*, 1999). Recently, it has been shown in neuroendocrine lung cancer cells that Notch may use a novel mechanism independent of *HES1* in down-regulating Hash-1. Overexpression of Notch1 in these cells increased ubiquitinylation of the Hash-1 protein and its subsequent degradation (Sriuranpong *et al.*, 2002).

Expression of *Ngn1* is also under the control of Notch signalling. Injection of a wild type *Delta1* into *Xenopus* embryos strongly suppressed the expression of *Ngn1* mRNA whereas the misexpression of a mutant *Delta1* (equivalent to blocking lateral inhibition) leads to an upregulation of *Ngn1* expression, suggesting *Ngn1* is a target of lateral inhibition (Blader *et al.*, 1997). Both Mash1 and Ngn1 can activate the *Delta* gene. In *Mash1* mutant mouse embryos, expression of both *Delta1* and the downstream effector *Hes5* is lost throughout the ventral telencephalon, spinal cord, and mesencephalon where *Mash1* is normally expressed (Casarosa *et al.*, 1999). Misexpression of *Ngn1* in both *Xenopus* and zebrafish leads to ectopic expression of *Delta1* (Ma *et al.*, 1996; Blader *et al.*, 1997). Thus it

appears that Ngn1 and Mash1 control the expression of *Delta* and are themselves down-regulated by lateral inhibition in a negative feedback loop which will help diversify cell types during development of the brain (Fig. 1.8B). In contrast, *NeuroD*, which is required for the terminal differentiation, is insensitive to direct inhibition by *Notch* signalling as demonstrated by the inability of the constitutively active *Notch* ICD to inhibit the ectopic neuronal differentiation when co-injected with *NeuroD* in *Xenopus* embryos (Chitnis and Kintner, 1996).

1.5 INTERACTION OF THE FGF AND *NOTCH* SIGNALLING PATHWAYS

One significant area that requires a closer examination is whether *Notch* signalling interacts with FGF-2 in regulating neurogenesis. It is not clear whether the maintenance of stem cells and cellular differentiation of their progeny are regulated independently by the two distinct signals or whether the different signals co-operate in specifying these cellular fates. As we have seen above, there is a regulatory loop involving *Notch* and the proneural proteins in controlling the cell lineages in the nervous system. There are not that many studies that have attempted to look at how FGF or other signalling molecules may interact with these. As was reviewed earlier, FGF-2 is primarily mitotic for neuroectodermal cells and is therefore possible that it may positively interact with the Notch signalling pathway to maintain these cells in a non-differentiated state. It has been shown that FGF-2 may use the Notch signalling pathway to inhibit the neuronal differentiation of E10 cortical precursors (Faux *et al.*, 2001). FGF-2 increased the expression of *Notch* and down-regulated the expression of the ligand *Delta*, suggesting that *Notch* signalling pathway may be downstream of FGF signalling. When activation of *Notch* is inactivated by a null mutation of the *Presenilin-1* gene or with antisense *Notch* oligonucleotides, treatment with FGF-2 at low concentrations resulted in a profound increase in neuronal production (Faux *et al.*, 2001). It has also been found that both pathways influence the fate of

the mammalian mouse telencephalon neural progenitors co-operatively. Cells expressing activated *Notch* show a 4-fold increase in their ability to proliferate in response to FGF (Gordon Fishell Lab, see URL in reference section). Both these studies suggest that the *Notch* pathway may be a downstream cascade that transduces FGF-2 signals that ultimately result in the inhibition of neurogenesis.

On the other hand, FGF-2 may act to inhibit Notch signalling thus allowing neuronal differentiation to take place. Currently, there is no direct evidence to support this. However, NGF, via its activation of the protein kinase C (PKC) pathway, inhibited the DNA-binding ability of HES1 by phosphorylating its basic DNA binding domain, thus allowing the PC12 cells to differentiate into neuronal cells (Ström *et al.*, 1997). As PKC can transduce FGF-2 signals (Fig 1.4), it is therefore possible that FGF-2 may therefore induce neuronal differentiation in a similar manner.

1.6 OLFACTORY NEUROGENESIS: A MODEL SYSTEM

The olfactory epithelium (OE) is well recognized as a simple model system to explore the molecular and cellular mechanisms of neurogenesis that have been mentioned above. It has several features that make it well suited for such studies. Its peripheral location makes it accessible. Like the neural tube in the nervous system, it has an epithelial structure in which neurons are generated. However, the OE has a much simpler structure. The tissue is made up of 3 cell types that can be distinguished from each other by morphology, their position in the epithelium, and cell type-specific antigenic markers. These are the basal cells, neurons, and sustentacular cells. Unlike the brain, the OE is populated by only one type of neuron, the olfactory receptor neuron (ORN). The most notable characteristic about this neuron is that it is replenished continuously throughout the life of an animal from a maintained population of undifferentiated precursor cells at the base of the epithelium, implying that stem cells of the ORN

lineage exist in this tissue. It is this regenerative capacity that has rendered the OE an excellent system in which to study the molecular and cellular events that occur during neurogenesis.

1.6.1 Early stages of mouse OE development

The OE develops from olfactory placodes which are formed at E9.5 from thickened patches of the ectoderm on the ventral sides of the head. This is followed by invagination of the placodes at E10.5, forming the olfactory pits which deepen and form recesses around E11.5. Over the next E12.5-13.5 period, the OE gets organized into layers (Farbman, 1994). The OE is stratified and the cell types found there are localised into 3 layers, the basal, middle and apical layers (Figure 1.12). The basal layer contains 2 types of basal cells that can be distinguished from one another. The cytokeratin expressing horizontal basal cells (HBCs) are small, flat and dark cells found on the basal lamina. Superficial to HBCs are the globose basal cells (GBCs) which do not express cytokeratin. The middle layer of the OE contains both bipolar immature and mature ORNs. The latter are characterised physically by the apical dendritic knob and cilia which are in direct contact with the external environment. The ORNs send their axons and synapse directly to the olfactory bulb (OB) in the forebrain. In the apical layer, sustentacular cells extend from the epithelial surface to the basal lamina.

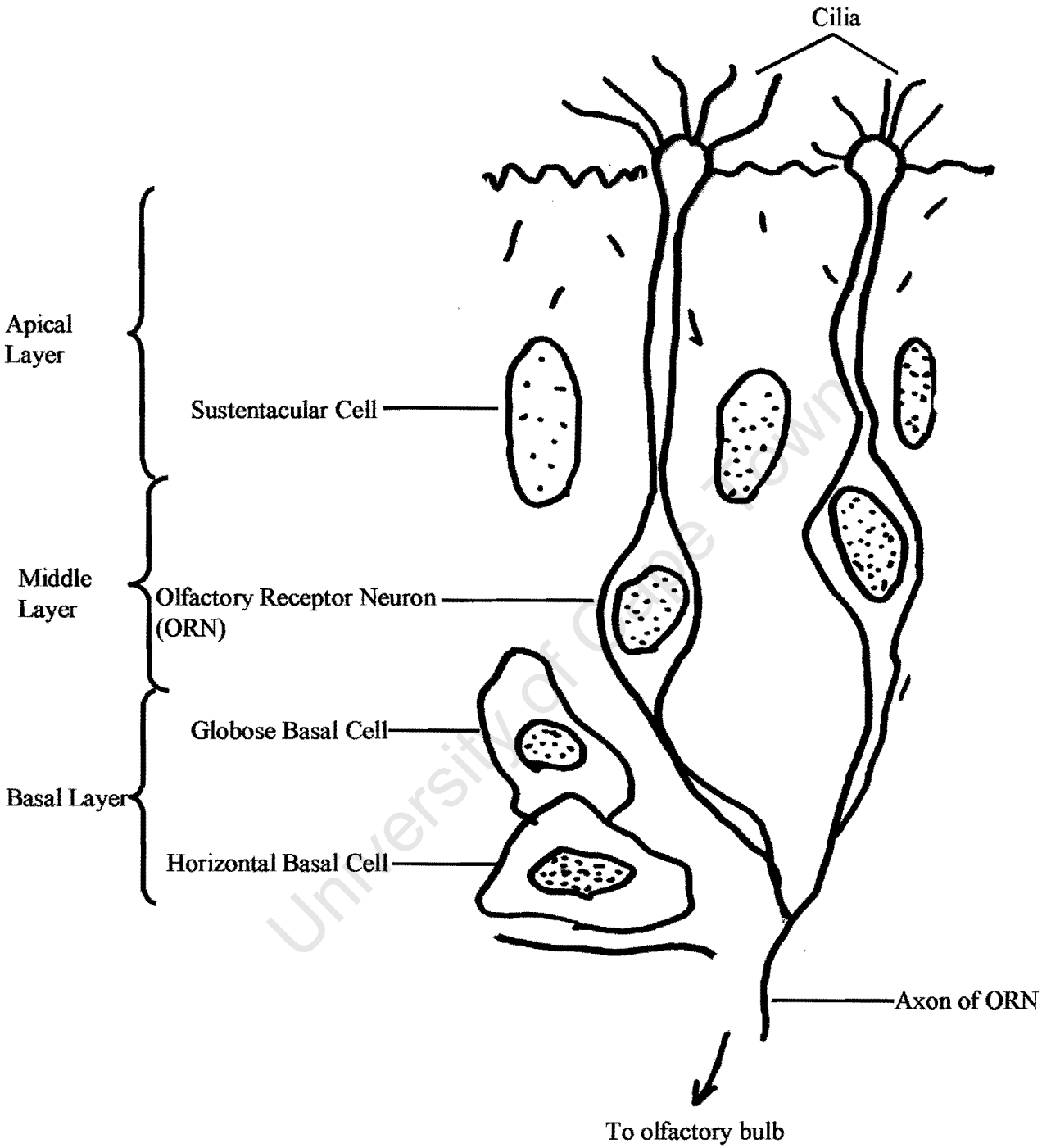

Figure 1.12 The diagram of the structure of the olfactory epithelium. The sustentacular cells are located in apical layer of the OE while the middle layer is populated by both immature and mature olfactory receptor neurons (ORN's) whose axons extend into the olfactory bulb with their dendrites into the nasal cavity, in direct contact with odorants. The basal layer contains both horizontal and globose basal cells (GBC) which are mitotically active.

1.6.2 The neuronal lineage in the mouse OE

A model of neuronal lineage in the OE has been proposed via the use of various tissue culture assays (reviewed in Calof *et al.*, 2002). The phenotype of the cells at various stages of the differentiation process can be characterized by defined markers (Fig 1.13).

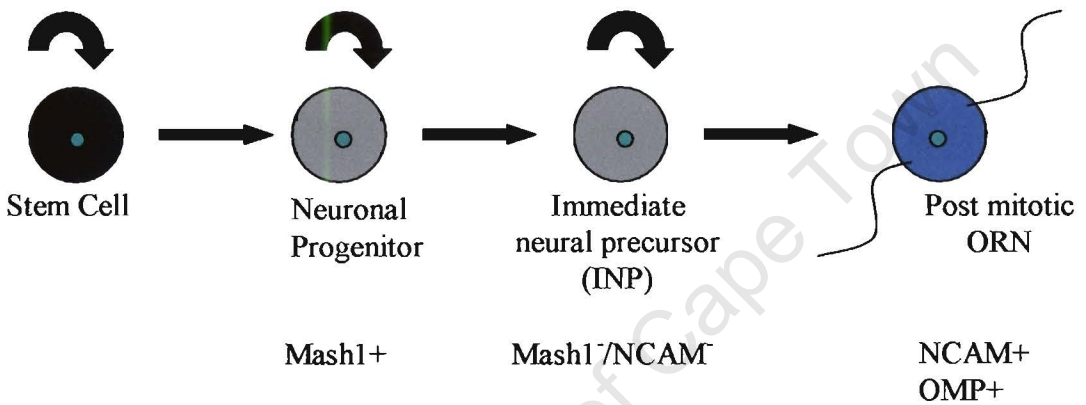

Figure 1.13 The OE neuronal lineage is characterized by 3 stages of actively dividing progenitor populations: the neuronal stem cell, the neuronal progenitor that expressed Mash1, and the last proliferating cells in this lineage, the Mash1$^-$/NCAM$^-$ immediate neuronal precursor. The INP differentiates into a postmitotic ORN which expresses the olfactory marker protein (OMP) and olfactory receptors.

There are at least 3 distinct sequential stages of mitotically active cells within the lineage. These are the neuronal stem cell, the neuronal progenitor cell and lastly, the immediate neuronal precursor (INP). To date, the identity of the neuronal stem cell is still unknown. A neuronal colony forming cell (CFU) has been tentatively identified as a neuronal stem cell -when grown *in vitro* on feeder cell layer, progenitor cells and ORNs are produced from this cell (Mumm *et al.*, 1996; Calof *et al.*, 2002). Found interposed between the postmitotic ORN and the neuronal stem cell are the two transit-amplifyng progenitors: the *Mash1* expressing progenitor and the INP. The *Mash1*+ neuronal progenitor cell is thought to be the progeny of the stem cell and this cell undergoes one to two rounds of division to give rise to *Mash1*$^-$/NCAM$^-$ INP, the terminal progenitor cells in the lineage.

The INP goes through several symmetrical divisions followed by differentiation of all progeny into ORNs. *In vivo*, the mitotically active cells of the neuronal lineage are found within the GBC population, a heterogenous cell population that has been shown to be direct precursors of ORNs. Mature ORNs are post-mitotic and express NCAM, proteins of the olfactory receptor transduction pathway and the olfactory marker protein.

1.6.3 Regulation of OE neurogenesis

Regulation of OE neurogenesis by both extrinsic and intrinsic signals follows similar themes to that reviewed earlier in this chapter. The effects of FGF-2 on this lineage has been studied *in vitro* using explant cultures and cell lines (reviewed in Chapter 3), while studies of regulation by bHLH proteins and Notch signalling have been spearheaded by the laboratory of Francois Guillemot (reviewed in Chapter 5).

1.7 AIMS OF THE STUDY

The general aim of this project has been to study the role of fibroblast growth factors (FGF), particularly basic FGF (FGF-2) in olfactory neuronal differentiation, using a novel embryonic cell line (OP27) as a model system. OP27, together with other similar cell lines (OP6, OP47 and OP55) were isolated by infection of primary cultures of olfactory epithelium from E10.5 mouse embryos with retrovirus carrying temperature sensitive alleles of the SV40 large T antigen (Illing *et al.* 2002). The retrovirus allows the cells to proliferate at the permissive temperature of 33°C, but the cells stop dividing when shifted to the non-permissive 39°C when the T antigen is inactivated. This allows us to

study the effects of various growth factors at the non-permissive temperature when the cells are not under the control of the large T antigen. These cell lines can be used as a model system to study neuronal differentiation in the olfactory epithelium *in vitro*.

The following approach was used in this study.

1.7.1. Determine whether FGF receptors are expressed by the cell line

As we have seen above, one FGF ligand can only activate several FGF receptors. Therefore I sought to determine whether the OP6, OP27, OP47, and OP55 cell lines express a limited number or the whole repertoire of FGF receptors.

1.7.2. Assay the response of OP27 to FGF-2 and characterise the response

Having shown that the OP27 cell line does express receptor(s) for FGF-2, tissue culture experiments were designed to test whether the OP27 cell line responds to FGF-2 at the non-permissive temperature by proliferating or by differentiating to mature olfactory neuronal cells. Markers that characterize the different stages of the OE lineage were used to characterize the phenotype of the cells following treatment with FGF-2. These included markers that are generic to neuronal cells (NCAM, GAP-43, PLCγ), and those that are specific to the ORNs (OMP and the proteins involved in the odorant signalling pathway e.g. olfactory receptors and G_{olf},).

1.7.3 Analysis of olfactory receptor gene expression in OP27 cells

ORNs express olfactory receptors during their differentiation and each ORN expresses one or very few of these receptors. OP27 cells were investigated whether they express only one or a small repertoire of olfactory receptors during their induction with FGF-2.

1.7.4. Characterization of the transcriptional expression of proneural bHLH transcription factors and *Notch* signalling pathway components in OP27 following treatment with FGF-2

Lateral inhibition plays an important role in neuronal fate determination. I wanted to find out whether FGF signals lead to activation of genes downstream of the Notch signalling cascade. Semi-quantitative RT-PCR was used to monitor expression levels of the various components of the *Notch* signalling pathway following treatment with FGF-2.

1.7.4. Differential display analysis of the OP27 cell line

The technique of differential display was employed to identify novel genes that respond to FGF-2 treatment and that might play a crucial role in neuronal differentiation. The identification of genes involved in the process of neuronal differentiation would provide an important step towards the understanding of the underlying molecular mechanisms. These genes would include those that have been activated and those that have been repressed, for neuronal differentiation to take place. In addition, genes that are good markers of the different stages in neuronal differentiation of olfactory sensory neurons may be identified.

Chapter 2

Methods

2.1 CELL LINES

Cell lines (Illing *et al.*, 2002) were routinely maintained in Dulbecco's modified Eagle medium (DMEM, Gibco-BRL) supplemented with 10 % fetal calf serum (FCS, Delta Bioproducts) at 33°C under a 10% CO_2 atmosphere. For passaging, cells were washed once with pre-warmed 1X phosphate-buffered saline (PBS: 0.14M NaCl, 2.7mM KCl, 8 mM Na_2HPO4, 1.5mM KH_2PO_4), and detached with 0.25% trypsin/2.5mM EDTA solution (Gibco-BRL) for 2 min and stopped with the addition of DMEM/10% FCS. After dissociation the cells were centrifuged at $1000min^{-1}$ for 5 min in a Hettich Rotanta bench centrifuge (Labotech) and the cell pellet was resuspended in fresh DMEM/10% FCS. Cells were seeded into tissue culture dishes at a density of $1X10^4$ cells/cm^2.

2.2 MULTIPLEX RT-PCR ANALYSIS OF FGFR EXPRESSION IN OP27 CELLS:

To determine which of the four FGFRs were present in the OP27 cells, simultaneous amplification of the receptors was accomplished with a multiplex PCR technique using a single primer pair followed by a restriction enzyme analysis as described by McEwen and Ornitz (1996), with modifications.

2.2.1 Isolation of RNA

Cells grown in culture were harvested by trypsinization and total RNA isolated using the single step method of acid guanidium thiocyanate-phenol-chloroform extraction (Chomczyński and Sacchi, 1987). Briefly, the cell pellet was homogenised in 500µl solution D (4M guanidine thiocyanate, 25mM sodium citrate pH7.0, 0.5% sarkosyl, 0.1M mercaptoethanol) followed by the sequential addition of

0.1x volume of 2M sodium acetate pH4, 1x volume of phenol pH4, and 0.2x volume of chloroform-isoamylalcohol (24:1). After a 15 min incubation on ice, the samples were centrifuged at 10 000g for 20 min at 4°C. The aqeous phase was mixed with an equal volume of isopropanol in a fresh eppendorf and incubated at -70°C for at least one hour followed by centrifugation at 10000g for 20 min at 4°C. The RNA pellet was resuspended in 300µl solution D and precipitated with an equal volume of isopropanol at -70°C for at least one hour. Following aspiration of the supernatant, the pellet was washed once with 70% ethanol and allowed to dry at room temperature. The RNA was finally dissolved in nuclease-free water and quantitated by UV spectrophotometry.

2.2.2 DNaseI treatment

Contaminating genomic DNA was removed from total RNA by treatment with DNaseI, followed by phenol–chloroform extraction and ethanol precipitation. Twenty µg of total RNA was treated with 20U RQ1 DNaseI (Promega) in a 200µl volume containing 1x RQ1 DNaseI buffer (40mM Tris-HCl pH8.0, 10mM $MgSO_4$, 1mM $CaCl_2$) and 200U Recombinant RNasin® Ribonuclease inhibitor (Promega) at 37°C for 1 hour. This was followed by extraction with 1x volume of phenol pH4: chloroform: isoamylalcohol (25:24:1). The aqueous phase was mixed with 0.01x volume of µCarrier (Molecular Research Centre), 1x volume 3M sodium acetate pH 5.2 and 2.5x volume ethanol, and precipitated at -70°C for at least 1 hour. The RNA solution was centrifuged at 13000RPM for 30 min in a benchtop centrifuge at 4°C and the pellet was washed once with 70% ethanol and dried at room temperature. The pellet was resuspended in nuclease-free water and quantitated by UV spectophotometry. The integrity of RNA was checked by agarose gel electrophoresis.

2.2.3 First- strand cDNA synthesis

Five µg of DNaseI-treated total RNA was heat-denatured at 92°C for 2 min in the presence of 500ng random hexamers (Promega) in a 20µl volume, followed by quenching on ice. To each sample, 6µl of 5x RT buffer (final concentrations: 50mM Tris-HCl pH 8.3, 75mM KCl, 3mM $MgCl_2$, 10mM DTT), 1.5µl of 10mM each dNTP, 1µl of 40u/µl recombinant RNasin® Ribonuclease Inhibitor and 1µl of 200U/µl Moloney murine leukemia virus Reverse transcriptase (M-MLV RT, Promega) were added. The samples were incubated at room temperature for 10 min, 42°C for 50 min and 95°C for 5 min.

2.2.4 Polymerase chain reaction (PCR)

Four microlitres of the cDNA were amplified in a 50µl total volume containing 1x PCR buffer (10mM Tris-HCl pH 9.0, 50mM KCl, 0.1% Triton X-100), 1.5mM $MgCl_2$, 0.2mM dNTPs, 10pmol of each D0156 and D0158 oligonucleotides (Table 2.1), and 1U Taq polymerase (Promega). The samples were then subjected to 30 cycles of 94°C for 1 min, 55°C for 2 min, and 72°C for 2 min, followed by a final extension at 72°C for 5min in the Omnigene thermocycler (Hybaid). The amplification of the expected product size (341bp) was confirmed by analysing 5µl of the reaction on a 2% agarose gel. Following the gel analysis, the PCR reactions were purified using the Wizard PCR Preps DNA Purification System® (Promega).

Table 2.1 RT-PCR primers used to characterize the OP27 cell line.

Gene Name	*Primers*	*Sequence 5'-3'*	*Sizes Expected (bp)* cDNA size	Genomic	*Reference*[a]
FGFR	D0156 D0158	TCNGAGATGGAGRTGATGAA[b] CCAAAGTCHGCDATCTTCAT[b]	341 bp	>530	McEwen and Ornitz, 1996
FGFR1	F1189 R1190 F1191	CTGGTCACAGCCACTCTCTGCAC CCAGGTACAGAGGTGAGGTCATC ACTTTGCGCTGGTTGAAAAACGGC	823; 1090 bp	~34700	This study
FGFR2	FGFR2-f FGFR2-r	CCTCCAAGCTGGACTGCC TGCCACGGTGACCGCCTC	777 bp	~21500	This study
FGFR3	FR3f FR3r	CCGGCCAACCAGACAGCC TTGCAGGTGAGCTGTTCCTC	997 bp	3731	This study
FGFR4	FR4f FR4rp	GCTATCTCCTGGATGTGC ACACCCAGCAGGTTGATG	936 bp	5987	This study
Olfactory Receptor	ORF3 ORC	AGATCTAGATGGCITAYGAYMGITAYGTIGC[b] GCTCTAGATARATRAAIGGRTTIARCAT[b]	530	530	Ngai *et al.*, 1993
OMP	OMPfp OMPrp	AAGGTCACCATCACGGGCAC TTTAGGTTGGCATTCTCCAC	242	242	Barber *et al.*, 2000

[a]The source of the nucleotide sequences of the primers used in this thesis

[b]**N**=A, C,G or T; **R**= A or G; **H**=A, C, or T; **D**=A, G, or T; **Y**=C, or T; **M**=A, or C; **I**=inosine

2.2.5 Restriction Enzyme digestion of the PCR products

Eight microlitres of the purified PCR products were digested separately with *EcoRI*, *PstI* and *PvuII* (Amersham) by adding 1µl of the appropriate 10x buffer and 1µl of the enzyme and incubating at 37°C for at least 1 hour. The digested samples were mixed with 2.5µl of 5x loading buffer (50mM EDTA pH8.0, 50mM Tris-HCl pH 8.0, 50% glycerol) for non-denaturing PAGE and subsequently analysed on a 12% non-denaturing 1X TBE (90mM Tris-borate pH 8.3, 1mM EDTA) polyacrylamide gel. After the electrophoresis, the gel was fixed and silver-stained as described previously (Bassam *et al.*, 1991). Briefly, the gel was fixed in 10% acetic acid for 20 min and rinsed in dH_2O for 2 min thrice. This was followed by impregnating the gel with a freshly made mixture of 0.1% $AgNO_3$ and 0.055% formaldehyde for 30 min. The colour reaction was developed with a solution of 3% Na_2CO_3, 0.055% formaldehyde and 0.0002% $Na_2S_2O_3.5H_2O$ (sodium thiosulphate) for 2-5 min and stopped with 10% acetic acid for 5 min.

2.3 DETERMINATION OF OP27 FGFR SPLICE ISOFORMS

2.3.1 First- strand cDNA synthesis

cDNA synthesis was performed in a 20µl reaction containing 5µg heat-denatured (65°C, 5 min) total RNA, 250ng random hexamers, 1mM dNTPs, 1x RT buffer, 0.1µg/ µl BSA, 20U recombinant RNasin® Ribonuclease Inhibitor, 500ng oligo-(dT) and 200U M-MLV RTase, incubated at 42°C for 1hour and heat-inactivated at 95°C for 5 min.

2.3.2 FGF receptor 1 RT-PCR

Twenty µl of the RT reaction were used in a 100µl reaction volume with 1x PCR buffer (2.5mM TAPS pH9.3, 50mM KCl, 2mM $MgCl_2$, 1mM β-mercaptoethanol), 1.5mM $MgCl_2$, 10pmol of each F-1189 and R-1190 oligonucleotides (Table 2.1), 5% DMSO and 2.5U SuperTherm DNA polymerase (Southern Cross Biotech.). The reactions were run for 30 cycles at 94°C for 1 min, 60°C for 1 min and 72°C for 3 min followed by a 5 min incubation at 72°C. The PCR-amplified products were analysed by agarose gel electrophoresis and transferred overnight onto a Hybond N^+ membrane (Amersham) for

Southern blot analysis to analyse the specificity of the RT-PCR products. The 3' ECL labelling and detection system (Amersham) was used for labelling the internal oligonucleotide, F-1191 (Table 2.1), hybridization and detection as recommended by the manufacturers. The RT-PCR products were cloned into the pGEM-T cloning system (Promega) and the nucleotide sequence of the inserts was verified by automated sequencing.

2.3.3 FGF receptor- 2 RT-PCR

PCR amplification of the FGF receptor 2 was performed using an aliquot of 4 µl of the above RT reaction, 1x PCR buffer, 20 pmol of each forward and reverse primers (Table 2.1), 0.2mM dNTP, 3mM $MgCl_2$ and 1U SuperTherm Taq in a 50 µl reaction volume. The cycling conditions were the same as those used for FGF receptor 1 above. The RT-PCR product was cloned into the pGEM-T cloning system and verified by partial sequencing of the cloned fragment using the Sequenase 2 sequencing kit (USB).

2.3.4 Restriction fragment analysis of RT-PCR products for detection of FGF receptor splicing isoforms

The RT-PCR products were purified using the Wizard PCR Preps DNA Purification System (Promega) as instructed by the manufacturers. To discriminate between the IIIb and IIIc isoforms of FGFR 1, 10µl of the RT-PCR product was subjected to a restriction digestion analysis with the endonucleases *AccI* and *VspI* (Amersham) in a 20µl reaction containing 1X final concentration of the appropriate buffer and incubated at 37°C overnight. For the FGF receptor 2, *EcoRV* was used to discriminate between the IIIb and IIIc isoforms in a similar digestion reaction set up. The digest products were analysed on 1% agarose gel and stained with ethidium bromide.

2.4.1 OP27 CELL CULTURE IN FGF-2

For the FGF-2 experiments, cells were plated in petri-dishes at the density of $5x10^4$ cells/cm^2 and allowed to grow in DMEM/10% FCS until 70% confluence at the permissive temperature (33°C). At time 0, the cells were shifted to the non- permissive temperature (39°C) in serum-free DMEM: Ham's F-12 (1:1, vol/vol) medium containing N2 supplement (5µg/ml insulin, 50µg/ml transferrin, 20nM progesterone, 100µM putrescein, 30nM sodium selenite, all Sigma), 5 U/ml heparin (Sigma) and FGF-2 at 5 ng/ml (a kind gift from John Heath, University of Birmingham, UK). The cells were grown at this temperature for different time points. After the specified times at 39°C, images of cells were captured using a 10x objective on an Olympus microscope. At least 3 images were captured per dish. The analySIS® software (Soft Imaging System GmbH) was used to analyse the digital images.

2.4.2 QUANTITATIVE ANALYSIS OF FGF-2-INDUCED DIFFERENTIATION OF OP27 CELLS

2.4.2.1 Number of bipolar cells

With the help of the analySIS® package, the percentage of cells with bipolar morphology was determined by counting the number of bipolar cells in a field per total number of cells in that field. Ten randomly photographed fields from 3-4 plates were counted for each time point and averaged. Bipolar cells were defined as cells with neurite-like extensions emanating from either side of the cell body, with one neurite longer than the size of two cell bodies.

2.4.2.2 Survival assay

10^4/ml cells were seeded in 6-well tissue culture dishes in DMEM/10% FCS and allowed to adhere at 33°C. At day 0, the medium in 3 wells from a dish was replaced with 2ml of serum-free DMEM: Ham's F-12 containing N2 supplement, heparin and FGF-2 per well while that in the other 3 wells was replaced with the same medium but with no FGF-2 (control cultures). The dishes were shifted to 39°C and the medium was replaced with fresh medium after every 2 days. To assess survival, cells from

each well were trypsinized, incubated in Trypan blue and unstained cells (live cells) were counted using a haemocytometer.

2.4.2.3 Cell proliferation assay

OP27 cells were differentiated as mentioned in 2.4.2.1. DNA synthesis was measured by labeling cultures with [^{3}H]thymidine (5Ci/mmol, Amersham) at 2μCi/ml per well for 24hrs. At the end of the 24hr-labelling period, the medium was removed and each well was washed twice with ice-cold PBS followed by 2 washes in ice-cold 5% (vol/vol) trichloroacetic acid and aspirated. The cells were then solubilized in 0.5ml of 0.25M NaOH. Incorporated ^{3}H-thymidine was quantified by liquid scintillation counting of 400μl of solubilised cells. Counts from the triplicate wells were averaged and plotted using the Microsoft® Excell 2000 software.

2.5 WESTERN BLOT ANALYSIS

OP27 cells were treated with FGF-2 as detailed in 2.4.1. Control and differentiated OP27 cells were washed twice with ice-cold PBS, and harvested using cell scrapers. The cell suspension was centrifuged at 1400rpm for 5min at 4°C and the cell pellets were resuspended in ice-cold lysis buffer (50mM Tris-Cl pH 7.5, 150mM NaCl, 1% NP-40, 5mM EDTA, 10μg/ml aprotinin, 10μg/ml leupeptin, 40μg/ml PMSF). Suspensions were homogenized, incubated on ice for 10 min and cleared by centrifugation at 14 000 rpm for 2min to remove cell debris. Protein assays were performed with the Bio-Rad Protein Assay kit (BioRad) based on the Bradford dye-binding procedure. For immunoblot analysis, 20μg of proteins from the control and differentiated OP27 cells were separated by SDS-polyacrylamide gel electrophoresis in 7.5% resolving gel using the Mini-Protean system apparatus (BioRad). Proteins were then electrotransferred to a Hybond P transfer membrane (Amersham) using the Mini Trans-blot Electrophoretic Transfer Cell (BioRad). The membranes were then blocked at room temperature for 1h using TBS (10mM Tris-HCl pH 7.4, 0.5M NaCl) containing 5% (w/v) fat-free dry milk. The blots were incubated overnight at 4°C with primary antibodies at various dilutions (Table 2.2) in TBS containing 2% (w/v) fat-free milk. Membranes were washed 3 times in TBS/0.1% Tween-20 for 5min at room temperature and incubated with horseradish perixodase-conjugated secondary antibodies for 1h at room temperature. After 3 washes with TBS/0.1% Tween-20,

immunoreactivity for NST, TrkB, PLCγ2, Gαolf, and β-actin was detected by chemiluminescence using a commercial kit (Pierce), while that for NCAM, TrkC and ACIII was detected as follows: (a) 13.3 µl P-coumaric acid (Sigma) (stock solution: 14mg P-coumaric acid /ml DMSO) and 1.66µl of 30% H_2O_2 were added to 3ml of 100mM Tris-HCl pH 8.5 (b) 30µl of 3-aminophalhydrazin (Sigma) (stock solution: 44mg/ml DMSO) was added to 3ml of 100 mM Tris-HCl pH 8.0 (c) both solutions were then mixed together and poured over the membrane and incubated for 5 min. The signals for all antibodies were visualised by exposing the plastic-wrapped membranes to X-ray film after removal of excess substrate.

Table 2.2: List of antibodies and the dilutions used for immunoblotting (western) and immunocytochemistry (ICC)

Primary antibody	*Species*	*Source*	*Dilution (Western)*	*Dilution (ICC)*
β-actin[a]	Mouse monoclonal	Sigma	1:5000	-
Adenyl cyclase type III (AC-III)	Rabbit polyclonal	Santa Cruz	1:500	-
Neural cell adhesion molecule (NCAM)	Rabbit polyclonal	Chemicon	1:5000	-
Neuron specific tubulin (NST, β-III)[a]	Mouse monoclonal	Babco	1:250	-
Olfactory G protein ($G_{\alpha s/olf}$)[a]	Rabbit polyclonal	Santa Cruz	1:1000	1:1000
Phospholipase C gamma (PLCγ)[a]	Rabbit polyclonal	Santa Cruz	1:500	1:1000
TrkB[a]	Rabbit polyclonal	Santa Cruz	1:500	1:1000
TrkC	Rabbit polyclonal	Santa Cruz	1:500	1:750[a]
HRP conjugated secondary antibodies				
Mouse IgG-HRP	Goat	Dako	1:2000	-
Rabbit IgG-HRP	Goat	Bio-Rad	1:10 000	-
Goat IgG (H+L)-HRP	Rabbit	Molecular Probes	-	1:1000
Fluoresceine conjugated secondary antibodies				
Mouse- Alexa 488	Goat	Molecular Probes	-	1:100
Rabbit- Alexa 488	Goat	Molecular Probes	-	1:100

[a]carried out in Dr J. Roskams' laboratory , University of British Columbia.

2.6 Immunocytochemistry

2.6.1 Coating slides

4-chamber slides and 12mm round glass coverslips were coated with the E-C-L cell attachment matrix (entactin-collagen IV-laminin) (Upstate biotechnology) at 7.5μg/cm^2 and 5μg/cm^2, respectively, and incubated at 33°C for 1 hour. The slides were then rinsed twice with 1x PBS.

2.6.2 Plating on slides

OP27 cells were plated onto E-C-L coated 4-chamber slides at 1.5x10^4/ml and expanded at 33°C. Cells were then differentiated at 39°C in the serum-free medium with FGF-2 for the indicated time periods; washed with PBS; fixed with 4% PFA for 10 minutes at room temperature; washed 3x5 min in PBS and stored at 4°C in 0.1% sodium azide in PBS until ready for use. Cells were permeabilised with 0.1% Triton X-100 in PBS for 30 min and blocked in 4% normal serum in PBS for 15 min at room temperature. Subsequently, cells were incubated overnight at 4°C with primary antibodies (Table 2.2) in 2% normal serum in PBS. Negative controls were incubated with 2% normal serum in PBS only. After washing with PBS twice for 5 min, the cells were incubated for 1hr at room temperature in the dark with the appropriate fluorescently conjugated secondary antibodies (Table 2.2) diluted 1:100 in 2% normal serum. The slides were washed 2x 5min with PBS and DAPI (Sigma) was used to visualise nuclei at a 1:15000 dilution of the 5mg/ml stock. The slides were then coverslipped using Vectashield mounting medium and images captured. Illustrations were assembled and processed digitally using the Adobe® Photoshop® 5.0 software (Adobe Systems).

2.7 Olfactory Receptor RT-PCR conditions and identification of receptors

The PCR was performed in a 20μl reaction volume on a GeneAmp® PCR System 9700 thermocycler (PE Biosystems) using 2.5μl of first-strand cDNA template (~625ng total RNA), 0.4U Super-Therm polymerase, 1x reaction buffer, 2mM $MgCl_2$, 0.2mM each dNTP, and 2μM each ORF3 and OR-C primers (Table 2.1). The cycling conditions for olfactory receptor (OR) PCR were as follows: 2 cycles of denaturation at 94°C for 4 min, annealing at 50°C for 2 min and extension at 72°C for 3 min and 28 cycles of denaturation at 94°C for 1 min, annealing at 60°C for 2 min and extension at 72°C for 3 min.

The PCR was concluded with a 10 min extension at 72°C. The RT-PCR product was gel-purified using the GeneClean II kit (BioRad) and sub-cloned into the pGEM®-T Easy vector system. Recombinant plasmids were identified by EcoRI digestion of miniprep DNA and sequence identity of clones was determined by automated sequence analysis. Characterization of receptor clones was achieved by PCR with SP6 and T7 primers followed by restriction enzyme digest analysis.

2.8 SEMI-QUANTITATIVE RT-PCR

Total RNA from FGF-2 induced OP27 cells was isolated using TRI REAGENT™ (Molecular Centre) and treated with DNase I to remove contaminating genomic DNA. Five µg of DNaseI-treated RNA was heat-denatured at 65°C for 5 min and then reverse transcribed in a 20 µl reaction volume consisting of 1X M-MLV reaction buffer, 1mM of each dNTP, 0.1mg/ml BSA, 0.25µg oligo$(dT)_{15}$ primer, 0.25µg random hexamers, 20U recombinant RNasin ribonuclease inhibitor, and 200U M-MLV reverse transcriptase, RNase H Minus (Promega Corp.). The reaction was carried out at room temperature for 10 min, at 37°C for 90 min, and finally at 75°C for 10 min. A negative control reverse transcription reaction for each sample was also performed in the absence of reverse transcriptase. Semi-quantitative RT-PCR was carried out using 1µl of each RT reaction or negative control (equivalent of 0.25µg total RNA) with primers for target cDNA and β-actin in the same reaction tube. The PCR reaction contained 1x NH_4 buffer [16mM $(NH_4)_2SO_4$, 67mM Tris-HCl (pH 8.8), 0.1% Tween-20], 0.2mM each of dNTP, 2µM each forward and reverse primer of the target cDNA, 0.05 µM each β-actin primer (Table 2.3), 2mM $MgCl_2$ (1.5mM $MgCl_2$ for Notch-1 amplification), either 5% DMSO (for *Hes-1*, *Ngn-1*, *Gap-43*, *NeuroD*) or 5% formamide (for *BF-1*) and 0.5U BIOTAQ™ DNA polymerase (BIOLINE) in a 25µl reaction volume. The annealing temperature for each transcript is shown in Table 2.3. The number of cycles for PCR was within the linear range of amplification (26 cycles). Following PCR, halve of the reaction mixture was analysed on 2% agarose gels and visualized by ethidium bromide staining. Images of stained gels were captured using the GeneSnap software (Sygene) and saved as TIFF files. Band intensities were analysed with the QuantityOne® software (BioRad) by placing rectangular objects over each band and quantitated. Expression levels were expressed relative to β-actin levels.

Table 2.3 Primers used for RT-PCR and semi-quantitative RT-PCR

Gene Name	Primers	Sequence (5'-3')	Sizes Expected (bp) cDNA size	Genomic	T_a (°C)[d]	Reference[a]
19G6	19G6F 19G6R	AAAGGAACCGGCCTATGAGCAAG ATCGCTCGACACAGCACCTTTTC	202	202	60	This study
20A4	20A4F 20A4R	CGCCTCAGGTGTTTGAAC CATGACTTGGATCCTCAATG	1139	>5000	55	This study
20A6	20A6F 20A6R	TCAAACCGATCTCTCGTCGAT GGAAGCCTCTTTGCAGATGC	207	596	60	This study
20G2	20G2s	CTGGTGGGGTTGCTAAGGGAGAGAAGTG GGACACAGCCCCTTCACATGTGCAAAG	219	219	60	This study
20G3	EST3p1 EST3p2	CAGGTGTCCACACGACGATGTCTC CCTAACTGCCGCCCTTGGTTTCTC	580	?	60	This study
β-actin[e]	MAC302 MAC480 MAC666	CATTGTTACCAACTGGGACGACA AGCCATGTACGTAGCCATCCAG GCTCGGTCAGGATCTTCATGAGG	360 186	360 186	55 or 60 55 or 60	Illing *et al.*, 2002
BF-1	F510 R1474	ACGAGGATCCGGGCAAGGGC TACGAATTCGGTGGAGAAGGAGTGG	350	350	59	Illing *et al.*, 2002
Delta-1	Delta1-5' Delta1-3'	TGTGACGAGCACTACTACGGAGAAG AGTAGTTCAGGTCTTGGTTGCAGAA	315	2739	55	Faux *et al.*, 2001
GAP43	F747 R1219	GACGCTGTAGACGAAGCC GACTCCTCAGAACGGAAC	473	473	55	Tloti and Illing[c]
Hes1	Hes1-A Hes1-B	TGGAGCTGGTGCTGATAACAG ATTCTTGCCCTTCGCCTCTTC	365	498	60	This study
Hes5	Hes5A Hes5B	CCGCTCCGCTCCGCTCGCTAA GCTGGGGGCCGCTGGAAGTGG	449	592	60	b
Mash-1	Mash1A Mash1B	CTCTTAGCCCAGAGGAAC GGTGAAGGACACTTGCAC	454	825	60	b
NeuroD	NeuroDA NeuroDB	TTAAGGCGCATGAAGGCCAAC TGAGGGGTCCGTCAAAGGAAG	499	499	60	This study
Neurogenin1	Ngn1A Ngn1B	TCCAGCAGCAACAGCAGCA TTCCTGCTCTTCGTCCTGGG	175	175	60	b
Neurogenin2	Ngn2A Ngn2A	GGACATTCCCGGACACACAC AGATGTAATTGTGGGCGAAG	545	813	60	b
Notch-1	5' primer 3' primer	TTACAGCCACCATCACAGCCACACC ATGCCCTCGGACCAATCAGA	360	360	60	Faux *et al.*, 2001
Olf-1	OLF-S2 OLF-AS3	TGTCCACAATAACTCCAAGCACGG CAGAACTGCTTGGACTTGTACGAC	306	306	60	Illing *et al.*, 2002
OTX2	Otx2f Otx2r	CTCTAGTACCTCAGTCCC GTCCAGGAAGCTGGTGAT	242	242		Calof *et al.*, 1996
PP2 B56γ isoform	B56GF B56GR	CCGTGGCCCTTCTCCACATTCG GCTCCCGTGGGATTGGAGGAAG	288	>30000	60	This study

[a]The source of the nucleotide sequences of the primers used in this thesis

[b]Dr Francois Guillemot kindly provided the nucleotide sequences of these primers.

[c]unpublished

[d]annealing temperature

[e]the MAC302 and MAC666 primers amplify a 360 bp fragment, whereas MAC480 and MAC666 amplify a 180 bp PCR product

2.9 mRNA DIFFERENTIAL DISPLAY

2.9.1 DNase treatment

Total RNA was extracted from the cells after 0, 6, 24 and 48 hours in FGF-2 at 39°C using the TriReagent method. The RNA samples were then DNaseI treated using the MessageClean™ kit according to the manufacturer's recommendations (GenHunter Corp.). Briefly, 10-50 µg of RNA was treated with 10 U of RNase-free DNaseI at 37°C for 30 min, followed by extraction with phenol-chloroform (3:1). The RNA was precipitated with 0.3 M sodium acetate and 2.5 volumes of ethanol at minus 70°C for at least 1 h, followed by centrifugation for 10 min at 4°C. The pellet was resuspened in DEPC-treated H_2O, quantified by absorbance at 260nm and analysed in a 1% formaldehyde agarose gel to check integrity of samples.

2.9.2 First-strand cDNA synthesis and PCR

Differential-display PCR was performed with the RNAimage Kit 3 following the manufacturer's instructions (GenHunter Corp). Briefly, 1µg of DNaseI treated RNA from each time point was reverse transcribed with the one base anchored 3' oligodT primers H-T_{11}A, H-T_{11}C and H-T_{11}G (H=AAGCTT, HindIII restriction endunuclease site Table 2.4). The resulting cDNAs were amplified in duplicate with these anchored primers and arbitrary primer set H-AP17 to H-AP24 (Table 2.4) in the presence of AB*TaqPlus* DNA polymerase (Southern Cross Biotech) and [α-^{33}P]dATP. Samples were then electrophoresed on 6% denaturing polyacrylamide gel and exposed to Hyperfilm β-max X-Ray films (Amersham) overnight.

Table 2.4: RNAimage 3 kit Differential Display Primers

Primer	Sequence 5'-3'
One-base anchored oligo(dT) primers	
H-T_{11}A	AAGCTTTTTTTTTTTA
H-T_{11}C	AAGCTTTTTTTTTTC
H-T_{11}G	AAGCTTTTTTTTTTG
Arbitrary primers	
H-AP17	AAGCTTACCAGGT
H-AP18	AAGCTTAGAGGCA
H-AP19	AAGCTTATCGCTC
H-AP20	AAGCTTGTTGTGC
H-AP21	AAGCTTTCTCTGG
H-AP22	AAGCTTTTGATCC
H-AP23	AAGCTTGGCTATG
H-AP24	AAGCTTCACTAGC

2.9.3 PCR reamplification

PCR amplification products exhibiting differences in treated, compared to non-treated OP27 cells, were excised and eluted by boiling in 100µl H_2O for 10min. Following ethanol precipitation, the cDNAs were reamplified by PCR using the appropriate primer combinations and PCR conditions similar to the differential display procedure, except that the final dNTP concentration was at 20µM, and no isotopic label was used. PCR products were analysed on a 1-2% agarose gel.

2.9.4 Reverse northern slot-blot

Reverse northern slot-blot was performed combining the protocols described by Zhang *et al.* (1996) and Jung *et al.* (2000) with modifications. The candidate differentially expressed cDNAs were re-amplified in a 50µl volume using the same conditions described in 2.9.3, PCR products analysed, gel-extracted using the GENECLEAN II gel extraction kit. PCR products of house-keeping genes, β-actin, glyceraldehyde-3-phosphate dehydrogenase (GAPDH) and 21C2 (excised and purified from the DD

screen) were also generated. For blotting, 30µl of each PCR re-amplified cDNA was mixed with 10µl of 2M, denatured by incubating at 100°C for 10min and neutralized with 10µl of 3M sodium acetate, pH 5.0. Finally, the samples were made up to 110µl with dH_2O and kept on ice. Fifty µl of each sample was blotted onto duplicate Hybond N^+ membranes using a 48 well slot-blot manifold (HoeferCo). The membranes were UV cross-linked and rinsed in 6xSSC before hybridization. The cDNA probes were prepared from 5µg of each of the two RNA samples (control vs cells that were treated with FGF-2 for 6hrs) by reverse transcription in a 50µl reaction that consisted of 1x M-MLV RT buffer, 30µM dNTP (without dCTP), and 0.5µg oligodT. After 5min incubation at 65°C, the samples were shifted to room temperature for 10 min, 50µCi of [α-^{32}P]dCTP (3000Ci/mM) and 500U M-MLV reverse transcriptase (Promega) were added followed by incubation at 37°C for 1hr. After reverse transcription, spin columns were used to remove the unincorporated label. Ten million cpm of each of the cDNA probes from the control and treated cells were heat denatured and used to probe the duplicate blots in 10ml of hybridization buffer containing 0.1% SDS; 50% formamide; 5x SSC; 50 mM $NaPO_4$; pH 6.8; 0.1% Sodium Pyrophosphate; 5x Denhardt's Solution and 50 µg/ml sheared Herring Sperm DNA at 42°C overnight. Filters were washed twice in 2x SSC, 0.1% SDS at room temperature for 30 min.; twice in 1x SSC, 0.1% SDS for 30 min. at room temperature; once in 0.2x SSC, 0.1% SDS for 30 min. at 55°C, and finally in 0.1x SSC, 0.1% SDS for 30 min. at 55°C until the background was low when detected using the Geiger counter. The filters were exposed to the phosphoscreen for up to 2 days. The phosphoscreen was scanned on a Molecular Imager FX system and hybridisation signals were quantitated using QuantityOne® software (BioRad, Hercules, CA). Band intensities were analysed by placing rectangular objects over each band and quantitated. The background intensity around each spot in each blot was subtracted from the signal intensity of each spot. No intensity was determined in cases where there was no visible signal in the blot. The intensities of the DD cDNAs in each blot were normalized to those of the house-keeping genes using 2 approaches. The first approach was adapted from Dilks *et al.* (2003). In this method, the intensities of the house-keeping genes were determined in both blots and the intensity of each house-keeping gene in blot 1 was then divided by its counterpart in blot 2. The ratios for GAPDH and 21C2 were then averaged and applied as a scaling factor to the intensities of the clones in blot 2. Finally, the intensities of the clones in blot 2 were divided by those in blot 1 and expressed as a fold-change difference in expression compared with the control experiment in blot 1. In the second approach the signals for the DD clones in each blot were

divided by the signals for GAPDH and 21C2 in each blot. Because both approaches produced similar results, only the results generate by the first method are presented in the thesis.

2.9.5 Northern- blot analysis

Twenty µg total RNA along with 5µg RNA molecular weight markers were size fractionated overnight on a denaturing gel containing 1% agarose, 20mM MOPS, 5mM sodium acetate, 6% formaldehyde and 1mM EDTA, transferred to a Hybond N+ membrane by capillary blotting and immobilised by UV crosslinking. cDNA fragments for the candidate differentially expressed were labelled with the MegaPrime DNA labelling kit using [α-^{32}P]dCTP (Amersham Pharmacia Biotech). Unincorporated dNTPs were removed with spin column chromatography. The probes were hybridized at 42°C overnight in a buffer containing 0.1% SDS; 50% formamide; 5x SSC; 50 mM $NaPO_4$; pH 6.8; 0.1% Sodium Pyrophosphate; 5x Denhardt's Solution and 50 µg/ml sheared Herring Sperm DNA. Blots were washed twice in 2x SSC; 0.1%SDS for 30 min at room temperature, once in 1x SSC; 0.1% SDS for 30 min at room temperature and once in 0.2x SSC; 0.1% SDS for 45 min at 55°C. The results were visualised by autoradiography on Hyperfilm MP X-ray films (Amersham Pharmacia Biotech).

2.9.6 Verification of differential expression by semi-quantitative RT-PCR

cDNA fragments were cloned using the pGEM-T Easy cloning system following the manufacturer's instructions. The plasmids containing the cloned inserts were sequenced in both 5' and 3' directions using a Molecular Dynamics Mega BACE 500 fluorescent sequencing facility available at the Department of Molecular and Cell Biology, University of Cape Town, South Africa. Gene-specific primers were then designed (Table 2.3) and semi-quantitative RT-PCR used to confirm diffferential gene expression as mentioned in section 2.8.

2.10 Rapid Amplification of cDNA Ends (RACE)

To determine the 5'- and 3'- ends of the cDNAs identified in the differential display screen, 5' and 3' RACE was performed by using the SMART RACE cDNA amplification kit (ClonTech). Briefly, the synthesis of 5'- RACE –Ready cDNA was performed in a final volume of 10µl containing 1µg of

heat-denatured (70°C for 2min) total RNA from OP27 cells treated with FGF-2 for 48hrs, 1μM 5'-RACE cDNA synthesis primer (5'-CDS), 1μM SMART II oligonucleotide, 1x first-strand buffer [50mM Tris-HCl (pH8.3), 75Mm KCl, 6mM $MgCl_2$], 2mM DTT, 1mM dNTP and 200U SuperScript II M-MLV RNaseH$^-$ reverse transcriptase (Gibco-BRL). The mixture was incubated at 42°C for 90 min, followed by dilution of the first-strand reaction with 100μl of Tricine-EDTA buffer [10mM Tricine-KOH (pH8.5), 1mM EDTA] and incubating at 72°C for 7 min. The 3'- RACE –Ready cDNA was synthesised using the same procedure except that the 5'-CDS and SMART II oligonucleotides were replaced with 1μM 3'- CDS primer. The PCR included 2.5μl of 5'- or 3'- RACE –Ready cDNA, 1x universal primer mix (UPM), 0.2μM gene specific primer, 1x Advantage 2 PCR buffer [(40mM Tricine-KOH, pH 8.7; 15mM KOAc; 3.5mM $Mg(OAc)_2$; 3.75μg/ml BSA; 0.005% Tween-20; 0.005% Nonidet-P40)], 0.2mM dNTPs and 1x Advantage 2 Polymerase mix in a total volume of 50μl. The sequences of the kit primers and all gene-specific primers are shown in Table 2.4. The PCRs were performed in a GeneAmp PCR System 9700 (Perkin- Elmer) using cycling parameters recommended by the kit manufacturers. Ten to 20μl of PCR reaction were analysed on 1.2% agarose and transferred overnight onto Hybond N^+ membrane for Southern blot analysis using an internal oligonucleotide as a probe to confirm identity of RACE product. The positive RACE products were purified by using the GENECLEAN II gel extraction kit (BIO 101 Inc.) and ligated into the pGem-T Easy system (Promega Corporation). The sequences of both strands were determined by cycle sequencing.

2.11 I.M.A.G.E. cDNA clones

The I.M.A.G.E. cDNA clones matching the cDNAs isolated in the differential display screen were purchased from Research Genetics as bacterial stocks grown in LB with 8% glycerol and 50μg/ml ampicillin. Individual clones were isolated by streaking out the stocks on LB agar plates containing 100μg/ml ampicillin. Plasmids were prepared from the glycerol stocks and analyzed by sequencing and bioinformatics.

Table 2.5: Oligonucleotides used for RT-PCR and SMART RACE PCR reactions

Oligonucleotide	*Sequence 5'-3'*
5'-CDS	5'-$(T)_{25}N_{-1}N$-3' (N_{-1}= A, C, or G; N= A, C, G, or T)
SMART II	AAGCAGTGGTAACAACGCAGAGTACGCGGG
3'-CDS	AAGCAGTGGTAACAACGCAGAGTAC$(T)_{30}N_{-1}N$-3'
Universal Primer Mix (UPM)	Long:CTAATACGACTCACTATAGGGCAAGCAGTGGTAACAACGCAGAGT Short:CTAATACGACTCACTATAGGGC
Gene specific primers	
20G2s	CTGGTGGGGTTGCTAAGGGAGAGAAGTG
20G2as	GGACACAGCCCCTTCACATGTGCAAAG
3.9s	GAGGCATTCAGGCAGCGAGAGC
3.9as	GGCCGACCTTCAAACTAGAACC
23Gpr1	CGTCACAGTCTCCTTCAACCATGGC
23Gpr2	TGGTAGGGAGTGTGTAGGTGCC
23Gf433	GAGTCCACGGCTAACATGGCTA

2.12 Bioinformatics

Searches for homologies or identities of cDNAs were performed using the BLAST algorithm (Altschul *et al.*, 1990) against the nucleotide and protein databases and also to expressed sequence tags databases (dbEST) at the NCBI (http://www.ncbi.nlm.nih.gov). Various web-based bioinformatics tools were used to analyze the sequences. These are described in Table 2.6.

Table 2.6 Bioinformatic Tools used in the analysis of the genes identified in the DD screen

Analysis	Tool	URL	Reference
Secondary structure prediction	MFOLD	http://www.bioinfo.rpi.edu/applications/mfold/old/rna/	Zuker, 2003
Sorting signals and subcellular localization	PSORTII	http://psort.nibb.ac.jp/form.html	Nakai and Horton, 1999
Identification of functional motifs	PROSITE	http://www.expasy.ch/prosite/	Hofmann *et al.*, 1999
Identification of domains	SMART	http://smart.embl-heidelberg.de/	Ponting *et al.*, 1999.
Identification of signal peptide and cleavage site	SignalP v1.1	http://www.cbs.dtu.dk/services/ SignalP	Nielsen *et al.*, 1997
Prediction of subcellular localization	TargetP v1.01	http:// www.cbs.dtu.dk/services/ TargetP	Emanuelsson *et al.*, 2000.
Analysis of mitochondrial target sequence	Predotar v 0.5	http://www.inra.fr/predotar	
Phylogenetic analysis	ClustalW	http://www.ebi.ac.uk/clustalw/	Higgins *et al.*, 1994.
Analysis of chromosomal localization of genes	MapViewer	http://www.ncbi.nlm.nih.gov/mapview	

Chapter 3

Effects of FGF-2 on the immortalized olfactory placodal cell line OP27

3.1 Introduction

The OE provides a useful model to identify molecular factors that regulate neurogenesis. There is increasing evidence indicating that cell numbers at each stage of the ORN lineage are regulated by extrinsic factors. A number of these signalling molecules have been reported to regulate olfactory neurogenesis, including FGFs, retinoic acid, epidermal growth factor (EGF), transforming growth factor (TGF-β) and leukemia inhibitory factor (LIF) (Calof *et al.*, 1991; Mahanthappa and Schwarting, 1993; DeHamer *et al.*, 1994; Satoh and Yoshida, 1997; Mackay-Sim and Chuah 2000; Illing *et al.*, 2002).

As shown in Chapter 1, FGF-2 has many roles in neuronal development, including effects on proliferation of progenitor cells, differentiation, migration and survival. There is increasing evidence that FGF-2 may play similar roles in OE neurogenesis. This has come from work done *in vitro* using explant cultures, and expression patterns of both FGF-2 and its receptors.

3.1.1 Expression of FGF-2 and its receptors in the OE

Although there is little consensus as to the type of cells that express FGF-2 or its subcellular localization, its expression in the OE has been shown by various laboratories. In one study using adult mice, the FGF-2 protein was detected in nuclei of the sustentacular cells and some apically located neurons (Goldstein *et al.*, 1997). In another study, high immunoreactivity was detected in the cytoplasm of sustentacular cells with lower levels in neurons and basal cells while the mRNA levels were high in the basal and neuronal layers with low levels detected in the sustentacular cells (Hsu *et al.*, 2001). In neonate mice there was extensive immuno-labelling throughout all layers of the OE (Chuah and Teague, 1999). There have been no studies of FGF-2 expression in the OE during embryonic development.

Knowing which FGF receptors are expressed in the OE can provide clues about the role of FGF in olfactory neurogenesis. From published reports, FGFR-1 and FGFR-2 seem to be the only FGF receptors that are present in the OE (reviewed by Mackay-Sim and Chuah 2000). Using RT-PCR, mRNA transcripts of both receptors were identified in olfactory mucosal extracts of both embryonic and adult mice (DeHamer *et al.*, 1994; Hsu *et al.*, 2001). High FGFR-1 immunoreactivity was observed in both basal and neuronal layers and very little in the sustentacular cells (Nibu *et al.*, 2000; Hsu *et al.*, 2001). The expression of the FGFR-2 protein has not been reported in this tissue.

Analysis of which receptor splice variants are expressed in the OE or in any other tissue can define the FGF ligands the cells can respond to (Ornitz *et al.*, 1996, see Table 1.1). Using RT-PCR with primers specific for each FGFR- splice variant, a limited set of the variants, namely FGFR-1 IIIb, FGFR-1 IIIc and FGFR-2 IIIc were identified in the mature OE (Hsu *et al.*, 2000; Mckay-Sim and Chuah, 2000).

This would suggest that these splice variants may mediate signals initiated by the following FGF ligands: FGF-1; FGF-2; FGF-4; and FGF-9. FGF-2 has a high affinity for FGFR-1 IIIc and to a lesser extent FGFR-2 IIIc (Table 1.1). FGF-1, FGF-2, FGF-4, FGF-7 and FGF-8 have been shown to stimulate proliferation of olfactory cultures but only FGF-2 (see below) and FGF-8 have been shown to be expressed in the OE (DeHamer *et al.*, 1994; Calof *et al.*, 20002;).

Currently, there is no information available regarding differential spatial or temporal expression of the 3 identified splice variants in the OE during development (i.e. whether a particular receptor isoform is expressed at a certain stage of the ORN lineage). This can be achieved through direct *in situ* hybridization studies using the splice variants as riboprobes and should help define the role of FGF in each stage of the ORN lineage.

3.1.2 Role of FGF-2 in the development of the OE neuronal lineage

There is no universal agreement on the role of FGF-2 in olfactory neurogenesis, although the general consensus is that it is a mitogen for the OE neuronal precursors. It seems that the role of FGF-2 in OE neurogenesis is to regulate the number of cell divisions that precursor cells go through and not to determine the fates of these progenitors. In explant cultures derived from E14.5-E15.5 mouse OE, FGF-2 was found to significantly increase the proliferation of transit amplifying cells and as a result delayed their differentiation. In these cultures, FGF-2 was also found to support the proliferation of a rare stem-like cell (DeHamer *et al.*, 1994). In the absence of any growth factor, the INPs divide only once and differentiate terminally to give rise to ORNs. In the presence of FGF-2 the number of INPs that went through 2 rounds of cell division instead of one, increased before they differentiated (DeHamer *et al.*, 1994).

Similar results were observed in studies conducted by MacKay-Sim and co-workers. The number of ORNs induced by TGFβ_2 (a differentiation factor in these cultures) increased in progenitor cell cultures that had been pre-treated with FGF-2, compared to control cultures that did not receive FGF-2. In these cultures, FGF-2 stimulated proliferation of the progenitor basal cells but had no effect on both the differentiation and survival of these cells (Newman *et al.*, 2000). Additionally, treatment of the adult rat olfactory epithelium-derived NIC cell line with FGF-2, was found to suppress neuronal differentiation as evidenced by the reduction in the expression of neuronal markers. Instead, the NIC cells were maintanied in a proliferative state (Goldstein *et al.*, 1997).

However, neuronal differentiation is not precluded by the mitogenic actions of FGF-2 in olfactory cultures. Cells of a line derived from human fetal OE increased [^{3}H]-thymidine incorporation in response to FGF-2 treatment and these cells later differentiated into neuronal cells, suggesting that FGF-2 may influence initial stages of differentiation (Ensoli *et al.*, 1998). FGF-2 induced neuronal differentiation in OE explant cultures of both embryonic mouse and adult human OE with the phenotype of the bipolar cells confirmed by expression of neuronal specific markers (MacDonald *et al.*, 1996; Murrel *et al.*, 1996). Lastly, FGF-2 was found to enhance ORN regeneration and the subsequent reinnervation of the olfactory bulb following chemical lesion of the adult rat neuroepithelium (Herzog and Otto, 1999).

To establish the absolute functions of FGF-2 in the ORN lineage, analysis of mice carrying null mutations in the FGF-2 gene would be necessary. *Fgf-2* knockout mice have been generated to study its effects in the development of the cerebral cortex (Dono *et al.*, 1998; Ortega *et al.*, 1998). However, these studies do not report on changes in the OE as a result of the absence of *Fgf-2* the gene.

This chapter describes the differentiation of a novel cell line, OP27, derived from E10.5 mouse OE (Illing *et al.*, 2002) and the molecular characterization of the cell line following treatment with FGF-2.

3.2 RESULTS

3.2.1 OP27 Cells Express FGF Receptors

FGF-2-mediated activities, including proliferation, differentiation, and/or survival require binding of the growth factor to its high-affinity tyrosine kinase receptors. To determine whether the OP27 cell line expressed any of the 4 FGF receptors, I used an approach that was described by McEwen and Ornitz (1997). A pair of degenerate primers based on conserved sequences in the tyrosine kinase domain of FGFR-1-4 (Fig. 3.1) was used to simultaneously amplify all FGFR-s by RT-PCR, followed by specific restriction enzyme analysis with enzymes that recognize each FGFR to yield unique digestion fragments (Table 3.1).

Table 3.1 Predicted restriction endonuclease digest patterns for mouse FGFR RT-PCR product amplified with the degenerate primers, D0156 and D0158 (McEwen and Ornitz, 1996). The sizes of the digested fragments are in base-pairs (bp).

Enzyme	*FGFR-1*	*FGFR-2*	*FGFR-3*	*FGFR-4*
PvuII	195/146	233/108	-	-
PstI	-	-	175/166	-
EcoRI	-	-	-	125/215

RT-PCR with the degenerate primers, D0156 and D0158 (Table 1.1; Fig. 3.1A) gave the expected 341bp product in the OP6, OP27, OP47 and OP55 olfactory placode cell lines (Fig 3.1B). To distinguish between the FGFRs expressed in OP27 cells, the RT-PCR product was digested with PvuII, PstI, and EcoRI. Each of the RE digest analysis gives unique fragments. PvuII recognizes both FGFR-1 and FGFR-2 but with distinct digest patterns, while PstI and EcoRI recognize FGFR-3 and FGFR-4, respectively (Table 3.1). Only PvuII was able to completely digest the PCR product to yield the expected fragments for FGFR-1 and FGFR-2, while PstI and EcoRI did not yield any digest fragments (Fig 3.1C). This analysis therefore suggested that only FGFR-1 and FGFR-2 were expressed in the OP27 cell line. The absence of FGFR-3 and FGFR-4 expression in these cells was further confirmed by RT-PCR using gene specific primers for both primers (Fig.3.2).

3.2.2 Alternative splice forms of FGFR-1 and FGFR-2 mRNAs in the OP27 cell line

All the FGFRs with the exception of FGFR-4 are expressed in multiple variant forms arising from alternative splicing of mRNA transcripts (Johnson and Williams, 1993). The isoforms of the FGFRs generated by splicing result in distinct binding specifities and affinities for their ligands. I determined by gene-specific RT-PCR which splicing variants of FGFR-1 and FGFR-2 are expressed in the OP27 cells. All FGF receptors contain the signal peptide, 3 extracellular immunoglobulin (Ig)- like domains (I-III), a string of acidic amino acid residues (known as the acidic box) between the first two Ig domains, a hydrophobic transmembrane (TM) domain, the juxtamembrane (JM) domain between the TM and the split tyrosine kinase (TK) domain. FGFR-1 was amplified using a sense primer, F1189 recognizing the signal sequence and the antisense primer, R1190 located in the juxtamembrane (Fig 3.3A).

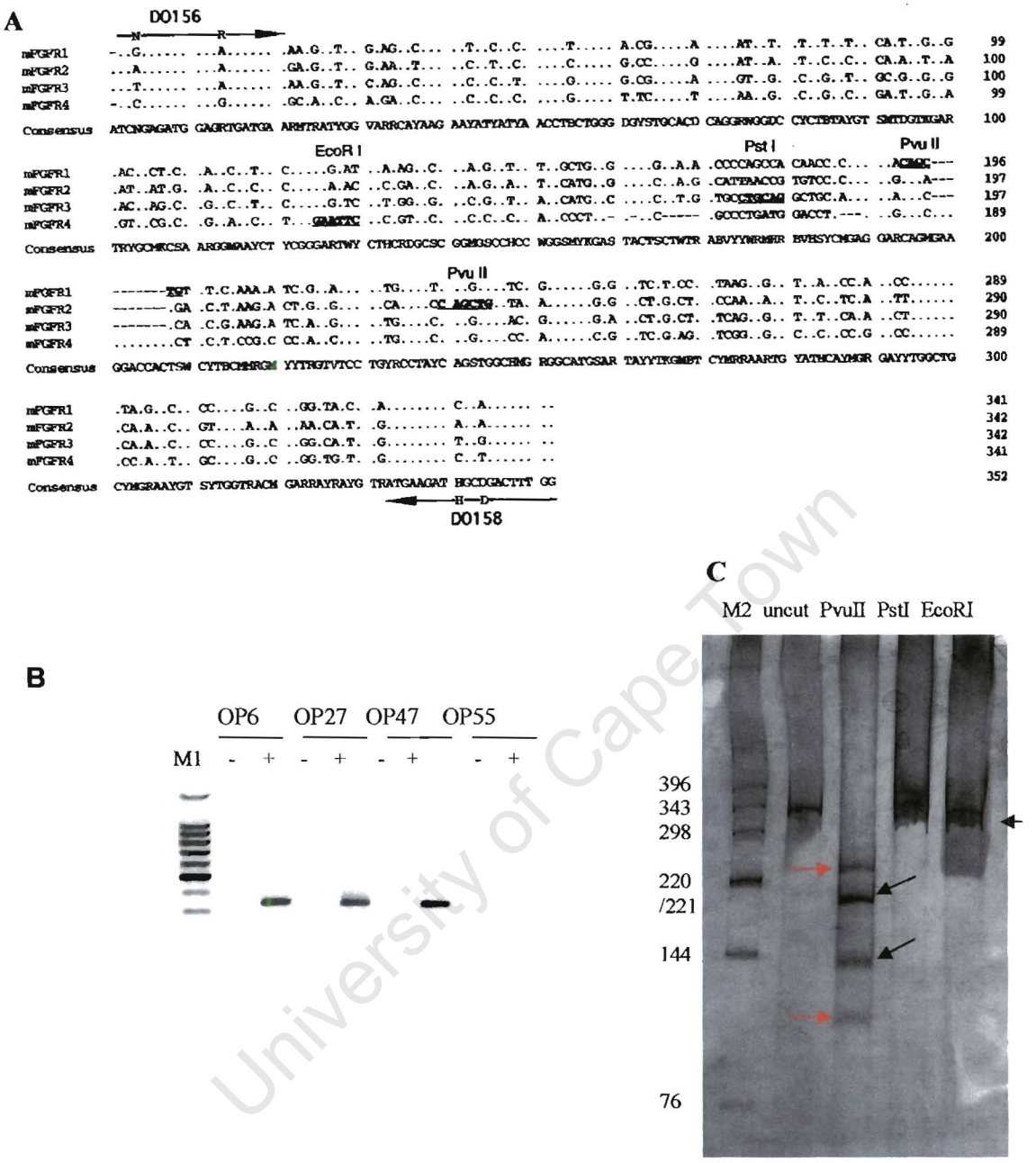

Figure 3.1 Identification of FGFR-s expressed in the OP cell lines. (A) Sequence alignment of tyrosine kinase domains of mouse FGFR-1-4, showing the conserved nucleotides (...) and restriction enzyme sites in bold and underlined. Primers D0156 and D0158 are indicated. Adapted from McEwen and Ornitz, 1996. (B) The 341bp RT-PCR product amplified in the OP cell lines. -, non reverse transcribed RNA sample; +, reverse transcribed RNA samples used as templates for RT-PCR. M1, 100bp marker (from the top 1500; 1000; 900; 800; 700; 600; 500; 400; 300; 200; 100 bp, Promega). (C) The RT-PCR product from the OP27 cell line was digested with the restriction enzymes and analysed on a non-denaturing polyacrylamide gel. The FGFR-1 specific digest patterns are indicated with black arrows, and the FGFR-2 specific digest patterns are indicated with red arrows. The undigested RT-PCR product is indicated with the black arrow-head. M2, pBR322-HpaII digest (sizes shown).

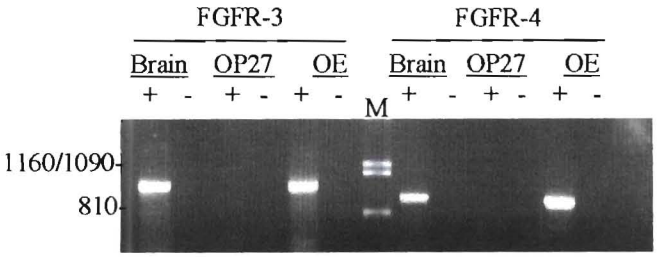

Figure 3.2 Expression of FGFR-3 and FGFR-4 in the brain, OP27 cell line, and olfactory epithelium. RT-PCR products of FGFR-3 (997 bp) and FGFR-4 (936 bp) were detected in brain and olfactory epithelium (OE). FGFR-3 and FGFR-4 were not detected in the OP27 cell line. -, non reverse transcribed RNA sample; +, reverse transcribed RNA samples used as templates for RT-PCR. M, λ DNA digested with PstI as a molecular weight marker, sizes (in bp) shown on the left.

The primers encompass at least 2 alternatively spliced regions of FGFR-1: the first Ig domain (Ig I) and the second half of IgIII which gives rise to either the IIIb or IIIc isoforms. Splicing in the Ig I domain generates isoforms known as FGFR-1α, which contains Ig I together with the other 2 Ig domains, FGFR-1β which lacks the 267 bp exon for the Ig I, or FGFR-1γ which, like the β-isoform lacks IgI but has an 144 bp insertion instead of the 267 bp exon (Fig 3.3A, Yamaguchi *et al.*, 1994). RT-PCR with the FGFR-1 oligonucleotides in the OP6, OP27, OP47 and OP55 cell lines yielded fragments of 1090 bp, 967 bp, 823 bp encoding the α, γ, and β isoforms, respectively. These RT-PCR products were subsequently confirmed as FGFR-1 transcripts by Southern blot analysis with a fluorescently labeled internal oligonucleotide, I-1191 (Fig. 3.3B). The FGFR-1β isoform is the predominant PCR product in all four cell lines, with the FGFR1-α and FGFR1-γ isoforms expressed in much less abundance. To distinguish between the IIIb and IIIc isoforms in OP27, the FGFR-1 RT-PCR product was digested with VspI and AccI restriction endonucleases which recognize the IIIb and IIIc isoforms, respectively (Fig. 3.3 C, Kalyani *et al.*, 1999). The product of the predominant 823 bp FGFR-1β RT-PCR product is clearly visible, while the less abundant FGFR-1α and FGFR-1γ isoforms are not visible by ethidium bromide staining.

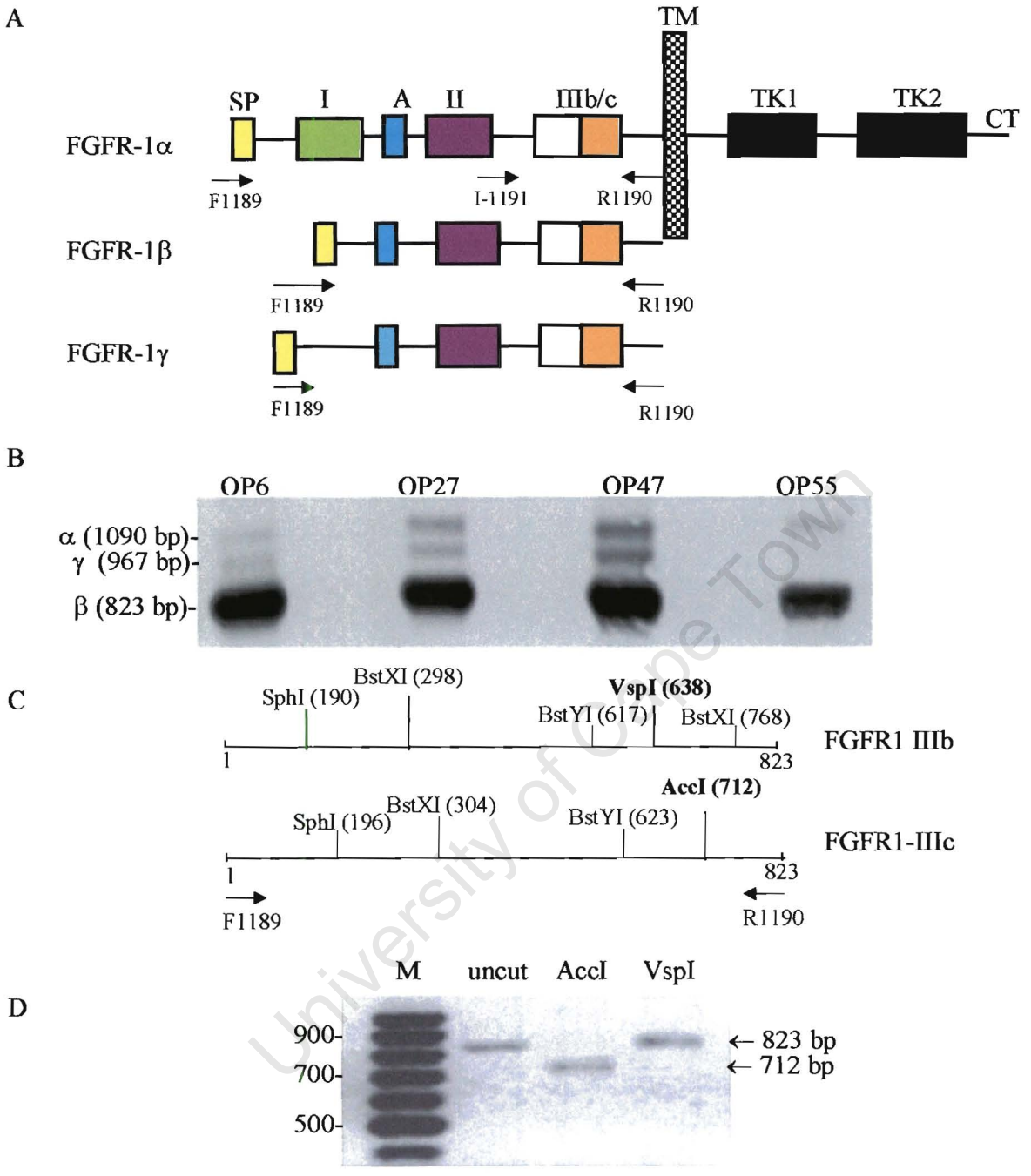

Figure 3.3 Identification of the isoforms of FGFR-1 expressed in OP27 cells. (A) General structure of FGFR-1 showing the alternatively spliced variants (presence or absence of IgI domain and alternative use of exons, IIIb or IIIc for the C-terminal end of IgIII); and the positions of RT-PCR primers as indicated by arrows. F1189 and R1190 primers are specific for the 3 variants of FGFR-1 viz. α (containing all 3 Ig domains); β (missing IgI); γ (contains a 144bp insert instead of IgI); I-1191 an internal oligonucleotide used for Southern blot analysis of FGFR-1 PCR products. SP, signal peptide; I, II, III, Ig-like domains; A, acid box; IIIb/c, either the IIIb or IIIc splice isoform; TM, transmembrane; TK1 and TK2, split tyrosine kinase domain; CT, C-terminal cytoplamic tail. (B) Southern blot analysis of FGFR-1 RT-PCR products using the internal oligonucleotide I-1191 in (A) as a probe. Three hybridising bands representing the 3 variants α, β, and γ are shown. (C) Restriction digestion of the IIIb and IIIc isoforms of FGFR1β. VspI recognizes the IIIb isoform and digests this isoform to generate two fragments of sizes 638 bp and 185 bp. AccI recognizes the IIIc isoform and gives rise to the 712 bp and 111 bp fragments. The sites for the restriction enzymes are shown in brackets. (D) The 823 bp FGFR-1β RT-PCR product digested with AccI and VspI. M; 100bp ladder (Promega), sizes in base pair shown on the left.

Digestion with AccI of the 823 bp PCR product gives rise to 712 bp and 111 bp digest fragments, thus confirming the presence of the FGFR-1 IIIc isoform (only the 712 bp fragment is visible on the gel in Fig. 3.3D). Digestion of the PCR product with VspI does not result in any fragments. The FGFR-1 RT-PCR product was subsequently cloned into the pGEM-T vector. Nucleotide sequence analysis confirmed that the IIIc variant of FGFR-1 was expressed in the OP27 cells.

For analysis of expression of FGFR-2 splice variants in OP27 cells, the PCR primers were also designed to amplify both the IIIb and IIIc isoforms. The sense primer (FR2f) was located in the region between IgII and the N-terminal end of IgIII while the antisense primer sequence (FR2r) was proximal to the tyrosine kinase domain (Fig. 3.4A). These primers were able to amplify the expected ~770 bp product (Fig 3.4C, lane 2). Digestion of the PCR product with EcoRV which recognizes the IIIc isoform of FGFR-2 isoform and not IIIb (Orr-Urtreger *et al.*, 1993) (Fig. 3.4B) resulted in complete cleavage of the FGFR-2 to give digest products of 279 bp and 498 bp (Figure 3.4C lane 3). This suggests that FGFR-2 IIIb is not present and only the FGFR-2-IIIc isoform is expressed in the OP27 cell line.

In summary, OP27 cells express a subset of the FGF receptors. FGFR-1 IIIc is expressed in OP27 cells as the 3 alternatively spliced variants, FGFR-1α, FGFR-1β and FGFR-1γ with the FGFR-1β being the predominant isoform. FGFR-2 was also detected in OP27 cells and identified as the IIIc isoform. FGFR-2 is also known to occur as a receptor with either three or two Ig domains (Bansal *et al.*, 1996). However, I was only interested in determining whether both FGFRs were expressed as either the IIIb or IIIc splice form since these determine ligand binding specificity, I did not determine whether FGFR-2 was expressed as a receptor with three or two Ig domains in OP27 cells.

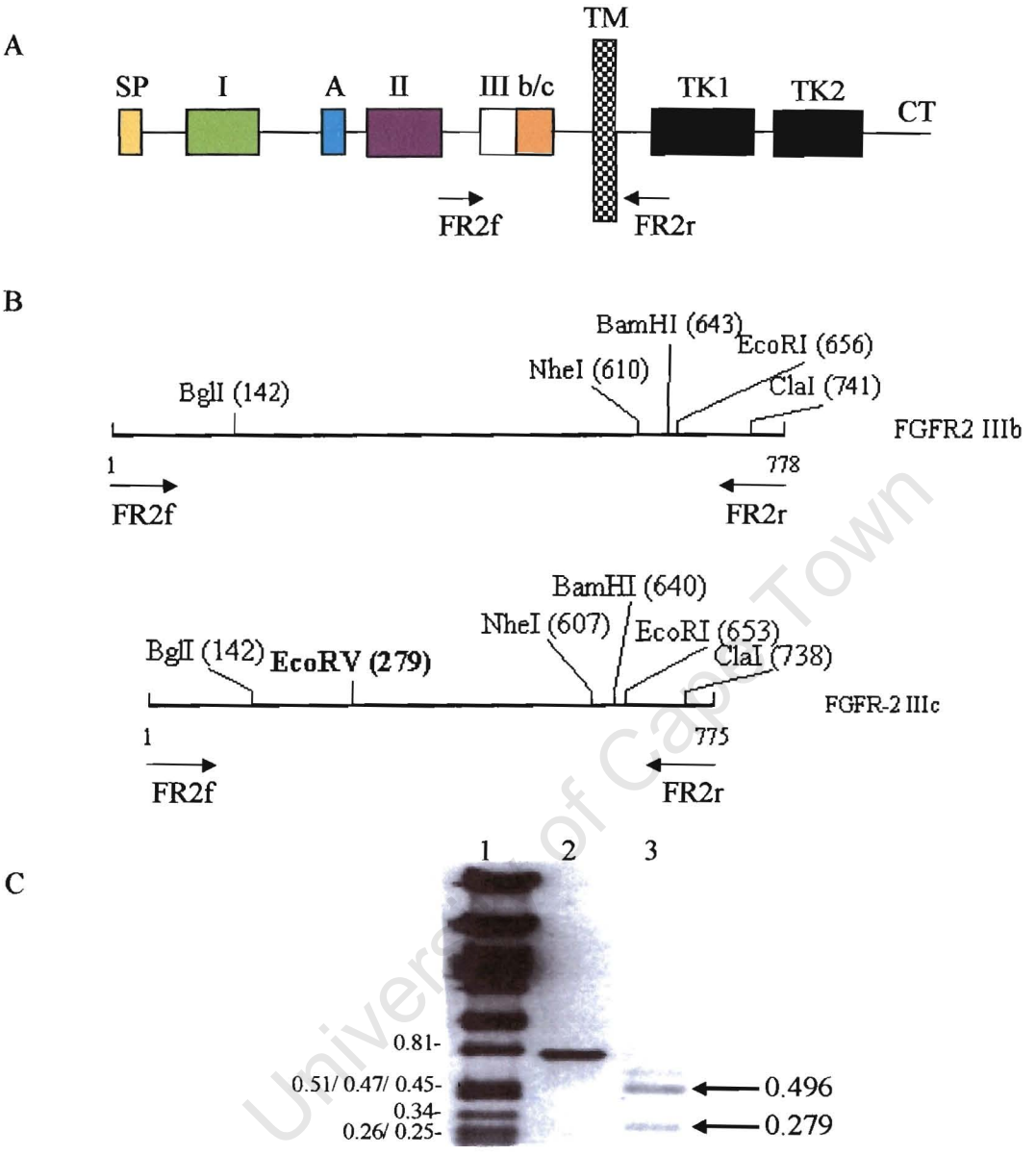

Figure 3.4 Identification of the isoforms of FGFR-2 expressed in OP27 cells. (A) General structure of FGFR-2 showing the positions of RT-PCR primers as indicated by arrows. SP, signal peptide; I, II, III, Ig-like domains; A, acid box; IIIb/c, either the IIIb or IIIc splice isoform; TM, transmembrane; TK1 and TK2, split tyrosine kinase domain; CT, C-terminal cytoplamic tail. (B) Diagrammatic representation of the restriction digest analysis of the IIIb and IIIc isoforms of FGFR2 RT-PCR product amplified with the FR2f and FR2r primers. EcoRV recognizes the IIIc isoform only resulting in digest fragments of 279 bp and 496 bp fragments. The site for each restriction enzyme in each of the FGFR-2 isoform is shown in brackets. (C) The FGFR-2 primers, FR2f and FR2r amplified the expected 775bp PCR product (lane 2) that was completely digested with EcoRV (lane 3) which is specific for the IIIc isoform of FGFR-2. The digest products of the FGFR-2 IIIc isoform are indicated by arrows in lane 3. Lane 1, lambda DNA digested with PstI, sizes (kilobase pair, Kb) indicated on the left.

Since I had established that the OP27 cells expressed FGFRs, I sought to study the effects of FGF-2 on these cells. FGF-2 has high affinity for the FGFR-1 IIIc isoform and to a lesser extent, the FGFR-2IIIc isoform (Ornitz *et al.*, 1996). Since the IgI is not essential for ligand binding, the FGFR-1α and FGFR-1β do not show any significant difference in ligand binding (Xu *et al.*, 1999).

3.2.3 FGF-2 promoted the outgrowth of bipolar cells

To study the effects of FGF-2 on the OP27 cells, the cells were cultured at 33°C in DMEM and 10% FCS until they reached 70% confluence. At time 0, the media was replaced with either N2 (control cultures) or with N2 plus 5ng/ml FGF-2 and cells were shifted to the non-permissive temperature (39°C). After 24 hours at 39°C, the control cultures had the same morphology as the cells at the permissive temperature (33°C) and no phase-bright cell bodies were visible (Fig. 3.5A and Fig 3.5C). In contrast, phase-bright cell bodies were clearly visible in OP27 cells treated with FGF-2 for 24 hours. Secondly, several cells had changed morphology at this time to take on a bipolar morphology, with neurite-like extensions emanating from either side of the cell bodies (Fig 3.5B). At this stage several cells still had the same morphology as the cells at 33°C. After 2 days the number of cells with the bipolar morphology had increased compared to the 24 hour time point and continued to be prominent until after 10 days (Fig. 3.5D-E, G-H). Meanwhile, the cell density of control cultures that were not treated with FGF-2 decreased as the cells were observed to detach from the culture dishes, round-up and float on the culture medium with very few cells still attached. This was especially evident after 4 days in culture (Fig. 3.5 F). The cell density of FGF-2 treated cultures also decreased with time but was never as severe as the control cultures.

Figure 3.5 Phase-contrast micrographs of OP27 cells cultured at 33°C and at 39°C under serum-free conditions with or without FGF-2 for 10 days. At the permissive temperature of 33°C (A), they grow as clusters of flat and irregularly shaped epithelial cells. When shifted to the non-permissive temperature of 39°C with FGF-2, the cells assume a bipolar shape, developing neurite-like processes (*arrows*), concommitant with the reduction in the size of the cytoplasm (B, D, F, G and H). Phase-bright cell bodies are evident in cells treated with FGF-2 (indicated by *). There were no morphological changes observed in cultures without FGF-2 (C and E). Instead, the cells looked unhealthy at first (C) with the nuclei not readily apparent. After 4 days without FGF-2 (E), a large proportion of the cells were rounded up, detached and found floating on the culture medium. There were very few cells still attached on the culture dishes.

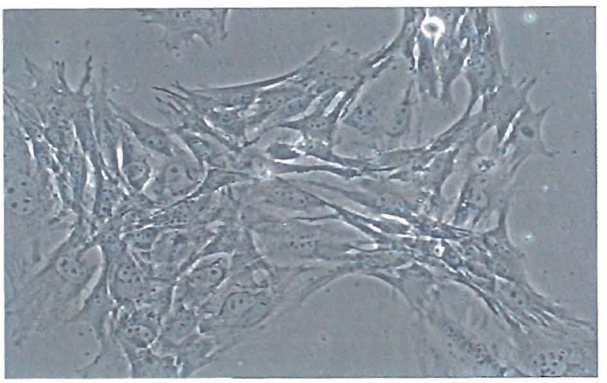

A: OP27 cells at day 0

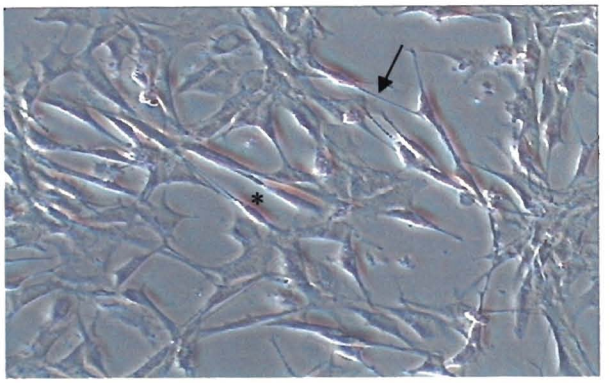

B: After 1 day at 39°C with FGF-2

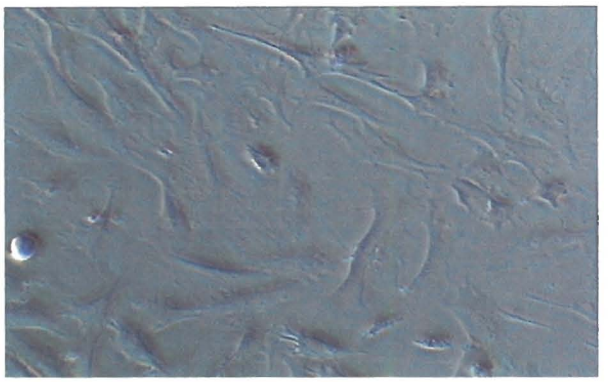

C: After 1 day at 39°C without FGF-2

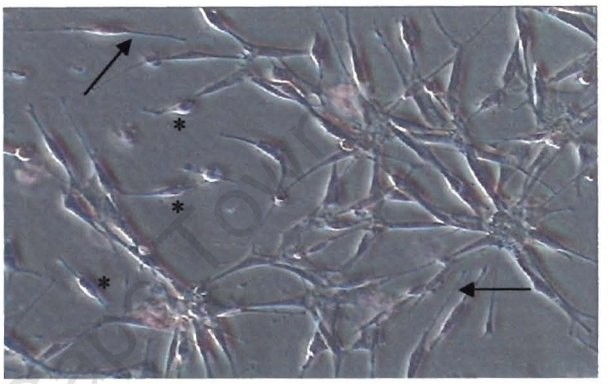

D: After 2 days at 39°C with FGF-2

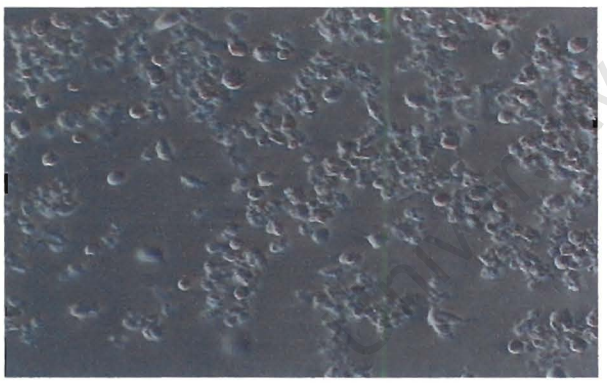

E: After 4 days at 39°C without FGF-2

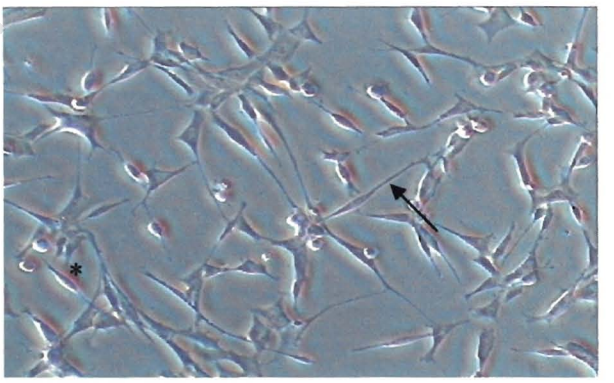

F: After 4 days at 39°C with FGF-2

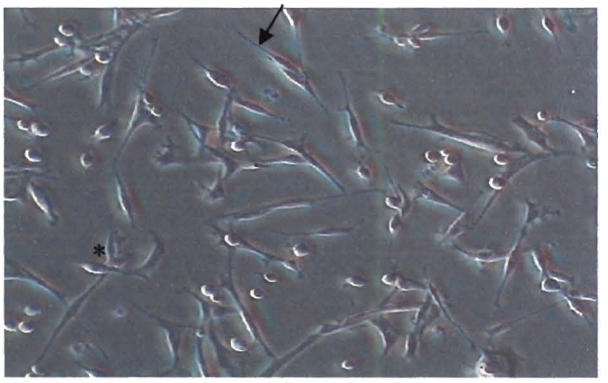

G: After 6 days at 39°C with FGF-2

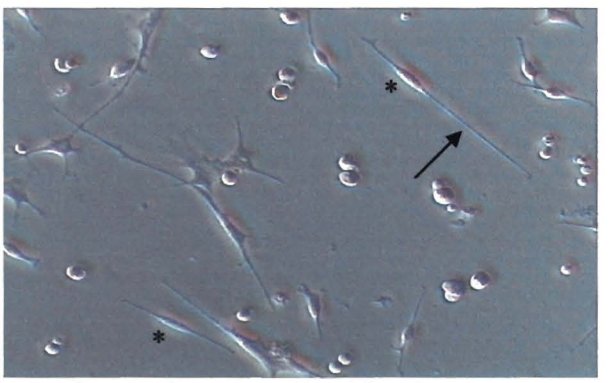

H: After 10 days at 39°C with FGF-2

3.2.4 Quantitation of bipolar cells in culture

The bipolar cells that appeared following treatment of OP27 cells with FGF-2 were quantified. The proportion of bipolar cells was determined over the time course of the FGF-2 assay. The first 2-4 days in culture was characterized by a lag phase in the appearance of bipolar cells, with the proportion of bipolar cells around 20-30% during this period. At 6 days *in vitro* (DIV) the proportion of bipolar cells had doubled that observed at 2-4 DIV and the increased proportion was maintained until 10 DIV (Fig. 3.6).

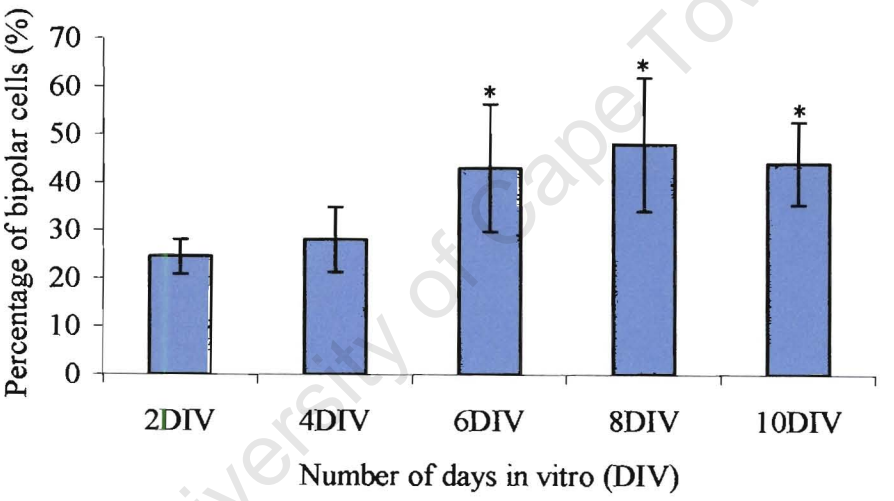

Figure 3.6 Time course of the percentage of bipolar cells in OP27 cultures treated with FGF-2. Each point represents the mean ± SEM of cell counts on each of ten randomly photographed fields (at magnification 10X) taken from 3-4 plates per time point from one representative experiment. Significance, *P<0.05, compared to 2-4 days.

3.2.5 Effect of FGF-2 on the survival of OP27 cells

The total number of viable OP27 cells in both N2 and N2 + FGF-2 was counted every 2 days beginning at 2DIV at 39°C, to quantify the effect of FGF-2 on their survival. When cultured in N2 only, the OP27 cultures showed a significant decline in number of viable cells (Fig. 3.7). After 10 days in culture, only 0.3% of the cells originally present at day 0 remained. To determine whether the decline in cell numbers in N2 began at 2 DIV, the number of cells was counted at day 0 and at day 1 following the shift to N2. At 1DIV the cell numbers had already declined, and by 2DIV approximately half the numbers at 33°C (day 0) remained (Fig. 3.7 insert). This suggests that the shift to the serum-free media and to the non-permissive temperature of 39°C compromised the survival of OP27 cells.

In contrast, the cultures had a better survival in the presence of FGF-2. Within 24 hrs following the shift to N2 + FGF-2 and to 39°C, the total number of cells was double the number present at day 0. This is in direct contrast to the cell numbers at the same period in control cultures without FGF-2 where the numbers were halved compared to day 0 (Fig. 3.7 insert). It is likely that the OP27 cells went through one round of cell division at 39°C in the presence of FGF-2, with cell numbers doubling. However, cell numbers declined steadily after 24 hrs even though they were maintained above those of control cultures (Fig. 3.7).

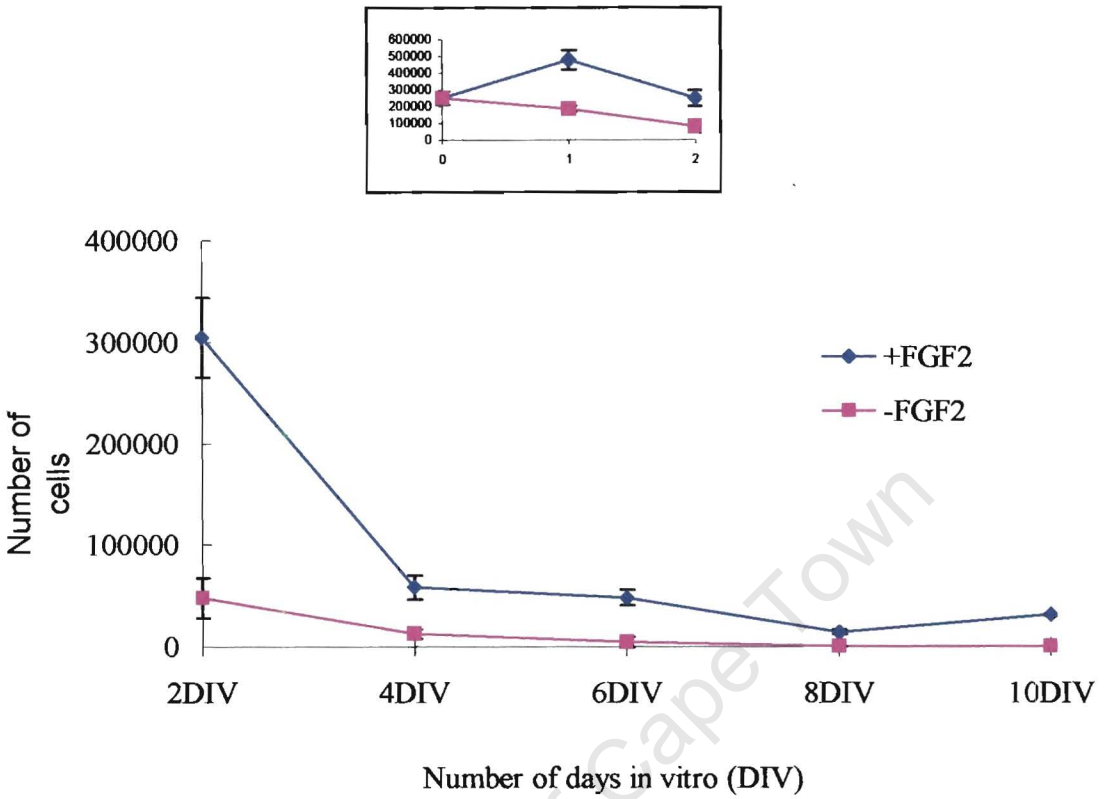

Figure 3.7 Effect of FGF-2 on OP27 cell survival at 39°C. $3x10^4$ cells were plated on six-well culture dishes and cultured with or without FGF-2 at the non-permissive temperature (39°C). After every 2 day interval the cells from a dish were harvested by by trypsinization and the number of viable cells was determined by the exclusion of the Trypan blue dye. The insert (from a separate experiment) shows the OP27 cell numbers determined at day 0 and at 1 and 2 days *in vitro*. The numbers increased for the first 24hrs at 39°C in the presence of FGF-2 and decreases thereafter. Values are the means and standard deviations of three wells for both the experiment and the control. The graph shown above is a representative of two independent experiments.

3.2.6 Effect of FGF-2 on the proliferation of OP27 cells

FGF-2 has a mitogenic role for the neuronal precursors in the OE and elsewhere in the nervous system (see section 3.1 and Chapter 1). It was therefore possible that the increased survival of OP27 cells at 39°C in the presence of FGF-2 (particularly within the first 24 hours when cell numbers were twice those at day 0) compared to control cultures without the growth factor was a result of increased proliferation mediated by FGF-2. To test this hypothesis, the effect of FGF-2 on the proliferation of OP27 cells at the non-permissive temperature was examined by [^{3}H]-thymidine incorporation.

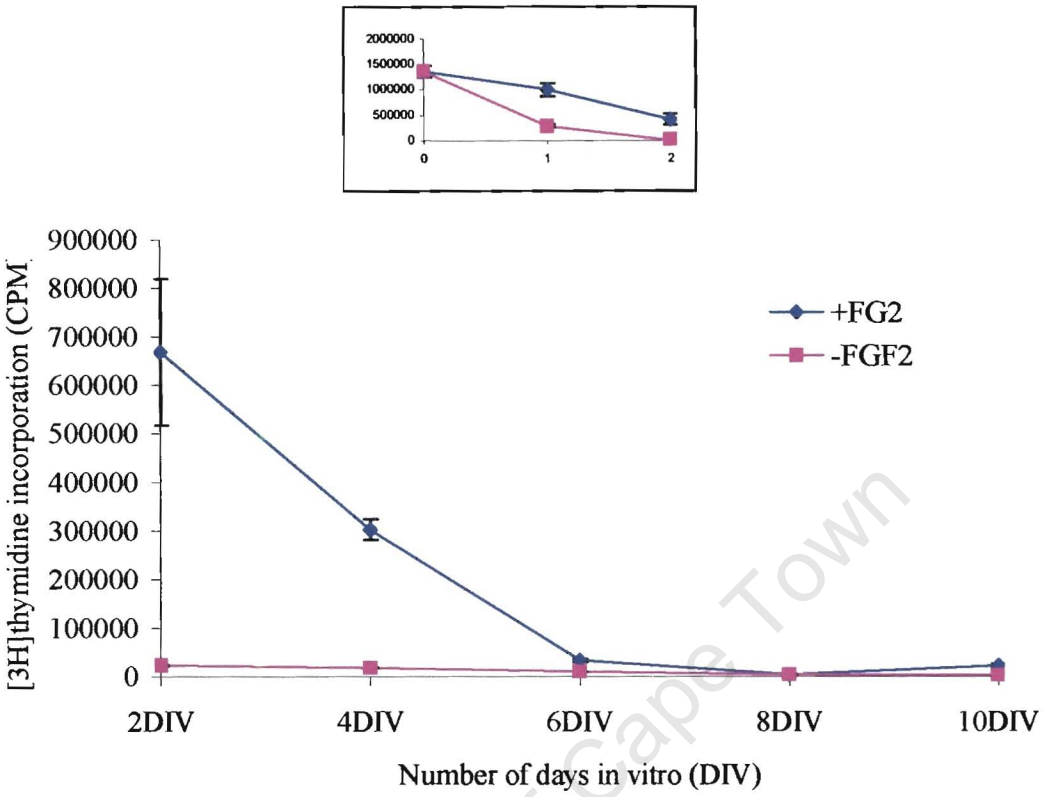

Figure 3.8 [^{3}H]-thymidine incorporation of OP27 cells in response to FGF-2. Cells were plated on six-well culture dishes and cultured with or without FGF-2 at the non-permissive temperature (39°C). Both the treated and control cells were incubated with [^{3}H]-thymidine for 24hrs prior to measuring [^{3}H]-thymidine incorporation by scintillation counting. The incorporation was determined for every second day at 39°C. The insert shows the [^{3}H]-thymidine incorporation determined for the OP27 cells at day 0 and the first 48hrs at 39°C (1 and 2 days *in vitro*). Values are the means and standard deviations of three wells for both the experiment and the control.

As shown in Fig 3.8, there was a significant reduction in the [^{3}H]-Thymidine incorporation when the OP27 cells were cultured in the absence of FGF-2 under serum-free conditions. In 24 hours [^{3}H]-thymidine incorporation had dropped to ~20% of the cells at day 0 and by 2DIV this dropped further to 0.3%. Cell cultures treated with FGF-2 showed a higher [^{3}H]-thymidine incorporation compared to control cultures. The [^{3}H]-thymidine incorporation at 1DIV was ~70% of that at day 0, compared to the 20% by the control cultures at the same time (Fig 3.8 insert). The relatively high [^{3}H]-thymidine incorporation in FGF-2 treated cultures is consistent with the doubling of the cell numbers at the same time (Fig. 3.7). However, even in the presence of FGF-2, [^{3}H]-thymidine incorporation declined from

2 to 4 days. From 6DIV onwards [^{3}H]-thymidine incorporation was low and similar to that of control cultures. This would suggest that the FGF-2 treated cells were gradually withdrawing from the cell cycle. However, since the apparent decline in [^{3}H]-thymidine incorporation beyond 4 days parallels the massive death of cells (Fig 3.7) it may not be possible to conclude rigorously that OP27 cells cultured beyond 4 days are not mitotically active. The data in Fig. 3.8 was thus normalized for the cell numbers shown in Fig. 3.7. This normalization appears in Fig. 3.9. Similarly to the data shown in Fig. 3.8, the first 2 days are characterized by a decline in [^{3}H]-thymidine incorporation in total cell numbers. However, between 2 and 4 days, there was a significant increase in [^{3}H]-thymidine incorporation which may suggest that a sub-population of OP27 cells was still mitotically active at this stage. Beyond 4 days there was a decline again thus indicating that OP27 cells at this stage were indeed not proliferating. Neuronal differentiation is preceded by exit from the cell cycle. The increase in the number of the bipolar cells at this time (Fig. 3.6) is consistent with the significant decline in the [^{3}H] thymidine incorporation.

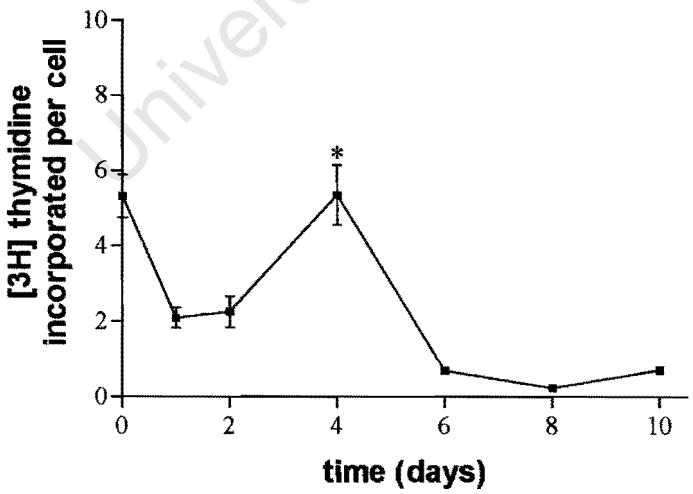

Figure 3.9 [3H] thymidine incorporation normalized for total OP27 cells. The data shown in 3.8 was normalized with that shown in Fig. 3.7. Significance, *P<0.05, compared to 1-2 days and 6-10 days.

3.2.7 Phenotypic characterization of FGF-2-induced neuronal differentiation of OP27 cells

Defined molecular markers can characterize the phenotype of the cells at the various stages of the ORN differentiation pathway. Various molecular biology techniques including RT-PCR, western blot analyses and immunocytochemistry have been used to define the phenotype of differentiated cells (Cunningham *et al.*, 1999; Murrell and Hunter, 1999; Barber *et al.*, 2000; Illing *et al.*, 2002). A selection of these markers had already been used to characterize the OP27 cell line following retinoic acid-induced differentiation (Illing *et al.*, 2002). I have used the same markers to characterise the behaviour of the OP27 cells under the influence of FGF-2, using the above-mentioned techniques.

3.2.7.1 RT-PCR characterization

RT-PCR assays were performed on total RNA isolated from the OP27 cells at different time points of differentiation using oligonucleotide primer pairs specific for growth associated protein-43 (GAP-43) and olfactory marker protein (OMP) (Tables 2.1 and 2.3). GAP-43 is a membrane associated phosphoprotein whose wide expression in the nervous system is correlated with process-outgrowth, axonal regeneration and synaptogenesis. In the olfactory epithelium GAP-43 is expressed in immature ORNs that are not terminally differentiated (Pellier *et al.*, 1994). Using a semi-quantitative RT-PCR assay, the message for GAP-43 was found to be transiently up-regulated as the OP27 cells differentiated. At the non-differentiated state and after 6 hours following FGF-2 treatment, very faint bands were detected. The mRNA levels for GAP-43 increased after 24 hours and peaked at 48 hours but the levels decreased to for the next 8 days in culture (Fig. 3.10).

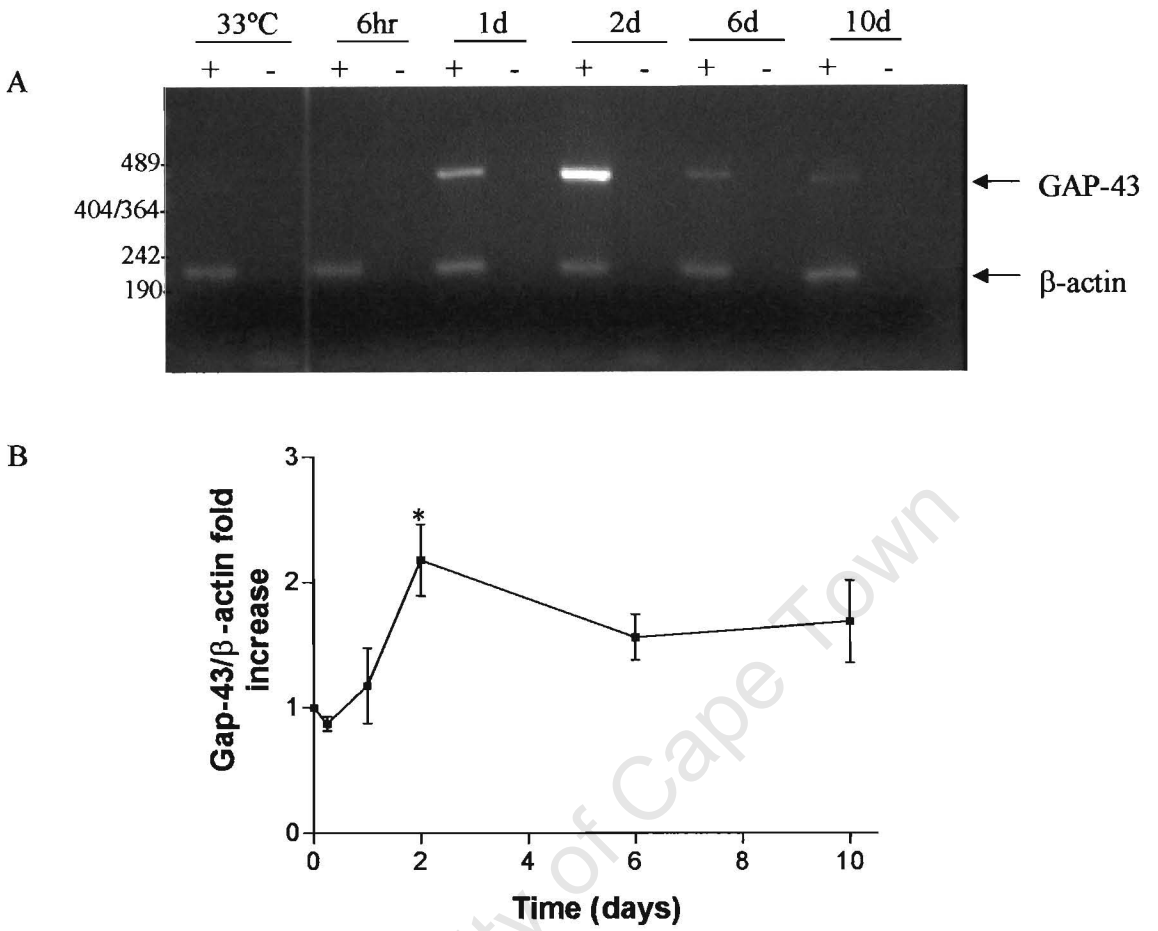

Figure 3.10 Transient up-regulation of GAP-43 mRNA expression by FGF-2 in OP27 cells. (A) A representative semiquantitative RT-PCR analysis of GAP-43 mRNA in OP27 cells treated with FGF-2 for the indicated times. Cells that had not been treated (33°C) were included as controls. GAP-43 and β-actin were amplified together in the same reaction tube. hr, hours; d, days. (+) amplification from RNA that had been reverse transcribed, (-) RNA that were not reverse transcribed as negative controls. Molecular weight sizes (in base pairs, bp) are indicated on the left. (B) GAP-43 and β-actin mRNA levels were determined by densitometric scan of the bands at each time-point. Data are expressed as fold increase in the ratio of Gap-43/β-actin with the value of the cells at 33°C (time 0 days) taken as 1 and represent mean ± SEM values of 3 independent experiments. Significance, *P<0.05, compared to 0-1 day and 6-10 days.

OMP is the classical marker for mature olfactory neurons *in vivo* (Rogers *et al.*, 1987). I determined whether the OP27 cells express any OMP transcripts as the cells differentiated. A faint transcript of 242 bp was amplified after 10 days following FGF-2 treatment but this was never reproducible from experiment to experiment (results not shown). This suggests that that even though these cells resemble differentiating cells morphologically, they do not differentiate into mature olfactory neurons in 10 days in the presence of FGF-2.

3.2.7.2 Western blot analyses

OP27 cells were induced to differentiate for 5 and 10 days *in vitro* (5DIV and 10DIV, respectively) and examined for the expression patterns of markers characteristic of differentiating olfactory neurons, using western blot analyses. Neuron specific type III β-tubulin (NST) is among the earliest characterized markers of neuronal differentiation. Its expression occurs just before or during the last division of neuronal precursors of both PNS and CNS (Roskams *et al.*, 1998). OP27 cells express high levels of NST at the non-differentiated state but expression levels decreased when the cells were induced to differentiate in the presence of retinoic acid (Illing *et al.*, 2002). When the cells are induced with FGF-2 at 39°C the NST levels were also found to decrease after 5DIV and 10DIV compared to the non-differentiated state (Fig. 3.11A).

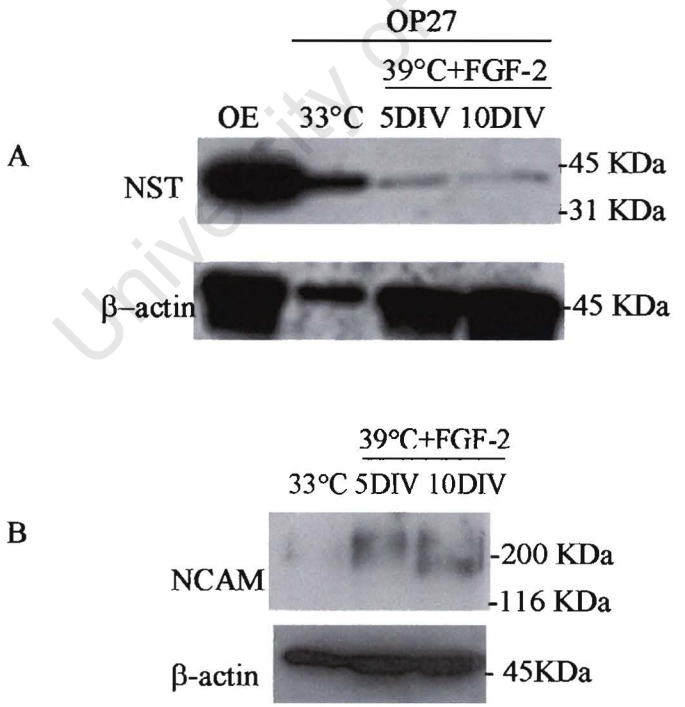

Figure 3.11 Expression patterns of β-III neuron-specific tubulin (NST) and neural cell adhesion molecule (NCAM) on OP27 cells treated with FGF-2. Immunoblot of OP27 cells was prepared using total protein lysates from cells at 33°C and cells that had been treated with FGF-2 at 39°C for 5 days *in vitro* (5DIV) and 10 days *in vitro* (10DIV). The olfactory epithelium (OE) was used as a positive control. Each blot was used for each of the olfactory neuronal developmental marker and later reprobed with β-actin to verify loading.

The neural cell adhesion molecule (NCAM) is widely expressed throughout the nervous system and has been implicated in the control of neural progenitor cell proliferation and differentiation (Amoureux *et al.*, 2000). During vertebrate development multiple splice variants of NCAM are expressed. The 3 major isoforms are the NCAM120, NCAM140, and NCAM180, based on their molecular weights. In addition, NCAM is posttranslationally modified by addition of long chains of polysialic acid residues. This polysialylation results in the abberant electrophoretic migration of smeared bands of NCAM in immunoblots (Fujimoto *et al.*, 2001; Illing *et al.*, 2002). As the neurons mature NCAM becomes less sialylated and appears as distinct bands on immunoblots (Illing *et al.*, 2002). At the non-differentiated state (33°C) the OP27 cells presented a very faint smeared band of whereas the band that was detected in the cells that were induced to differentiate for 5DIV was broad and smeared. The band at 10DIV was broader than that at 5DIV, with the molecular weight band increased. This may indicate an up-regulation in the expression of the shorter NCAM isoforms (NCAM120 and NCAM140). Alternatively, the increased smearing at 10DIV may indicate an increased polysialylation (Fig. 3.11B).

The pattern of expression of the tyrosine receptor kinases, TrkB and TrkC, was also analyzed in differentiating OP27 cells. These are the cognate receptors for the neurotrophins, brain-derived neurotrophic factor (BDNF) and neurotrophin-3 (NT-3), respectively, that have been suggested to have roles in a number of cellular processes, including development, differentiation, survival and neuronal regeneration. Both TrkB and TrkC receptors are alternatively spliced to yield isoforms containing a catalytic tyrosine kinase (TK+) and truncated isoforms (TK-) which lack the TK domain (reviewed by Carter and Roskams, 2002). It has already been shown that OP27 cells express both the TK+ and TK- isoforms of both TrkB and TrkC. As the OP27 cells differentiate in response to retinoic acid the predominant isoform of TrkB expressed becomes the ~90KDa kinase inactive truncated form (Illing *et al.*, 2002). As shown in Fig. 3.12A one immunoreactive protein band that migrated at ~90KDa was

detected in OP27 cells at 33°C with the anti-TrkB antibody. A 140KDa band representing the full-length receptor was not detected in the OP27 cells. Secondly, the ~90KDa band was lost in OP27 cells as they differentiate with levels barely detectable after 5DIV and 10DIV (Fig. 3.12A).

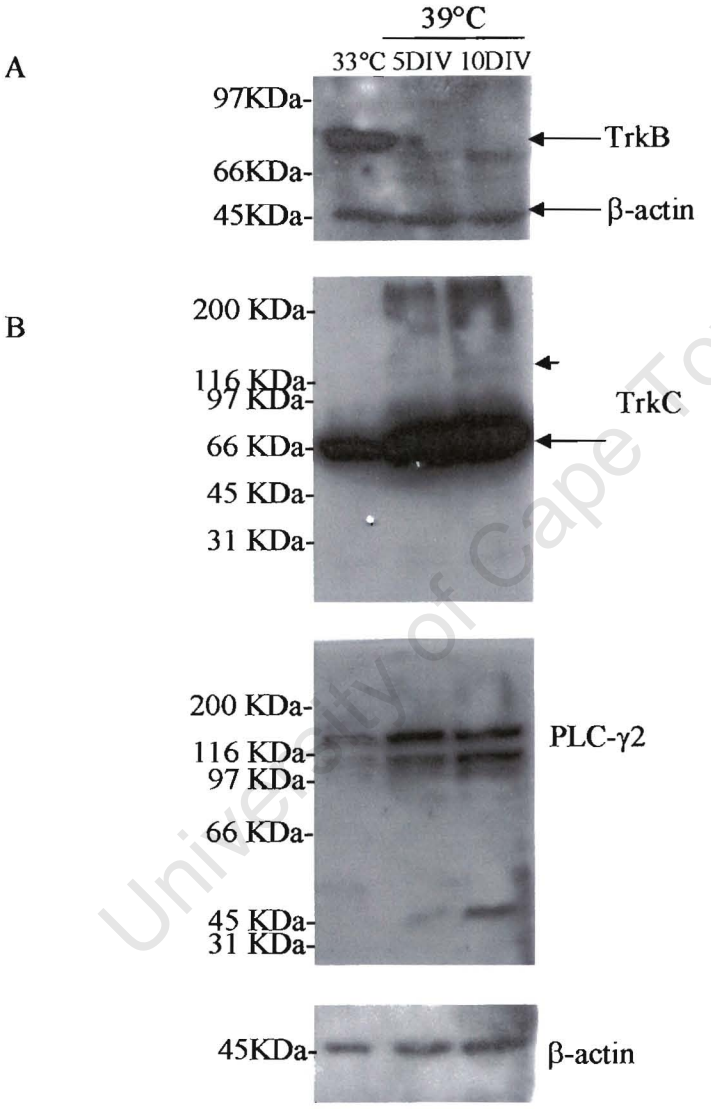

Figure 3. 12 Expression patterns of the components of the neurotrophin signal transduction cascade in OP27 cells treated with FGF-2. Immunoblot of OP27 cells was prepared using total protein lysates from cells at 33°C and cells that had been treated with FGF-2 at 39°C for 5 days *in vitro* (5DIV) and 10 days *in vitro* (10DIV). (A) OP27 cells express mainly the truncated isoform of TrkB (indicated with an arrow) at 33°C which is downregulated as the cells differentiate. (B) Predifferentiated and differentiating OP27 cells express both the full-length (arrowhead) and truncated (arrow) isofoms of TrkC. PLC-γ2 is also expressed as both its full-length (140KDa) and processed (100KDa) forms. Each blot was used for each antibody and later reprobed with β-actin to verify loading.

TrkC, on the other hand was detected as two protein bands that migrated at ~140KDa (for the TK+ isoform) and 90KDa (the TK- isoform). At the non-differentiated state, only the 90KDa TK- isoform form is present. At 39°C, expression of the 90KDa TK- isoform increases and the 140KDa TK+ isoform is detected (Fig. 3.12B). This pattern of expression of TrkC observed in OP27 cells treated with FGF-2 is similar to that observed when these cells were induced to differentiate with retinoic acid (Illing *et al.*, 2002).

The effector enzyme, phospholipase C gamma 2 (PLC-γ2) is tyrosine phosphorylated in response to neurotrophins acting on TrkB or TrkC receptors and is also implicated in FGF-2 signalling (Yamada *et al.*, 2002). OP27 cells express two forms of PLC-γ2: the phosphorylatable 140KDa full-length form and the 100KDa cleavage product that cannot be phosphorylated. As the cells were induced to differentiate with retinoic acid they continued to express both forms with the full-length form predominating (Illing *et al.*, 2002). In this study the full-length form of PLC-γ2 predominated at all time points. Both were also up-regulated after 5 and 10 days of FGF-2 treatment compared to the control cells at 33°C (Fig. 3.12B).

Finally, antibodies recognizing the olfactory signal transduction components, G_{olf} and the olfactory specific effector adenylate cyclase (ACIII) were demonstrated by western blot analysis to react with appropriately sized proteins in OP27 cell at different time points of differentiation (Fig 3.13). Both G_{olf} and ACIII are expressed in OP27 at 33°C when the cells are not differentiated and G_{olf} continues to be expressed at 39°C when cells are differentiating under the influence of FGF-2. ACIII on the other hand, gets down-regulated with FGF-2-induced differentiation of these cells, with expression levels barely detectable after 5 days *in vitro* (Fig. 3.13). The expression patterns of both G_{olf} and ACIII are

similar to that observed in OP27 cells when induced to differentiate with retinoic acid (Illing *et al.*, 2002).

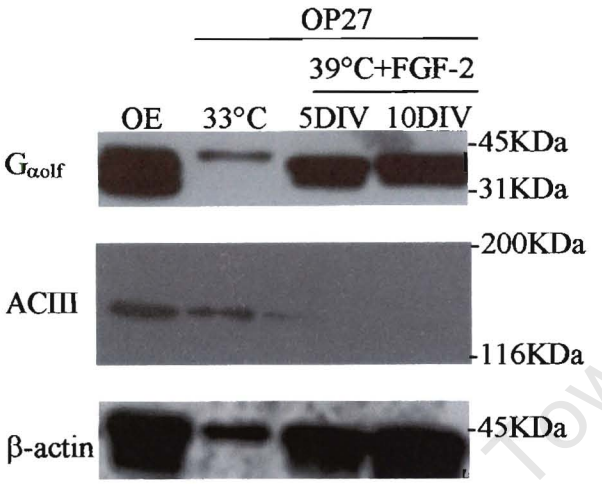

Figure 3.13 Expression patterns of Gαolf and type III adenylate cyclase (ACIII) on OP27 cells treated with FGF-2. Immunoblot of OP27 cells was prepared using total protein lysates from cells at 33°C and cells that had been treated with FGF-2 at 39°C for 5 days *in vitro* (5DIV)and 10 days *in vitro* (10DIV). The olfactory epithelium (OE) was used as a positive control. The same blot was used for each of the olfactory signal transduction components (and those shown in Fig. 3.10) and later reprobed with β-actin to verify loading.

3.3.7.3 Immunocytochemical characterization of FGF-2-differentiated OP27 cells

The FGF-2-induced differentiation in OP27 cells was also characterized by immunocytochemistry using some of the antibodies used for western blot anlyses to establish their cellular localization in the differentiating cells. The anti-TrkB polyclonal antibody was detected closer to cell bodies of cells with shorter neurites while staining in cells with longer neurites was evident in the processes (Fig 3.14A). Similarly, the high affinity NT3 receptor TrkC was also immunolocalized closer to cell bodies of cells with shorter neurites whereas cells with longer processes had staining both in the cell bodies and at the distal ends of the neurite-like processes (Fig 3.14B). The staining for PLCγ2 was noted for being

localized throughout the processes in all the cells that were stained (Fig 3.14C). The olfactory G-protein (G_{olf}) was mainly found localized to cell bodies in a majority of cells and in out-growing neurite processes in few of cells (Fig 3.14 D). Negative controls with no primary antibody failed to reveal any staining (data not shown).

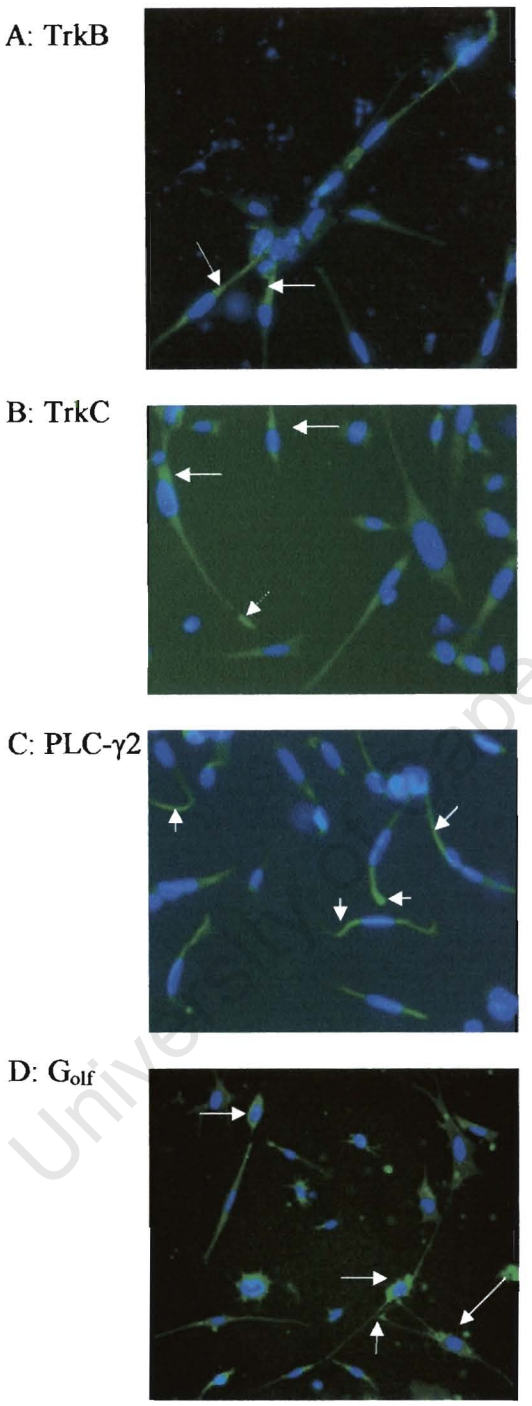

Figure 3.14 Immunocytochemical characterization of OP27 cells with olfactory signalling proteins. Shown are images of OP27 cells treated with FGF-2 for 10 days at 39°C and immunostained (green) with anti-TrkB (A), anti-TrkC (B), anti-PLC-γ2 (C) and Gαolf (D). Staining in the cell bodies is indicated with long arrows while staining in processes is indicated with shorter arrows. Nuclei were counterstained blue with DAPI. The photographs were taken at 40X magnification.

3.3 DISCUSSION

The OP27 cell line was isolated by infection of primary cultures of E10.5 mouse olfactory placode with the retrovirus containing the tempereature sensitive SV40 large T antigen. The cells proliferate under the control of SV40 large T antigen at the permissive temperature (33°C). Shifting the cells to 39°C allows the study of the effects of growth factors of neuronal differentiation when the cells are not under the control of the SV40 large T antigen. The OP27 cells have been shown to respond to retinoic acid and differentiate into olfactory receptor neurons (ORN) that express endogenous olfactory receptors and neuronal markers (Illing *et al.*, 2002). I have extended these studies and examined the response of OP27 cells to FGF-2, a growth factor which has been shown to be important for neuronal differentiation.

To test whether FGF-2 had any effects in the proliferation, differentiation, and/ or survival of OP27 cells, I first checked whether these cells express the receptors for this growth factor. RT-PCR was used to examine the expression of FGFR-1 to FGFR-4 and the isoforms of these receptors. I discovered that the OP27 cells express a limited set of FGFR-s, these being FGFR-1 and FGFR-2. This pattern of expression is consistent with that found in E14.5-E15.5 explant cultures of mouse OE (DeHamer *et al.*, 1994). This FGFR- expression pattern is also similar to that observed in adult mouse OE *in vivo* (Hsu *et al.*, 2001) but differes in the subtype of the receptor that is expressed in both systems. OP27 cells express only the IIIc isoforms of both FGFR-1 and FGFR-2 wherease the adult mouse OE contained the IIIb isoforms of both FGFR-1 and FGFR-2 and the IIIc isoform of only FGFR-1 (Hsu *et al.*, 2001). The expression of the IIIc isoform of FGFR-2 in the embryonic OP27 cells versus the IIIb in the adult mouse OE may suggest a stage-specific switch in the expression of the FGFR-2 splice isoform.

In addition, the FGFR-1 IIIc expressed in OP27 cells appears as the 3 variants, α, β, and γ which differ in the sequence concerning Ig-I domain in the extracellular region. Another olfactory cell line, JFEN, which was derived from a human olfactory neuroblastoma tumour was shown to also express the α, β, and γ isoforms of FGFR-1, although it was not shown whether the FGFR-1 was either the IIIb or IIIc (Nibu *et al.*, 2000).

In addition to the alternative splicing of the IgIII domain in the extracellular region of FGFR, a second splicing event occurs in the juxtamembrane region, resulting either in the inclusion or deletion of the dipeptide Val-Thr (VT) (Gillespie *et al.*, 1995; Twigg *et al.*, 1998). VT is required for the interaction of FGFR with the signalling adapter protein FRS2 (Burgar *et al.*, 2002) and to initiate downstream signalling through the RAS/MAPK pathway (Twigg *et al.*, 1998). The analysis of FGFR splice variants expressed in OP27 cells is therefore not comprehensive. However, the main focus here was to demonstrate that OP27 cells express both FGFR-1 IIIc and FGFR-2 IIIc and can therefore respond to FGF-2.

By extrapolation of BaF3 mitogenic assays which assayed FGFR-FGF ligand interactions (Table 1.1), it is likely that OP27 cells could interact with the following FGF ligands, FGF-1, FGF-2, FGF-4, and FGF-9, and to a lesser extent, with FGF-5, FGF-6 and FGF-17 (Table 3.2). The actions of some of these ligands have already been demonstrated in OE explant cultures. FGF-1, FGF-2, and FGF-4 were found to stimulate proliferation of INPs in E14.5-E15.5 OE explant cultures (DeHamer *et al.*, 1994). The function of FGF-9 in OE development has not been demonstrated yet. There is evidence that FGF-9 is required for survival and not for the differentiation of bulbospinal neurons (Pataky *et al.*, 2000). The actions of two other FGFs, FGF-7 and FGF-8 have been demonstrated in explant cultures as well.

FGF-7 was also found to support the proliferation of the INPs but at lower effect compared to FGF-1, 2, and –4 (DeHamer *et al.*, 1994). FGF-8 was found to stimulate the proliferation of the putative OE neuronal stem cell (Calof *et al.*, 2002). The binding study by Ornitz *et al.* (1996) in BaF3 cells showed that FGF-7 and FGF-8 exert their effects through activation of FGFR-2-IIIb, FGFR-3-IIIc and FGFR-4 receptors. FGFR-2-IIIb has been detected in purified adult OE by RT-PCR but FGFR-3-IIIc and FGFR-4 were not detected in the OE (Hsu *et al.*, 2001). It is therefore unclear how the effects of FGF-8 in OE lineage can be mediated.

Table 3.2 FGF ligands that the OP27 cells could respond to, as a result of expression of the IIIc isoforms of both FGFR-1 and FGFR-2 in these cells. These FGF-FGFR interactions are extrapolated from the mitogenic assays using BaF3 cells (Table 1.1). +++, ++ represent level of interaction of ligand and receptor.

Interaction	FGFR-1 IIIc	FGFR-2 IIIc
+++	FGF-1, FGF-2, FGF-4	FGF-1, FGF-4, FGF-9
++	FGF-5, FGF-6	FGF-2, FGF-6, FGF-17

In this study the effect of FGF-2 on OP27 cells was analysed under serum-free conditions at the non-permissive temperature (39°C). I found that FGF-2 had effects on both the rate of cell division and differentiation of OP27 cells under these conditions. The rate of cell division of FGF-2 treated OP27 cells was higher in than in control cells. As a result, the total number of viable cells at each time point were always greater in the presence of FGF-2 compared to controls. However, there was a progressive decline in [^{3}H]thymidine incorporation in FGF-2 treated cells with time, and by 6 days cells had ceased dividing. This is similar to the observation that a fraction of OP27 cells continue dividing for up to 4 days after shifting them to 39°C in the presence of retinoic acid (Illing *et al.*, 2002).

Neuronal differentiation is preceeded by exit from the cell cycle. The decrease in thymidine incorporation with time in culture thus suggested cessation of DNA replication and cell division and beginning of differentiation. Indeed, the cells began to undergo a morphological change indicative of differentiating ORNs. The decline in thymidine incorporation was accompanied by a gradual increase in the number of bipolar cells. The increase was particularly noticeable between 6 and 10 days when cell division had stopped.

Both treated and untreated cells displayed cellular death as judged by the decrease in numbers. However, OP27 cells treated with FGF-2 were always maintained in higher numbers than control cultures without FGF-2. It appeared that FGF-2 may be protecting the cells from death. Apoptosis is induced by the activation of the cellular death protease Caspase (Bae *et al.*, 2000). FGF-2 was found to protect rat hippocampal cells from death by delaying the onset and peak activation of caspases (Eves *et al.*, 2001). FGF-2 may thus protect OP27 cells in a similar manner. It is clear though that FGF-2 is not sufficient on its own to prevent apoptosis. Thus additional molecules may be required. The neurotrophin BDNF has been shown to promote cell survival in mouse OE both *in vivo* and *in vitro* (Holcomb *et al.*, 1995) and its cognate receptor TrkB is expressed in OP27 cells.

The expression patterns of various markers which characterize different stages of olfactory neuron development were analyzed in OP27 cells that had been treated with FGF-2. GAP-43 is the among the first neuron-specific markers to be expressed in differentiating olfactory receptor neurons (ORNs) during embryogenesis. It is a marker for immature ORNs and is expressed transiently during the early stages of differentiation. Its expression coincides with process outgrowth and synaptogenesis in the mouse OE (Biffo *et al.*, 1990). A semi-quantitative RT-PCR assay showed a transient up-regulation of GAP-43 mRNA in OP27 cells following treatment with FGF-2. High levels were first detected after 24

hours with maximum levels reached after 48 hours. After 2 days the GAP-43 mRNA levels decreased but were still higher than at the predifferentiated state. This is an indication that the OP27 cells were indeed differentiating into neuronal cells. The GAP-43 protein was also shown to up-regulated in OP27 cells following retinoic acid induced differentiation (Illing *et al.*, 2002). The high levels of GAP-43 mRNA at 24 and at 48 hours coincided with the appearance of the first OP27 cells with neurite-like extensions.

The expression of NST, NCAM, TrkB, TrkC, PLC-γ2, G_{olf} and ACIII was also analyzed using western blots. These proteins were expressed both at 33°C and at the non-permissive temperature but there were characteristic changes in their expression patterns as the cells were induced to differentiate. The NST protein is present at 33°C but its expression is down-regulated as OP27 cells differentiate and mature into ORNs. Although this mirrors what has already been reported in ORNs both *in vivo* and *in vitro* (Roskams *et al.*, 1998; Illing *et al.*, 2002), it is not clear what the significance of NST down-regulation following FGF-2 induction is.

Another proof that the OP27 cells differentiate into neuronal cells in the presence of FGF-2 is the expression of NCAM. In the OE, NCAM is used as a marker to distinguish between the immediate neuronal precursors which are negative for NCAM and the post-mitotic neurons (both immature and mature) which do express NCAM (Calof *et al.*, 1991). I have shown, using western blots, that FGF-2 induced the OP27 cells to up-regulate NCAM expression in culture.

Do the OP27 cells become terminally differentiated under the conditions used here?. The best example of specific marker for ORNs is the OMP, a developmentally regulated, abundant 19KDa cytoplasmic protein whose expression is largely the hallmark of ORN maturity (Carr *et al.*, 1998). I could not reproducibly show that OP27 cells express OMP mRNA transcripts following their induction to differentiate. OMP mRNA transcripts were present in FGF-2 treated cells only after 10 days (one out of 4 experiments) but this was never reproducible from experiment to experiment. It has been shown that cells that express GAP-43 are not terminally differenitated neurons since they are devoid of OMP expression (Pellier *et al.*, 1994). OP27 cells still express GAP-43 transcripts even after 10 days in culture, albeit at lower levels compared to at 48 hours. It was therefore concluded that under the conditions used in this thesis OP27 cells did not achieve terminal differentiation. It is, however, possible that with longer time points in culture I would have been able to detect OMP expression in OP27 cells. It is also possible that FGF-2 is not enough on its own to promote the OP27 cells to progress from the immature neuronal state to a terminally differentiated and mature OMP expressing cell state. Other signals may be required for the maturation of these cells. In a study using the 3NA12 cell line, the neutrophins BDNF and NT-3 were demonstrated to promote the progression of these cells into mature and OMP expressing cells (Barber *et al.*, 2000). TrkB and TrkC, the cognate receptors for BDNF and NT-3, respectively, and their signalling component PLC-γ2 were shown to be present in OP27 cells. The expression of TrkB was, however lost as the OP27 cells differentiated while TrkC and PLC-γ2 prevailed. NT-3, the ligand for the TrkC receptor, could therefore be the neutrophin that may be required for the maturation of OP27 cells.

In summary, I have shown that the OP27 cell line expresses the receptors that are known to transduce FGF-2 signals. These cells respond to FGF-2 and initiate a differentiation programme that is

characteristic of differentiating immature olfactory receptor neurons *in vivo*, as analyzed by the expression of various neuronal markers. However, the culture conditions used here did not support the maturation of the OP27 cells as they do not express OMP, the definitive marker for mature olfactory neurons. In Chapter 4 I demonstrate that the differentiating OP27 cells express olfactory receptors as would be expected for differentiated olfactory receptor neurons.

Chapter 4

Analysis of olfactory receptor gene expression in OP27 cells

4.1 Introduction

The neurons in the olfactory epithelium (OE) specify their functional identity by selecting one olfactory receptor (OR) to express (Malnic *et al.*, 1999; Reed, 2000). ORs are G-protein coupled seven transmembrane proteins responsible for mediating the interaction of odours from the external environment with the brain resulting in smell detection.

4.1.1 Discovery of OR genes

OR genes were first cloned from the rat using degenerate RT-PCR with primers that annealed to conserved regions of the G-protein coupled receptor (GPCR) superfamily (Buck and Axel, 1991). This landmark discovery was based on the assumption that since G-proteins had been found in earlier experiments to mediate olfactory signal transduction, it was therefore highly likely that ORs belong to the GPCR superfamily of proteins that are characterized by seven hydrophobic transmembrane (TM) domains. The initial discovery in rats was soon followed by cloning of more genes from species such as chickens, Zebrafish, *Drosophila*, mouse, dog and human (Selbie *et al.*, 1992; Ngai *et al.*, 1993; Issel-Tarver and Rine, 1996; Leibovici *et al.*, 1996; Clyne *et al.*, 1999).

The OR gene products are encoded by an ~1kb intronless open reading frame (ORF). There are several amino acid sequence motifs that are conserved in all ORs and that distinguish them from other GPCRs (Fig. 4.1, Mombaerts, 1999). These include the **LHTPMY** motif in intracellular loop 1; **MAYDRYVAIC** at the end of TM3 and beginning of intracellular loop 2; **SY** at the end of TM5; **FSTCSSH** in the beginning of TM6 and **PMLNPF** in TM 7. The high degree of variability among the ORs is evident in TMs 3, 4 and 5. It has been suggested that these variable regions may form odorant-binding sites.

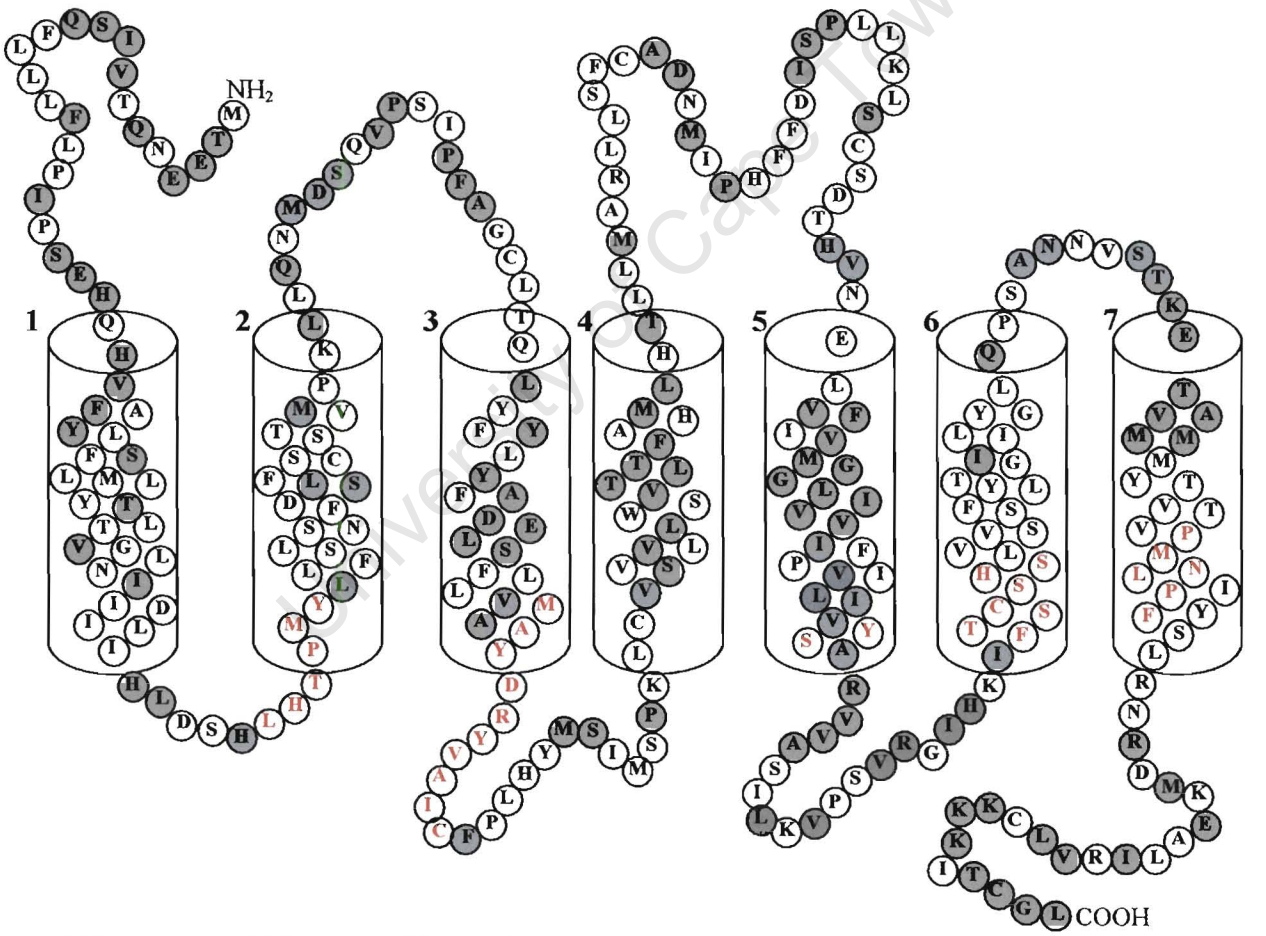

Figure 4.1 The structure of OR as exemplified by the receptor OR I15 which was cloned by Buck and Axel (1991). The cylinders represent the hydrophobic transmembrane (TM) domains with 1 the most N-terminal TM domain and 7 the last TM (the TM domains are numbered 1-7). Conserved residues of a OR subfamily are shown as white balls while the gray balls represent the variable amino acids. The regions that contain the conserved motifs that distinguish ORs from other GPCRs are marked with red letters (see text).

4.1.2 OR Repertoire and genomic organization

ORs represent the largest family in the mammalian genome, encompassing different subfamilies. Current estimates of the complexity of the OR gene repertoire stand at about 1200-1300 genes in mice, 1000 in humans and 100 in zebrafish (Zhang and Firestein, 2002; Godfrey *et al.*, 2004). These genes are randomly clustered in a number of chromosomal locations in all species studied. In some locations the cluster(s) can be characterised by intergenic distances of anything between 5-50kb. There is no ordered arrangement of the genes in a cluster and transcription may occur in either direction (Mombaerts, 1999; Kratz *et al.*, 2002).

It is thought that the OR gene repertoire has expanded through numerous duplications of entire chromosomal portions, followed by mutations within the duplicated regions to increase diversity (Dryer and Berghard, 1999). Some of these mutations may have resulted in pseudogenes: 60-70% of human OR genes do not code for any functional OR proteins as these have ORFs that are either interrupted with stop codons, or that lack conserved motifs (Glusman *et al.*, 2000).

4.1.3 Patterns of olfactory receptor expression

The patterns of expressions of OR genes in the OE have been largely studied using a series of *in situ* hybridization experiments with riboprobes derived from cloned OR cDNAs. Expression is first detected in immature neurons and has never been observed in the mitotically active ORN precursors (Qasba and Reed, 1998; Fan and Ngai, 2001; Iwema and Scwob, 2003). Additionally, experiments using bulbectomized animals have shown that the expression of ORs is activated independently of the olfactory bulb (OB), their target organ (Sullivan *et al.*, 1995).

A number of studies have reported that in mice each ORN expresses only one or very few of the 1000 OR genes. This hypothesis was based on the finding that a given riboprobe hybridized to a very small subset (about 0.1%-1%) of mature ORNs (Malnic *et al.*, 1999). A limited number of single-cell RT-PCR data support this hypothesis: using degenerate primers recognising conserved regions in OR sequences, it was found that a single neuron expressed only one OR gene (Malnic *et al.*, 1999; Touhara *et al.*, 1999). There is, however, one study where it was shown that one cell expressed at least two different OR genes (Rawson *et al.*, 2000). Moreover, each ORN expresses either the maternal or the paternal allele of the transcript and never both, a phenomenon known as monoallelic expression (Chess *et al.*, 1994).

Various laboratories have independently shown that a given OR probe is restricted to one of four parallel topographic zones in the OE of mammals (Ressler *et al.*, 1993; Strotman *et al.*, 1994; Vassar *et al.*, 1993). ORNs expressing a given OR are randomly distributed in a punctate pattern within a zone, intermingled with ORNs expressing different receptors. However, the axons of the ORNs that express the same OR gene, while randomly distributed in that zone, converge to the same glomerulus in the olfactory bulb (Ressler *et al.*, 1994; Vassar *et al.*, 1994).

Examination of the pattern of expression in zebrafish, chick and fruit-fly has revealed a temporal pattern of expression during development. In zebrafish a staggered onset of expression of a subset of OR genes was observed in four consecutive time-periods after fertilization. Most genes with same onset of period were found clustered in the genome (Argo *et al.*, 2003). A similarly staggered onset of expression was observed with 3 different Drosophila OR (DOR) genes. Expression of 2 DORs was shown to begin much later than that of the other one. However, unlike in Zebrafish, the two synchronous DOR genes were not clustered together in the genome of the fly (Clyne *et al.*, 1999).

At least two onset groups of OR have also been reported in chicks, with 6 ORs easily detected at E5 whereas a second group could be detected later (Nef *et al.*, 1996). In contrast to the asynchrony in the expression of the different ORs observed in chick, fly and fish, a group of different ORs were expressed simultaneously during embryogenesis in rodents (Strotmann *et al.*, 1995; Sullivan *et al.*, 1995).

4.1.4 Regulation of OR gene expression

The regulatory mechanisms that are responsible for the choice of just one OR to be expressed by an ORN are largely unknown. There are hypotheses that have been suggested or that are currently being explored to unravel these control mechanisms. One theory that has been suggested involves DNA rearrangement events in either the ORNs or the basal cells whereby a single OR gene gets translocated from a cluster by DNA recombination into close proximity to an active promoter for expression or else the active promoter itself gets translocated upstream of a single OR gene (Mombaerts, 1999; Kratz *et al.*, 2002). This hypothesis has been tested by two independent laboratories using cloning experiments by nuclear transfer of a postmitotic, OMP^+ cell into enucleated oocytes. It was hypothesized that, if an irreversible DNA rearrangement event occurred in the locus of the OR gene of the cell used for the transfer, then all the ORNs of the cloned mouse should express the same receptor. This was not the case. The ORNs of the cloned mice expressed a repertiore of OR genes and their patterns of expression were not different from that of the ORNs of the wild-type mice (Eggan *et al.*, 2004; Li *et al.*, 2004).

Yeast artificial chromosome (YAC) transgenic mice carrying OR clusters have been used to define cis-regulatory elements or locus control regions (LCRs) that may be involved in the choice of OR to express. These regulatory elements have been suggested to be located at widely varying distances from

the transcription initiation site of a given OR gene, with some at hundreds of kilobases away while some were found at close proximities to the OR gene (Qasba and Reed, 1998; Kratz *et al.*, 2002; Serizawa *et al.*, 2003). One such LCR, known as the H region, has recently been shown to control the expression of clustered OR genes by stochastically selecting just one gene at a time and activating its expression from that cluster. When the H region was deleted from a YAC containing tagged OR genes in a cluster, the expression of these transgenic ORs was completely abolished (Serizawa *et al.*, 2003).

A negative feedback regulation mediated by the OR themselves has recently been proposed to ensure that one ORN selects and expresses only one OR gene. Two groups using transgenic mice carrying OR genes with either full-length or deleted ORFs have independently shown that when one OR gene is stochastically selected from a cluster and activated, the expressed OR protein then generates a feedback signal that will inhibit the activation and expression of the other OR genes either in that cluster or in other clusters in that cell. When an OR gene with a deleted coding region is selected there is no feedback signal and as a result the cell can choose a second functional OR (Serizawa *et al.*, 2003; Lewcock and Reed, 2004).

There is also the hypothesis that the selection of one OR gene to activate may be a consequence of specific combinations of transcription factors interacting with binding sites in the proximal promoter of that OR (Kratz *et al.*, 2002). Potential binding sites of various transcription factors have been identified in promoters of mouse and human OR genes. These were identified using either *in silico* methods or yeast one-hybrid screens. The identified transcription factors included the olfactory neuron specific factor 1/early B cell factor-like 1 (O/E-1); O/E-2, pituitary homeobox 1-factor (Ptx-1); binding factor for early enhancer (BEN); aristaless-like homeobox 3 (Alx-3); lim-homeobox-2 factor (LH2/Lhx2), activator protein 2β (AP-2β); nuclear factor-1 (NF-1); CREB; hepatocyte nuclear factor

3β (HNF3β); and aryl hydrocarbon nuclear translocator (Arnt) (Glusman *et al.*, 2000; Hoppe *et al.*, 2000; Hoppe *et al.*, 2003; Sosinsky *et al.*, 2000). The interaction of these OR promoter motifs with the transcription factors has been demonstrated using electrophoretic mobility gel shift assays (Hoppe *et al.*, 2003). Whether these proteins regulate the expression of the ORs is yet to be demonstrated. A few transcription factors have been shown to regulate the expression of an OR or a subset of these genes in non-vertebrates. In *C. elegans* the olfactory-specific transcription factor odr-7 (a member of the nuclear receptor superfamily) has been shown to regulate the expression of the OR gene *odr-10* (Sengupta *et al.*, 1996). The expression of *odr-10* was barely detectable in *odr-7* mutant worms when compared to the wild-type. Expression of a subset of *Drosophila* ORs (DORs) was shown to be differentially regulated by the transcription factor Acj6. A group of DOR genes that expressed in the maxillary palp (one of two olfactory organs found in the fly) were affected by a null mutation in the *acj6* gene whereas the absence of the gene had no effect in the expression of a subset of DOR genes expressed in the antenna (the second olfactory organ) (Clyne *et al.*, 1999).

It has been postulated that the choice of OR may be either a cell-autonomous event, may be affected by local environmental factors and/or the choice may be a result of a stochastic selection of a single OR from a cluster in the genome (Fan and Ngai, 2001; Iwema and Schwob, 2003).

In a previous study, the OP27 cell line was shown to express a single OR, OR27-3, following induction with retinoic acid (Illing *et al.*, 2002). I therefore sought to establish whether the OP27 cells expressed any endogenous OR genes in response to FGF-2 treatment, and to determine whether these cells express only the OR27-3 receptor or a limited set of ORs.

4.2 Results

4.2.1 OP27 cells express OR transcripts when differentiated

OP27 cells that had been treated with FGF-2 at 39°C were analyzed for the expression of OR genes by performing RT-PCR with RNA isolated from 5 pooled tissue culture petri-dishes. A pair of degenerate primers, OR-F3 and OR-RC (Table 2.1), which are based on the conserved motifs MAYDRYVA at the end of TM3 and MLNPFIY in TM7 (Fig. 4.1), respectively, amplified the expected ~530bp PCR product on OP27 cells treated with FGF2 for 48hrs onwards (Fig. 4.2). In order to analyze the identity and diversity of the OR gene transcripts expressed in OP27 cells *in vitro*, the amplification product from the 2-day time point was cloned into the pGEM-TEasy® and pCRII® vector systems and the nucleotide sequence was initially determined for 3 recombinant plasmids, 27OR-69, 27OR-70 (both in pCRII) and 27OR-71 (cloned in pGEM-TEasy®). The clones were sequenced in both directions to reveal 534 bp nucleotide sequences.

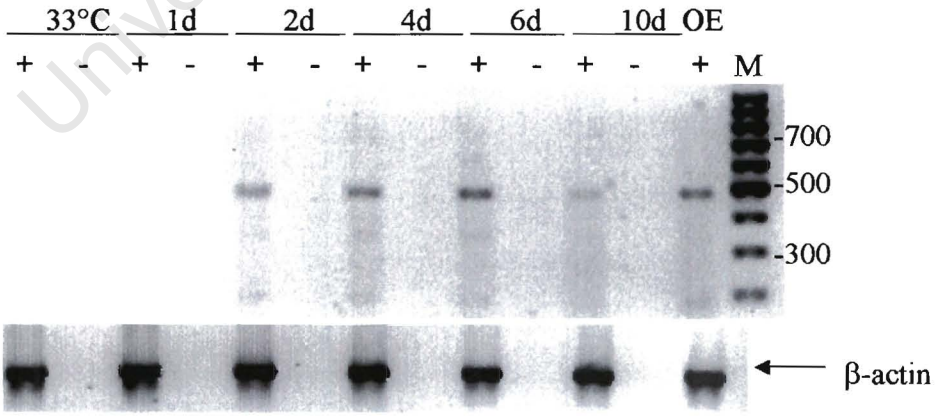

Figure 4.2 RT-PCR analysis of the expression of olfactory receptors in differentiating OP27 cells. Expression was determined in OP27 cells at 33°C and in cells that had been treated with FGF-2 for 1, 2, 4, 6, and 10 days at 39°C. +, reverse transcribed RNA templates, -, non-reverse transcribed RNA samples used as negative controls, M, 100 bp ladder as a molecular weight marker with sizes shown on the left in base pairs (bp). cDNA from the olfactory epithelium (OE) was used as a positive control.

The nucleotide sequences of the 3 clones were compared to each other and revealed at least 99% sequence identity between them, with 4 base substitutions. 27OR-70 and 27OR-71 were 99.8% identical with one base difference, whereas 27OR-69 had 3 base differences with 27OR-70 and 4 with 27OR-71 (Fig. 4.3A). Figure 4.3B shows representative chromatograms for the base substitutions in the 3 OR clones. The 4 base differences between the clones resulted in a few amino acid substitutions in the deduced protein sequence of 27OR-71. However, BLASTp searches against GenBank database with all 3 clones showed the greatest homology to the OR6-13 (Illing *et al.*, 2002, accession number AF042359) and Olfr57 (also known as MOR139-3, accession number XP_137190) odorant receptors (Fig. 4.4). I concluded that the determined nucleotide sequences of the 3 clones represented one OR gene (referred to as Type 1 in this study). It is possible that the base substitutions in the three clones could be a result of misincorporation by *Taq* DNA polymerase.

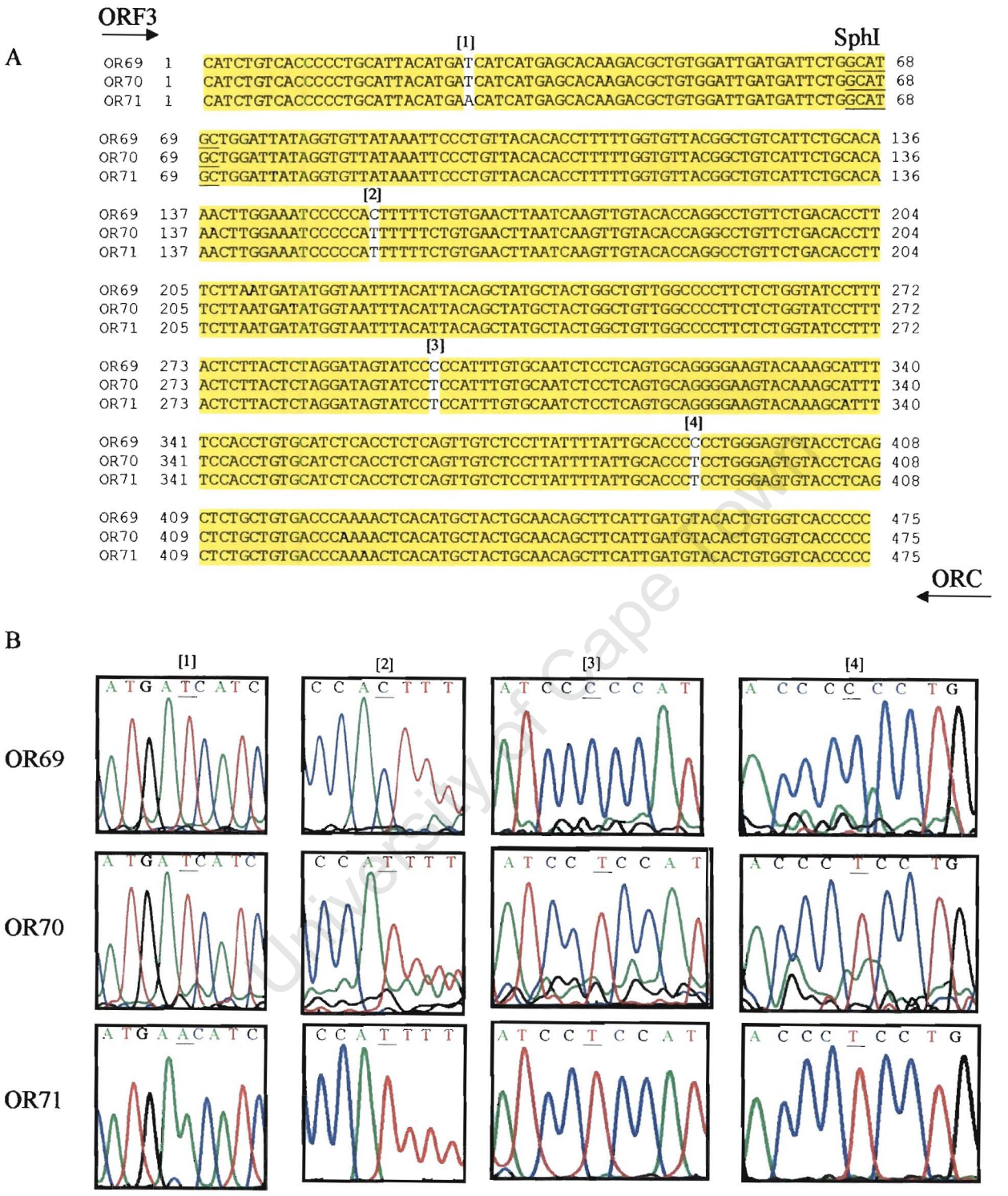

Figure 4.3: Nucleotide sequence alignment of OR-69; OR-70; and OR-71 clones from the OP27 cell line treated with FGF2. **A**. Identical nucleotide sequences are shaded. The nucleotide sequences of the primers ORF3 and ORC are not included in the alignment. The SphI recognition site in all 3 OR genes is indicated. **B**. Representative chromatograms showing the base substuitions (underlined). Top row, OR69; middle row, OR70; bottom row, OR71. The positions where there are base substitutions in the three OR clones are indicated with bracketed numbers in the alignment (A) and in the sequence chromatographs (B).

```
MOR139-3   1   ICHPLHYMIIMSTRRCGLMILACWIIGVINSLLHTFLVLRLSFCTNLEIPHFFCELNQVVHQAC  64
OR71       1   ICHPLHYMNIMSTRRCGLMILACWIIGVINSLLHTFLVLRLSFCTNLEIPHFFCELNQVVHQAC  64
OR6-13     1   ICHPLHYMIIMSTRRCGLMILACWIIGVINSLLHTFLVLRLSFCTNLEIPHFFCELNQVVHQAC  64
OR69       1   ICHPLHYMIIMSTRRCGLMILACWIIGVINSLLHTFLVLRLSFCTNLEIPHFFCELNQVVHQAC  64

MOR139-3   65  SDTFLNDMVIYITAMLLAVGPFSGILYSYSRIVSSICAISSVQGKYKAFSTCASHLSVVSLFYC  128
OR71       65  SDTFLNDMVIYITAMLLAVGPFSGILYSYSRIVSSICAISSVQGKYKAFSTCASHLSVVSLFYC  128
OR6-13     65  SDTFLNDMVIYITAMLLAVGPFSGILYSYSRIVSSICAISSVQGKYKAFSTCASHLSVVSLFYC  128
OR69       65  SDTFLNDMVIYITAMLLAVGPFSGILYSYSRIVSPICAISSVQGKYKAFSTCASHLSVVSLFYC  128

MOR139-3   129 TLLGVYLSSAVTQNSHATATASLMYTVVTP 158
OR71       129 TLLGVYLSSAVTQNSHATATASLMYTVVTP 158
OR6-13     129 TLLGVYLSSAVTQNSHATATASLMYTVVTP 158
OR69       129 TPLGVYLSSAVTQNSHATATASLMYTVVTP 158
```

Figure 4.4 Amino acid alignment of OR69 and OR71 with the published odorant receptors that revealed high homology, MOR139-3 and OR6-13, between the primer regions MAYDRYVA at the end of TM3 and MLNPFIY in TM7.

4.2.2 Differentiated OP27 cells express a small repertoire of the OR gene family

I wanted to established whether the cell line expressed only one of the reported ~1300 mammalian OR genes when induced to differentiate. The cells expressed the OR27-3 receptor when induced to differentiate in the presence of RA (Illing *et al.*, 2002) which is a different OR reported for the 2 day time point of FGF-2 induction. I analyzed an additional 21 randomly selected recombinant plasmids containing the PCR products from the 2 day time point, to see whether other ORs were expressed. The inserts were PCR-amplified using the SP6 and T7 primers which flank the multiple cloning site of pGEM-TEasy® cloning vector, generating a 714bp product. The amplicons were subsequently digested with the restriction enzyme SphI and analyzed on a 2% ethidium bromide stained agarose gel to determine the digest pattern of each clone. SphI restricts the 27OR-69, -70 and -71 clones (Fig. 3.4) to generate fragments of sizes 470bp and 200bp (orientation 1, Fig. 4.5A) or 534bp and 140bp (orientation 2, Fig. 4.5A).

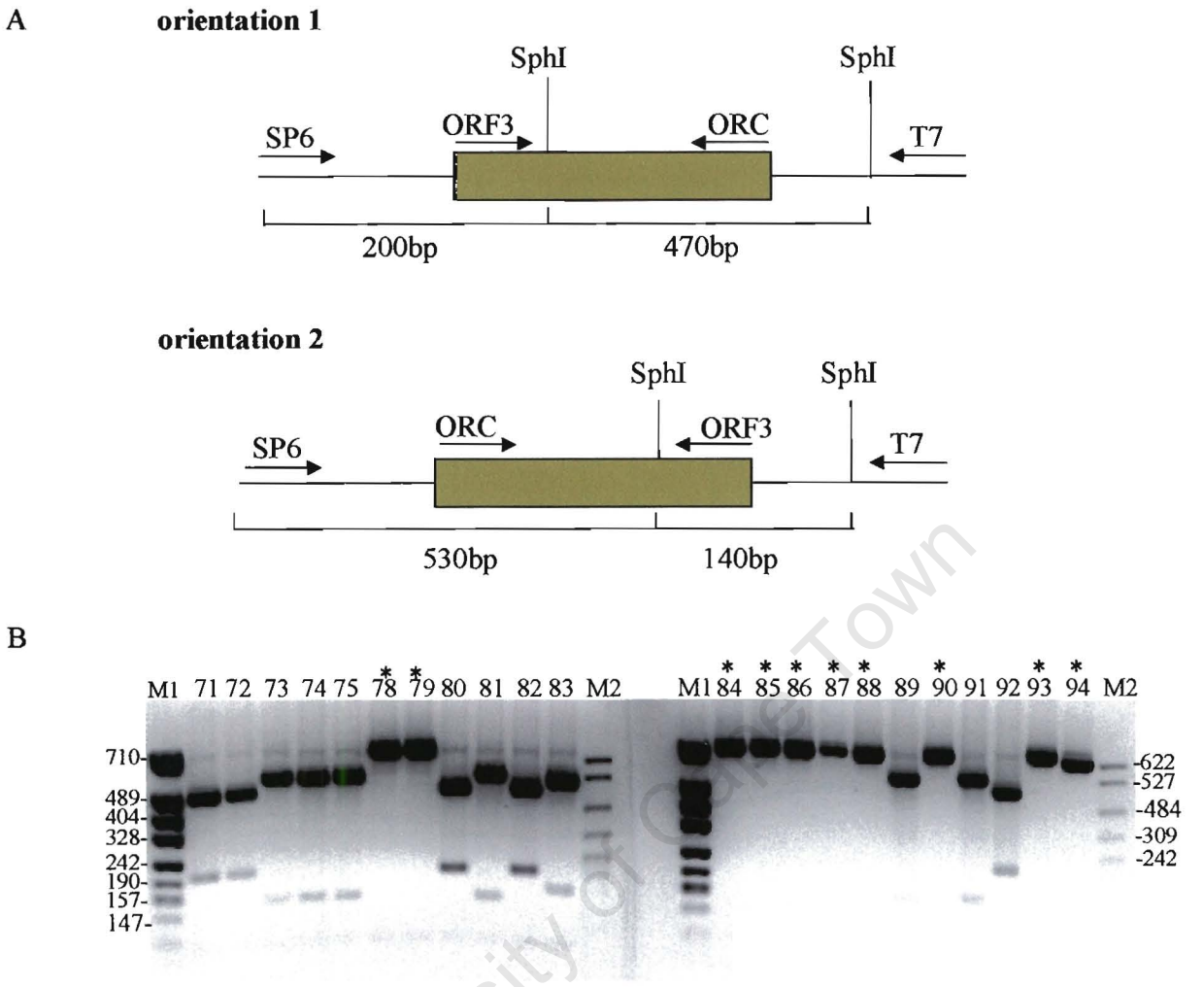

Figure 4.5 Restriction analysis of 27OR clones from the 2-day time point. **A**. The OR PCR products were subcloned into the pGEM®-T Easy vector and inserts amplified with the T7 and SP6 primers to give a 714bp product. The orientation of the insert in the vector is one of two possibilities such that digestion of Type 1 OR PCR products with SphI would result into one of the two digestion patterns shown. **B**. SphI digestion of the PCR products from recombinant plasmids cloned from the 2 day time point. 71, control plasmid OR71 showing the diagnostic 470bp and 200bp SphI digestion pattern. M1 and M2 are the pBluescript II SK+ -HpaII and pBR322-HpaII molecular weight markers, respectively. Sizes of molecular weight markers are shown in base pairs, bp. Ten of the 21 PCR products, indicated by asteriks, were not digested with SphI.

Digestion of the PCR products with SphI is shown in Fig. 4.5B. Analysis of the digestion pattern shows that 11/21 of the PCR products were Type 1 OR, giving a characteristic SphI digestion pattern. Five of the 21 clones (27OR-72; 77; 80; 82 and 92) gave digest patterns corresponding to orientation 1; while the other six (27OR-73; 74; 81; 83; 89 and 91) gave patterns corresponding to orientation 2. PCR products from ten OR clones (27OR-78; 79; 84; 85; 86; 87; 88; 90; 93 and 94) were not digested by SphI. This suggested that these clones were either different ORs or the digestion reactions failed for

these PCR products. The nucleotide sequences of all the clones that did not digest and 3 clones that did digest (OR74; 89; and 92) were determined. Sequence analysis of these clones showed that OR74; 89; and 92 were Type 1 ORs with 98.3% identity to OR69 and 98.5% identity to OR71, thus confirming the restriction digest patterns. On the other hand, OR78; 79; 84; 85; 86; 87; 88; 90; 93; and 94 were sequences of 3 completely different OR genes (OR types 2, 3, and 4). In short, I could identify 4 different OR genes that were expressed by OP27 cells at the 2 day time point following induction with FGF2. These are summarized in Table 4.1.

Table 4.1 The different types of OR genes identified in OP27 cells pooled from 5 petri-dishes, following FGF-2 induced differentiation for 2 days. The published mouse OR genes that have high homologies with the 27OR genes are also shown.

OR TYPE	Clones representing the particular OR Type	BLAST MATCH	Accession Number	Amino acid homology
Type 1	27OR-69; -70; 71; 72; 73; 74; 75; 76; 77; 80; 81; 82; 83; 89; 91; 92	OR6-13 MOR139-3	AF042359 XM_137190	99%
Type 2	27OR-84; 87; 88; 90; 93; 94	Olfr18	XM_146869	100%
Type 3	27OR-78; 79; 85	MOR141-3	XM_146415	98%
Type 4	27OR-86	MOR135-7	NM_147008	98%

4.2.3 Sequence homology of the OP27 OR clones

Nucleotide and the deduced amino acid sequences of a representative of each OR type was compared with those of the other three. Differences in both the nucleotide and amino acid sequences between the OR genes were quite significant. An amino acid sequence alignment of the 4 OR genes is shown in Fig 4.6. The presence of the amino acid motifs that are conserved in all OR's demonstrates that these clones belong to the OR superfamily. Highest sequence similarity was in TM6 whilst TM4 and TM5, the putative odorant binding pockets, had the greatest sequence diversity.

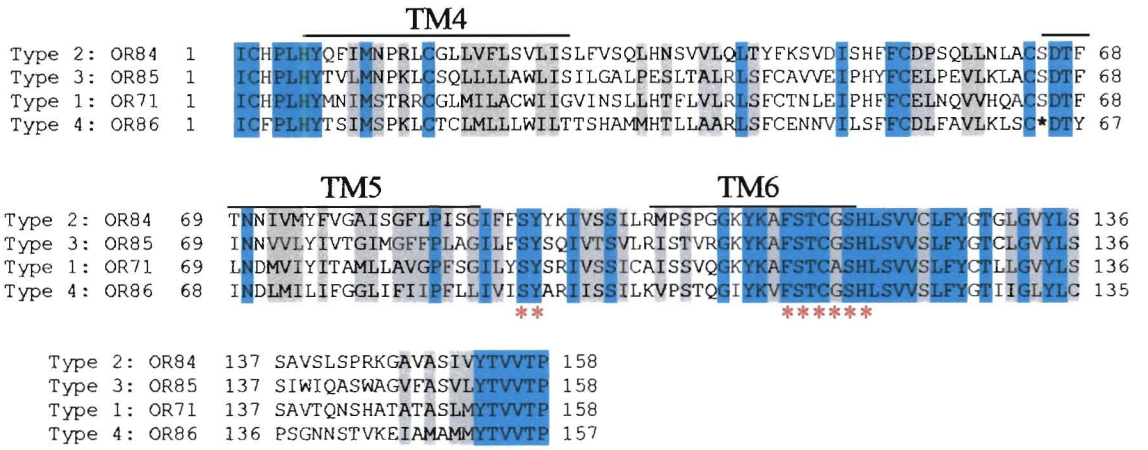

Figure 4.6: Alignment of the amino acid sequences of 27OR clones. The deduced amino acid sequences of the 4 types of OR transcripts from the end transmembrane domain TM3 to TM7 are aligned. The blue shading indicates identical amino acid residues while conserved residues are shaded in gray. The positions of the transmembrane domains TM4-TM6 are indicated. The consensus amino acid motifs for olfactory receptors are indicated with red asteriks. The position of the termination signal in 27OR86 is indicated by a *.

The sequences of the 4 OR gene transcripts identified in OP27 were compared to the GenBank nucleotide and amino acid databases. The sequences were homologus to other known olfactory receptors. The results are described below and summarized in Table 4.1. Even though the ORF of the type 4 OR (represented by 27OR-86) was interrupted by a single stop codon (Fig. 4.6), there was an overall 99% identity with the olfactory receptor MOR135-7 (accession number NM_147008). Both the forward and the reverse sequences of the 27OR-86 showed this stop codon. However, the stop codon in 27OR-86 was not conserved in the nucleotide sequence alignment with MOR135-7. It is possible that the stop codon introduced into the OR86 clone could be a result of misincorporation by *Taq* DNA polymerase.

4.2.4 Amplification of OR gene transcripts from genomic DNA results in a more heterogenous mixture of sequences

The ORFs of OR genes have no introns, thus making it impossible to design degenerate primers spanning an intron. Consequently, PCR products resulting from amplification of either cDNA or genomic DNA cannot be differentiated. The cloning of the 4 different types of OR genes instead of just one specific OR in the OP27 cells might therefore be a consequence of genomic DNA contamination. However, the RNA that was used for the first strand cDNA synthesis was always pretreated with DNaseI to remove any contaminating DNA. Subsequent to the treatment, the RNA was used as a template in a PCR with the degenerate primers or any other primers to check if any PCR product would result. Indeed these reactions failed to amplify any PCR product. Lastly, as shown in Figure 4.2 the RNA samples that were not reverse transcribed did not result in any amplification as expected of a sample with no genomic contamination. A second control experiment to exclude any possibility of contamination was therefore to perform a PCR on genomic DNA, clone the PCR products and determine the distribution of OR expression in these clones. Amplification from genomic DNA should result in a large variety of OR genes. To confirm this hypothesis, a PCR on genomic DNA was therefore performed; the PCR products were subcloned and nucleotide sequences of inserts from 9 randomly chosen recombinant plasmids were determined. Indeed, the PCR products cloned from the PCR on genomic DNA were a more heterogenous mixture of OR sequences than the RT-PCR product. Nucleotide sequence alignment (Fig. 4.7) revealed that all the clones were different ORs with 45-72% sequence homology.

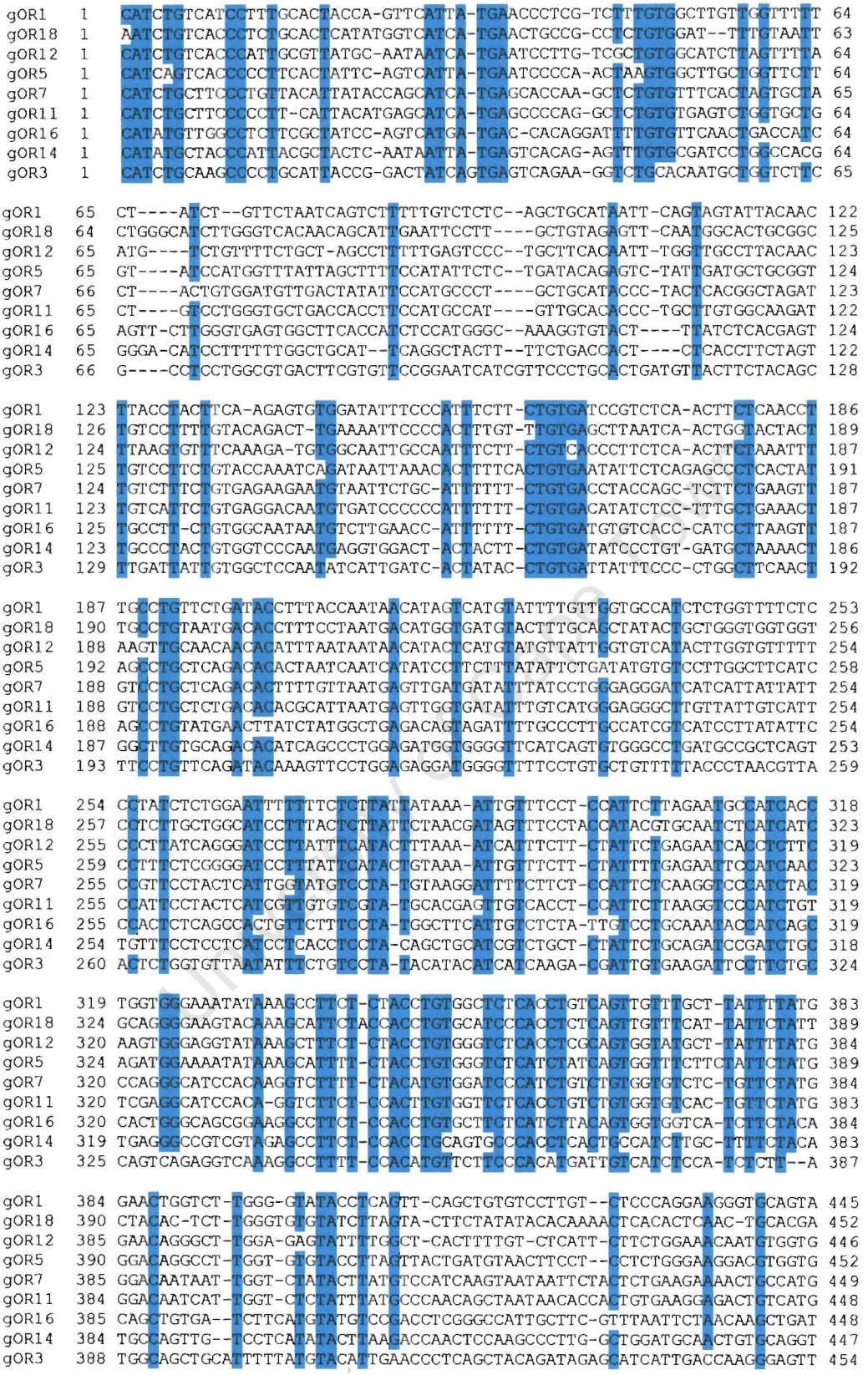

Figure 4.7: Nucleotide sequence alignments of the genomic olfactory receptor clones.

4.2.5 Repertoire of OR expression in differentiating OP27 cells changes at a later time point

In order to see whether OP27 expressed the same reportoire of ORs following FGF-2 induced differentiation, I analysed expression of ORs at a later time point. RNA was extracted from 5 pooled plates after 4 days of FGF-2 treatment. OR PCR products were cloned, the inserts were PCR-amplified as described above, and the PCR products digested with restriction enzymes that recognized each specific OR type described earlier (Table 4.4). SphI (specific for type 1) and PvuII (recognizes type 2) digested only one of the 18 day 4 OR clones to give the expected digestion pattern (Fig. 4.8A and B). PvuII additionally digested two other clones (27OR-1 and 27OR-24) but these did not result in the same digestion pattern as type 2, nor each other, thus suggesting that these were different OR genes. NheI and VspI which recognize type 3 and type 4, respectively, did not result in any digests at this stage of differentiation (Fig. 4.8C and D). These digest patterns would suggest that type 1, and type 2 are expressed again in an independent experiment. However, the majority of the OR clones were different. Nucleotide sequences of 9 randomly selected clones from this time point viz. 27OR-7, -10, -12, -14, -15,-18, -19, -20, and -23 were therefore determined and analyzed. All 9 clones encoded 4 additional putative OR types that were different from the clones described earlier. The 4 day time-point OR clones and the matching olfactory receptor proteins whose sequences are available in GenBank are summarized in Table 4.3. A sequence alignment of the deduced amino acid sequences of both the 2 day and 4 day time-point OR clones is shown in Fig. 4.9.

Table 4.2: Restriction enzyme digest patterns used to identify OR PCR products cloned from OP27 cells following 4 days of treatment with FGF-2. Digestion of PCR products of Type 1, 2, 3, and 4 ORs with SphI, PvuII, NheI, and VspI, respectively gives a unique restriction enzyme digest profile, shown in bp.

	SphI	PvuII	NheI	VspI
Type 1: OR-71	200/471 144/536			
Type 2: OR-84		157/200/313 191/197/313		
Type 3: OR-85			300/413 323/390	
Type 4: OR-86				334/377 311/400

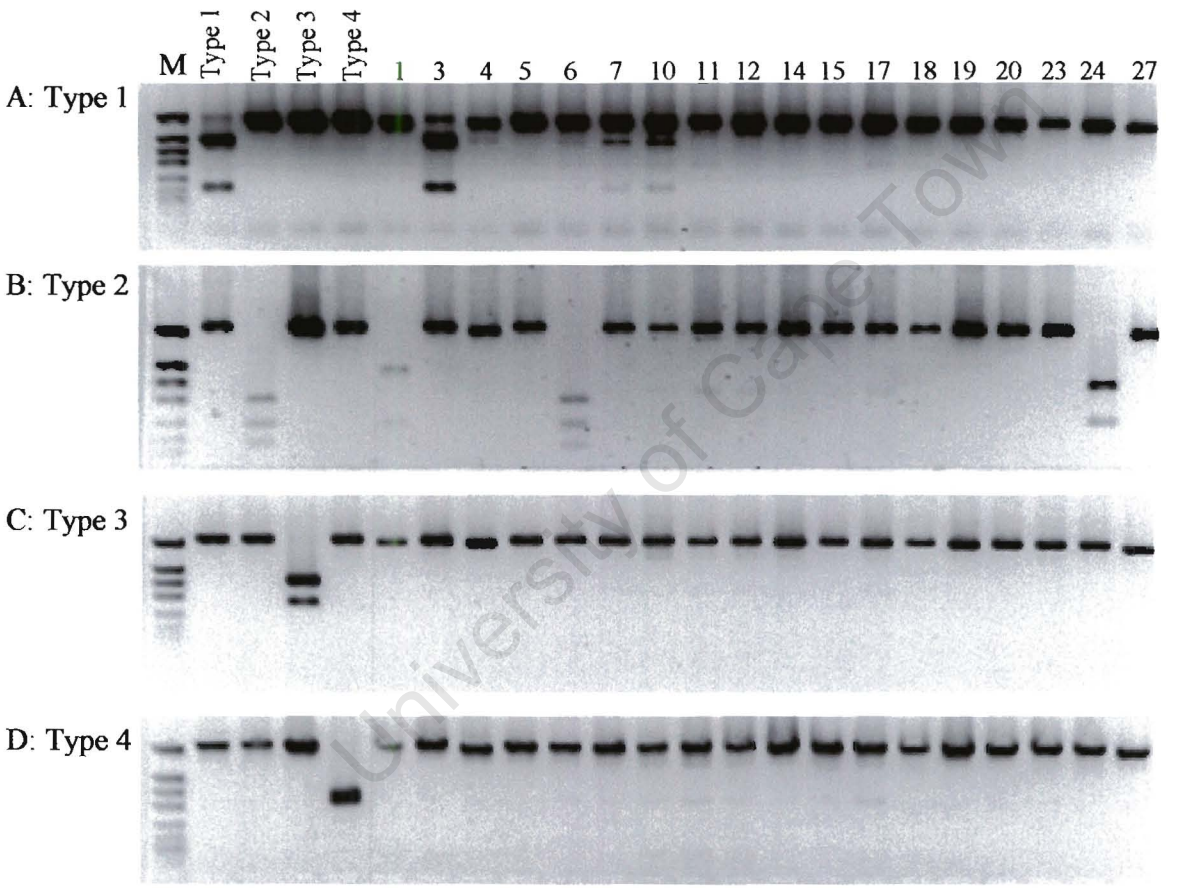

Figure 4.8: Restriction digestion analysis of OR transcripts cloned from OP27 cells that had been treated with FGF2 for 4 days. SphI (A), PvuII (B), NheI (C) and VspI (D) RE digests which recognised Type 1, Type 2, Type 3, and Type 4 OR, respectively, were used to characterise 18 OR PCR products cloned from OP27 cell cultures following 4 days treatment with FGF-2. SphI (A) digested OR3 PCR product while digestion of OR6 PCR product with PvuII (B) gave RE digest pattern consistent with Type 2 OR. PvuII also digested PCR products from OR1 and OR24 giving a different digest pattern. NheI (C) and VspI (D) did not digest any of the clones. OR71, 84, 85 and 86 were included as controls for Type 1, 2, 3, and 4 OR digests, respectively.

Table 4.3: Summary of 4 additional OR types that were expressed in OP27 cells after 4 days in FGF-2. The BLAST matches of the OR types are also included.

OR Type	Clones representing OR type	BLAST MATCH	Accession Number	Amino acid homology
Type 5	27OR-7, -10, -14, -18, -19	MOR256-23	XM_195302	96%
Type 6	27OR-15	MOR257-1	NM_146987	100%
Type 7	27OR-20	MOR165-6	NM_146787	100%
Type 8	27OR-12, -23	MOR257-4	AY073654	100%

```
Type 4: OR86  1   ICFPLHYTSIMSPKLCTCLMLLLWILTTSHAMMHTLLAARLSFCENNVILSFFCDLFAVLKLSCD-TY 67
Type 7: OR20  1   ICNPLLYNIVMSPKMCSYLMLGSYLMGFSGAMIHTGCVLRLSFCDGNIINHYFCDLLPLLQLSCTSTY 68
Type 2: OR84  1   ICHPLHYQFIMNPRLCGLLVFLSVLISLFVSQLHNSVVLQLTYFKSVDISHFFCDPSQLLNLACSDTF 68
Type 3: OR85  1   ICHPLHYTVLMNPKLCSQLLLLAWLISILGALPESLTALRLSFCAVVEIPHYFCELPEVLKLACSDTF 68
Type 1: OR69  1   ICHPLHYMIIMSTRRCGLMILACWIIGVINSLLHTFLVLRLSFCTNLEIPHFFCELNQVVHQACSDTF 68
Type 6: OR15  1   VCNPLRYTVVMNPRLCMGLAGVSWFVGVVNSAVETAVTMSLPTCGHNVLNHVACETLALVRLACVDIT 68
Type 8: OR23  1   VCNPLRYTVVMNPRLCMGLAGVSWFVGVVNSAVETAVTMRLPTCGHNVLNHVACETLALVRLACVDIT 68
Type 5: OR10  1   VCHPLHYTSIMHPLLCHALAISSWVGGLVNSLTQTSLIMTIPLCGH-HLNHFFCEMLVLLKLACEDTV 67

Type 4: OR86  68  INDLMILIFGGLIFIIPFLLIVISYARIISSILKVPSTQGIYKVFSTCGSHLSVVSLFYGTIIGLYLC 135
Type 7: OR20  69  VNEIEVLIVAGKDIIVPTVIIFISYGFILSSIFQMKSTKGMSKAFSTCSSHIIAVSLFFGSGAFMYLK 136
Type 2: OR84  69  TNNIVMYFVGAISGFLPISGIFFSYYKIVSSILRMPSPGGKYKAFSTCGSHLSVVCLFYGTGLGVYLS 136
Type 3: OR85  69  INNVVLYIVTGIMGFFPLAGILFSYSQIVTSVLRISTVRGKYKAFSTCGSHLSVVSLFYGTCLGVYLS 136
Type 1: OR69  69  LNDMVIYITAMLLAVGPFSGILYSYSRIVSPICAISSVQGKYKAFSTCASHLSVVSLFYCTPLGVYLS 136
Type 6: OR15  69  LNQVVILASSVVVLLVPCSLVSLSYAHIVAAIMKIRSTQGRRKAFETCASHLTVVSMSYGMALFTYMQ 136
Type 8: OR23  69  LNQVVILASSVVVLLVPCCLVSLSYAYIVTAILKIRSTQGRRKAFGTCASHLTVVSMSYGMALFTHME 136
Type 5: OR10  68  GTEANLFVAGAIILVCPVALILGTYAHIAHAVLKIKSRSGRRKALGTCGSHLTVVFLFYGSAMYMYLQ 135

Type 4: OR86  136 PSGNNSTVKEIAMAMMYTVVTP 157
Type 7: OR20  137 PNSTGTMNNGKIPSIIYTILIP 158
Type 2: OR84  137 SAVSLSPRKGAVASIVYTVVTP 158
Type 3: OR85  137 SIWIQASWAGVFASVLYTVVTP 158
Type 1: OR69  137 SAVTQNSHATATASLMYTVVTP 158
Type 6: OR15  137 PRSTASAEQDKLVVLFYAVVTP 158
Type 8: OR23  137 PTSTASAEQDKVVVVFYAVVTP 158
Type 5: OR10  136 PVHVYSGSEGKFAALFYTIITP 157
```

Figure 4.9 Alignment of the deduced amino acid sequences of the 27OR clones, between the primer regions MAYDRYVA at the end of TM3 and MLNPFIY in TM7. The clones were from both the 2 day time-point (Type 1-4) and 4 day time-points (Type 5-8) following treatment of OP27 cells with FGF-2.

4.2.6 Genomic organization of 27OR clones

A different set of ORs were expressed in OP27 cells in the retinoic acid experiment (Illing *et al.*, 2002), at the 2 day time-point and at the 4 day time point in FGF-2. In order to see whether these ORs were clustered together, or randomly distributed in the genome, I used the Entrez MapViewer tool available at the NCBI to determine the chromosomal localization of the ORs identified in differentiating OP27 cells. This analysis revealed that the OR types are widely distributed in the genome and most are found within OR clusters with OR genes from either the same family or different families. Some were found on the same chromosome but were mapped to distinct loci (Fig. 4.10). Type 2 and type 7, for an example, were located on chromosome 9 with an intergenic distance of ~18.5M (Fig. 4.10B,G). Similarly, type 4 and type 5 ORs occupy distinct positions on chromosome 11 (Fig. 4.10D, E). OR types 6 and 8 which had a very high amino acid sequence homology (Table 4.4; Fig. 4.9) were mapped adjacent to one another on chromosome 6 and have the same transcriptional orientation (Fig. 4.10F). Both genes belong to the same OR gene family (family 257, Zhang and Firestein, 2002). The type 1 OR and type 3 ORs were mapped to chromosomes 10 and 8, respectively (Fig. 4.10 A, C). Type 3 OR is one of only two OR genes housed in chromosome 8 (Zhang and Firestein, 2002). There was, therefore, no evidence for ORs being expressed in OP27 cells on basis of genomic organization.

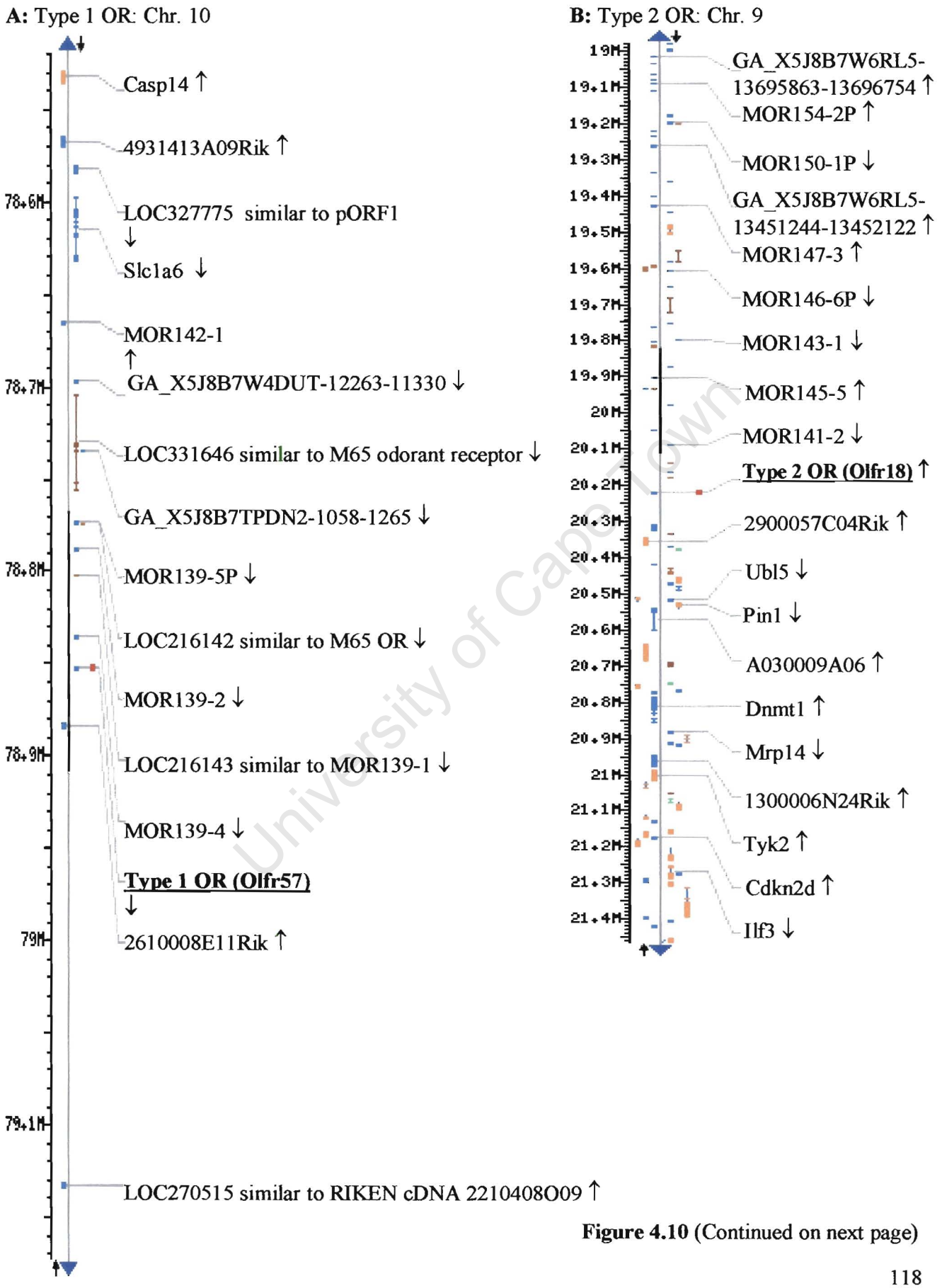

Figure 4.10 (Continued on next page)

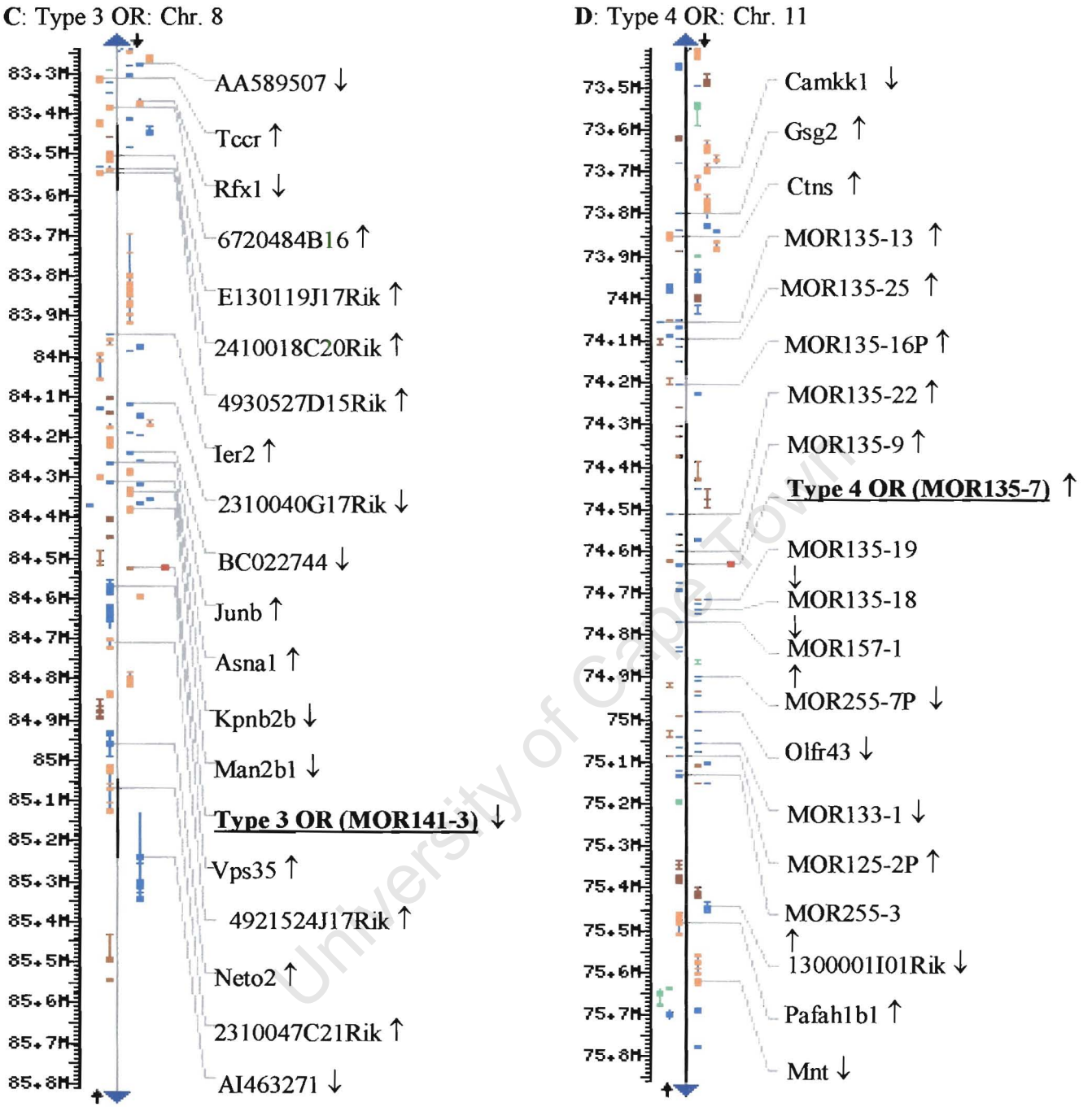

Figure 4.10 (Continued on next page)

E: Type 5 OR: Chr. 11

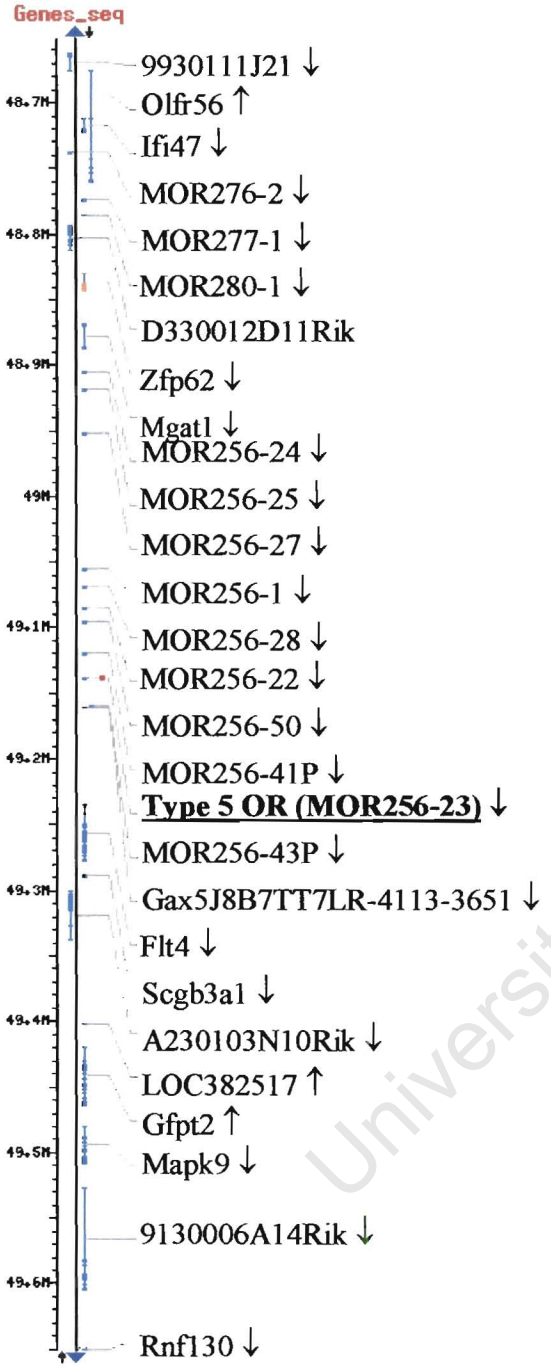

F: Type 6 and type 8 ORs: Chr. 6

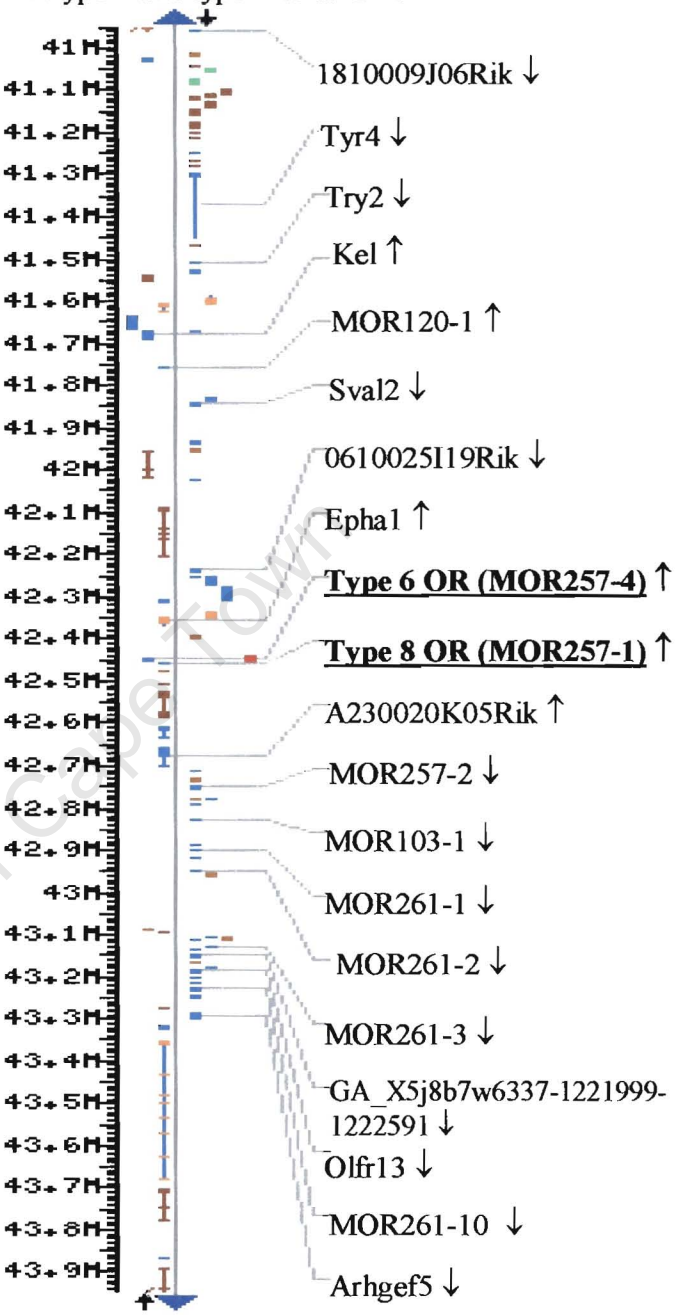

Figure 4.10 (Continued on next page)

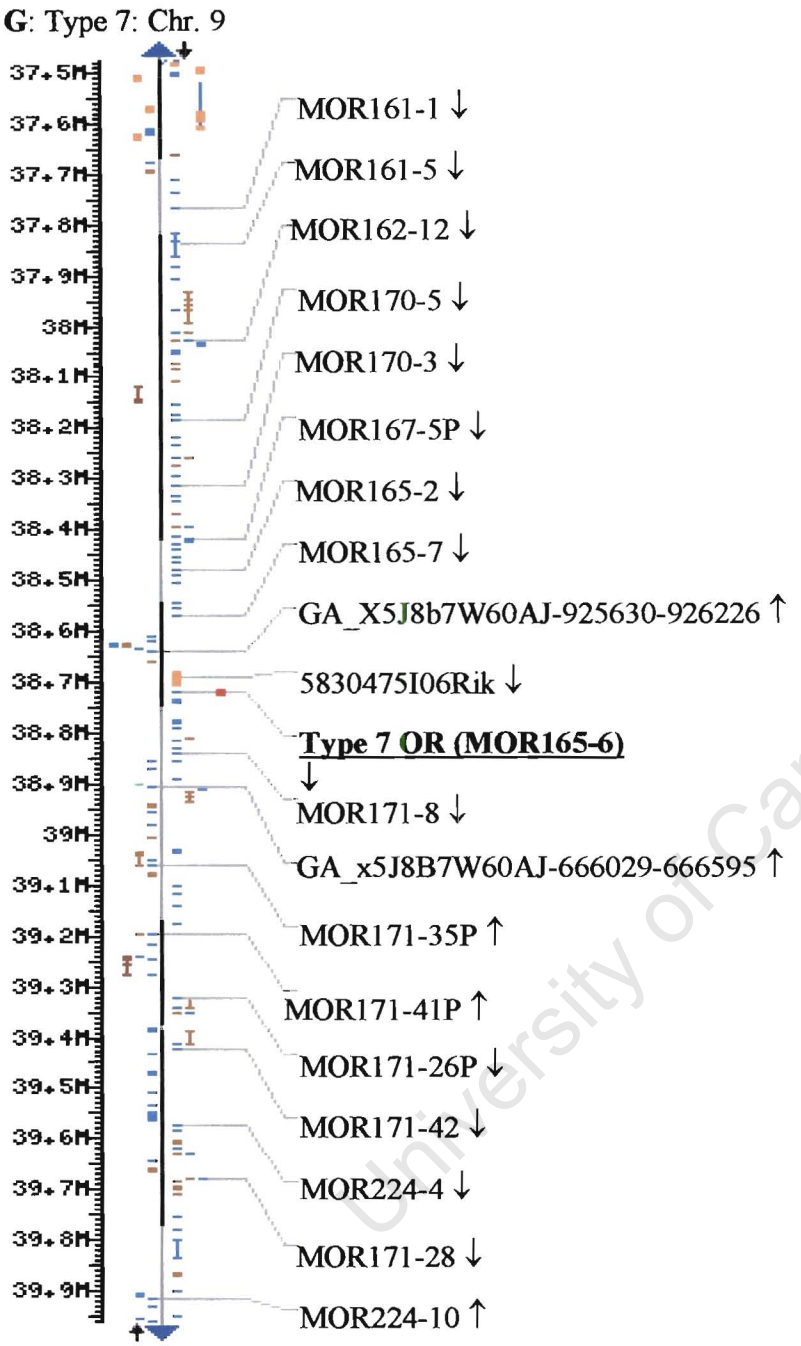

Figure 4.10 A Map View output of the genomic organization of the olfactory receptors identified in OP27 cells. The OR genes highly homologous to those expresssed in OP27 cells are shown in bold. The transcriptional orientation of the genes is indicated by the arrows. Arrows facing down represent the positive strand whilst arrows facing up represent the negative strand. The chromosome (Chr.) which houses the OR genes are indicated at the top of the map.

4.3 DISCUSSION

One fundamental characteristic of OR gene expression is that each ORN selects only one of the reported 1300-1500 genes in mice to express. Following induction with retinoic acid, the OP27 cell line was shown to express just one OR gene, the OR27-3 receptor (Illing *et al.*, 2002). I have investigated whether these cells were committed to express this particular receptor, or whether they could express different OR(s) following FGF-2 treatment. This investigation was carried-out using RT-PCR with degenerate primers that recognize conserved regions in OR sequences. A PCR product obtained from cells pooled from several culture dishes after 2 days of treatment with FGF-2 was cloned and restriction enzyme digest analysis of 24 clones indicated that they encoded 4 different types of OR transcripts with little homology between them and OR27-3. Moreover, a different OR repertoire was expressed by OP27 cells after 4 days of differentiation. RE digest analysis of 18 clones from a PCR product obtained at the 4-day time-point indicated that there were at least 4 types of OR transcripts expressed. These results are different from the results obtained in the retinoic acid experiment in which only the OR27-3 receptor was identified (Illing *et al.*, 2002). I have excluded any possibillty that the results obtained in this study may have been a consequence of genomic DNA contamination. Secondly, the expression of only OR27-3 in the retinoic acid experiment was reported from one time point only and from a single culture dish whereas in this study the expression of the small repertoire of OR transcripts was based on RNA extracted from OP27 cells pooled from several plates and from different time points. These observations would therefore suggest that the OP27 cell line is not committed to express a single receptor as previously suggested in Illing *et al* (2002). Instead, these cells are capable of expressing a small repertoire of OR genes each time they differentiate. It is likely that within the pool of OP27 cells a small percentage of the neurons express ORs, with each cell selecting one OR to express randomly and as a result, PCR was able to pick up expression of the

ORs from single cells. Whether individual cells indeed expressed only one OR could be resolved using single-cell RT-PCR.

An important question in this field is how an individual ORN selects an OR gene to express and how to ensure that only one and no other ORs are expressed. Several theories have been proposed. One of these was the genomic DNA rearrangement hypothesis that has since been disproved (Eggan *et al.*, 2004; Li *et al.*, 2004). There is also the possibility that specific combinations of transcription factors acting on gene-specific promoter regions activate the expression of only one gene. However, when two copies of the same OR transgene having the same regulatory sequence were tagged with different markers, it was found that only one of the two copies was expressed by individual ORNs (Serizawa *et al.*, 2000). This therefore makes theory that transcription factors may be involved in selecting one OR gene to activate unlikely. There is also the theory that a LCR may regulate the expression of individual OR genes within a cluster. Recent data have shown that a negative feedback mechanism mediated by the OR protein itself ensures that all the other ORs are not expressed in that cell (Serizawa *et al.*, 2003; Lewcock and Reed, 2004).

It has been suggested that the stage at which these genes are expressed along the neuronal lineage is likely to be important for understanding how a neuron chooses a single OR to express (Fan and Ngai, 2001; Brunjes and Greer, 2003; Iwema and Schwob, 2003). In their study using catfish, Fan and Ngai (2001) sought to determine the onset of OR gene expression along the ORN developmental pathway. They proposed that if the expression of these ORs was activated early in the lineage (i.e stem cells, transit amplifying cells or the immediate neuronal precursors) that would imply that the ORNs derived from a common mitotically active precursor would all express a specific OR transcript. However, their results were inconsistent with this hypothesis. They found that ORs were expressed only in

differentiated neuronal cells (no cells were doubly labelled with BrdU and OR riboprobes). They therefore concluded that the ORN precursors were not committed with regard to expression of OR. The onset of expression was activated later, such that ORNs derived from a common presursor would all express different ORs. The results that I have described in this study are consistent with this model of expression. At the non-differentiated state (at 33°C) the OP27 cell line has properties of a transit amplifying cell population (Illing *et al.*, 2002) that does not express OR genes as yet. The ORs were first detected at 2 days following treatment with FGF-2 and this was coincident with the up-regulation of GAP-43, a marker for immature ORNs, in these cells (Chapter 3). This suggests that both the commitment to express a particular OR (receptor choice) and the activation of ORs likely take place at the immature neuronal stage. Two other studies conducted in mice have reported similar patterns of expression. In one study, the expression of ORs was found to precede both the dissapearance of GAP-43 and the onset of OMP expression in adult mice (Iwema and Schwob, 2003). Similarly, the earliest expression of the mouse *M4* OR within the OE neuronal lineage was detected first in immature ORNs (Qasba and Reed, 1998).

The results obtained in this study with respect to OR expression in OP27 cells also confirm already published *in vivo* data that OR expression can be activated independent of signals from the olfactory bulb (Sullivan *et al.*, 1995; Fan and Ngai, 2001; Iwema and Schwob, 2003). Thus the OP27 cell line is the first OE *in vitro* model system to be shown to express endogenous ORs and this might render them useful in studying the regulatory mechanisms involved in OR expression. They could be useful for gene targeting and transfection studies in an attempt to elucidate these mechanisms. Another cell line, 3NA12, derived from the OE of H-2K^{b}-tsA58 transgenic mice has also been suggested to express ORs although this has not been experimentally demonstrated. This suggestion was based on the response

profiles of single cells of this line to a number of structurally different odorants. There was an even distribution of cells responding to each of the odorant ligands tested, with ninety percent of responsive cells being stimulated by only one odorant whereas only 10% responded to 2 odorants. None of cells were stimulated by more than 2 odorants (Barber *et al.*, 2000).

In conclusion, the OP27 cells are not committed to express a single OR. The expression of a small spectrum of OR genes in the cell line would suggest that there was simultaneous differentiation of a subpopulation of OP27 progenitor cells along different lineages with regard to OR gene expression. Secondly, because different spectra of OR genes were expressed at both the 2-day and 4-day time-points, it is likely that the decision of which OR to express is made *de novo* each time the neurons differentiate. Lastly, the ORs identified in this study are not co-localized in the genome but are widely distributed in different chromosomes thus suggesting that these cells are not committed to express ORs that are clustered in the genome.

Chapter 5

Characterization of the transcriptional expression of proneural bHLH transcription factors and Notch signalling pathway components in OP27 cells following treatment with FGF-2

5.1. Regulation of olfactory neuron development by bHLH and rHLH transcription factors

Data from analysis of pattern of gene expression and genetic studies has identified several transcription factors that regulate cell fate at different stages in the development of olfactory neurons. These transcription factors include members of the bHLH family (*Mash1, Ngn2, Ngn1, NeuroD, Hes1, Hes5*); the mammalian Olf1/EBF (O/E) family of repeated helix-loop-helix (rHLH) transcription factors (O/E1, O/E2, O/E3); homeodomain transcription factors (*Dlx5*); paired-box proteins (*Pax-6*), homeobox (*Otx2*) and winged-helix transcription factor (*Foxg1/BF-1*).

Studies conducted in mouse have shown that members of HLH proteins are sequentially activated to regulate olfactory neuronal development (Cau *et al.*, 1997; 2000; 2002), in a similar manner to that observed in primary neurogenesis (Fig. 1.6, Chapter 1). Analysis of the spatial and temporal pattern of expression of the bHLH genes, *Mash1, Ngn1,* and *NeuroD*, relative to markers for mitotic cells (identified by BrdU incorporation) and immature neurons (identified by expression of class III β-tubulin) revealed that they are expressed in different populations of cells during mouse olfactory placode development (Cau *et al.*, 1997).

Mash1 is the first of these transcription factors to be expressed. High expression levels were found preferentially in $BrdU^+$ apical and basal progenitor cell clusters that were found outside of the β-tubulin expression domains (Cau *et al.*, 1997; 2002). *Ngn1*, on the other hand, was transiently expressed in mitotically active basal cells that intermingled with β-$tubulin^+$ cells although there was no overlap between β-tubulin and *Ngn1* expression. *NeuroD* expression was expressed in the last cell division and at the beginning of differentiation of the postmitotic neurons as shown by double-labelling with β-tubulin. These patterns of expression would suggest that, in the mouse OE development the bHLH proteins are sequentially expressed, with *Mash1* at the beginning, followed by *Ngn1* and lastly *NeuroD* (Fig. 5.1), and that *Mash1* may specify the ORN fate by activating the expression of the other two bHLH genes. Indeed, deletion of *Mash1* results in the loss of *Ngn1* and *NeuroD* expression and, as a consequence, the block of neuronal differentiation (Cau *et al.*, 1997). Another bHLH transcription factor, *Ngn2* was found expressed in a subset of ORN progenitors that were independent of *Mash1* function. These *Ngn2* positive progenitors persist and continue to express *Ngn1* and *NeuroD* in the absence of *Mash1*. This suggests that *Ngn2* may have a similar function to that of *Mash1* in this cell population, activating both *Ngn1* and *NeuroD* (Fig. 5.1, Cau *et al.*, 1997).

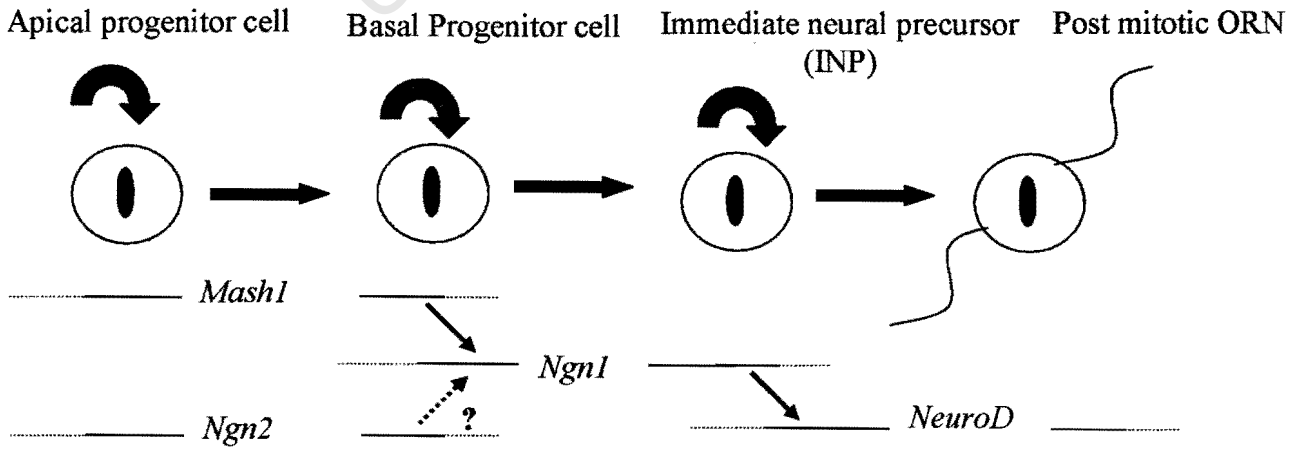

Figure 5.1 Sequential activation of bHLH transcription factors in mouse olfactory neuronal lineages. *Mash1* is expressed in the progenitor cell population (both apical and basal) and is followed by the expression of *Ngn1* in the immediate neuronal precursor (INP) and *NeuroD* by cells that are leaving the cell cycle to begin to differentiate into olfactory receptor neurons (ORN). *Ngn2* is also expressed in the OE but in a separate domain to that of *Mash1* but has not been determined whether it is expressed upstream of *Ngn1*.

5.1.1 The role of O/E-1 in olfactory development

O/E-1 was first cloned by genetic selection for transcription factors that bind to a conserved, *cis*-acting element found in promoters of several olfactory neuronal-specific genes, including OMP, olfactory cyclic nucleotide gated cation channel (OCNC), type III adenylate cyclase (ACIII), and $G_{olf\alpha}$ (Wang and Reed, 1993). Recently, several potential O/E-1 binding sites have also been identified in promoters of a human olfactory receptor gene cluster (Glusman *et al.*, 2000).

In the OE, the O/E-1 protein is transiently expressed in neuronal precursor cells that are leaving the cell cycle and begin to differentiate, well before the onset of expression of OMP, OCNC, $G_{olf\alpha}$ etc. Its expression is maintained in the neuronal cell layers of the OE. This pattern of expression suggests that O/E-1 has a critical role in ORN differentiation and may function to activate transcription of the ORN specific genes (Davis and Reed, 1996). It is likely that O/E-1 is a downstream target of *Mash1* since expression of O/E-1 mRNA transcripts was abolished in *Mash1* mutant OE (Cau *et al.*, 2002). Two O/E-1 mouse homologs, O/E-2 and O/E-3 have been identified. Genetic analyses have revealed that the functions of these proteins are, to a degree, redundant in olfactory development. While the expression of olfactory specific genes like OMP and components of the olfactory transduction pathway was not affected in *O/E-2* and *O/E-3* mutant mice, the olfactory bulb was reduced in size and ORNs failed to project to the olfactory bulb (Wang *et al.*, 2004).

5.1.2 Expression of *Otx2* in the olfactory neuronal lineage

Otx2 is a member of the homeobox gene family that has been implicated in the development of anterior regions of the nervous system, including the OE (Robel *et al.*, 1995; Mallamaci *et al.*,

1996). Immunocytochemical analysis of the OTX2 protein showed it was already expressed at the mouse placodal stage (E9.5-E10.0) before the formation of olfactory pits (Mallamaci *et al.*, 1996). In E14.5 OE explant cultures, *Otx2* mRNA was generally expressed in ORN precursor cells that were migrating away from the explant to begin to differentiate. Little or no expression was detected in differentiated ORNs and expression of the transcription factor was therefore proposed as a general marker for ORN progenitors (Calof *et al.*, 1996).

5.1.3 FoxG1 as a regulator of timing of neuronal differentiation

FoxG1, formerly known as brain factor 1 (BF-1), is a winged-helix transcription factor specifically expressed early in the telencephalic neuroepithelium and in the olfactory placode during embryonic development (Tao and Lai, 1992). In the telencephalon, the expression levels of *Foxg1* gene are highest in rapidly proliferating cells and levels decline once the cells become post-mitotic and begin to differentiate (Xuan *et al.*, 1995).

In *Foxg1* null embryos, the cerebral hemispheres of the telencephalon fail to expand as a result of the depletion of the neural progenitor pool. In these mutants, the neural progenitors exit the cell cycle and begin to differentiate prematurely thus retarding the growth of the telencephalon (Xuan *et al.*, 1995). The cerebral cortex of *Foxg1* null mice is characterized by an overproduction of early cortical neurons, the Cajal-Retzius neurons, at the expense of neurons that are normally generated later (Hanashima *et al.*, 2004). On the other hand, ectopic expression of *Foxg1* in the neural plate of *Xenopus* embryos leads to the expansion of the neuroectoderm while inhibiting neuronal differentiation (Bourguignon *et al.*, 1998). These studies suggest that the function of *Foxg1* is to maintain neural progenitor cells in a proliferative state and to control the timing of neuronal differentiation. FoxG1 has recently been shown to repress transcription directly via its DNA

binding domain, and indirectly by interacting with the transcription co-repressor Groucho/TLE and HES1 (Yao *et al.*, 2001).

FoxG1 is also an important regulator of cell proliferation and neurogenesis in the OE. Its mRNA transcripts are expressed early during the placodal stage (Tao and Lai, 1992; Illing *et al.*, 2002) and also in the OE at E14.5 (Calof *et al.*, 2002). The OE is also greatly reduced in size and most proliferating cells are missing in transgenic mice in which *Foxg1* is deleted, compared to wild-type embryos (Xuan *et al.*, 1995; Calof *et al.*, 2002). *Foxg1* may therefore play a very important role in the regulation of olfactory neurogenesis.

5.1.4 Regulation of olfactory neurogenesis by *Notch* signalling

A clue that lateral inhibition may be operating in the OE first came from *in situ* hybridization expression studies of the *Notch* signalling pathway components (Lindsell *et al.*, 1996). *Notch1* and its ligand *Delta1* were expressed in the basal progenitors whereas two other *Notch* homologues, *Notch2* and *Notch3* were found throughout the OE, except in the basal layer. Genetic studies carried out in the laboratory of Guillemot showed that lateral inhibition is instrumental in regulating the number of neuronal cells that are generated in the OE (Cau *et al.*, 2000; 2002). From these studies, it was shown *Notch* signalling regulates the ORN production at the level of the proneural transcription factors *Mash1* and *Ngn1* (Fig.5.2). This action is mediated by the *Notch* effectors, *Hes1* and *Hes5*, which have distinct expression patterns in the OE progenitors. At E12.5, when the OE has attained its layers, *Hes1* transcripts are found only in most progenitors at the apical side of the OE before the onset of *Mash1* expression. *Hes1* mutants display ectopic expression of *Mash1* in cells that do not normally express it and an increase in the number of *Mash1*$^{+}$ cell clusters. At this stage *Hes1* functions as a prepattern gene, independent of Notch signalling, to restrict expression of

Mash1 in the apical progenitors. *Hes1* is expressed together with the *Notch* ligand *Ser1(Jag1)* in apical progenitors downstream of *Mash1* as shown by targeted mutation of *Mash1*. It is proposed that *Mash1* selects apical progenitors that will become basal progenitors by activating *Notch* signalling. Therefore, the *Notch* ligand *Ser1* and effector *Hes1* regulate production of basal progenitors by targeting *Mash1* (Fig 5.2).

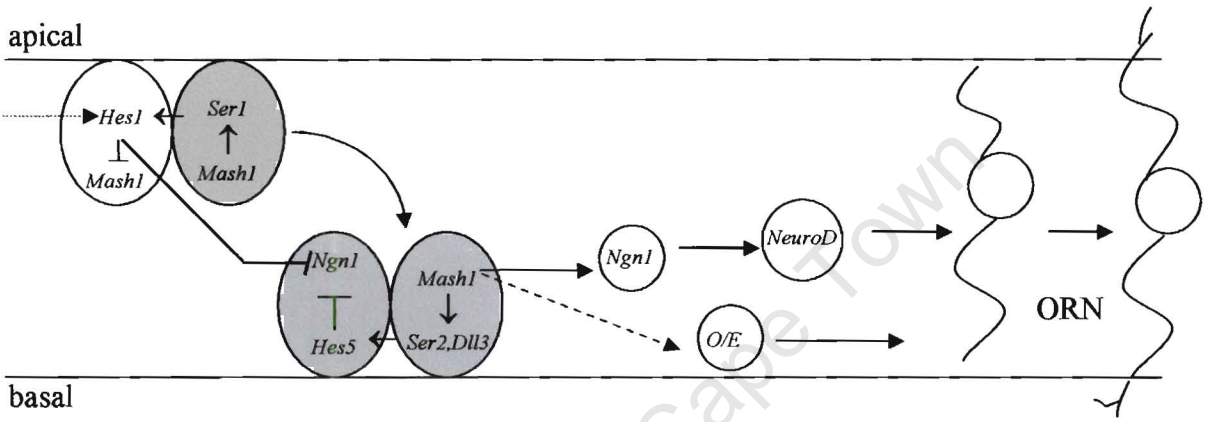

Figure 5.2 Interaction of positive bHLH transcription factors *Mash1*, *Ngn1*, and *NeuroD* and the negative bHLH regulators *Hes1* and *Hes5* in regulating olfactory neurogenesis. Shown above is a schematic representation of the OE at E12.5 showing the apical (top) and basal (bottom) sides of the neuroepithelium. Both sides are populated by lineage related progenitor cells that express defined sets of positive and negative regulators of olfactory neurogenesis. The apical progenitors express *Mash1*, the *Notch* ligand *Serrate1* (*Ser1*), and the effector *Hes1*. *Mash1* selects progenitors that will differentiate into basal progenitors by activating the expression of *Ser1* and *Hes1* through *Notch* signalling (lateral inhibtion). Through *Hes1* activation (downstream of *Notch* signalling), *Mash1* expression is repressed in some apical progenitors and as a result these cells are not fated to become basal progenitors. *Hes1* is also activated independently of *Notch* signalling (indicated by the dashed arrow in the diagram) to limit the expression of *Mash1* in the apical progenitors (Cau *et al.*, 2000). The apical progenitors fated to become basal (shown in grey) translocate into the basal side of the neuroepithelium and continue to divide. In this population of progenitors *Mash1* has been shown to also activate lateral inhibition through a distinct set of *Notch* ligands and effectors. The ligands, *Delta like 3* (*Dll3*) and *Serrate2* (*Ser2*) and the effector *Hes5* are activated downstream of *Mash1* function. *Hes5* then synergizes with *Hes1* to repress expression of the transcription factor *Ngn1* which is required for neuronal differentiation of the basal progenitors. *Mash1* also activates at least 2 downstream programs of ORN differentiation in the basal progenitors. In one programme, *Ngn1* is required to activate the expression of the differentiation gene *NeuroD* and to generate ORNs. Members of the Olf1/EBF family (*O/E-1*, *O/E-2* and *O/E-3*), shown to be functionally redundant for the expression of olfactory-specific genes (Wang *et al.*, 2004), are also activated in a programme of ORN differentiation downstream of *Mash1* function but independently to *Ngn1* expression (Cau *et al.*, 2002).

The basal progenitor population is characterized by the expression of a distinct set of *Notch* ligand and effector molecules from that found in apical progenitors, namely, *Dll3*, *Ser2*, and *Hes5*. These have been shown to regulate the production of ORNs at the level of *Ngn1*. At this level, *Hes5* co-operates with *Hes1* to negatively regulate ORN neuronal differentiation by repressing the

expression of *Ngn1* which is required for the differentiation of ORNs. Thus, Notch signalling regulates olfactory neurogenesis in at least 2 different steps along the neuronal pathway (Fig.5.2).

The regulatory loop involving *Mash1* and *Notch* signalling ensures that not all the apical progenitors generate basal progenitors that are destined to become the ORNs. Instead, an alternative fate is probably promoted at the expense of the neuronal lineage. The sustentacular cells, the non-neuronal cells in the OE, are thought to be generated by apical progenitor cells in the adult OE (Cau *et al.*, 2002). Targeting of *Mash1* by the *Notch* pathway in apical progenitors would probably promote the generation of these cells. Recent *Mash1* knockouts studies have shown that the majority of the cells in the mutant OE express *Steel,* a marker for sustentacular cells (Murray *et al.*, 2003).

5.1.5 Regulation of intrinsic molecules by extrinsic signals in olfactory neurogenesis

As shown earlier, vertebrate neurogenesis is regulated by both intrinsic and extrinsic factors, starting from the early commitment of multipotential neural progenitors, right to their terminal differentiation into neuronal cells. How the various secreted signals and the intrinsic transcription factors co-operate in regulating this process remains largely unknown. There is evidence that extrinsic signals regulate expression of these transcription factors. In the differentiation of neural crest progenitor cells into autonomic neurons, *Mash1* is required for competence of the cells to respond to BMP2, a member of the BMP subclass of TGFβ proteins. Exposure of the neural crest progenitor cells to BMP2 maintains *Mash1* expression and leads to differentiation. *Mash1* on its own is not sufficient to drive neurogenesis and cells that initially express the transcription factor but not exposed to BMP2 fail to differentiate (Edlund and Jessel, 1999; Lo *et al.*, 2002). In the OE, members of both FGF and BMP families have been shown to play integral roles in the regulation of

neurogenesis in this tissue (Chapter 3; Shou *et al.*, 1999; 2000). BMPs have been shown to regulate neuron number in E14.5-15.5 OE explant cultures by targeting *Mash1*. At low concentrations (0.1ng/ml), BMP4 has a stimulatory effect on neurogenesis, promoting the survival of newborn neurons. At high concentrations (10ng/ml) it blocks proliferation of $MASH1^+$ progenitors and their subsequent differentiation by mediating a rapid proteasome-dependent degradation of MASH1 (Shou *et al.*, 1999). Overexpression of *Notch* in small-cell-lung cancer cells has been shown to also down-regulate the HASH1 protein (the human homolog of MASH1) via the same degradation pathway (Sriuranpong *et al.*, 2002). It is therefore possible that in the OE, *Notch* signalling and high BMP levels may co-operate to negatively regulate OE neurogenesis.

FGF-2, on the other hand, has been shown to have a stimulatory effect on OE neurogenesis by promoting proliferation of the putative ORN stem cell and that of the INP (DeHamer *et al.*, 1994; Calof *et al.*, 2002). I have also shown that FGF-2 promotes neurogenesis in OP27 cells, first promoting proliferation and subsequently, neuronal differentiation. However, whether FGF-2 exerts any effects on the regulation of the transcription factors has not been explored. In this chapter I have studied the effect of FGF-2 on the expression of transcription factors that are important for OE neurogenesis. I have also studied the expression patterns of the components of the Notch signalling pathway during FGF2- induced differentiation of OP27 cells.

5.2 RESULTS

5.2.1. Expression of intrinsic components of neuronal differentiation in OP27 cells

To begin to determine whether FGF-2 has any role in the regulation of the various transcription factors, I first analysed the expression patterns of these proteins at the mRNA level in OP27 cells.

RT-PCR analysis with specific primers was used to determine which of these components were contained in OP27 cells at the undifferentiated state (at 33°C) and at 6, 24 and 48 hours following FGF-2 treatment.

The earliest marker in the OE neuronal lineage is *Mash1*, with high expression levels in apical and basal progenitor cells before *Ngn1* and *NeuroD* (Fig. 5.1). I could not detect any *Mash1* mRNA transcripts in OP27 cells whether at the undifferentiated state or following treatment with FGF-2 (Fig. 5.3A). mRNA transcripts of another early marker, the bHLH transcription *Ngn2* were also not detected in these cells (Fig. 5.3B). *Ngn2* is expressed by a subset of progenitor cells in the ventrocaudal domain of the olfactory placode independent of *Mash1* expression (Fig. 5.1 Cau *et al.* 1997). The primers used to amplify both *Mash1* and *Ngn2* were able to amplify the specific products of expected sizes from genomic DNA (Fig. 5.3A, B).

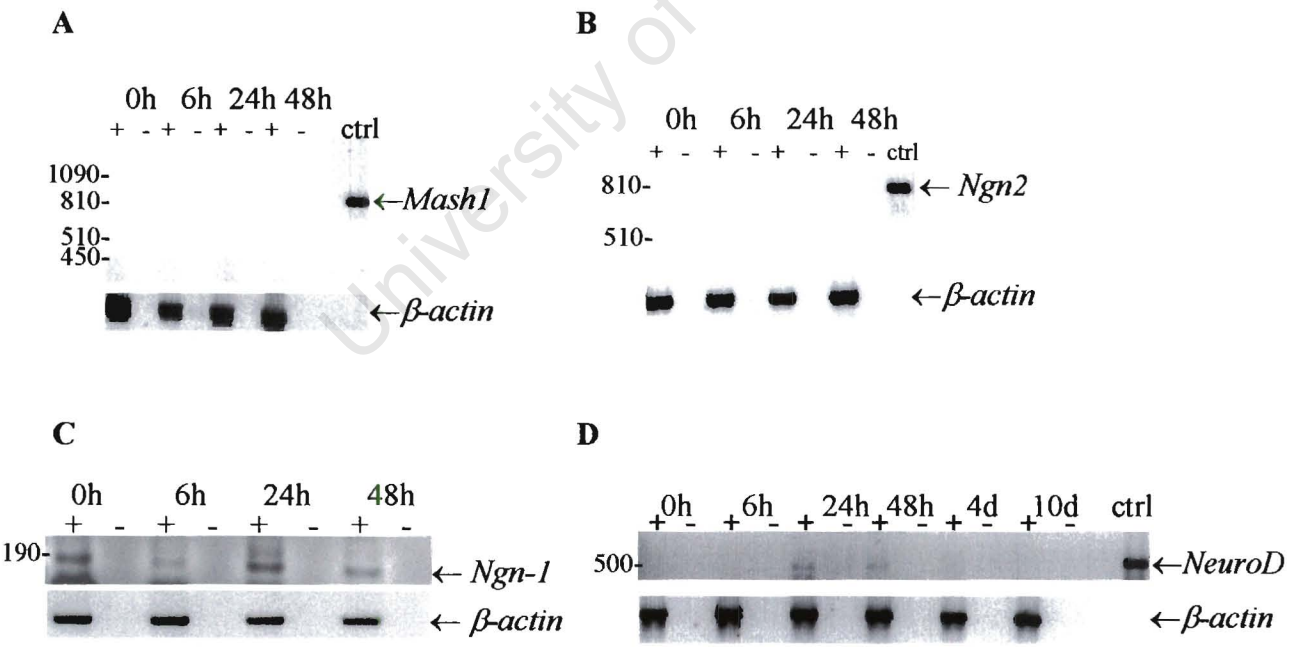

Figure 5.3 Expression profiles of positive regulators of ORN lineage development in OP27 cells. RT-PCR analysis for the various positive regulators of olfactory neuronal differentiation was conducted in OP27 cells when maintained at 33°C (0h) and when treated with FGF-2 at 39°C for various times (h, hours; d, days). Mouse genomic DNA was used as a positive control (ctrl) in all the RT-PCRs. OP27 cells do not express the cDNAs for *Mash1* (454 bp) and *Ngn2* (545 bp). +, reverse transcribed cDNA template; -, RNA sample that was not reverse transcribed used as a negative control. Primers for β-actin were used as control for loading of samples. Molecular weight sizes (in base pairs, bp) are shown on the left of each gel.

The expression of *Ngn-1* and *NeuroD* has been shown to under the control of *Mash1*and mark the population of dividing immediate neuronal precursors and the onset of neuronal differentiation of the postmitotic cells (Cau et al., 1997; 2002). *Ngn1* transcripts could be detected at in OP27 cells at 33°C and up to 2 days following treatment with FGF-2 (Fig. 5.3C). No *Ngn1* transcripts were ever detected after 2 days. *NeuroD,* on the other hand, was not present in OP27 at the non-differentiated state but could be detected after 24 hours and 48 hours following treatment with FGF-2, with the levels lower at the 48-hour time point. No PCR product was ever detected after 48 hours in FGF-2 (Fig. 5.3D).

Next to be analysed were the transcript profiles of *Otx-2* and *O/E-1*. *Otx-2* has been suggested to be expressed by neuronal precursor cells or transit amplifying cells down-stream of *Mash1* in the olfactory neuronal lineage (Calof *et al.*, 1996; 2002). OP27 cells expressed both *Otx-2* and O/E-1 transcripts both at 33°C and after treating the cells with FGF-2. Levels did not change in response to FGF-2 treatment during the 48 hours (Fig 5.4).

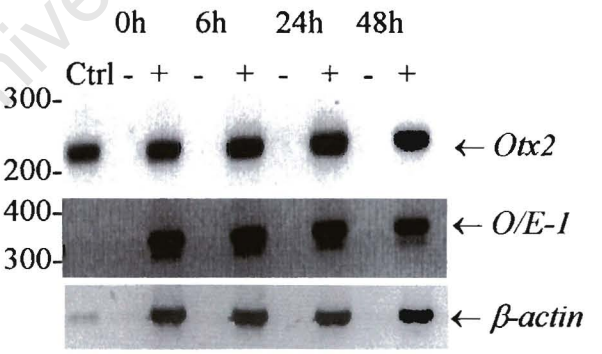

Figure 5.4 Expression of *Otx-2* and *O/E-1* transcription factors in OP27 cells. RT-PCR analysis for *Otx-2* and *O/E-1* was conducted in OP27 cells when maintained at 33°C (0h) and when treated with FGF-2 at 39°C for various times (h, hours). Mouse genomic DNA was used as a positive control (ctrl) in all the RT-PCRs. +, reverse transcribed cDNA template; -, RNA sample that was not reverse transcribed used as a negative control. Primers for β-actin were used as control for loading of samples. Molecular weight sizes (in base pairs, bp) are shown on the left of each gel.

The expression profiles of *Notch*, its ligand *Delta* and both effectors, *Hes1* and *Hes5*, were also examined in OP27 cells. The messages for both *Notch1* and *Delta1* could be readily detected in OP27 cells at 33°C and at 39°C with FGF-2 treatment (Fig. 5.5A), with *Delta1* levels beginning to increase around 2 days after FGF-2 treatment (Fig. 5.5B).

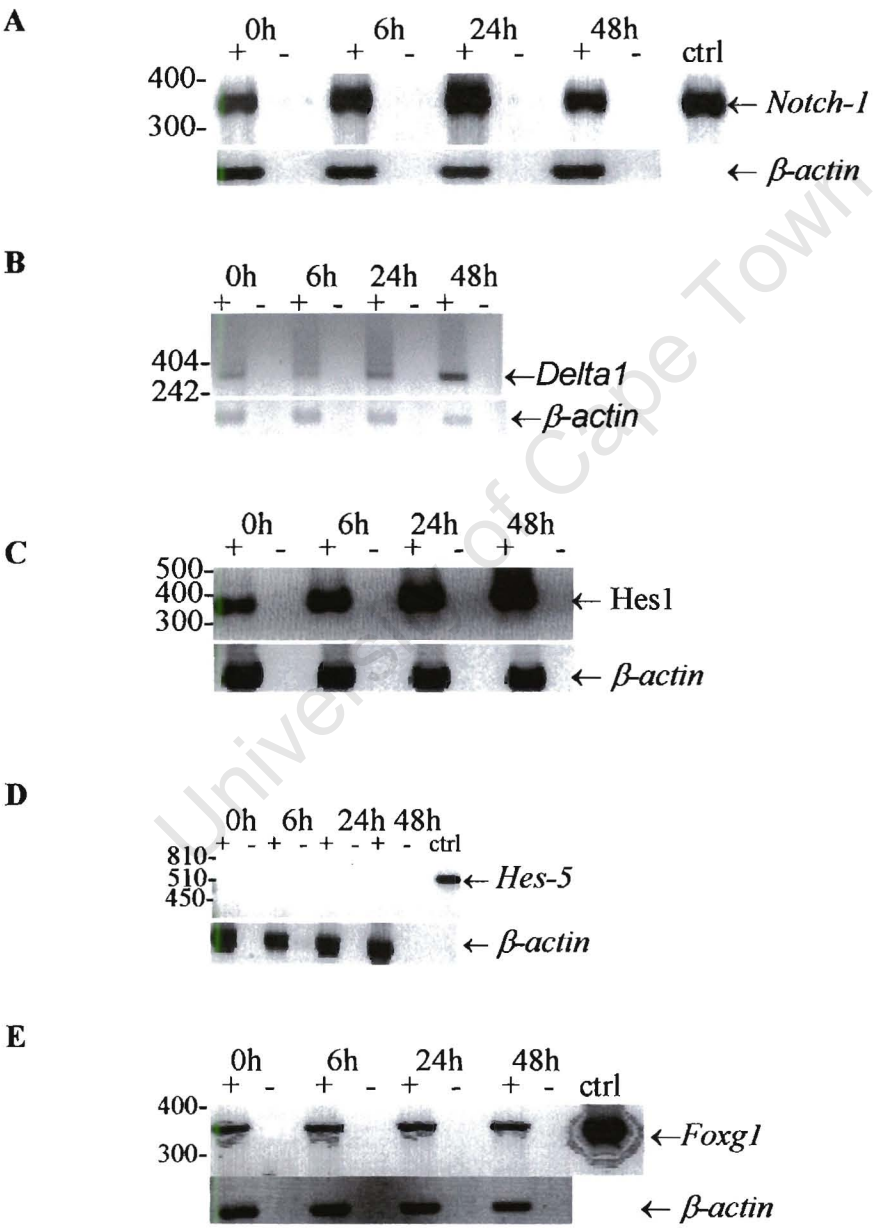

Figure 5.5 Expression of *Notch1*, its ligand and bHLH effectors in OP27 cells. RT-PCR analysis for *Notch* signalling components was conducted in OP27 cells when maintained at 33°C (0h) and when treated with FGF-2 at 39°C for various times (h, hours). Mouse genomic DNA was used as a positive control (ctrl) in all the RT-PCRs. OP27 cells do not express the cDNA for *Hes5* (449 bp) but the 592 bp genomic fragment could be detected using the sampe primers. +, reverse transcribed cDNA template; -, RNA sample that was not reverse transcribed used as a negative control. Primers for β-actin were used as control for loading of samples. Molecular weight sizes (in base pairs, bp) are shown on the left of each gel.

Notch signalling suppresses neuronal differentiation through the induction of bHLH transcription factors, *Hes1* and *Hes-5* that inhibit both the expression and/or transcriptional activity of *Mash1* and *Ngn-1*. Only *Hes1* transcripts could be detected in OP27 cells with levels increasing once the cells were cultured at the non-permissive temperature with FGF-2 (Fig. 5.5C). The primers for *Hes-5* were able to amplify the expected transcript in the genomic DNA template (592 bp) but never in the OP27 cDNA (449 bp) (Fig.5.5D). The transcription factor *Foxg1* (BF-1) which was shown to interact with *Hes1* to repress transcription (Yao *et al.*, 2001), was expressed in OP27 cells before and after treatment with FGF-2 with levels not changing with treatment (Fig. 5.5E).

5.2.2 Changes in expression levels of the various transcriptional markers following treatment with FGF-2.

Only one model that integrates the regulation of transcription factors with extracellular signals during the olfactory neuronal lineage has emerged (see section 5.1.5). I therefore sought to examine whether FGF-2 had any influence on the expression levels of the messages contained in the OP27 cells. In Fig.5.3- Fig.5.5 it was established that the OP27 cells expressed a panel of both positive and negative regulators of neuronal differentiation thus making these cells suitable for use as model system to study the interplay between extrinsic signals and transcription factors during olfactory neurogenesis. A semi-quantitative RT-PCR approach, using fewer PCR cycles, was therefore used to analyse the transcriptional levels of the genes following FGF-2 induced differentiation.

Semi-quantitative RT-PCR is a very useful technique to measure changes in the level of expression of very low abundant mRNA transcripts (e.g. transcription factors) between samples during cellular processes such as differentiation (Foley *et al.*, 1993). It is still widely used and is much more sensitive than the more commonly used northern blotting and ribonuclease protection assays (Marone *et al.*, 2001; Santagati *et al.*, 1997). The gene of interest is amplified either in parallel or

co-amplified with a house-keeping gene that acts as an internal control whose expression does not vary with the experimental condition. The internal controls that are commonly used in semi-quantitative RT-PCR include β-actin, glyceraldehyde-3-phosphate dehydrogenase, 18S ribosomal RNA and tubulin (Thelin *et al.*, 1999). The co-amplification of both the gene of interest and the housekeeping gene controls for the variation in template concentration and amplification efficiency. This permits the quantitation of the gene under study relative to the internal control. Quantitation is performed when the PCR reactions are in the linear range of amplification for both transcripts before the reaction components become limiting (Foley *et al.*, 1993). The β-actin was used as an internal control in this study as it was shown by northern blotting that its mRNA levels do not change with FGF-2 treatment of OP27 cells (see Chapter 6).

When the OP27 cells were shifted to the non-permissive temperature and induced to differentiate with FGF-2, transcript levels of *Delta* and *Hes1* genes were observed to change while that of others did not. *Notch-1* levels were not observed to change significantly with FGF-2 treatment when compared with the control cultures (Fig. 5.6A). On the other hand, the *Delta* mRNA levels were significantly up-regulated 48 hours after FGF-2 treatment and levels remained significantly higher than the levels of cells at the non-differentiated state (Fig. 5.6B). In a similar fashion, *Hes1* transcripts were significantly increased in FGF-2 treated OP27 cells but the up-regulation preceeded that of *Delta* by 24 hours. *Hes1* levels were maintained higher until 10 days after treatment with FGF-2 (Fig. 5.6C).

The transcripts of another negative regulator, *Foxg1* were also analysed. *Foxg1* has been shown to potentiate the repressive effects of *Hes1*. However, no appreciable changes were observed in its transcripts following induction of OP27 cells with FGF-2 (Fig. 5.6D).

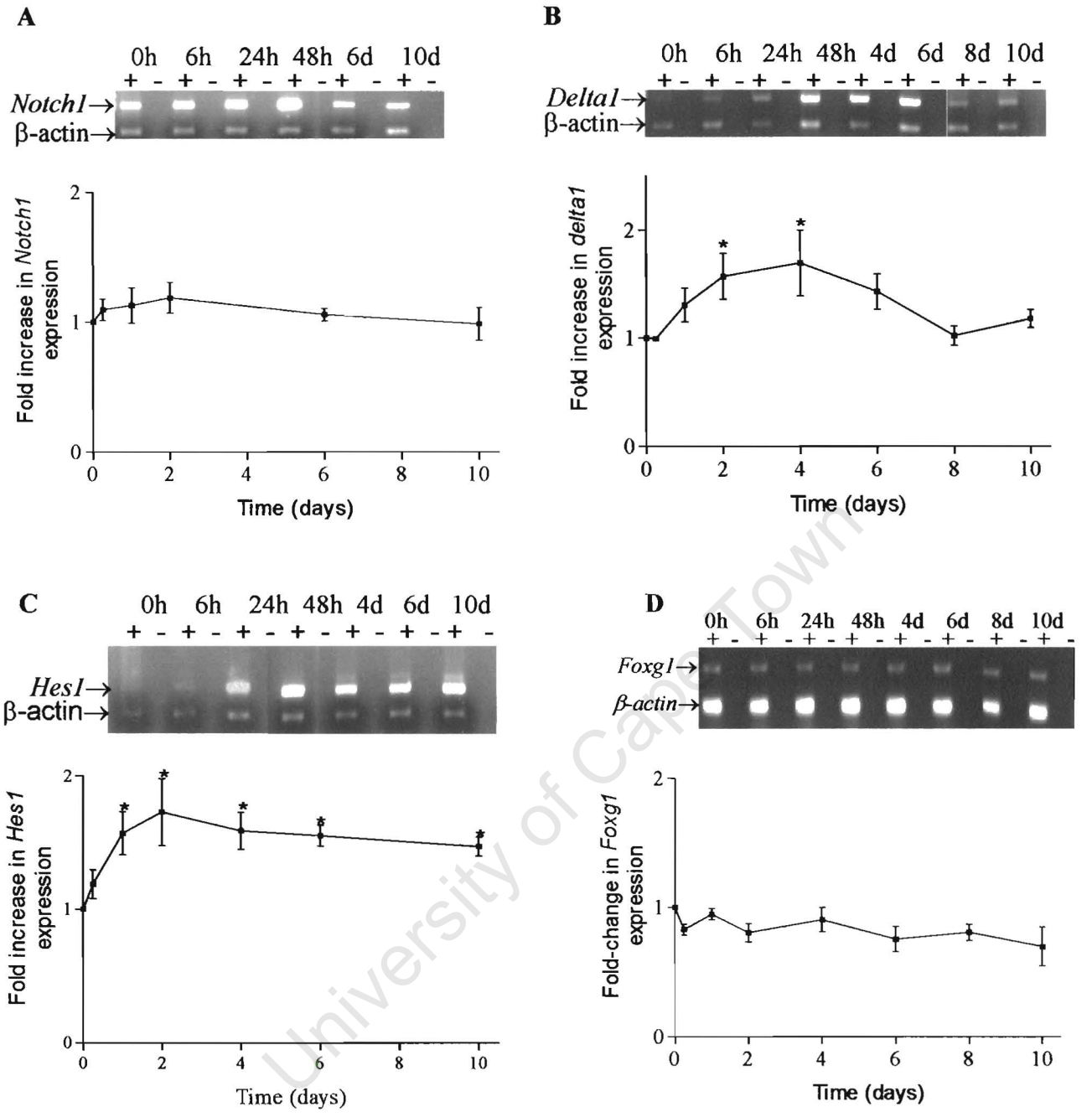

Figure 5.6 Regulation of *Notch* signalling components in OP27 cells. Representative semi-quantitative RT-PCR analyses of *Notch1*, *Delta1*, *Hes1* and *Foxg1* mRNAs in OP27 cells treated with FGF-2 for the indicated times. Cells that had not been treated (33°C) were included as controls. The genes were co-amplified with β-actin. h, hours; d, days. (+) amplification from RNA that had been reverse transcribed, (-) RNA that were not reverse transcribed as negative controls. mRNA levels were determined by densitometric scan of the bands at each time-point and normalized to β-actin. Data are expressed as fold increase in the ratio of gene-of-interest/β-actin with the value of the cells at 33°C (time 0) taken as 1. Data represent mean ± SEM values of 3 independent experiments. Significance, *P<0.05 compared to control experiment at 0 days.

After 2 days in FGF-2 OP27 cells were observed to change into a bipolar morphology. This apparent neuronal differentiation should be accompanied by changes in transcript levels of positive neuronal regulators. In the OE neuronal lineage *NeuroD* marks the population of cells at the last cell cycle before they differentiate. In OP27 cells *NeuroD* was expressed after 24 hours with FGF-2 (Fig. 5.3D). This is the time that transcript levels of *Hes1* have reached a maximum. O/E-1, like *neuroD*, is transiently expressed during the last cell cycle and beginning of neuronal differentiation (Davis and Reed, 1996). In OP27 cells O/E-1 is expressed before the onset of *NeuroD* expression. There was no significant change in *O/E-1* mRNA levels within the first 6 days but levels decreased thereafter (Fig. 5.7).

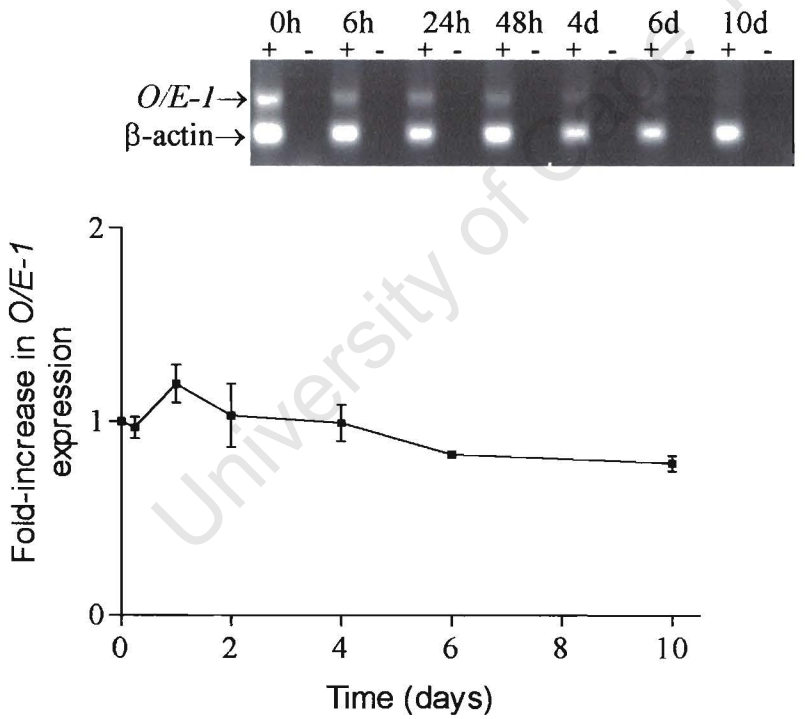

Figure 5.7 Regulation of *O/E-1* in OP27 cells. Representative semi-quantitative RT-PCR analyses of *O/E-1* mRNAs in OP27 cells treated with FGF-2 for the indicated times. Cells that had not been treated (33°C) were included as controls. The genes were co-amplified with β-actin. h, hours; d, days. mRNA levels were determined by densitometric scan of the bands at each time-point and normalized to β-actin. Data are expressed as fold increase in the ratio of gene-of-interest/β-actin with the value of the cells at 33°C (time 0) taken as 1. Data represent mean ± SEM values of 3 independent experiments.

5. 3 Discussion

RT-PCR analysis of OP27 cells has shown that the Notch receptor, its ligand Delta and the effector Hes1 are all expressed in these cells. This expression pattern indicates that Notch signalling, which mediates lateral inhibition between neighbouring cells, may be active in OP27 cells. While FGF-2 had no significant effect on the transcript levels of *Notch*, levels of both *Hes1* and *Delta1* were significantly up-regulated by FGF-2 treatment with the up-regulation of *Hes1* preceding that of *Delta1*. *Hes1* was up-regulated within 24 hours following treatment with FGF-2. This is the time when the OP27 cells have not displayed any gross morphological changes yet (Fig. 3.5). It has been shown that overexpression of the *Hes1* gene results in the delay or suppression of neuronal differentiation by maintaining neural stem cells in a proliferative state (Ohtsuka *et al.*, 2001). The up-regulation of the *Hes1* gene in OP27 cells at 24 hours may be required to delay the differentiation of these cells. The inhibition of neuronal differentiation is mediated via the transcriptional repression of other bHLH transcription factors such as Mash-1 and Ngn-1 by HES1. In the OE neuronal lineage HES1 has been shown to restrict the expression of *Mash-1* and later to repress the transcription of *Ngn1* downstream of *Mash1* (Fig. 5.2). While no *Mash1* transcripts could be detected in OP27 cells, *Ngn1*, which marks the population of INPs in the OE neuronal lineage (Fig. 5.1) was present in low levels (judging by the faint bands following 35 cycles of PCR, Fig. 5.3C). Low *Ngn1* levels in these cells probably indicate an enhanced *Notch* signalling that restricts the expression of this transcription factor.

The actions of FGF-2 within the first 24 hours are consistent with the work done by Faux *et al.* (2001) on murine forebrain neuroepithelial precursor (NEP) cells. FGF-2 was found to influence the differentiation of NEP cells by differentially regulating the expression of both *Notch* and

Delta1. In the presence of FGF-2, NEP cells were maintained the NEP cells in a proliferative state by up-regulating *Notch* expression while *Delta1* was repressed.

By the definition of lateral inhibition, the cells that are fated to become neurons up-regulate Delta1 and subsequently activate Notch signalling in the neighbouring cells thus inhibiting them from differentiating into neuronal cells. The significant up-regulation of *Delta1* at 2 days and its maintained high levels after that (Fig. 5.6B) is concomitant with the emergence of differentiating OP27 cells with a bipolar morphology at 2 days and an increase in the number of the bipolar cells with time (Fig. 3.6). Up-regulation of *Delta1* in OP27 cells is also concomitant with the onset of *NeuroD* expression, which is indicative of a pathway leading to neuronal differentiation. In *Xenopus* the expression of *X-Ngnr-1* precedes then overlaps that of *X-Delta-1* whereas *XneuroD* is expressed later (Ma *et al.*, 1996). Ngn-1 has been shown to activate the expression of both *Delta1* and *NeuroD* (Ma *et al.*, 1996; Cau *et al.*, 2002). Thus, following treatment of OP27 cells with FGF-2 for 2 days, Ngn1 probably up-regulates *Delta1* expression and in addition, it may also lead to expression of *NeuroD* and the subsequent neuronal differentiation. The patterns of expression of both *Ngn1* and *NeuroD* suggested that these were transient in OP27 cells, consistent with their expression in olfactory progenitors *in vivo* (Cau *et al.*, 1997) and in cerebral cortex primary cultures in vitro (Katayama *et al.*, 1997).

It is paradoxical that the neuronal differentiation of OP27 cells occurs in the midst of high levels of *Hes1*given that it is a negative regulator of this process. *Hes1* is first up-regulated at 24 hours before *Delta1* levels are increased. Whether the initial up-regulation *Hes1* was mediated by Notch signalling is unclear. However, later lateral inhibition activated by increased Delta1 may have maintained levels of *Hes1* high. Following up-regulation of the ligand in some cells, Delta1 signals to adjacent cells which increase *Hes1* expression, which mediates the suppression of neuronal

differentiation. This suggests that there are two subpopulations of OP27 cells, with one differentiating (with high *Delta1* levels) and other proliferating (with high *Hes1* levels). This is consistent with the data that I have presented in Chapter 3 that while there was a progressive increase in the number of bipolar cells beginning at 2 days there were cells that were still not differentiated (Fig. 3.6). It is likely that these cells under the influence of FGF-2 would reveal differential expression patterns of both HES1 and Delta1. The use of either *in situ* hybridizations and/or immunocytochemistry would perhaps help resolve these.

It is also possible that HES1 may be inhibited thus allowing for neuronal differentiation to take place. NGF was shown to phosphorylate the basic DNA binding domain of HES1 via the activation of the protein kinase C (PKC) pathway. The DNA binding ability of HES1 was as a result effectively inhibited thus allowing for the neuronal differentiation of PC12 cells (Ström *et al.*, 1997). Since PKC is one of several pathways downstream of FGF-2 signalling (Fig. 1.4), it is therefore likely that FGF-2 may interfere with the activity of HES1 in a similar manner in OP27 cells.

In conclusion, I have presented data that show that FGF-2 may regulate FGF-2 induced olfactory neuronal differentiation by altering the transcript levels of the components of the Notch signalling cascade.

Chapter 6

Isolation of genes differentially expressed in OP27 cells following FGF-2 induced differentiation

---

6.1 Introduction

Cellular development is characterized by proliferation of progenitor cells, exit from cell cycle and then differentiation. These are always accompanied by continuous changes in patterns of gene expression. Certain gene transcripts may be down-regulated or turned off to allow for cells to exit the cell cycle while genes may be specifically expressed during differentiation. This ultimately gives rise to the great diversity of cell types that are found in multicellular organisms. These changing patterns are well-regulated both temporally and spatially to allow for normal development. However, in disease such as cancer the cells escape the confines of growth control and continue to proliferate, as a result of aberrant gene transcription. Thus, to understand development, disease and various other biological processes, researchers would need to find methods to identify these genes and study how their expression is modulated. The identification of genes that are differentially regulated and the analysis of their role in changing the properties of cells is one way in which we can start to unravel the complex processes of development and disease. There are a number of tools that are available that one could use to measure differential gene expression at the mRNA level. These include differential hybridization, subtractive hybridization, differential display, microarrays, serial analysis of gene expression (SAGE), representational difference analysis (RDA) and many others (reviewed by Green *et al.*, 2001).

6.1.1 Differential display PCR as a tool to clone genes that are differentially regulated.

Differential display PCR (DD) was introduced in 1992 as a tool to compare the expression levels of a subset of mRNA transcripts from different but related cells, and to identify differentially expressed genes (Liang and Pardee, 1992). The subset of mRNA transcripts is selected for amplification by PCR by using a combination of primers that selects between 50 and 100 templates from the total template pool. The products of the PCR reactions are then compared on a denaturing polyacrylamide sequencing gel. Any PCR product that is differentially amplified between the cell types under study can be recovered and cloned. The basic outline of the protocol is shown in Fig.6.1.

6.1.1.1 The principles of DD

The first step of DD involves the reverse transcription of a subset of the mRNA population into cDNA. This is achieved by using an anchored-oligo(dT) primer with one or two additional bases at its 5-'end to help anchor the cDNA at the 3'-end of the RNA transcript. Different anchored-oligo(dT) primers with different additional bases can therefore be used to synthesize first-strand cDNA from different mRNA subsets in different reaction tubes. The anchored oligo(dT) used for reverse transcription of cDNA is then used together with an arbitrary primer to allow for PCR amplification of a subset of cDNAs. The arbitrary primer, typically at least 10 bases long, should in theory be randomly distributed in distance from the oligo(dT) for different cDNAs, resulting in products of varying sizes which can be resolved by polyacrylamide gel electrophoresis.

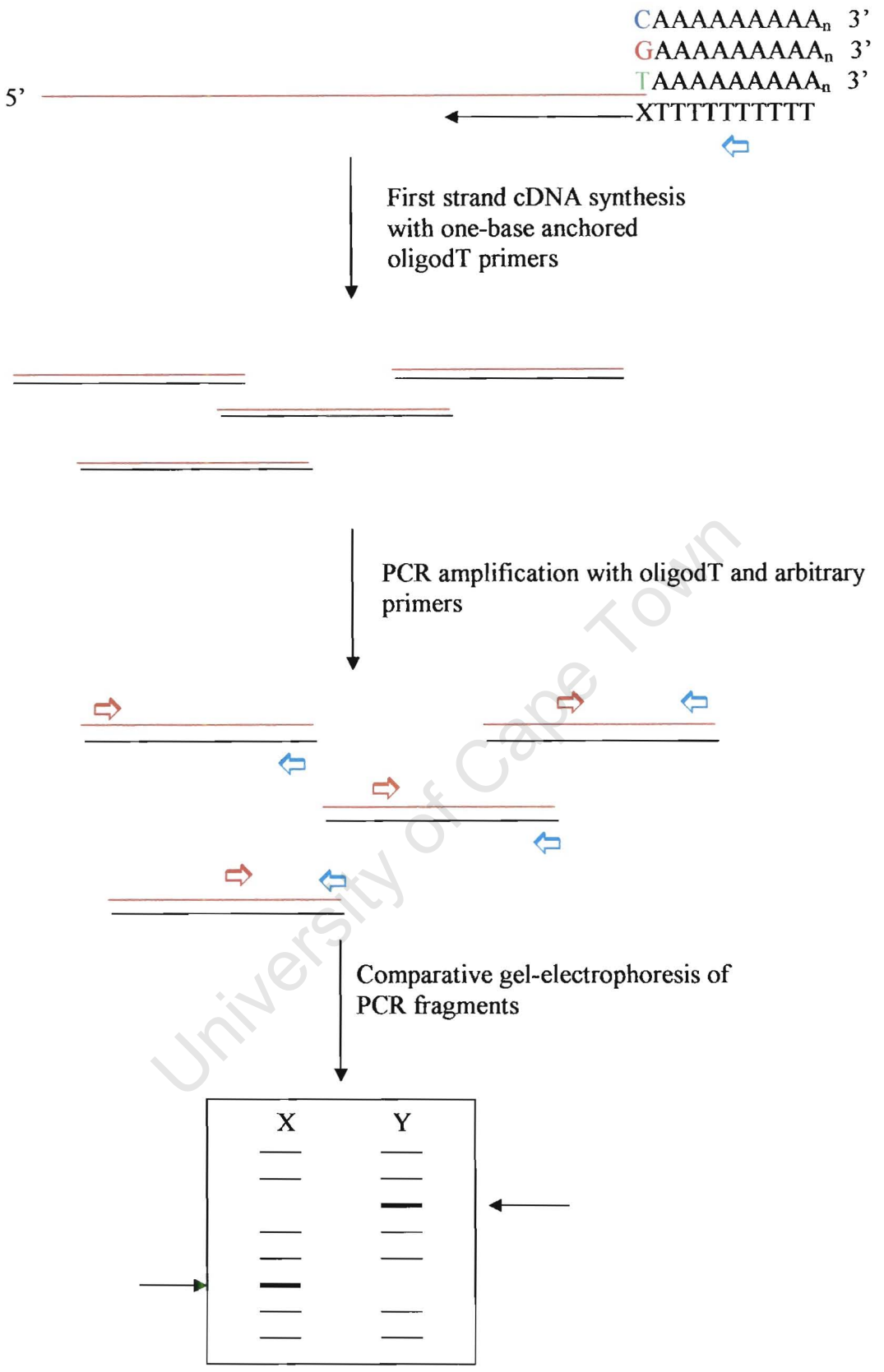

Figure 6.1: Schematic representation of the differential display PCR technique. Each anchored oligo(dT) primer (blue arrow) is used to reverse transcribe a subset of mRNA transcripts from the total RNA pool, extracted from cell types (X and Y) under comparison. The anchored oligo(dT) primer is then used in combination with a series of arbitrary primers (red arrows) for amplification of the mRNAs by PCR. The PCR products are then analyzed and bands that are differentially expressed between cells X and Y (shown by arrows in the scheme above) are recovered and analyzed.

The cDNAs are amplified in the presence of a radiolabelled deoxynucleotide (dNTP) and a low concentration of unlabelled dNTPs to label the products to a high specific activity for detection. As the PCR primers are short, a low annealing temperature of 40°C is used in the PCR reaction to allow for efficient priming. Under these conditions, a certain amount of degeneracy in priming is allowed, resulting in the amplification of mRNA templates that do not have a perfect fit to the arbitrary primer sequence. The radiolabelled PCR products are then resolved on a denaturing polyacrylamide gel electrophoresis to obtain clear separation of the large number of products that have been amplified. Side by side comparison of the banding patterns (visualized by autoradiography) of the PCR products derived from two different cells, allows the identification of gene transcripts that are differentially expressed (i.e. present in one cell type and absent in the other). Bands that are present in one lane of the sequencing gel but not in the other can be recovered from the gel, and reamplified by PCR (Fig. 6. 1). A theoretical number of primer combinations can be calculated to generate patterns of bands that might represent almost all 10 000-15 000 genes expressed in a particular cell. The number of primer combinations that have been suggested to allow a complete coverage of all the mRNAs have been hypothesized to be well over 200 (Bauer *et al.*, 1993; Watson and Flemming, 1994).

Once a potential differentially expressed gene has been isolated it is important to verify by northern blot analysis that it represents true differential expression. Alternative strategies that have been used to confirm differential expression include reverse northern blot analysis when multiple candidate genes have been isolated (Zhang *et al.* 1996; Dilks *et al.*, 2003), semi-quantitative RT-PCR with primers designed from the candidate differentially expressed genes (Brown *et al.*, 1999), ribonuclease protection assays (Gesemann *et al.*, 2001), virtual northerns (Franz *et al.*, 1999) and *in situ* hybridizations (Gupta *et al.*, 1998; Chambers *et al.*, 2000).

The last part of DD before the functional characterization of the candidate differentially expressed gene is determining their nucleotide sequences following confirmation of their differential expression.

6.1.1.2 Advantages of differential display PCR

Although techniques like subtractive hybridization and microarrays can also be used to analyse differential gene expression between two cell types, differential display PCR has some advantages. Firstly, the method is cheap, relatively simple and easy to use because it uses basic molecular biology procedures such as PCR and gel electrophoresis to search for differentially regulated genes. Differential display PCR is also useful when RNA is limited. Techniques like subtractive hybridization required a large quantity of RNA (Wan *et al.*, 1996).

The technique is versatile in that it allows a large number of comparisons to be done simultaneously. Examples of this are the identification of a wide representation of differentially expressed gene transcripts in different stages of development (Zimmermann and Schultz, 1994), isolation of cDNAs from different time points following treatment of cells (Garnier *et al.*, 1997), and screening for tissue specific genes (Pascolo *et al.*, 1999; Santhanam and Naz, 2001). Genes that are up- and down-regulated can also be simultaneously identified in the same experiment.

DD is carried-out without prior hypothesis as to which genes should be examined. Often with microarrays, a collection of pre-determined cDNAs or expressed sequence tags (EST) are used. Thus, DD has more potential to identify novel genes.

6.1.1.3 Limitations of differential display

Even though differential display PCR is an attractive approach in isolating differentially expressed genes, there are two main limitations associated with it. The high rate of false positives present among cloned candidate genes is one of these. False positives are those candidate cDNAs which are apparently differentially expressed on the differential display screen but whose patterns of differential expression cannot be reproduced on a northern blot. Some studies have reported a false positive rate as high as 85% (Zegzouti *et al.*, 1997). The low annealing temperatures used in the PCR reaction and genomic DNA contamination have been suggested to contribute to decreased reproducibility and the increase in the rate of false positives (Zhao *et al.*, 1995; Diachenko *et al.*, 1996). There are a number of precautions that have been suggested in order to reduce the number of false positives before time and effort were invested in characterizing a potential clone. Firstly, it is of paramount importance that the RNA template be of high quality and is free of genomic DNA contamination. To ensure that there is no genomic DNA contamination, PCR should be performed on a sample of DNase-treated RNA that has not been reverse transcribed. This should not give any bands in the differential display gel. It is also vital to use equal amounts of template for DD PCR, so that any observed difference between RNA samples under study are not due to slight differences in RNA concentrations (McClelland *et al.*, 1995) or due to variations in reverse transcription efficiencies (Kretzler *et al.*, 1996). Lastly, it is essential to run reactions in duplicate or triplicate to sort out true differences from non-reproducible false positives.

The second problem with the technique is that only the 3' non-coding regions of gene transcripts are cloned. As a consequence, identifiable open reading frames are often not found in the isolated cDNA fragments thus necessitating the screening of cDNA libraries or performing 5' RACE

reactions to clone the full-length sequences (Chen *et al.*, 1996; Dandoy-Droy *et al.*, 1998). A few technical modifications in the DD protocol have been performed in an attempt to clone genes with a coding sequence. The use of the r*Tth* DNA polymerase which has the ability to generate cDNAs between 200bp and 2kb in length, has been shown to improve the amplification of cDNA fragments that contain the coding regions (Jurecic *et al.*, 1998). In an attempt to maximize the amplification of cDNA fragments with coding sequences, Brown *et al.* (1999) used a set of statistically designed octadecanucleotides that showed a strong bias towards coding regions of mammalian genes. Lastly, the availability of more and more EST sequences in the dbEST database should facilitate the full-length *in silico* cloning of differentially expressed genes. This approach would involve starting from the known sequence obtained in a differential display screen and identify overlapping EST sequences from the dbEST database and assemble these in contigs to obtain the coding sequence (Senju and Nishimura, 1997).

6.1.1.4 Applications of differential display PCR in neuronal development

Since 1992 when the DD technique was invented there have been 3800 publications describing the use of the DD technique and its popularity continues to grow even in the presence of the fast emerging DNA microarrays (Liang, 2002). The technique has found wide applications in developmental, oncogenic and various other eukaryotic paradigms, and has contributed to the identification of a number of genes. I discuss a few examples of the application of DD in the study of neurogenesis in the following section.

During early vertebrate brain development the neural tube is patterned along the dorsoventral and rostrocaudal neural axes to form the forebrain, midbrain, and the hindbrain. To identify genes that might be important in the brain regionalization along the anteroposterior axis, Chambers *et al.* (2000) used a modified DD protocol by comparing gene profiles of midbrain and anterior hindbrain. *Sprouty2*, an antagonist of receptor tyrosine kinase signalling and a target of FGF-8, was found to be specifically expressed at the midbrain-hindbrain junction. *Sprouty2* was therefore postulated to play a crucial role in the specification and regionalization of the midbrain and hindbrain.

Various cell lines of neural origins have been used to screen for genes that respond to treatment with growth factors and which may be important for neuronal development (Table 6.1). PC12 cells undergo neuronal differentiation when cultured in the presence of FGF and NGF. DD PCR has identified a number of NGF responsive genes in PC12 cells. MARK1, a serine/threonine kinase and MAP kinase 3 (MAPKK3) were two of the majority of genes that were up-regulated by NGF while *Notch4*, a known inhibitor of neuronal differentiation, was down-regulated by the treatment (Table 6.1, Brown *et al.*, 1999).

EG6, a neural cell line immortalized from embryonic rat septum has also been used to screen for genes regulated by FGF-2 during neuronal differentiation. Ten differentially expressed genes (Table 6.1) were identified in this study, 4 of which were genes known to be either expressed in the brain or shown for the first time, in that study, to be expressed in the brain. One of the novel genes, clone 2C, identified in the study as being induced by FGF-2, was specifically expressed in the developing rat brain (Miyasaka and Matsuoka, 2000).

Table 6.1 Some of the genes identified by DD PCR in various cells of neural origins.

Cell type	Growth factor treatment and effect on cells	Up-regulated genes	Down-regulated genes	Reference
PC12 cell line	NGF growth arrest and neuronal differentiation	α-catenin, SatB1, MARK1, Sec61, MAPKK3, Eif-5A, ornithine decarboxylase, gluthione reductase, p54 nucleoporin, RNA binding protein, 2 brain derived cDNAs, 5 EST clones	Guanylate cyclase β subunit, p150 chromatin assembly factor, Notch4	Brown *et al.*, 1999
EG6 cell line Immortalized from embryonic rat septum by transfection with SV40 T antigen	FGF-2 Induction of morphological changes and extension of neurite extensions	Calmodulin, novel clone 1C, brain specific clone 2C	Thrombospondin 1 (TSP1), cytokine-inducible nuclear protein, osteoblast specific factor 2 (OSF2), clone 12, clone 24C-b	Miyasaka and Matsuoka, 2000
Bipotential human neuroblastoma NUB-7 cell line	dibutyryl cAMP induces neuronal differentiation	HMG-CoA reductage, clone 5-2, clone 5-1, clone 5-4	N/A	Dimitroulakos *et al.*, 1999
Bipotential human neuroblastoma NUB-7 cell line	retinoic acid differentiate into Schwann cells	clone 5-4, novel zinc finger zf5-3	N/A	Dimitroulakos *et al.*, 1999
Rat lens epithelial explant culture	FGF-2 Differentiaton into fiber cells	βB1-crystallin	Novel clone # 2	Cai *et al.*, 1999
Human neuroblastoma cell line SH-SY5Y	Retinoic acid Neurite outgrowth evident after 5-10 days in culture	Neurofilament, monocyte chemotactic protein (MCP-1)	HLH protein Id-2H, 90KDa heat shock protein HSP90, high mobility group protein-1 (HMG-1), threonine kinase, ribosomal proteins S25 and L7	Kito *et al.*, 1997
Pax6 heterozygous vs. normal mouse lenses	N/A	N/A	Phosphate inhibitor protein Pip-1, heat shock protein Hsp40, Purkinje cell protein Pcp4, mitochondrial cytochrome oxidase, ESTAA331381	Chauhan *et al.*, 2002
Gsh-1 homozygous mutant hypothalamic cell line	Transfected with a tet-inducible Gsh-1 expression construct	protease Cathepsin L, mitochondrial rRNA, novel clone 45A, β-activin A subunit homolog, homolog of the rat DRM gene that inhibits cell growth	MCL-1 homolog that promotes cell survival, novel clone 40B	Li *et al.*, 1999

In the bipotential neuroblastoma cell line NUB-7, cells differentiate into neurons in the presence of dibutyryl cAMP and into Schwann cells in the presence of retinoic acid. DD PCR was used to identify 3 different sets of inducible cDNAs from the NUB-7 cell line, namely those induced by dibutyryl cAMP, those induced by retinoic acid and those reponsive to both (Table 6.1, Dimitroulakos *et al.*, 1999). Comparison of non-induced and FGF-2 induced cultured chick lens epithelial explants identified a novel lens specific cDNA, clone 2, which was down-regulated upon differentiation of the cells (Cai *et al.*, 1999).

DD has also been used to identify transcriptional targets of transcription factors involved in neuronal development. Li *et al.* (1999) used a hypothalamic progenitor cell line carrying a homozygous mutation in the *Genetic screen homeobox-1* (*Gsh-1*) gene and transfected the cells with an inducible *Gsh-1* expression construct to identify candidate downstream target genes of the transcription factor. Several growth and differentiation related genes were identified in this study (Table 6.1, Li *et al.*, 1999). Similarly, eight gene transcripts either directly or indirectly regulated by PAX6 were identified in a DD screen comparing wild type versus *Pax6* heterozygous mouse lenses (Table 6.1, Chauhan *et al.*, 2002).

Current research on olfactory neuron development is focussing on known transcription factors and signalling molecules e.g. FGF and BMP, which have been shown to be important regulators of ORN development. In an attempt to further increase our understanding of ORN development, I set out to identify differentially expressed genes as the OP27 cells differentiate, by using differential display RT-PCR.

6.2 RESULTS

6.2.1 Differential Display analysis of FGF-2 regulated gene transcripts

DD was performed on OP27 cells that had been treated with FGF-2 for 0, 6, 24, and 48 hours except for 4 experiments in which the 48hr time point was omitted. The zero hour time-point represents untreated, control OP27 cells that were maintained at 33°C. A total of 24 primer combinations comprising the 8 different arbitrary sense primers and the 3 different one-base anchored antisense oligo(dT) primers (Table 2.4) were used. The PCR products from duplicate reactions from the same experimental sample were electrophoresed in parallel in a denaturing acrylamide gel. The results of the DD screen are shown in Fig. 6.2. One primer combination, H-T_{11}A / H-AP24, did not result in any PCR products while the H-T_{11}C / H-AP23 combination was less efficient compared to others. For each primer combination used, approximately 50-100 bands could be visualized per lane as expected.

Theoretically, anchored oligo(dT) primers reverse transcribe different mRNA sub-populations and when these are amplified with the arbitrary sense primers, distinct display patterns are generated (Liang and Pardee, 1992). This is clearly evident in the display patterns generated in OP27 cells (Fig. 6.2). When one sense (arbitrary) primer was used with each of the antisense oligo(dT) primers, distinct display patterns were observed. The majority of the bands within each primer combination showed equal intensity with the FGF-2 treatment while very few bands showed varying intensities with the treatment. Those that showed changing intensities were identified as candidate differentially expressed genes. Initially, 71 cDNA fragments were scored as differentially

expressed based on visual inspection of the autoradiographic X-ray films (Fig. 6.2). Some of the candidate differentially expressed transcripts were represented by very faint bands on the X-Ray films and as a result were not visible on the images shown in Fig. 6.2. The candidate differentially expressed differentially expressed cDNAs were identified according to the primer combination used to display that fragment. For example, 17A1 is a cDNA fragments that resulted from the display using H-AP17 and H-T_{11}A. Thirty-two of the cDNA fragments scored as being differentially expressed represented up-regulated genes while 39 gene transcripts that were apparently down-regulated. A list of both the up-regulated and down-regulated genes identified in this study is included in the Appendix.

Figure 6.2 Gene expression profiles in OP27 cells following FGF-2 treatment. The differential display patterns produced by specific primer combinations at the different time intervals of FGF-2 treatment were run in parallel. Anchored primer/arbitrary primer combinations used for each display are shown at the top and the time intervals of FGF-2 treatment are indicated in hours (0, 6, 24, and 48). Candidate differentially expressed transcripts are labelled according to the primer combination used. The mRNA transcripts that were successfully re-amplified as single PCR products, and whose change in expression levels was subsequently confirmed by either reverse northern blot, northern blot or RT-PCR are shown with an asterix (*). † 21C2 was evenly expressed across all time points.

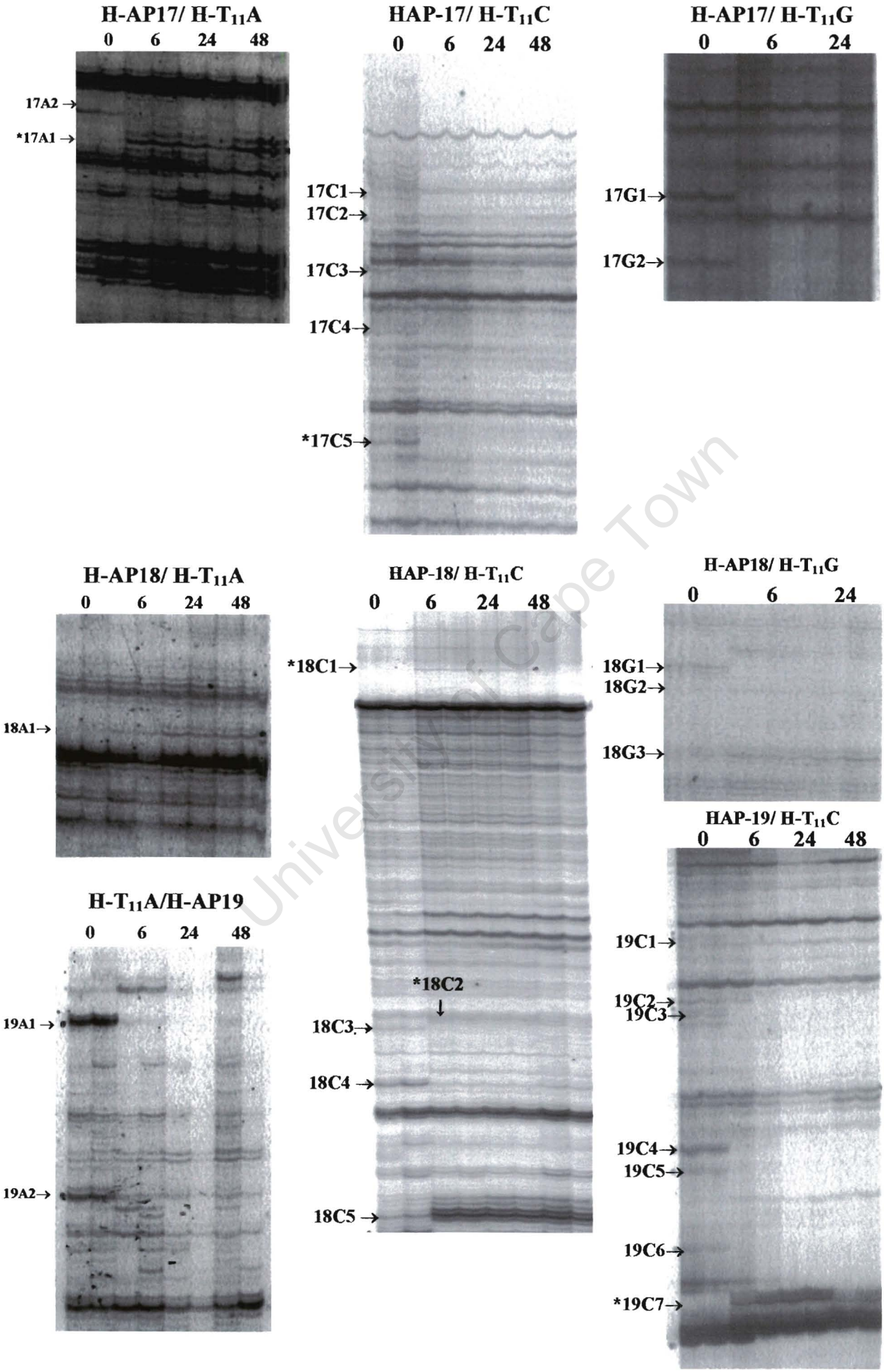

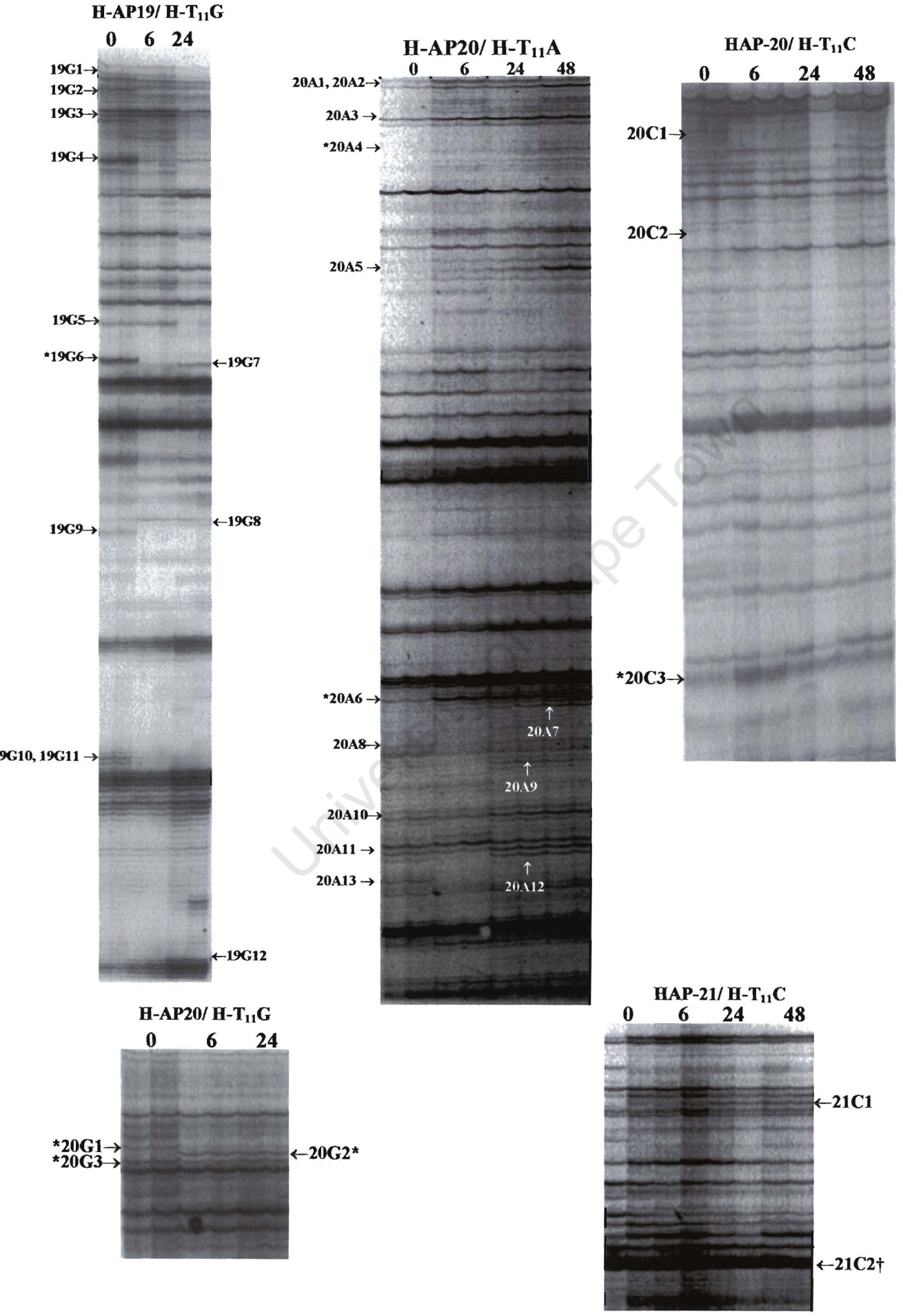

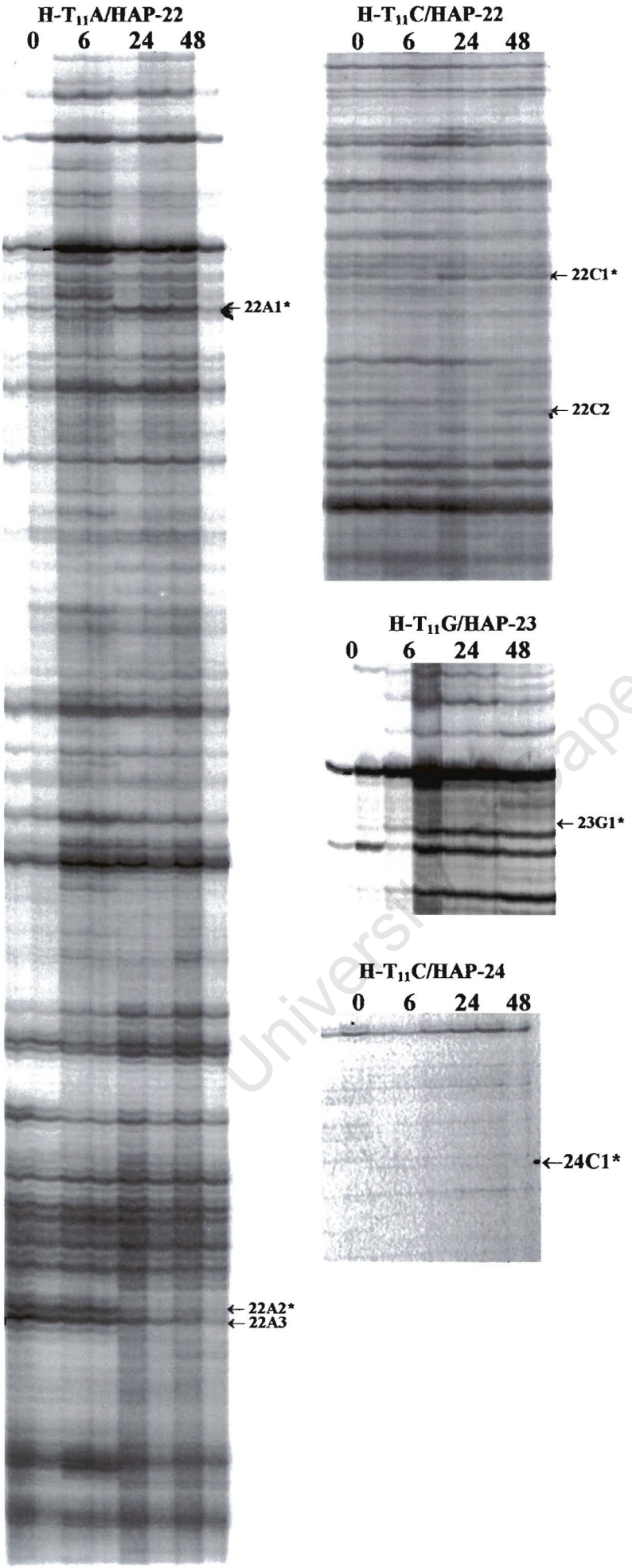

All 71 bands were excised from the sequencing gel and reamplified using the primer combination originally used to display them. One apparently equally expressed cDNA, 21C2 was also excised and used as a control in reverse northern slot blot analysis. The reamplified fragments ranged in size from approximately ~100 bp to ~800 bp. PCR reamplifications of some cDNAs (see Appendix) failed while some resulted in the co-amplification of at least 2 PCR products in one tube (Fig. 6.3 and Appendix).

6.2.2 Verification of differential expression by reverse northern blot analysis

Reverse northern slot blot analysis was used to confirm the differential expression of the candidate differentially expresed genes. Out of 71 cDNAs that were identified, forty-five that were successfully reamplified and gave single PCR products were blotted along with cDNAs for β-actin, glyceraldehyde dehydrogenase (GAPDH) and 21C2 which were used as internal controls. The clone 21C2 was excised and purified from the differential display gel. Duplicate blots were generated and were hybridized to cDNA probes prepared from total RNA extracted from OP27 cells at 33°C and from cells that had been treated with FGF-2 for 6 hours. The samples used for preparing the probes were from an independent FGF-2 experiment from that used in the differential display screen. The reverse northerns are shown in Fig. 6.4. Thirty-one of the candidate differentially expressed genes could be detected in both blots whereas a few did not give any signals. The intensities of some of the clones (e.g 17A1 in slot A1, 19G6 in slot D3, and 22C1 in slot C3, Fig. 6.4) differed between the 2 blots. These represented differential regulated clones that could be confirmed using this method.

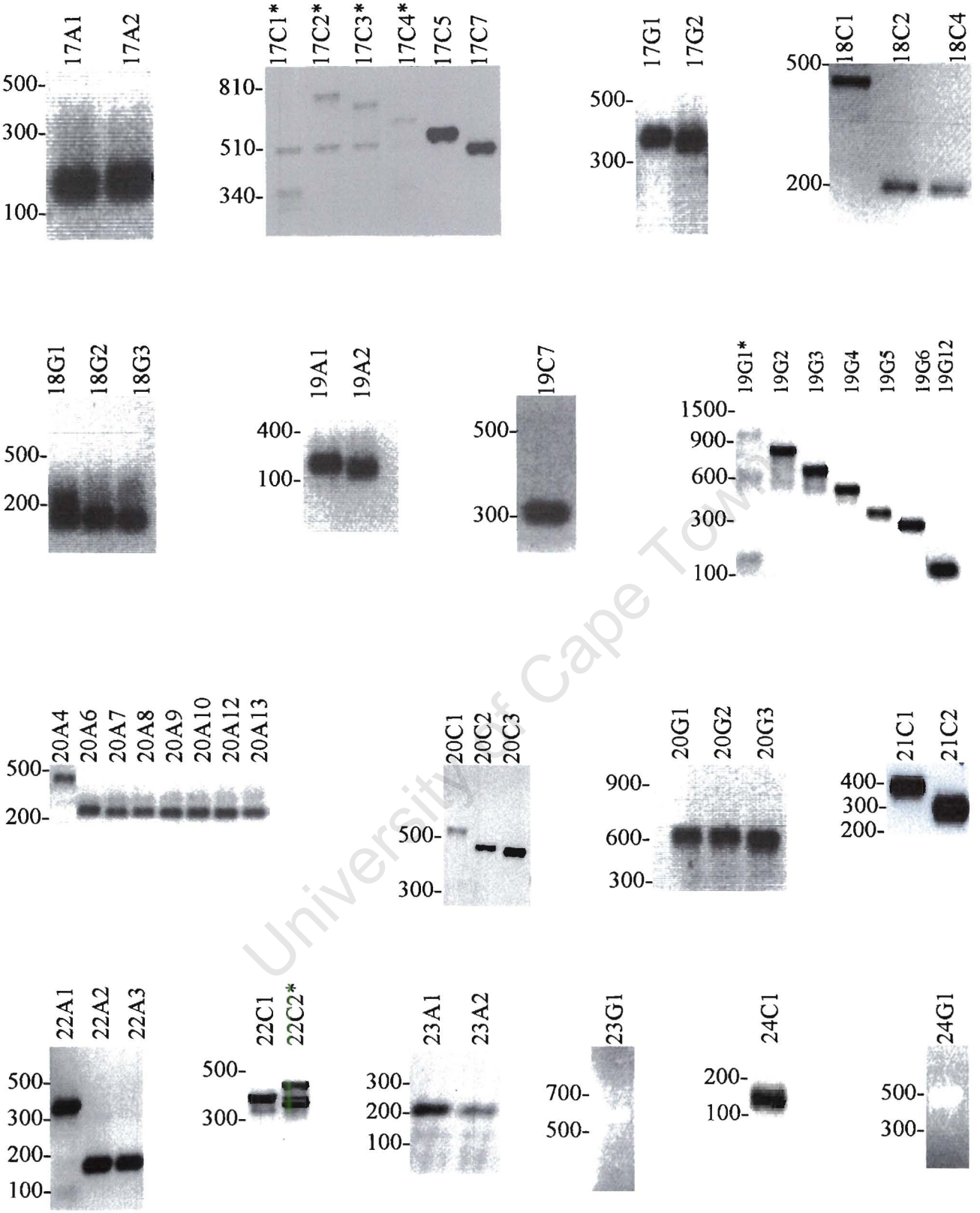

Figure 6.3 Agarose gel electrophoresis of the PCR reamplified candidate differentially expressed cDNAs. The cDNAs were excised from the polyacrylamide gels, purified and reamplified using the primer combination used in the differential display protocol. Few of the reamplifications failed even after a second round of PCR (data not shown). Some of the PCR reactions resulted in more one PCR product (marked with an asterix). These clones were excluded from subsequent analysis. Clone numbers corresponding to DD PCR products identified in Fig. 6.2 are shown above each photograph. Molecular weight markers (Promega's 100bp ladder and lambda DNA digested with PstI) are shown on the left hand side of each gel. Sizes are shown in base pairs, bp.

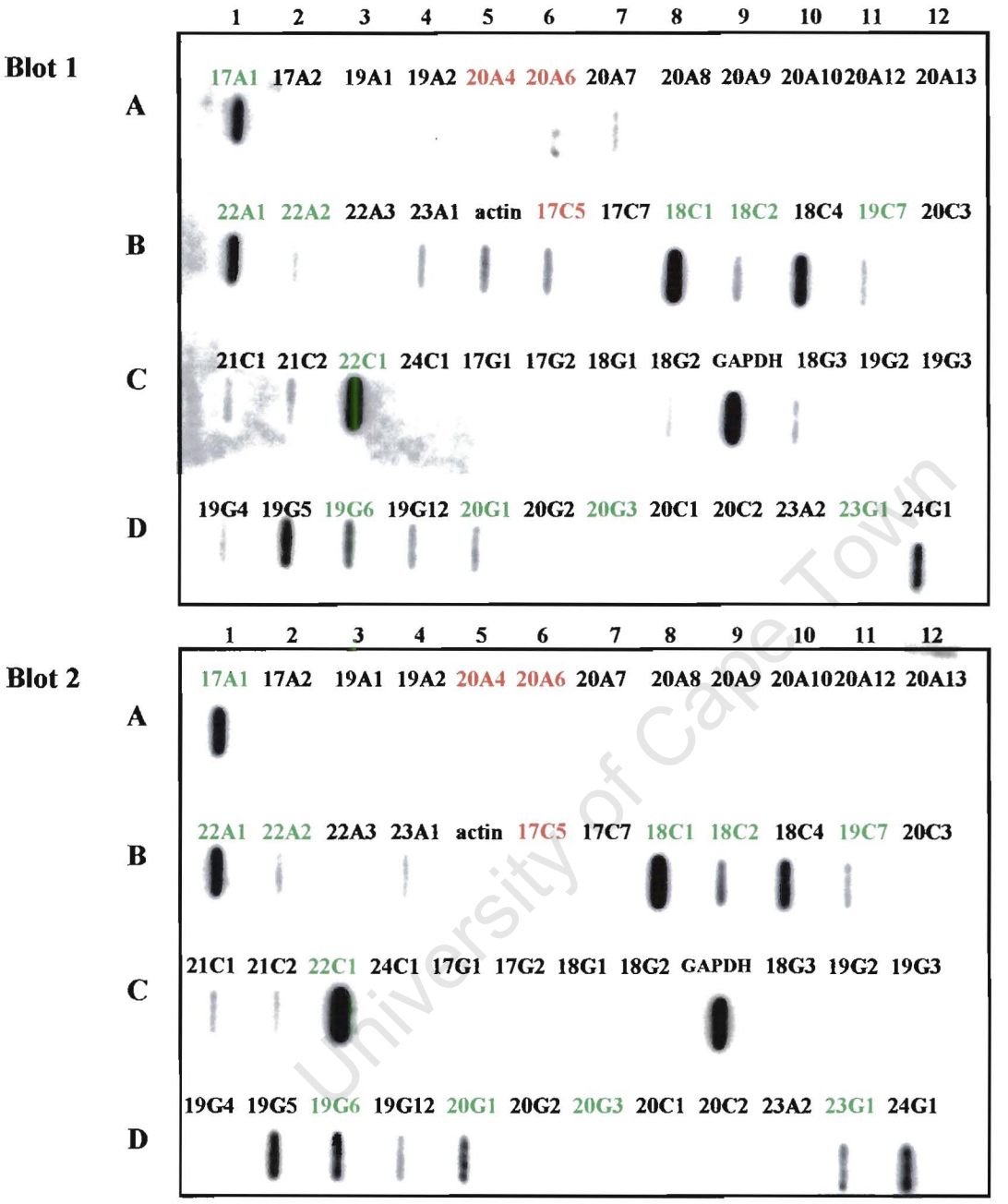

Figure 6.4 Verification of candidate differentially expressed cDNAs using reverse northern slot blot analysis. Blots showing signal of 32P-labelled cDNA probes hybridized against PCR reamplified cDNAs. Blot 1 was probed with radiolabelled cDNA synthesized from total RNA extracted from OP27 cells grown at 33°C while blot 2 was probed with [α-^{32}P]-labelled cDNA synthesized from total RNA from OP27 cells cultured at 39°C for 6 hours in the presence of FGF-2. ß-actin (in slot B5), GAPDH (slot C9), and 21C2 (slot C2) were also blotted as controls to equalize differences in efficiency of reverse transcription. Differentially expressed cDNA clones following normalization (Fig. 6.5) are indicated in green (up-regulated genes) and in red (down-regulated genes).

To ensure that the observed differences arose as a result of FGF-2 treatment rather than from external variations such as efficiency in probe labelling or inaccurate quantitation of labelled probe, the signal intensities of the 3 house-keeping genes, β-actin, 21C2 and GAPDH were measured and compared between the 2 blots. Their intensities were found to be consistently higher in blot 1 compared to blot 2 thus implying differences in probe labelling. The signal for β-actin in blot 1 was 2.6 times that in blot 2, whereas the signals for 21C2 and GAPDH in blot 1 were 1.4 and 1.2 times that in blot 2, respectively. It was therefore necessary to normalize the data. The method used by Dilks *et al.* (2003) was then applied to normalize the signals of clones used in the reverse northerns. In this approach, the signals of each of the house-keeping genes are determined in both blots and compared in a ratiometric fashion between both blots. The average ratio of all the house-keeping genes is then applied as a scaling factor to the signals of the clones in the blot that has a lower intensity (in this case, blot 2). Since 21C2 and GAPDH showed a similar variation in the 2 blots (mentioned above), their average ratio (i.e 1.3) was used as a scaling factor for the signals in blot 2. β-actin was totally excluded in the analysis as the ratio of 2.6 suggested that it was not evenly expressed. The scaled-up signals in blot 2 (experiment) were then compared with those in blot 1 (control) and expressed as a fold- change difference in expression. The normalized fold-changes of each clone used in reverse northern analysis are shown in Table 6.2 and summarized in Fig. 6.5. The results obtained using both 21C2 and GAPDH were consistent with the verification by northern blot analyses (Fig. 6.6). On the other hand when β-actin was used to normalize the data the up-regulated genes were more pronounced whereas the down-regulated genes showed no apparent change (results not shown).

Table 6.2 Normalized fold-change (OP27 cells at 33°C versus 6 hours at 39°C with FGF-2) in expression of DD clones that were detected in reverse northern blot analysis. The fold-changes were then plotted on a LOG_2 scale in Fig. 6.5

DD clone	Fold-change	LOG_2
17A1	1.68	0.75
17A2	0.8	-0.32
17C5	0.49	-1.03
17G1	1.34	0.42
18C1	1.86	0.89
18C2	1.91	0.93
18C4	1.06	0.08
18G2	1.17	0.23
18G3	1.05	0.07
19C7	1.57	0.65
19G2	1.06	0.08
19G4	0.99	-0.01
19G5	1.19	0.25
19G6	1.73	0.79
19G12	1.22	0.29
20A4	0.43	-1.21
20A6	0.38	-1.39
20A7	1.07	0.1
20A8	1.38	0.46
20A9	1.39	0.47
20A10	1.01	0.01
20G1	2.59	1.37
20G3	1.6	0.68
21C1	1.12	0.16
21C2	0.95	-0.07
22A1	1.6	0.68
22A2	1.63	0.7
22A3	1.22	0.29
22C1	2.2	1.14
23A1	1.3	0.38
23G1	2.99	1.58
24G1	1.41	0.49
GAPDH	1.1	0.14

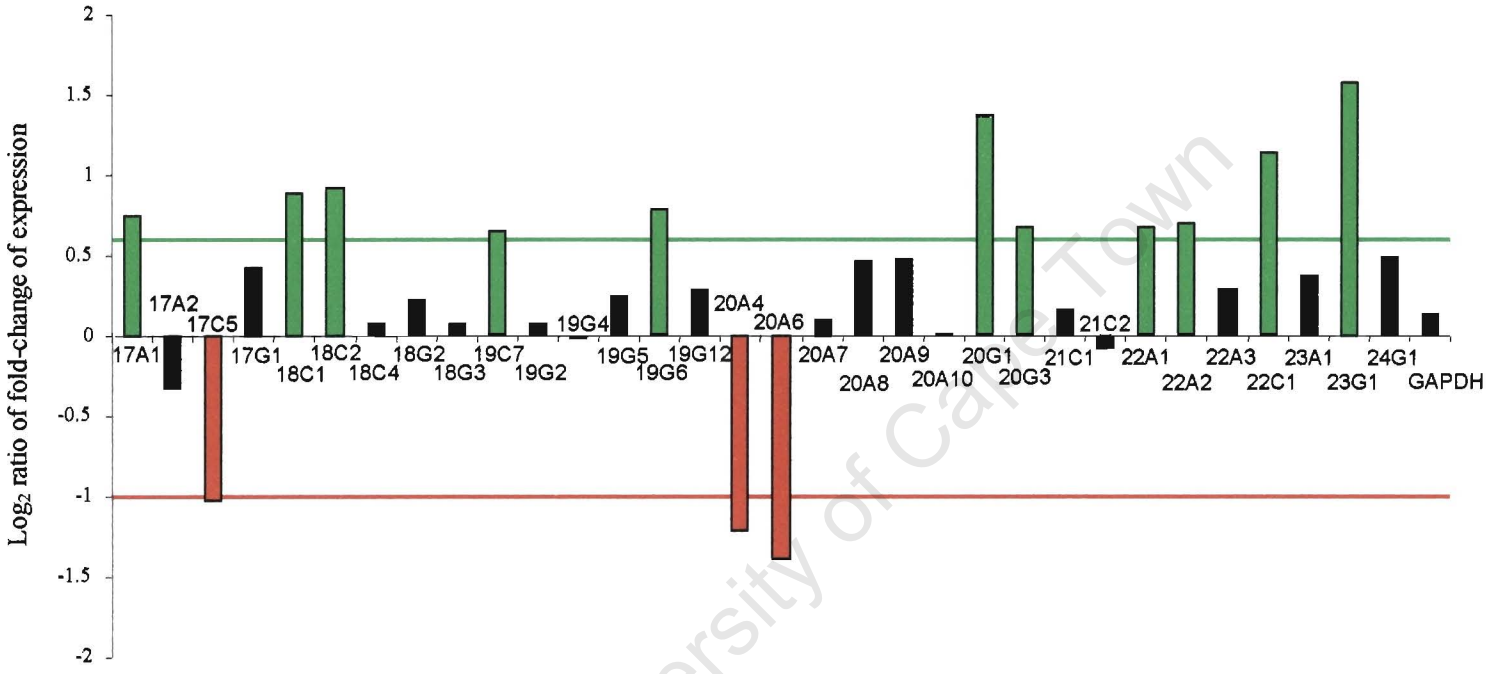

Figure 6.5 A summary of the expression patterns of cDNA clones used in reverse northern blot analysis. The signal intensities for each clone at 6 hours after FGF-2 treatment (blot 2 in Fig. 6.4) was compared with that at 0 hours (blot 1 in Fig. 6.4) and expressed as a fold-change (Table 6.2) following normalization using the internal controls 21C2 and GAPDH. The fold-change in expression was then plotted on a log scale as a $\log_2$ ratio shown above. DD clones that had at least 1.5-fold increase or 2-fold decrease in expression (shown as +0.65 or –1on the plot) were thus confirmed as being differentially regulated by FGF-2 treatment. Up-rgulated genes are shown in green on the plot while down-regulated transcripts are shown in red.

The fold-changes in expression between the 2 blots ranged from 0.38 (for 20A6) to 3.0 (for 23G1). All the genes that had a fold-change of expression close to 1 were designated as genes whose expression was not affected by treatment with FGF–2. Genes that had a 0.5 fold change were designated as genes that showed a robust down-regulation by FGF-2 treatment. cDNAs that fall into this category include 17C5, 20A4, and 20A6. On the other hand, genes that had a fold-change of at least 1.5 in expression levels were designated as up-regulated gene transcripts. The genes that fall into this group are the following: 17A1, 18C1, 18C2, 19C7, 19G6, 20G1, 20G3, 22A1, 22A2, 22C1, and 23G1 (Fig. 6.5). However, the expression pattern of several of these DD cDNAs in this assay contradicted that in the DD screen. For example, 19G6, 20G1, 20G3 and 23G1 were identified on the basis of down-regulation but the subsequent reverse northern analysis showed that their transcripts were up-regulated. Similarly with 20A4 and 20A6, the DD screen showed an up-regulation of these cDNAs whereas the reverse northern showed an opposite pattern of expression (Fig. 6.2, 6.4 and 6.5). Often with DD, it is possible to isolate multiple other transcripts when single bands are purified and reamplified (Averboukh *et al.*, 1996; Callard *et al.*, 1994). It was therefore necessary to confirm expression changes of these cDNAs using northern blot analysis as an alternative assay.

6.2.3 Verification of differential expression by northern blot analysis and RT-PCR

Northern blot analyses were performed to confirm the differential expression of the candidate cDNAs. Selected cDNAs were cloned and inserts used to probe blots of OP27 cells that had been treated with FGF-2. The cDNAs included transcripts whose expression change in the by reverse northern analysis was consistent with that in the DD screen, those whose expression changes in the reverse northern contracted with the DD analysis and transcripts that could not be detected.

The clone 17C5 was isolated on the basis of its down-regulation in the DD screen and that was confirmed with the reverse northern analysis (Fig. 6.5). The northern blot using this clone as a probe on the other hand showed a transient down-regulation of its extremely large transcript. It was first down-regulated at 6 hours, consistent with both the DD and reverse northern results, but it was up-regulated again at 24 hours (Fig. 6.6A). The clones 19C7, and 22A1 were confirmed as being up-regulated on the reverse northern analysis and this was reconfirmed with their respective northern blot analyses. The clone 19C7, represented by a ~4.8 kb message on the blot, displayed an up-regulation in differentiating OP27 cells. However, its up-regulation was more evident after 24 hours following FGF-2 treatment on the northern compared with the 6 hours on the reverse northern (Fig. 6.6B). The northern blot for 22A1 revealed that the clone is a product of an alternatively spliced transcript that is up-regulated with FGF-2 treatment (Fig. 6.6 D). Thus the northern blot analysis of 17C5, 19C7, and 22A1 was consistent with the results of both the DD screen and the verification by reverse northern.

20C3, 20G2 and 24C1 were among clones that did not give detectable hybridization signals on the reverse northern. However, signals for 20C3 and 24C1 could be detected with the northern hybridization after long exposures of their respective X-ray films. The clone 20C3, isolated on the basis of its transcriptional up-regulation in the DD screen, could be detected on the 6-hour time point only. This probably reflects a transient up-regulation of its transcript over 6 hours, which was followed by a down-regulation over the following 24 and 48 hours (Fig. 6.6C). The northern blot for the clone 24C1 also showed a transient up-regulation of its ~1.8 kbp transcript within the first 6 hours of FGF-2 treatment. It could still be detected after 24 and 48 hours although at a lower level compared to 6 hours (Fig. 6.6F). The clone 20G2 did not give any signal with the northern blot. The northern blots of clones 20C3 and 24C1 were therefore in agreement with the DD screen.

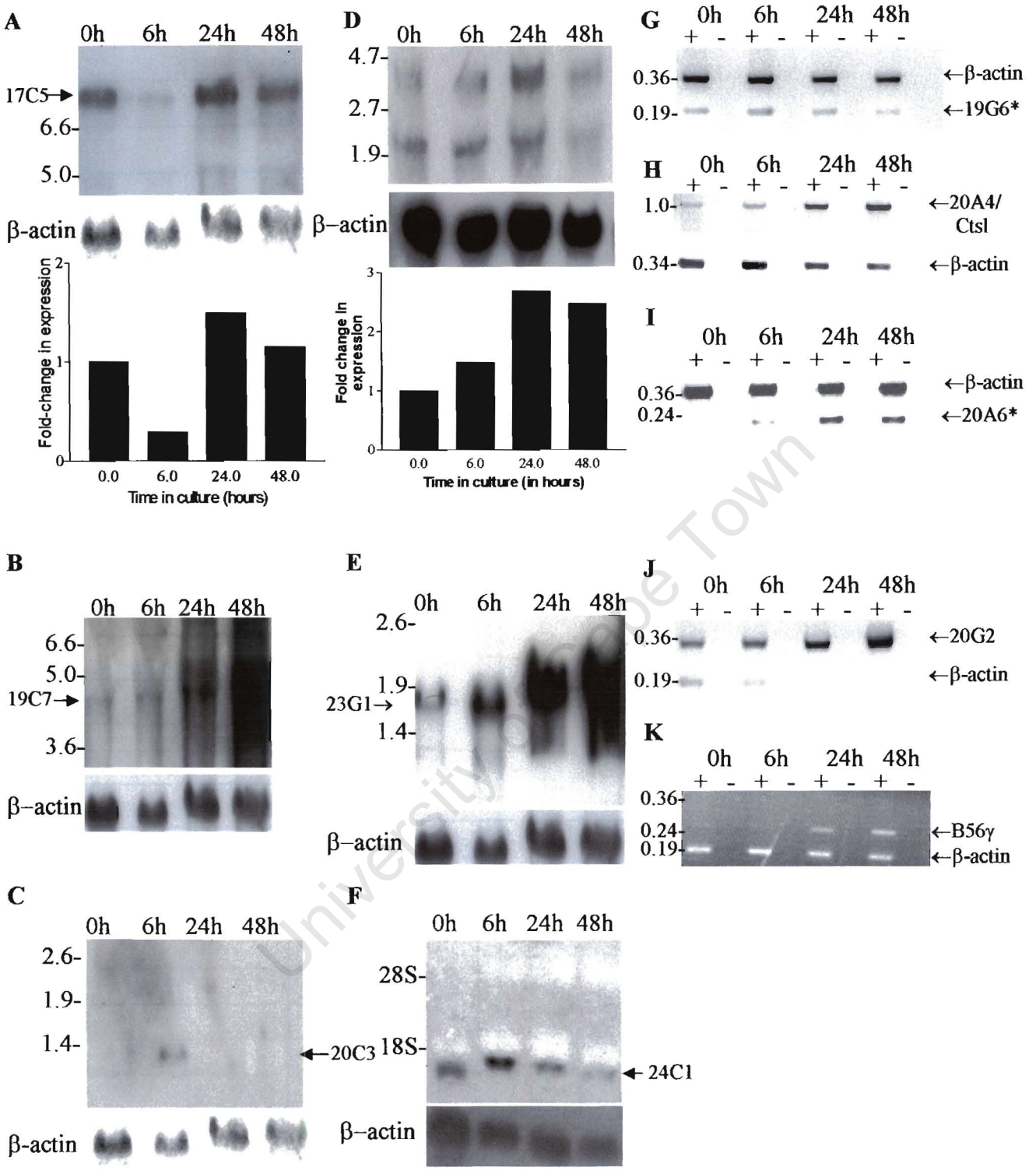

Figure 6.6 Verification of differential expression by northern blot hybridization and RT-PCR. Total RNA from OP27 cells treated for 0, 6, 24, and 48 hours with FGF-2 was transferred onto a membranes and hybridized with radiolabelled probes for DD clones 17C5 (A), 19C7 (B), 20C3 (C), 22A1 (D), 23G (E), and 24C1 (F) in northern blot analyses. The probes were removed and membranes were hybridized to a β–actin probe to control for loading. Densitometer readings from northern hybridization signals of 17C5 (A, bottom) and 22A1 (D, bottom) were generated, normalized with respect to β-actin levels and expressed as a fold-change in expression over the reading at 0 hours. (G-K) Semi-quantitative RT-PCR analysis was performed to verify the differential expression of DD clones PP2 B56γ, 19G6, Cathepsin L (*Ctsl*), 20A6, and 20G2 on first strand cDNA prepared from total RNA which was extracted from OP27 cells treated for the same time points as for northerns. β–actin primers were also included in each PCR reaction. * A different pair of β–actin primers (that amplify a 360 bp fragment) was used for the RT-PCR assays for 19G6 (G) and 20A6 (I). The PCR was run for a limited number of cycles (25 cycles) to limit the amplification to the linear range.

Northern blot analyses were also performed with clones that showed opposite patterns of expression in the DD screens and in the reverse northern blot. However, none of these cDNAs, with the exception of 23G1, gave a detectable signal on the northern blots even though their hybridization signals were clearly detected on the reverse northern. The clone 23G1, on the other hand, showed a robust up-regulation within 6 hours of its ~1.8 kb message and its levels continued to increase thereafter (Fig. 6.6E).

The nucleotide sequences of the clones that could not be detected with the northern blot analysis (19G6, 20A4, 20A6, and 20G2) were therefore determined and gene specific primers designed for semi-quantitative RT-PCR assays. 19G6 could not be confirmed to be differentially regulated using the semi-quantitative RT-PCR (Fig. 6.6G) and was therefore excluded from further analysis. Although the reverse northern assay showed that the 20A4 and 20A6 clones were down-regulated with FGF-2 treatment, the semi-quantitative RT-PCR result was consistent with their expression changes in the DD screen (Fig. 6.6H and I). It was therefore concluded that both 20A4 and 20A6 were up-regulated in FGF-2 induced OP27 cells. 20G2 whose signal could not be detected on the reverse northern was confirmed using this assay to be indeed up-regulated in OP27 cells following induction with FGF-2 (Fig. 6.6J).

6.2.4. Sequence analysis of differentially expressed cDNAs

The nucleotide sequences of the genes that were confirmed to be differentially expressed by the different assays were analyzed by BLAST searches against both the non-redundant (i.e nr) and EST databases (i.e dbEST) at the NCBI. The results revealed both previously identified mouse genes and genes that have not been characterized (Table 6.3).

Table 6.3 Summary of clones isolated by differential display following FGF-2 treatment of OP27 cells. ↑= Up-regulation in FGF-2, ↓= down-regulation in FGF-2, ↑↓= transient up-regulation, ↓↑= transient down-regulation,
ND= not detected.

DD clone	Clone size (bp)	GenBank Accession numbers of DD clones	Expression profile in DD screen	Expression change in reverse northern	Expression change in northern/ RT-PCR	GenBank match	Accession number	E-value
17A1	170	CK850014	↑	↑	↑	Protein phosphatase 2A B56γ regulatory subunit	BC003979	3e-72
17C5	534	CK850015	↓	↓	↓↑	Collagen IV α2 (COL IVα2)	NM_009932	Exact match
18C1	426	CK850016	↑	↑		IMAGE:6514303, similar to 60S ribosomal protein L34	XM_357642	Exact match
18C2	205	CK850017	↑	↑	ND	Protein phosphatase 4, regulatory subunit 2 (Ppp4r2)	NM_182939	2e-76
19C7	313	CK850018	↑	↑	↑	Amyotrophic lateral sclerosis (Als2)	NM_028717	2e-59
20A4	485	CK850020	↑	↓	↑	Cathepsin L	NM_009984	e-174
20A6	169	CK850021	↑	↓	↑	Metallothionein II (MT-II)	NM_008630	6e-58
20C3	457	CK850022	↑	ND	↑↓	IMAGE:9442282, similar to mouse arginine rich protein	AA545476	Exact match
20G1	620	-	↓	↑	ND	BAC clone RP23-119F18	AC122219	2e-86
20G2	618	-	↑	ND	↑	BAC clone RP23-400N18	AC123842	Exact match
20G3	594	CK850023	↓	↑	↑	2610002J02Rik	XM_131827	Exact match
22A1	351	CK850024	↑	↑	↑	Ocular development-associated gene (ODAG)	AB047921	Exact match
22A2	135	CK850025	↑	↑		EST D330002D23	AK084462	6e-45
22C1	374	-	↑	↑		Human Chr14 BAC R-596D21	AL136418	e-167
23G	540	CK850026	↓	↑	↑	Hypothetical GCN5-related NAT protein	AK015640	Exact match
24C1	179	CK850027	↑	ND	↑↓	Transgelin 2	AF465519	9e-79

Several of these clones matched to genes that have been implicated in neuoronal differentiation. The 17A1 clone, up-regulated by FGF-2 treatment in OP27 cells, revealed a 99% identity to the brain-specific γ isoform of the regulatory subunit B (also known as B56) of the mouse protein phosphatase 2A (PP2A). The B56 γ isoform has been shown to induce neuronal differentiation *in vitro* (Strack, 2002). Semi-quantitative RT-PCR analysis using B56 γ isoform specific oligonucleotides showed that this gene is indeed up-regulated in FGF-2 induced OP27 cells (Fig. 6.6K). The clone 17C5 which was first down-regulated then up-regulated by FGF-2, represented transcript for the extracellular matrix protein α2 collagen IV which has also been implicated in neurogenesis (Ali *et al.*, 1998). 19C7, up-regulated in OP27 cells exhibited high similarity to a gene designated as *Als2* (amyotrophic lateral sclerosis 2) which encodes for the protein ALSIN. Although the function of this gene is unknown, its high expression levels have been detected in the CNS (Yang *et al.*, 2001). The 22A1 clone which is up-regulated by FGF-2 is homologous to ODAG, a ocular development-associated gene, recently identified in a screen for genes that may play a role in eye development (Tsuruga *et al.*, 2002). The clone 24C1 which was transiently up-regulated by FGF-2 had high homology to the cytoskeletal protein transgelin 2. Its mRNA transcripts were up-regulated in PC12 cells following NGF induced neuronal differentiation (Angelastro *et al.*, 2000). Clones 20A4 and 20A6, both up-regulated in FGF-2 induced differentiation of OP27 cells, revealed high homology the protease cathepsin L and metallothionein 2 (MT-II).

Although homologs for the clones 18C1, 20C3, 20G3, 22A2, and 23G1 could be identified, the functions of those genes are unknown. Clones 18C1, 20C3, 20G3, and 22A2 exhibited high homologies to mouse ESTs. The ESTs that match 18C1 and 20C3 have been identified among potential *Otx2* target genes that are up-regulated in $Otx2^{-/-}$ early gastrulating mouse embryos (Zakin *et al.*, 2000). Clone 23G1 encodes a hypothetical GCN5-related N-acetyltransferase (NAT) (Table

6.3). These clones were therefore characterized with the use of web based bioinformatic tools (Table 2.6). On the other hand, 3 DD clones 20G1, 20G2, and 22C1 had no homology to any previously identified sequences nor ESTs but searches against the mouse High Throughput Genomic Sequence (HTGS) database revealed matching genomic clones (Table 6.3).

6.2.4.1 20C3, a novel and putative scaffold/matrix attachment region binding protein

The nucleotide sequence encoded by the clone 20C3 was found to have high homology with several mouse ESTs that were annotated as highly similar to the human arginine-rich, mutated in early stage tumours protein ARMET (ARMET is also known as Arginine Rich Protein, ARP). The function of ARMET is unknown but it has been found mutated in a number of cancers, including those of the lung, breast, prostate, head and neck (Shridhar *et al.*, 1996). It is also among OTX2 target genes up-regulated in *Otx2*$^{-/-}$ early gastrulating mouse embryos (Zakin *et al.*, 2000). One EST that matched 20C3, the IMAGE:944282 clone (accession no. AA545476) was purchased from Research Genetics and sequenced fully. A nucleotide sequence alignment of 20C3 and the 849 bp IMAGE:944282 is shown in Fig. 6.7A. As shown in the nucleotide sequence alignment, 20C3 is missing a 172 bp insert at position 414. It is possible that 20C3 is a product of an alternatively spliced transcript. To determine whether this was the case, the genomic structure of IMAGE 944282 was analyzed. The information on the genomic structure of the entire transcript was derived from a BLAST search of the HTGS database at NCBI. A 158137 bp mouse BAC clone RP23-239F13 from chromosome 9 (Accession number AC123065) was found to contain the whole of the IMAGE:944282 nucleotide sequence. Both the mRNA and the corresponding genomic DNA were aligned using the program Spidey at the NCBI. The transcript consists of 4 exons and 3 introns that span a 3154 bp between bases 63799 and 66953. No exon splice or donor sites were found in the 172 bp deletion identified in the clone 20C3. Instead, the sequence missing in the DD clone 20C3 was found within the 3' exon 4 (Fig. 6.7B). This therefore suggested that the region missing in 20C3 was not a result of alternative splicing. An alternative explanation is that the 172bp sequence is capable of forming a stable secondary structure that would cause the reverse transcriptase to jump across this junction and continue with cDNA synthesis thus resulting in a shortened cDNA (Zhang *et al.*, 2001).

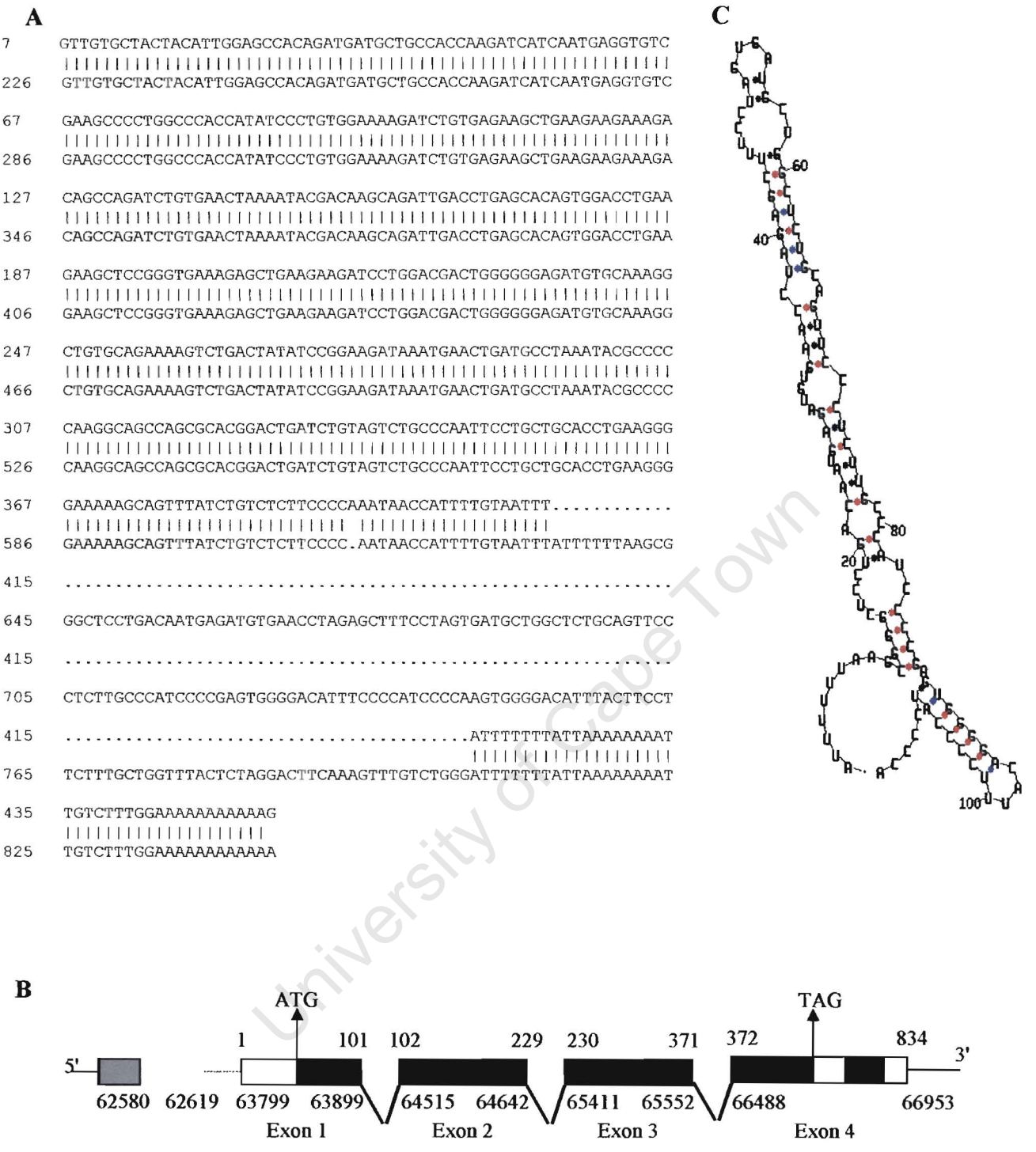

Figure 6.7 Analysis of the nucleotide sequence of the 20C3 clone. **(A)** Nucleotide sequence alignment of the differential display clone 20C3 with its matching EST IMAGE 944282 clone (accession no. AA545476). The top sequence in the alignment is the DD clone 20C3. The dashes represent the region missing in the 20C3 cDNA. **(B)** The exon-intron organization of the IMAGE 944282 clone was determined from nucleotides 63799-66953 of the BAC clone RP23-239F13. The exons are represented by open and black-shaded boxes. The hatched box within exon 4 represents the 172 bp sequence missing (nucleotides 632-805 of IMAGE 944282) in the DD clone 20C3. Introns are represented as lines joining the exons. The mRNA and genomic co-ordinates are shown above and below, respectively. The coding exons are shaded in black and both start and stop codons are shown. Further analysis of the BAC clone RP23-239F13 using GENSCAN revealed a putative 40 bp promoter at bases 62580-62619, indicated by the block shaded in grey. **(C)** The hairpin structure of the 172 bp deletion identified in clone 20C3. The structure was predicted using the MFOLD tool and has a ΔG of -31.5 kcal/mol.

Indeed, RNA structure analysis using the MFOLD program revealed that the missing 172 bp is capable of forming a stem loop structure (Fig 6.7C) that may have eluded reverse transcription of this mRNA transcript during cDNA synthesis.

A northern blot analysis was performed to determine whether the IMAGE:944282 clone had the same pattern of expression as 20C3 in FGF-2 induced OP27 differentiation. 20C3 hybridized to a distinct a transiently up-regulated (Fig. 6.6C). The IMAGE:944282 also showed a similar pattern of expression as that of 20C3 in an independent FGF-2 experiment. A signal is transiently up-regulated in OP27 cells with FGF-2 treatment, with levels barely detectable in cells at 33°C while a band was visible after 6 hours follwing treatment with FGF-2. The transcript was not detected after 6 hours (Fig. 6.8).

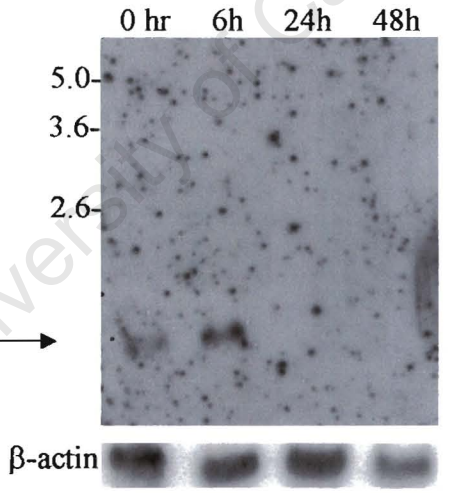

Figure 6.8 Northern blot analysis of IMAGE 944282 in OP27 cells following FGF-2 treatment. Total RNA from an independent FGF-2 experiment was analyzed and blotted. The membrane was hybridized with the IMAGE 944282 probe. IMAGE 944282 hybridized to a message of ~ 1kbp on the northern blot (arrow).

Translation of the IMAGE cDNA revealed a 537 bp open reading frame which codes for a 179 amino acid polypeptide, extending from 17 to 553 bp, thus giving a very short 5' UTR (16 bp) and a 296 bp 3' UTR (Fig. 6.9A). The putative 179 amino acid polypeptide has a molecular weight of

20.3 KDa and a pI of 8.26. IMAGE 944282 contains an N-terminal hydrophobic signal peptide that may target the protein to the secretory pathway. The signal peptide, which shows a high hydrophobicity index (Fig. 6.9B), is predicted to be cleaved between the residues Ala21 and Leu22, according to SignalP V1.1 (Nielsen *et al.*, 1997).

Several consensus phosphorylation sites (Table 6.4) were also identified, including 2 for casein kinase II dependent phosphorylation, one for a c-AMP and c-GMP dependent phosphorylation, one for tyrosine kinase phosphorylation and a protein kinase C phosphorylation site right at the C-terminus (Fig. 6.9A). The presence of these phosphorylation sites suggests that phosphorylation events are involved in regulating the activity of this protein.

Table 6.4 Consensus phosphorylation recognition motifs (Kemp and Pearson, 1990).

Protein kinase	Consensus recognition motif
Casien kinase II	S/TXXD/E
cAMP and cGMP dependent kinase	R/KXXS/T
Tyrosine kinase	R/KXXXD/EXXXY
Protein kinase C	S/TXR/K

A

```
1      GAGACGGCTGAGGAGGATGTGGGCTACGCGCGGGCTGGCGGTAGCGCTGGCCCTGAGCGT
1                      M  W  A  T  R  G  L  A  V  A  L  A  L  S  V

61     GCTGCCTGACAGCCGGGCGCTGCGGCCAGGAGACTGTGAAGTTTGTATTTCTTATCTGGG
16       L  P  D  S  R  A  L  R  P  G  D  C  E  V  C  I  S  Y  L  G

121    ACGATTTTACCAGGACCTCAAAGACAGAGATGTCACATTTTCACCAGCCACTATTGAAGA
36       R  F  Y  Q  D  L  K  D  R  D  V  T  F  S  P  A  T  I  E  E

181    AGAACTTATAAAGTTTTGCCGTGAAGCAAGAGGCAAAGAGAATCGGTTGTGCTACTACAT
56       E  L  I  K  F  C  R  E  A  R  G  K  E  N  R  L  C  Y  Y  I

                                                        20C3 primer 1
241    TGGAGCCACAGATGATGCTGCCACCAAGATCATCAATGAGGTGTCGAAGCCCCTGGCCCA
76       G  A  T  D  D  A  A  T  K  I  I  N  E  V  S  K  P  L  A  H

301    CCATATCCCTGTGGAAAAGATCTGTGAGAAGCTGAAGAAGAAAGACAGCCAGATCTGTGA
96       H  I  P  V  E  K  I  C  E  K  L  K  K  K  D  S  Q  I  C  E

361    ACTAAAATACGACAAGCAGATTGACCTGAGCACAGTGGACCTGAAGAAGCTCCGGGTGAA
116      L  K  Y  D  K  Q  I  D  L  S  T  V  D  L  K  K  L  R  V  K

421    AGAGCTGAAGAAGATCCTGGACGACTGGGGGGAGATGTGCAAAGGCTGTGCAGAAAAGTC
136      E  L  K  K  I  L  D  D  W  G  E  M  C  K  G  C  A  E  K  S

                                                  20C3 primer 2
                                                3'-GGGTTCCGTCGGTCGCG
481    TGACTATATCCGGAAGATAAATGAACTGATGCCTAAATACGCCCCCAAGGCAGCCAGCGC
156      D  Y  I  R  K  I  N  E  L  M  P  K  Y  A  P  K  A  A  S  A

       TGCCTGACT-5'
541    ACGGACTGATCTGTAGTCTGCCCAATTCCTGCTGCACCTGAAGGGGAAAAAGCAGTTTAT
176      R  T  D  L  *
601    CTGTCTCTTCCCCAATAACCATTTTGTAATTTATTTTTTAAGCGGGCTCCTGACAATGAG
661    ATGTGAACCTAGAGCTTTCCTAGTGATGCTGGCTCTGCAGTTCCCTCTTGCCCATCCCCG
721    AGTGGGGACATTTCCCCATCCCCAAGTGGGGACATTTACTTCCTTCTTTGCTGGTTTACT
781    CTAGGACTTCAAAGTTTGTCTGGGATTTTTTTATTAAAAAAAATTGTCTTTGGAAAAAAA
841    AAAAAAAAC
```

B

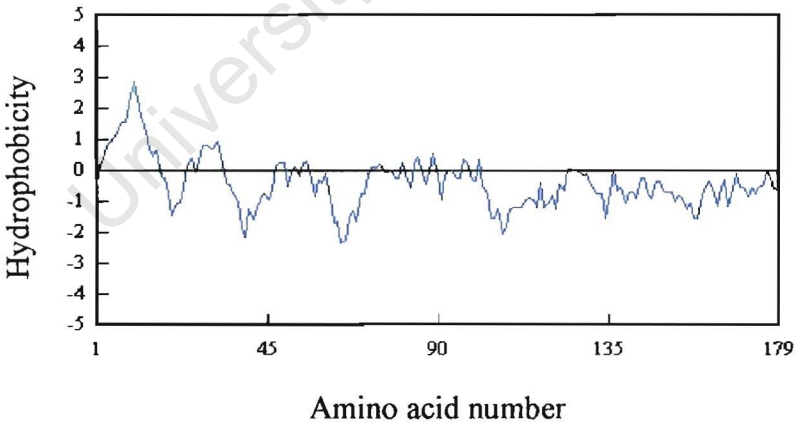

Figure 6.9 Analysis of the amino acid sequence of IMAGE 944282. **(A)** Translation of the nucleotide sequence of IMAGE clone 944282. The numbers written in black refer to the cDNA sequence and those in blue refer to the amino acid sequence. Both the start (ATG) and the stop (TGA) codons are written in bold. The signal peptide is underlined and the cleavage site is indicated by an arrow. The putative SAF-Box is double underlined. The casein kinase II dependent phosphorylation sites are shaded in yellow, the c-AMP and c-GMP dependent phosphorylation site is shaded in grey, the tyrosine kinase phosphorylation site is shaded in green and the protein kinase C phosphorylation is shaded in red. See Table 6.4 for consensus phosphorylation motifs (Kemp and Pearson, 1990). **(B)** Hydrophobicity plot of the amino acid sequence of 20C3. The signal peptide at the N-terminus has a high hydrophobicity index.

Searching the SMART domain database using the amino acid sequence of the IMAGE 944282 clone discovered the scarffold attachment factor box (SAF-Box) (PFAM model PF02037) between positions 129 and 165 (Fig. 6.9A). The SAF-Box is a conserved DNA binding domain that is found in diverse nuclear proteins that bind the scaffold attachment region (SAR) DNA (Aravind and Koonin, 2000; Kipp *et al.*, 2000). The region containing this motif has a high content of positively charged amino acids, particularly Lys, that may make contact with the negatively charged backbone of the DNA. An alignment of the putative SAF-Box of IMAGE 944282 with those of the other SAR binding proteins is shown in Fig. 6.10. Most of the conserved amino acid residues within the SAF-Box are present in IMAGE 944282. Unlike in the other proteins, the putative SAR binding domain of the EST IMAGE (the SAF Box) maps to the C-terminus of the protein while the SAF-Box of the other SAR binding proteins is located in the N-terminus (Aravind and Koonin, 2000).

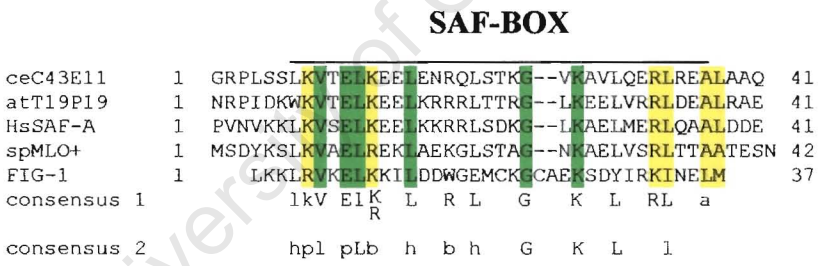

Figure 6.10 Alignment of the putative SAF-Box of FIG-1 with SAF-Boxes from other species. The other 4 SAF boxes shown in the alignment that have been shown to bind to SAR DNA (Kipp *et al.*, 2000). The consensus sequences of the SAF-Box have been manually inserted in the alignment from Kipp *et al.*, 2000 (consensus 1) and Aravind and Koonin, 2000 (consensus 2). In consensus sequence 2 'h' is for hydrophobic residues; l, aliphatic; p, polar; b, bulky. The species abbreviations are ce, *Caenorhabditis elegans*; at, *Arabidopsis thaliana*; Hs, *Homo sapiens*; sp, *S. pombe*.

A BLASTP search of the NCBI database revealed a high sequence similarity with both the published sequences of the human ARMET protein (P55145), mouse Armet (NP_083379) and with ARMET-like putative proteins from various species. A multiple sequence alignment of the ARMET homologous proteins is shown in Fig. 6.11. The mouse Armet sequence NP_083379 which is 100% identical to the amino acid sequence of the IMAGE clone was used in the alignment.

The putative SAF-Box is also conserved across all species in the alignment. Phylogenetic analysis of the various sequences revealed that the mouse Armet sequence is 99% identical to the rat sequence (XP_2366142) and 97% identical to the human ARMET sequence (Fig. 6.12). An orthologue of the rat sequence (XP_341562) was also identified. This orthologue shares a 50% sequence identity with both the rat and mouse Armet sequences (Fig. 6.11).

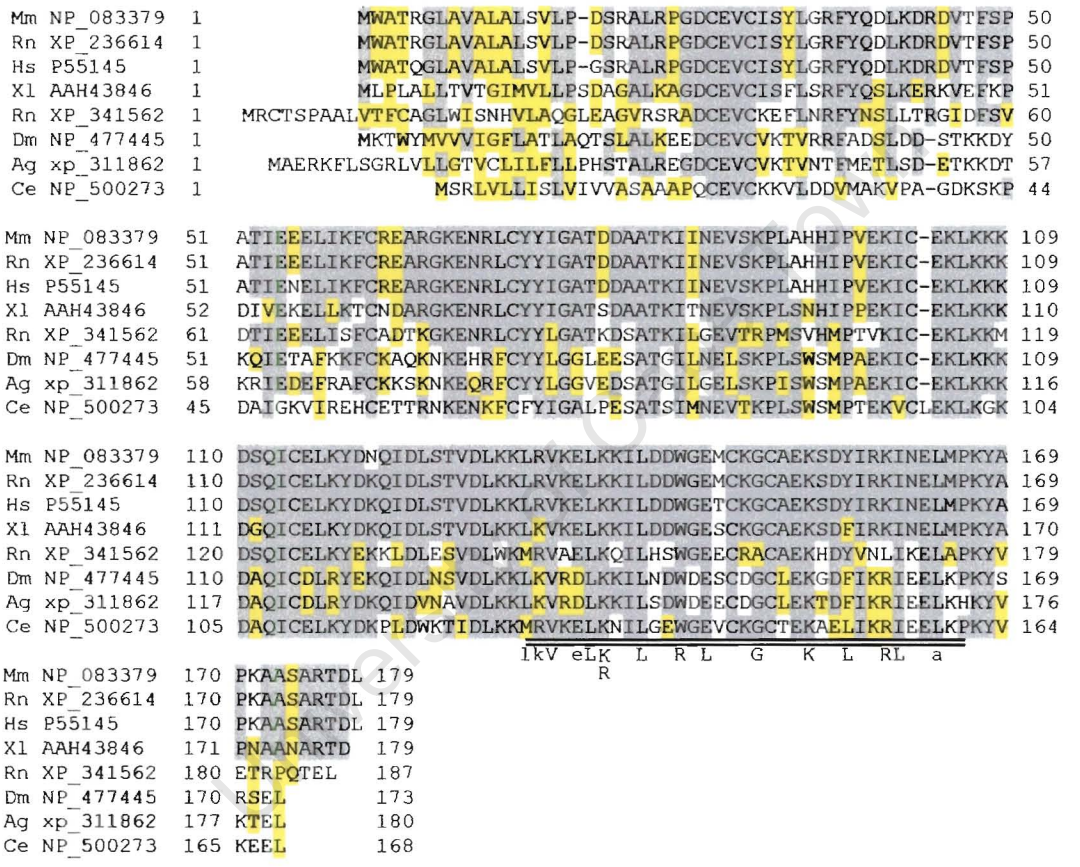

Figure 6.11 Multiple alignment of the IMAGE 944282 amino acid sequence (represented by the mouse Armet sequence Mm NP_083379) with sequences from various species. GenBank accession numbers are shown next to the species prefix. *Mm*, *Mus musculus*; *Hs*, *Homo sapiens*; *X l*, *Xenopus laevis*; *Rn*, *Rattus novergus*, *Dm*, *Drosophila melanogaster*; *Ag*, *Anopheles gambiae*; *Ce*, *Caenorhabditis elegans*. Identical amino acid residues are shown in grey while conserved residues are in yellow. The putative SAF-Box/SAP domain which is conserved is double underlined. The consensus sequence of the SAF-Box is shown underneath.

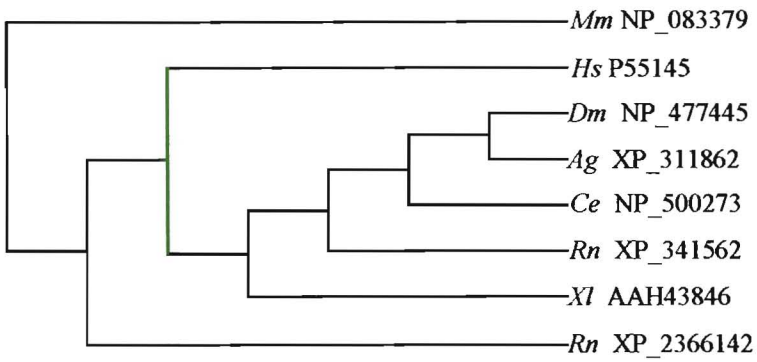

Figure 6.12 Phylogenetic analysis of the Armet-like sequences from the different species. The phylogenetic tree is based on the ClustalW multiple sequence alignment of the various sequences (shown in Fig. 6.11 above). GenBank accession numbers are shown next to the species prefix. *Mm*, *Mus musculus*; *Hs*, *Homo sapiens*; *X l*, *Xenopus laevis*; *Rn*, *Rattus novergus* , *Dm*, *Drosophila melanogaster*; *Ag*, *Anopheles gambiae*; *Ce*, *Caenorhabditis elegans*.

While the N-terminal signal peptide may target Armet for secretion, the presence of the putative SAF-Box would also suggest a nuclear localization of the protein. Using the PSORTII software, no nuclear localization signal sequences were identified in the Armet amino acid sequence. However, Reinhardt's method for cytoplasmic/nuclear discrimination which is based on the composition of basic residues (Reinhardt and Hubbard, 1998), predicted a nuclear localization with a reliability of 71%. Thus, the presence of both the N-terminal signal peptide and the SAF-Box would suggest that Armet is probably fated for a dual subcellular fate.

The distribution of the Armet mRNA on mouse tissues was analyzed with RT-PCR using gene specific primers (Fig. 6.9 for primer location). The transcript was present in the brain, OE and the heart but no expression was detected in both the kidney and liver (Fig. 6.13).

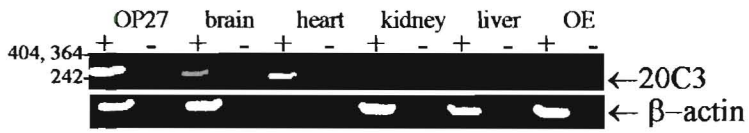

Figure 6.13 Tissue distribution of the Armet mRNA as detected by RT-PCR on mouse tissues. Primers designed from the nucleotide sequence of the DD clone 20C3 were used to amplify the transcript from OP27 cells at 33°C and from various mouse embryonic tissues. β-actin was also amplified from the tissues to control for loading.

6.2.4.2 Sequence analysis of 20G2, a clone with no homology

The 618 bp 20G2 clone was one of 4 DD clones that had no homology to any sequences in both the nr and dbEST databases. However, BLAST searches against the HTGS database revealed high homology to the mouse BAC clone RP23-400N18 (Accession number AC123842). To determine the full-length sequence of 20G2, 5' RACE was performed by using the SMART™ RACE amplification technique (Fig. 6.14A). Several PCR products of varying intensities sized ~0.5 to 3kb were obtained when the gene specific antisense primer, 20G2αs was used together with the 'universal primer' supplied in the kit (lane 1, Fig. 6.14B). The identity of the PCR products was confirmed by probing a Southern blot of the PCR products with a labelled internal sense primer, 20G2s. Several PCR products ranging from 0.5-1 kb in size gave a positive signal on the Southern blot thus confirming their identity as 5' sequence of the DD clone 20G2 (Fig. 6.14C). The largest PCR product running just below 1 kb (see arrow in Fig. 6.14C) was recovered from the agarose gel, cloned and sequenced. Sequence analysis of the 919 bp clone (known as cln3.9) confirmed the presence of the nucleotide sequence that overlaps with the original DD clone. No open reading frame was found within the nucleotide sequence of cln3.9. A northern blot analysis using cln3.9 as a probe confirmed the up-regulation of 2 transcripts at ~6 and ~3-4 kbs on OP27 cells following FGF-2 treatment (Fig. 6.14D), in agreement with the RT-PCR result in Fig. 6.6J. Both the nucleotide sequences of the original DD clone 20G2 and the SMART RACE PCR product cln3.9 were assembled into the 1104 bp contig AS1 (depicted in Fig. 6.14A). The contig AS1 was then analyzed by BLAST searches against the sequence databases at the NCBI. Only nucleotides 1-414 at the 5' end of contig AS1 matched to nucleotide sequences of cDNA clones deposited in the GenBank. The alignment of the cDNAs with contig AS1 is depicted in Fig. 6.15. Contig AS1 had a 100% homology with the 5' ends of several RIKEN clones but was never contigous with any of these clones towards the 3' end nucleotide sequences (Fig. 6.15).

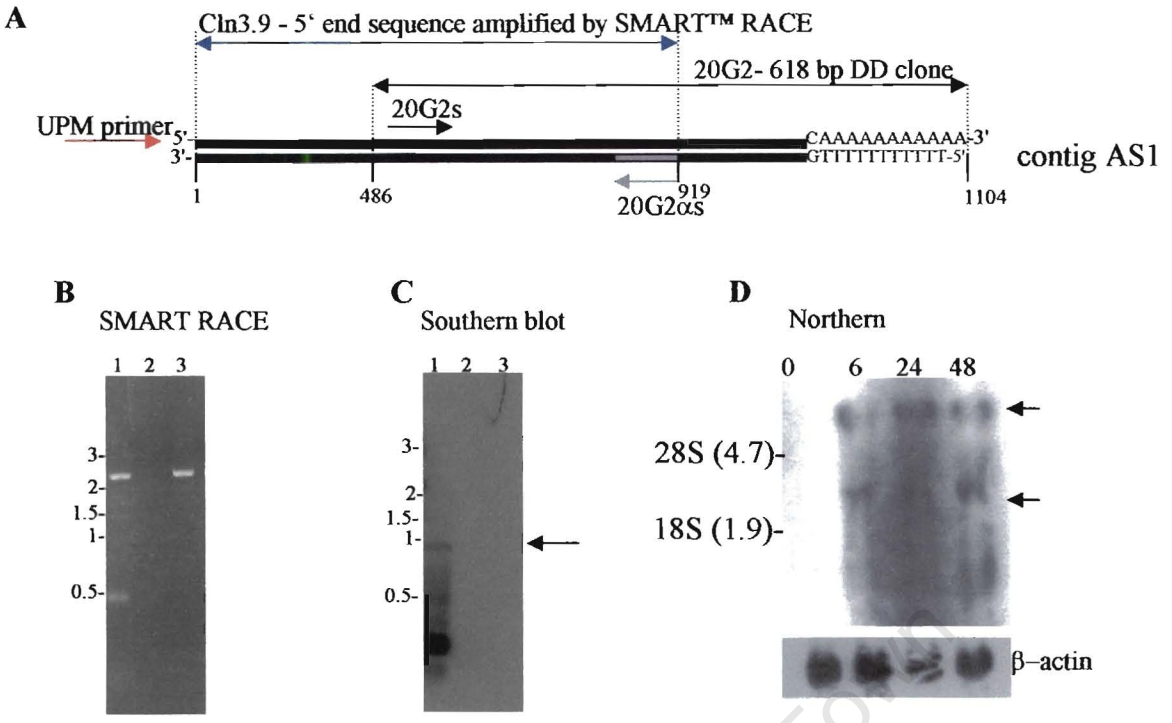

Figure 6.14 Cloning of the full-length sequence of the 20G2 clone. **(A)**. Gene specific primers were designed from the nucleotide sequence of the DD clone 20G2 (shown with black arrows above). The antisense primer 20G2αs was used in combination with the UPM primer (shown with a red arrow on the left) to amplify the 5' sequence of 20G2. The resulting clone cln3.9, 919bp in size (blue arrows), overlapped with 20G2. Both the nucleotide sequences of 20G2 and cln3.9 were assembled into 1104 bp contig AS1 **(B).** The SMART RACE reactions were conducted using the universal primer mix (UPM) supplied in the kit in combination with the primers shown above. Lane 1, UPM plus the antisense primer, 20G2αs. Lane 2, 20G2αs on its own. Lane 3, UPM on its own. Lanes 2-3 served as negative controls. Primer locations shown in the diagram in A. Molecular weight sizes are shown on the left, in kilobase pairs (kb) **(C).** Southern blot analysis of the SMART RACE PCR products. The oligonucleotide 20G2s was labelled and used to probe the Southern. The ~0.9kb PCR product that was recovered, cloned and sequenced is indicated with an arrow. **(D).** Northern blot hybridisation with cln3.9 as a probe on OP27 cells treated with FGF-2 for various time points. Times shown in hours (h). The hybridising signals are indicated by arrows. The membrane was stripped and reprobed with β-actin to control for loading.

The BLAST search also revealed a 100% homology over a 220 bp region (nucleotides 17-237 of contig AS1) with the 3' UTR of the mouse ramp2 gene (Accession number NM_019444). The 3' end of the contig AS1 (nucleotides 454-1104) which had no homology with any of the cDNA clones mentioned above, shared a high sequence identity with the genomic BAC clone RP23-400N18 (Accession number AC123842) (Fig. 6.15). Contig AS1 was also aligned with sequences deposited in the dbEST databases. Similarly, only nucleotides 1-414 of contig AS1 matched to mouse ESTs.

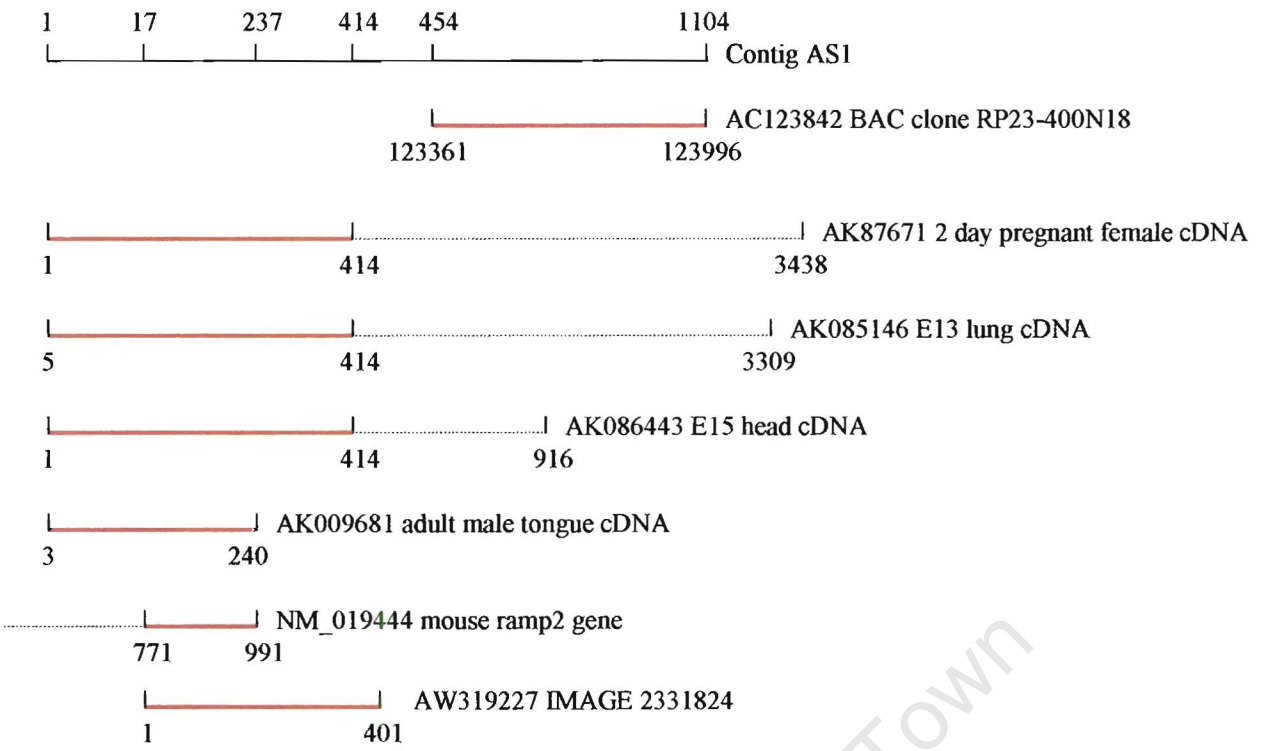

Figure 6.15 BLAST search analysis of contig AS1 against the nucleotide databases. The clones that match contig AS1 at either the 5' or 3' ends are indicated by their accession numbers and their descriptions. The alignment positions are shown. Red lines represent regions of 100% sequence homology while dotted lines represent regions of no homology.

Since only the nucleotide sequences in the 5' ends of these ESTs were deposited in the database, we purchased and analyzed one EST, IMAGE:2331824 (accession number AW319227, Fig. 6.15) to determine whether this EST and contig AS1 had the same nucleotide sequence at the 3' end. A northern blot was first performed with IMAGE 2331824 as a probe to determine whether it had a similar expression pattern to that of cln3.9 shown in Fig. 6.14D. Like cln3.9, the EST hybridized to two transcripts of ~6kb and ~ 4kb transcript that were up-regulated with FGF-2 treatment. The up-regulation of these transcripts was, however, delayed. The signals for the transcripts were evident starting after 48 hours and continued to increase with time (Fig. 6.16). IMAGE 2331824 was then fully sequenced to determine whether the nucleotide sequence at its 3' end was similar to that of contig AS1. Sequencing revealed a 1313 bp insert which was then aligned with contig AS1.

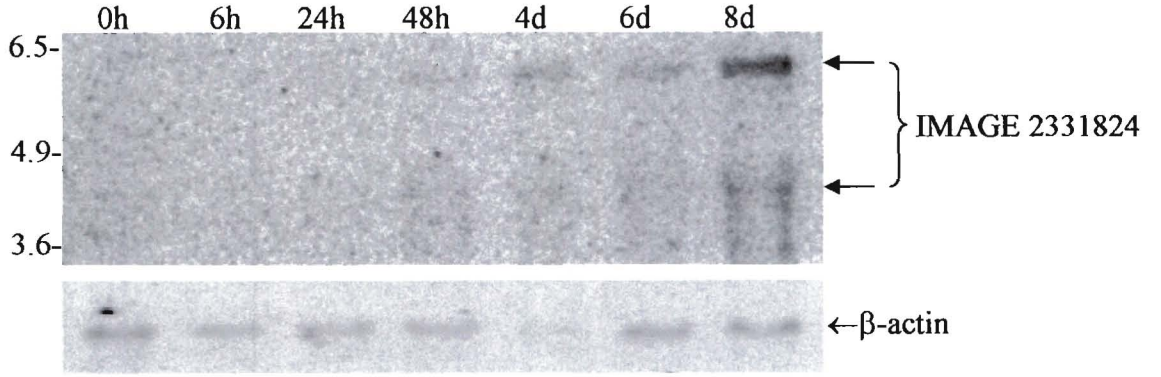

Figure 6.16 Northern blot hybridisation with IMAGE:2331824 as a probe on OP27 cells treated with FGF-2 for various time points. Times shown in hours (h) and in days (d). The hybridising signals are indicated by arrows. The blot was stripped and reprobed with β-actin a shown below.

Nucleotides 17-419 at the 5' end of contig AS1 matched perfectly with nucleotides 1-401 of IMAGE 2331824 whereas the sequences at the 3' end had no match with the EST (Fig. 6.17). It was therefore concluded that the EST and contig AS1 were not the same cDNA.

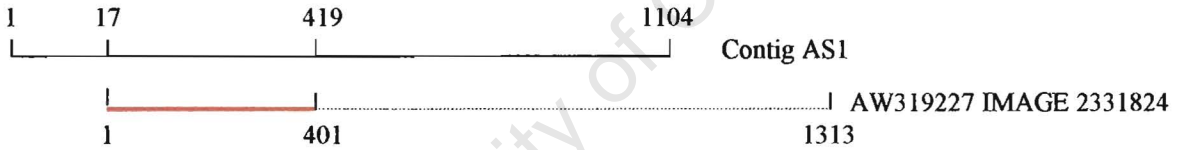

Figure 6. 17 Nucleotide sequence alignment of the contig AS1 and IMAGE:2331824. The 2 clones match only at the 5' ends and no sequence homology was evident at the 3' end. The region of high sequence similarity is indicated by the red line while the region of no homology is represented by the dotted line.

No PCR products were identified from a second round of SMART RACE PCR using the nucleotide sequence of the cln3.9 to obtain more 5' sequence information. Secondly, I had established that the cln3.9 had high sequence similarity with the 3' UTR of the mouse ramp2 gene (Fig. 6.15). I therefore designed a sense primer upstream of the coding region of ramp2 and used it together with the 20G2αs primer in RT-PCR to attempt to amplify the nucleotide region that might be flanked by the primers. No sequence was ever amplified by this primer combination, thus suggesting that cln3.9 was not the 3' UTR of the mouse ramp2 gene. Further attempts to find more sequence information using the mouse genome were not successful and as a result further analyses were aborted.

6.2.4.3 Identification of 20G3, a protein that is targeted to the mitochondria

The clone 20G3 was one of cDNAs that were identified as being differentially regulated by FGF-2 in OP27 cells. BLAST analysis of the GenBank non-redundant nucleotide database revealed high sequence identity to a mouse RIKEN cDNA 2610002J02 gene (Accession number XM_131827). An IMAGE clone (IMAGE: 4191674, Accession number BF540440) that matched both 20G3 and the RIKEN cDNA was purchased and sequenced fully to reveal a 1480 bp insert. The nucleotide sequence of 20G3 was located at positions 885-1480 bp in the insert sequence (Fig. 6.18).


```
1    aaGCttGTTGTGCCAGAA.GCGTTTGCCCCGAAGTTGCCCCAGCTAGATGTGGATAGCCACC
       ||  |||||||||||| ||||||| ||||||| || ||||||||||||||||||||||||
883  TTGCCCGTTGTGCCAGAAGGCGTTTGACCCGAAGCTGACCCAGCTAGATGTGGATAGCCACC

62     TTGCTCAGTGCTTGGCTGAGTGCACCGAAGATGTGGTGTGGTGAGCATCAGGGTGCCTTG
       ||||||||||||||||||||||||||||||||||||||||||||||||||||||||||||
945    TTGCTCAGTGCTTGGCTGAGTGCACCGAAGATGTGGTGTGGTGAGCATCAGGGTGCCTTG

122    CTGTATCTCC.TTCAAACCTACACACCGACATTGGATGTGGCTTCTGAGACATCGTCGTG
       |||||||||| ||||||||||||||||||||||||||||||||||||||||||||||||
1005   CTGTATCTCCGTTCAAACCTACACACCGACATTGGATGTGGCTTCTGAGACATCGTCGTG

181    TGGACACCTGAGTATTGGCTCCTTCTGGTTTTGTTCATGGGCATTGGACATAATGCTGGT
       ||||||||||||||||||||||||||||||||||||||||||||||||||||||||||||
1065   TGGACACCTGAGTATTGGCTCCTTCTGGTTTTGTTCATGGGCATTGGACATAATGCTGGT

241    CACTGACAGCAGGCAGCACTGATCCTCTGTGGACTCATCTTCATTGTCAGCCTGACAGGA
       ||||||||||||||||||||||||||||||||||||||||||||||||||||||||||||
1125   CACTGACAGCAGGCAGCACTGATCCTCTGTGGACTCATCTTCATTGTCAGCCTGACAGGA

301    TGTGGAATCACCCAGGAGACACATCTCAGGTGTGCCTGTGAAACCGTTCCCAGAGATTAC
       ||||||||||||||||||||||||||||||||||||||||||||||||||||||||||||
1185   TGTGGAATCACCCAGGAGACACATCTCAGGTGTGCCTGTGAAACCGTTCCCAGAGATTAC

361    CTGGGACAGGAAGTCCCAGCTGAATGTGGGTGGCACCGTGGCCT.GGGTCCCACTGATTG
       |||||||||||||||||||||||||||||||||||||||||||| ||||||||||||||||
1245   CTGGGACAGGAAGTCCCAGCTGAATGTGGGTGGCACCGTGGCCTGGGGTCCCACTGATTG

420    AAAAGGGAAAATGGAGAAATTGAGCTGTTTCCTCACTGGGGATGTGATGAGATGCACCGC
       ||||||||||||||||||||||||||||||||||||||||||||||||||||||||||||
1305   AAAAGGGAAAATGGAGAAATTGAGCTGTTTCCTCACTGGGGATGTGATGAGATGCACCGC

480    TCGCCTGCTACGGCAGCCATAGCTACTTTTGCTACTGTGCCCTCCTTGCCACAGGGACTG
       ||||||||||||||||||||||||||||||||||||||||||||||||||||||||||||
1365   TCGCCTGCTACGGCAGCCATAGCTACTTTTGCTACTGTGCCCTCCTTGCCACAGGGACTG

540    TACCTTAACTGTGAGCCAGAATAAATTTTAAGTTGCTTTCCAAAAAAAAAAA
       |||||||||||||||||||||||||||||||||||| ||||||||||
1425   TACCTTAACTGTGAGCCAGAATAAATTTTAAGTTGCTTTCCGAAAAAAAAAA
```

Figure 6. 18 Nucleotide sequence alignment of the differential display clone 20G3 with its matching EST IMAGE 4191674 clone (accession no. BF540440). The upper line in the alignment is the DD clone 20G3. The DD primers are shown in bold in the alignment. The mismatches between the H-AP20 primer and the IMAGE clone are shown in small letters.

Since the differential expression of 20G3 in the reverse northern analysis contradicted that in the DD screen, RT-PCR primers were designed from the nucleotide sequence of IMAGE 4191674 and were used to analyze the pattern of expression of 20G3 in FGF-2 induced OP27 cells. A semi-quantitative RT-PCR assay showed an up-regulation of the 20G3 transcripts as the cells differentiate in the presence of FGF-2 at 39°C (Fig. 6.19) consistent with the reverse northern blot analysis (Fig. 6.5).

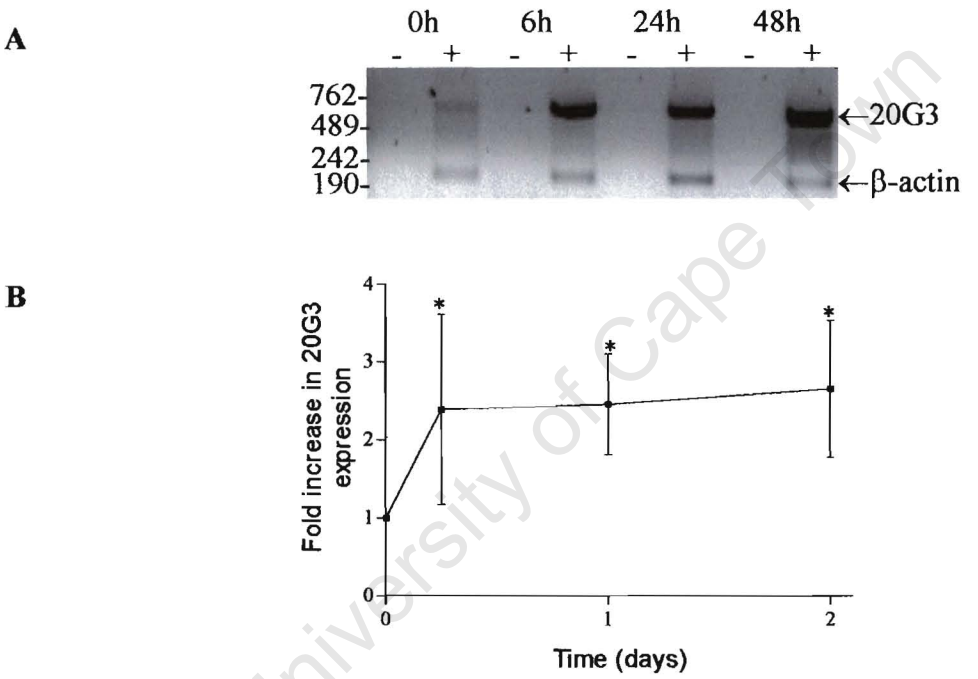

Figure 6.19 Semi-quantitative RT-PCR analysis of 20G3 in differentiating OP27 cells. **(A)** Up-regulation of 20G3 mRNA transcripts by FGF-2 in OP27 cells. A representative semi-quantitative RT-PCR analysis of 20G3 in OP27 cells treated with FGF-2 for various times (in hours, h). 20G3 and β-actin were co-amplified in the same reaction tube. +, amplification from total RNA that had been reverse transcribed; -, amplification from total RNA in a reverse transcription reaction in which the reverse transcriptase was omitted. Molecular weight sizes (in base pairs) are indicated on the left of the gel. **(B)** 20G3 and β-actin signals were quantitated at each time-point and plotted as fold-increase in the ratio of 20G3/β-actin with the ratio at 0h taken as 1. Data represent mean ± SEM values of 3 independent experiments. Significance, *$p<0.05$ compared to time 0 hours.

The same oligonucleotides were used to study the expression of 20G3 in mouse tissues. Several E12.5 embryonic tissues, including brain, heart, kidney and OE expressed the gene encoded by 20G3 (Fig. 6.20).

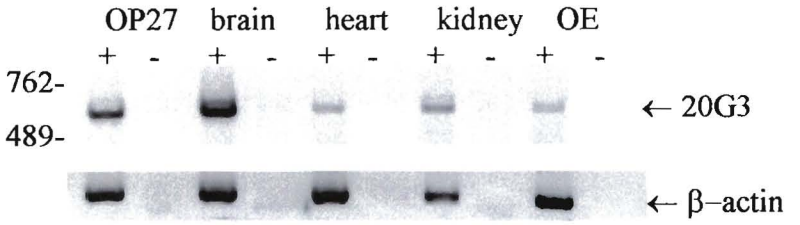

Figure 6.20 RT-PCR analysis of 20G3 in mouse tissues. Primers designed from the nucleotide sequence of IMAGE 4191674 clone were used to amplify the transcript from OP27 cells that were treated with FGF-2 for 6 hours at 39°C and from adult mouse tissues. β-actin was also amplified from the tissues to control for loading.

Translation of the 1480 bp EST sequence revealed a 528 bp ORF extending from 458 to 986 bp. This ORF codes for a hypothetical 176 amino acid protein, refered to as 20G3 in this study (Fig. 6.21). The 20G3 protein sequence was analysed for the presence of functional domains using various bioinformatic tools (Table 2.6). Two consensus phosphorylation motifs (Table 6.4) were identified by the PROSITE motif programme: 4 potential CKII phosphorylation sites at amino acids 24-27, 61-64, 127-130, and 155-158, and 3 potential PKC phosphorylation sites at 95-97, 113-115, and 122-124 (Fig. 6.21).

The subcellular localization of the 20G3 was investigated to suggest a possible function of the protein. The PSORTII programme revealed a mitochondrial targeting sequence motif at residue 18 on the N-terminus (Fig. 6.21). Targeting predictions with 2 other software packages, TargetP version 1.01 and Predotar version 0.5 supported a mitochondrial localization of 20G3 with high scores of 0.709 with TargetP and 0.820 with Predotar.

A

```
1          GACTGCGGGGGAGGCTGAGCCGTCGGAGGCCGCCCGCGGGGGGCGGGTGAGGCGGGACAG
61         AGCGGAAGGGTGGGGTCCTGGGGGCTTTGGAAGGCGCtgaGACACCGGGAAGGCGATGGG
121        GACGCCTCGATGTTCCCGCCTAGCTGCGGGGTTCCTCGCACGCGTGCATCTCGCTACCAG
181        CCGCGCTCCGCCTCTCTCGGGGCGCGGTCGCTTCTTCCGCCCCAACGCTGCTGTTCCCCA
241        CCACCACCTCCGCCACCCCTCTTCACGTCGCCCATTTATCCACTTCTTTCTCAGCCCCAG
301        GCTCCGTTTCCCCCAAGAGTCCATTTACCCTTCTAAGtgaGGTTCCTTCCCGGTCTCTTA
361        CTATGGACTCCCTCCTCCATTACCCCATTGTGGACCTGCTCCCtagCCCTGGTACCCCTC
421        ACTGtagAATCAACTCTTCACGATATCTCTACCATGGATGCCCCGGCTGACTCTTCCTGT
  1                                                M  P  R  L  T  L  P  V

481        GCTTCCCAGGCCCCCTAACTGCCGCCCTTGGTTTCTCTCGGAGGGAAGTAAGAGTGAGCC
9            L  P  R  P  P  N  C  R  P  W  F  L  S  E  G  S  K  S  E  P

541        CTGGGCTGCTCTGTTGCGCAGCACCGTGAGCGGGACCGCGGATTGGACCCCGAACCGTCA
29           W  A  A  L  L  R  S  T  V  S  G  T  A  D  W  T  P  N  R  Q

601        GCCATTACCACCGCTGCCTGCTTTTCCCAGCCAGGAGTCTCTACCTGACCCAGAGTCCAC
49           P  L  P  P  L  P  A  F  P  S  Q  E  S  L  P  D  P  E  S  T

661        TGTGCCTCCTGAGGCCTTCACTGTGGGATCCAAGACTTTCTCCTGGACGCCTTTGCCACC
69           V  P  P  E  A  F  T  V  G  S  K  T  F  S  W  T  P  L  P  P

721        TGCCCTTCGTGGCTCTGGAAGCTCCCGCCACCTGTTCTGTGAACCTGAAGGCTCCCTGGG
89           A  L  R  G  S  G  S  S  R  H  L  F  C  E  P  E  G  S  L  G

781        GTCACCTACTCCGTCCCTGAAAGGATGCCCTGCACTAAATTCTGGTCGAACTCCCAGCGC
109          S  P  T  P  S  L  K  G  C  P  A  L  N  S  G  R  T  P  S  A

841        CCAGGAGTGTGTGCCTGTGCAGAGTCCACTTGCGTTGCTGAGTTGCCCGTTGTGCCAGAA
129          Q  E  C  V  P  V  Q  S  P  L  A  L  L  S  C  P  L  C  Q  K

901        GGCGTTTGACCCGAAGCTGACCCAGCTAGATGTGGATAGCCACCTTGCTCAGTGCTTGGC
149          A  F  D  P  K  L  T  Q  L  D  V  D  S  H  L  A  Q  C  L  A

961        TGAGTGCACCGAAGATGTGGTGTGGTGAGCATCAGGGTGCCTTGCTGTATCTCCGTTCAA
169          E  C  T  E  D  V  V  W  *
1021       ACCTACACACCGACATTGGATGTGGCTTCTGAGACATCGTCGTGTGGACACCTGAGTATT
1081       GGCTCCTTCTGGTTTTGTTCATGGGCATTGGACATAATGCTGGTCACTGACAGCAGGCAG
1141       CACTGATCCTCTGTGGACTCATCTTCATTGTCAGCCTGACAGGATGTGGAATCACCCAGG
1201       AGACACATCTCAGGTGTGCCTGTGAAACCGTTCCCAGAGATTACCTGGGACAGGAAGTCC
1261       CAGCTGAATGTGGGTGGCACCGTGGCCTGGGGTCCCACTGATTGAAAAGGGAAAATGGAG
1321       AAATTGAGCTGTTTCCTCACTGGGGATGTGATGAGATGCACCGCTCGCCTGCTACGGCAG
1381       CCATAGCTACTTTTGCTACTGTGCCCTCCTTGCCACAGGGACTGTACCTTAACTGTGAGC
1441       CAGAATAAATTTTAAGTTGCTTTCCGAAAAAAAAAAAAAA
```

Figure 6.21 Analysis of 20G3 putative amino acid sequence. Translation of the full-length 20G3 nucleotide sequence. The numbers written in black refer to the cDNA sequence and those in blue refer to the amino acid sequence. The polyadenylation signal sequence is underlined. Both the start (ATG) and the stop (TGA) codons are written in bold. Several stop codons (written in bold small capital letters) are present upstream of the ATG start codon. The mitochondrial targeting sequence motif is double underlined. The casein kinase II dependent phosphorylation sites are shaded in yellow, and the protein kinase C phosphorylation is shaded in red. The consensus recognition motifs of the phosphorylation sites are shown in Table 6.4

BLASTp analysis using the 20G3 protein sequence revealed high homology to other rodent and human hypothetical proteins (Fig. 6.22). 20G3 shares a 94% sequence identity with another mouse sequence (XP_131827) with differences in the N-terminus. The rat sequence also has a high sequence identity with both 20G3 and XP_131827 (with 81% and 88% identity, respectively). The two human sequences (BAC86730 and BAB70965), while sharing a 88% sequence identity

between them, have very limited sequence identity (50%) with the rodent sequences. This suggests that the 2 human sequences are probably orthologues of 20G3 like sequences not identified in the human genome yet. No other homologues were identified in other vertebrates.

```
XP_131827   1                                                              0
20G3        1                                                              0
XP_342995   1                                                              0
BAB70965    1                                                              0
BAC86730    1   MCGPEHLLCCPKDLAMFPRQLSLTACLPGTPVSHKCHHIWLWVGVPAWHPRASRCGGAQPSSW 63

XP_131827   1     MEEERRLRGRLS------------RR----------RPPAGG-------------G---PP 23
20G3        1           MP--------------RL----------TLPVLP-------------R---PP 13
XP_342995   1     MEEERRLRGRLS------------RR----------RPPAGG-------------G---PP 23
BAB70965    1     MEAARRPRLGLS------------RR----------RPPPAG-------------G---PS 23
BAC86730    64  LHQKAARAFWLSLPAAKLRHHSSRWLRRSGAFSSGSTLKPPPSPSPAPLCHADNLRTGRTRPS 126

XP_131827   24  NCRPWFLSEGSKSE-PWAALLRSTVSGTADWTPNRQPLPPLPAFPSQESLPDPESTVPPEAFT 85
20G3        14  NCRPWFLSEGSKSE-PWAALLRSTVSGTADWTPNRQPLPPLPAFPSQESLPDPESTVPPEAFT 75
XP_342995   24  NCRPWFLSEESKSE-PWAALLRSTVGGNTDWTPNSQPLPPLPAFPSQESLPDPESTVPPEVFT 85
BAB70965    24  GGRPWFLLGGDERERLWAELLRTVSP----ELILDHEVPSLPAFPGQEPRCGPE---PTEVFT 79
BAC86730    127 GGRPWFLLGGDERERLWAELLRTVSP----ELILDHEVPSLPAFPGQEPRCGPE---PTEVFT 182

XP_131827   86  VGSKTFSWTPLPPALRGSGSSRHLFCEPEGSLGSPTPSLKGCPALNSGRTPSAQECVPVQSPL 148
20G3        76  VGSKTFSWTPLPPALRGSGSSRHLFCEPEGSLGSPTPSLKGCPALNSGRTPSAQECVPVQSPL 138
XP_342995   86  VGSKTFSWTPFPPALRGSGSSCRLLRCPEGSPGSPAPSLKGCPALDSRQTPSTQECV--QSQL 146
BAB70965    80  VGPKTFSWTPFPPDLWGPGRSYRLLHGAGGHLESPARSLPQRPAPDPCRAPRVEQQPSVEGAA 142
BAC86730    183 VGPKTFSWTPFPPDLWGPGRSYRLLHGAGGHLESPARSLPQRPAPDPCRAPRVEQQPSVEGAA 245

XP_131827   149 ALLSCPLCQKAFDPKLTQLDVDSHLAQCLAECTEDVV---W              186
20G3        139 ALLSCPLCQKAFDPKLTQLDVDSHLAQCLAECTEDVV---W              176
XP_342995   147 VLLNCPLCQKAFDPKLTQLDVDSHLAQCLAESTEDVV---W              184
BAB70965    143 ALRSCPMCQKEFAPRLTQLDVDSHLAQCLAESTEDVTCLSWMCKTLNDPGSQG 195
BAC86730    246 ALRSCPMCQKEFAPRLTQLDVDSHLAQCLAESTEDVT---W              283
```

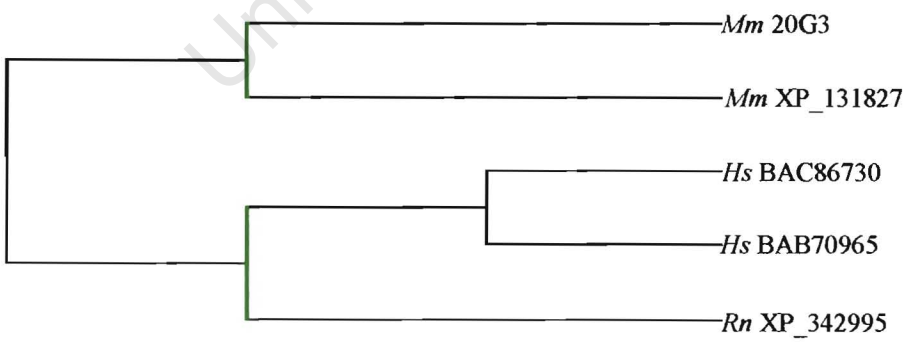

Figure 6.22 Multiple alignment of the 20G3 amino acid sequence with sequences from mouse, rat and human. (B). Phylogenetic analysis of the 20G3-like sequences. The phylogenetic tree is based on the ClustalW multiple sequence alignment of the sequences (A). GenBank accession numbers are shown next to the species prefix. *Mm*, *Mus musculus*; *Hs*, *Homo sapiens*; *Rn*, *Rattus novergus*

6.2.4.4 Identification and sequence analysis of 23G1, a putative N-acetyltransferase

The clone 23G1 was originally identified as a down-regulated cDNA transcript in the DD screen but subsequent verification by reverse northern and northern analyses showed an up-regulation with the FGF-2 treatment (Fig 6.5 and 6.6). The 540 bp 23G1 insert contained both H-AP23 and H-T_{11}G primer sequences used to display the transcript. A 1427 bp mouse cDNA (Accession number AK015640) that was 98% identical (9 nucleotide differences, Expect = 0.0) to 23G1 was identified during BLAST searches of the nucleotide sequence databases. As expected for a cDNA identified in a DD screen, 23G1 matched the 3' UTR of AK015640 between bases 901 to 1427 (Fig. 6.23). The mouse cDNA (Accession number AK015640) was annotated as a gene that codes for a hypothetical GCN5-related N-acetyltransferase (NAT). The AK015640 nucleotide sequence is smaller in size compared to the message (which is approximately 1.8 kb) predicted for 23G1 on the northern blot analysis shown in Fig. 6.6E. Attempts to identify the full-length cDNA of 23G in OP27 cells using the SMART™ RACE technology were not successful possibly as a result of severe secondary structures in the mRNA transcript. A conceptual translation of the AK015640 sequence predicted a 183 amino acid (549bp) open reading frame (ORF) extending from 675-1226 bp (Fig 6.23). The original DD clone 23G1 matched the 901-1427 region that includes the C-terminal 108 amino acids of the protein (Fig. 6.23).

The amino acid sequence of the predicted protein encoded by AK015640 (refered to here as 23G1NAT) was subjected to various bioinformatic tools to characterize the protein. A transmembrane (TM) domain was predicted between residues 74 and 97 and a bipartitie nuclear localization signal (NLS) sequence was found by PSORTII at positions 101-116. The NCBI Conserved Domain Search predicted a GCN5-related N-acetyltransferase (GNAT) domain between residues 77-159 that encompass both the TM domain and the NLS (Fig. 6.23).

A

```
1       GGAGAGGCTCGGCAGCGGCGGCGACAGGGTGGCGGTGGTGGCGGCGGACGGCCGCGGCGG
61      TGAAGGCGACTGCGGCGCGGCGGTGGCTGAGGGAGAGGAGCGGCGGAAACGGCGGCGGGG
121     AGCGGCGCGGGGATGGCGGAGGTACCGCCTGGGCCTAGCAGCCTCCTCCCACCACCAGCG
181     CCTGCGGCCCCAGCGGCGGCGGACTCCGCTGCCCGTTCCCGGCGGGGGCCGCGCTCGCTT
241     GCTGCAGCGAGGACGAGGAGGACGACGAGGAGCACGAAGGCGGCTGCGGGACCCAGCGGG
301     CGGNCGAGGCGGCGACCTCGGCCAAGGCGCGTTCTTGCCTTCGCTGCCCGCAGCTGCCTC
361     CGGAGCAGCAGCAGCAGCAGCTCAACGGCTTGATCGGCCCAGAACTGCGACACCTCCGGG
421     CCGCGGCGACCCTCAAGAGTAAGGTTCTGAGTGCAGCGGAGGCGGCCGCCCCCGACGGGG
481     CCTCCAAAGTGACTGCCACAAAAGGAGCCGAGGGACACCCGGGGGAGAGACCTCCCCACT
541     CGGTCCCCAACAATGCAAGAACTGCACTCCCCGGCCGGTCAGAGGCAGCGGCGGCGGCGG
                                Rik621 primer
601     CGGGGGCGGCGAGCGACCCCGCTGCGGCCCGAAATGGACTGGTGGAGGGCACCGAGCAGC
661     AGGAGGAGGAGGAGATGGACGAGCAGGTGCGGCTGCTGTCTTCGTCTCTGACCACCGGCT
1                       M  D  E  Q  V  R  L  L  S  S  S  L  T  T  G

721     GCAGTTTAAGGAGCTCCCAGGGCAGGGAGGCCGAGCCCGGGGAGGATCGGACGATACGAT
16      C  S  L  R  S  S  Q  G  R  E  A  E  P  G  E  D  R  T  I  R

781     ACGTCCGATATGAATCTGAGCTCCAAATGCCTGATATCATGAGACTGATCACCAAAGATC
36      Y  V  R  Y  E  S  E  L  Q  M  P  D  I  M  R  L  I  T  K  D

841     TGTCTGAACCCTACTCCATTTATACGTATAGATATTTTATCCACAACTGGGCCACAGCTGT
56      L  S  E  P  Y  S  I  Y  T  Y  R  Y  F  I  H  N  W  P  Q  L
```

B

```
          H-AP23 primer
       5'-aagCTTGGCtATG-3'
901     GTTTCTTGGCCATGGTAGGGGAGGAGTGTGTAGGTGCCATCGTTTGCAAGTTGGATATGC
76      C  F  L  A  M  V  G  E  E  C  V  G  A  I  V  C  K  L  D  M

                                      fp433 primer
                                   3'-ATCGGTACAATCGGCACCTGAG-5'
961     ACAAAAAGATGTTCCGCAGAGGTTATATAGCCATGTTAGCCGTGGACTCCAAATACAGGA
96      H  K  K  M  F  R  R  G  Y  I  A  M  L  A  V  D  S  K  Y  R

1021    GAAATGGCATTGGTACTAACTTGGTAAAGAAAGCTATATATGCCATGGTTGAAGGAGACT
116     R  N  G  I  G  T  N  L  V  K  K  A  I  Y  A  M  V  E  G  D

1081    GTGACGAGGTTGTTTTGGAAACAGAAATTACAAATAAGTCTGCTTTGAAACTTTATGAAA
136     C  D  E  V  V  L  E  T  E  I  T  N  K  S  A  L  K  L  Y  E

1141    ATCTTGGTTTTGTTCGAGATAAGAGGCTGTTCAGATACTATTTAAATGGAGTTGACGCAC
156     N  L  G  F  V  R  D  K  R  L  F  R  Y  Y  L  N  G  V  D  A

1201    TGCGACTTAAACTGTGCGTGCGCTGAGGAACTGACAGCAAGGAACGACTCCACCCACACG
176     L  R  L  K  L  C  V  R  *
1261    GAAGCGACTTTTGCATGCAATGCAATTTGTGCAGAATTGCTTTGCAGGTGGATTTAGTGA
1321    TTCCCATGCAGCTGTTATCTGTCAGTGTCCATTGAGTGTTGCACAATATTTGTTGCACTT
1381    TGGCATGGCGCATTTGTTCTGAATTAAATGAGATTGTTTTAAACTTCAAAAAAAAAAAn
                                                    3'-GTTTTTTTTTTTCGAA-5'
                                                          H-T11G primer
```

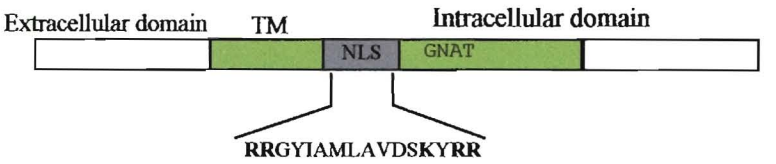

Figure 6.23 Nucleotide sequence of 23G1NAT cDNA (accession AK015640), and the deduced amino acid sequence. **(A)** The cDNA region (23G1) identified by differential display is boxed. The DD primers, H-AP23 and H-T_{11}G, which were used to display this cDNA are shown inside the box. The mismatches between the H-AP23 primer sequence and the 23G1NAT sequence are shown in small capital letters. The numbers written in black refer to the cDNA sequence and those in blue refer to the amino acid sequence. Both the start (ATG) and the stop (TGA) codons are written in bold. The polyadenylation signal is located at nucleotides 1403-1408 (bold and underlined)with the poly(A) at beginning at nucleotide 1427. In the amino acid sequence, the bipartite nuclear localization signal sequence is underlined and the putative transmembrane is double underlined. The location of the primers, Rik621 and fp433 which were used for RT-PCR in Fig. 6.26 are shown in red letters. **(B)** Schematic diagram showing the localization of the GNAT domain (shaded in green), the potential transmembrane domain (TM, within the GNAT domain) and the bipartite nuclear localization signal (NLS, shown in gray) in the 23G1NAT sequence. The NLS contains 2 positively charged amino acid clusters (shown in bold) that are separated by 10 amino acids.

All members of the GNAT superfamily transfer an acetyl group from acetyl CoA to different amino groups of different proteins. This superfamily has members from all kingdoms of life, including yeast, bacteria, plants, and vertebrates (Neuwald and Landsman, 1997). Blast analysis using the protein sequence of 23G1NAT revealed that the best matches represented hypothetical acetyltransfereases from rat, human, arabidopsis, fruit-fly and worm. The yeast N-acetyltransferase gene MAK3 also revealed high homology to the mouse 23G1NAT. A multiple sequence alignment of the protein sequences shows highly conserved sequences (Fig. 6.24).

The GNAT superfamily of NATs is characterized by four conserved sequence motifs (C, D, A, B) which span over 100 residues (Neuwald and Landsman, 1997). Motif A (Arg/Gln-X-X-Gly-X-Gly/Ala) which is involved in binding the AcCoA, is the most highly conserved among NATs in general. This is also the case in the protein alignment shown in Fig. 6.24A. Site-directed mutagenesis of any one of the conserved residues in this short segment reduces NAT activity of the protein (Wolf *et al.*, 1998). This short segment is present in the protein sequence of 23G1NAT at position 115 and is well conserved across species. Additional highly conserved amino acid sequences are found downstream of the motifs C, D and B (Fig 6.24A).

Mouse genomic databases were searched using the AK015640 cDNA, revealing a genomic clone RP24-142A23 (Accession number AC102726) that contained the gene in its entirity. Alignment of the full length cDNA sequence with the genomic clone using Spidey revealed a 5 exon structure for the 23G1NAT gene spanning 15173 bps (Fig. 6.25).

A

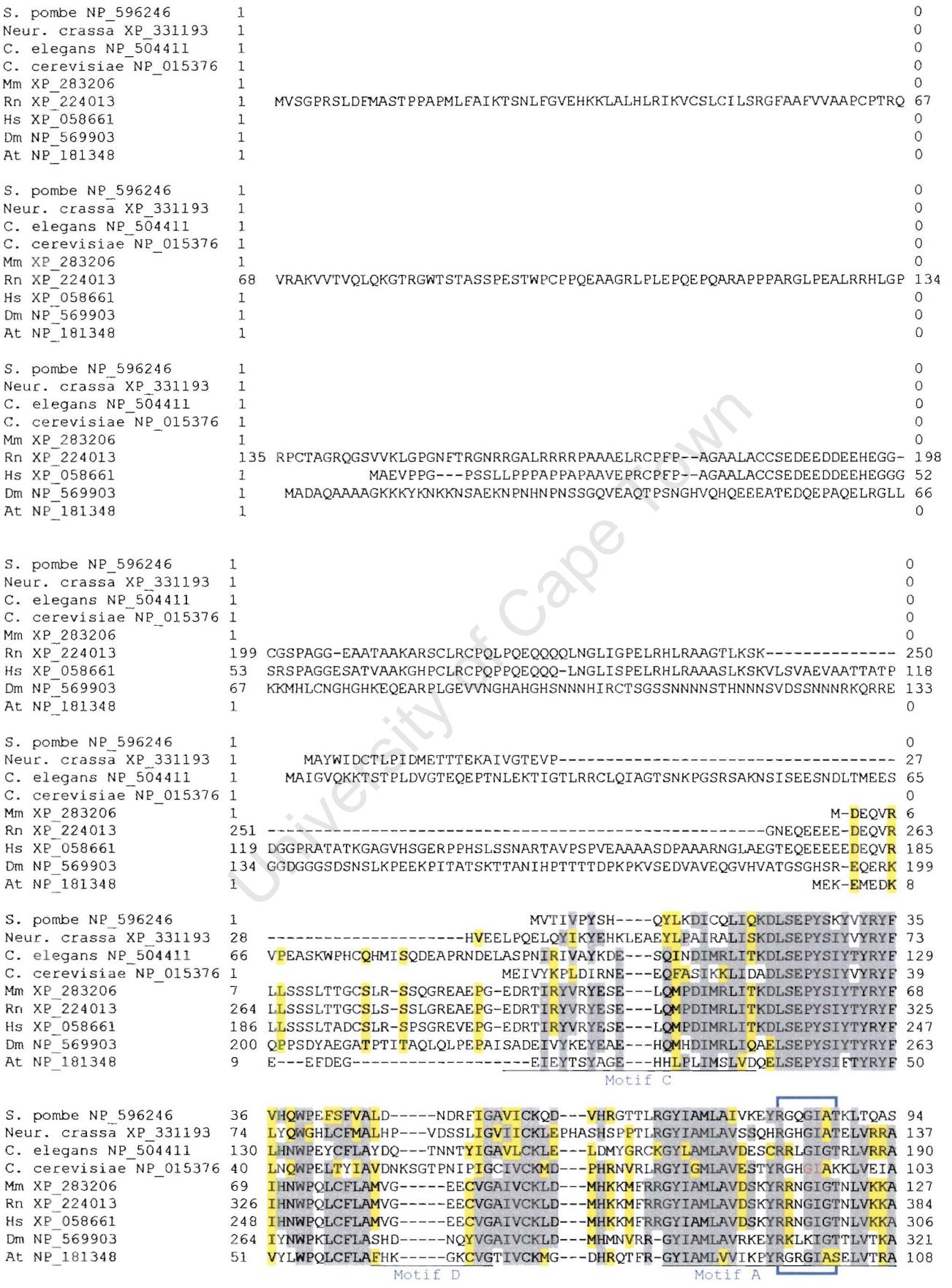

```
S. pombe NP_596246          95  LDVMKNRGAQE----------------------------IVLETEVDNEAAMSFYERLGFCRYKRL 132
Neur. crassa XP_331193     138  IDAMAQRDADE----------------------------IVLETEETNIPAMRLYERLGFVRSKKL 175
C. elegans NP_504411       191  LDAMQSKGCDE----------------------------IVLETEVSNKNAQRLYSNLGFIRQKRL 228
C. cerevisiae NP_015376    104  IDKMQREHCDE----------------------------IMLETEVENSAALNLYEGMGFIRMKRM 141
Mm XP_283206               128  IYAMVEGDCDE----------------------------VVLETEITNKSALKLYENLGFVRDKRL 165
Rn XP_224013               385  IYAMVEGDCDEKVKDHGWSRDWQLNAEHAEEEEGDPVKLSVVLETEITNKSALKLYENLGFVRDKRL 451
Hs XP_058661               307  IYAMVEGDCDE----------------------------VVLETEITNKSALKLYENLGFVRDKRL 344
Dm NP_569903               322  IEAMLADNADE----------------------------VVLETEMRNQPALRLYENLGFVRDKRL 359
At NP_181348               109  IKAMMESGCEE----------------------------VTLEAEVSNKGALALYGRLGFIRAKRL 146
                                                                                    Motif B

S. pombe NP_596246         133  YRYYLNGTDAFRYILYPN                                  150
Neur. crassa XP_331193     176  HRYYLNGNSAYRLVLLLRSVDADATN---DYAPDDRDIALR           213
C. elegans NP_504411       229  LKYYLNGGDAFRLKLIFTSRRVRSLNNQENYQPRCRVNEDDTPDEEEGTY  278
C. cerevisiae NP_015376    142  FRYYLNEGDAFKLILPLTEKSCT----RSTFLMHGRLAT             176
Mm XP_283206               166  FRYYLNGVDALRLKLWLR                                  183
Rn XP_224013               452  FRYYLNGVDALRLKLWLR                                  469
Hs XP_058661               345  FRYYLNGVDALRLKLWLR                                  362
Dm NP_569903               360  FRYYLNGVDALRLKLWFR                                  377
At NP_181348               147  YHYYLNGMDAFRLKLLFPKPRVPQIPSQVQTQQEYETFPRPRVP        190
```

B

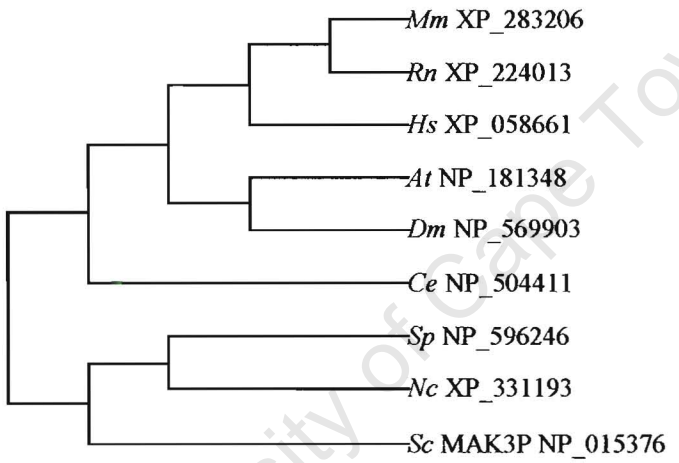

Figure 6.24 Multiple sequence alignment and phylogenetic analysis of the GCN5-related N-acetyltransferases. **(A)** Identical residues are shaded in green and strongly similar residues are in gray shading. The underlined regions in the alignment correspond to motifs C, D, A, and B as designated by Neuwald and Landsman (1997). The Arg/Gln-X-X-Gly-X-Gly/Ala segment found in motif A is boxed in blue. Residues in *S. cerevisiae* MAK3p that abolish NAT activity when mutated are shown in red letters. The GenBank accession numbers of the putative NATs from the various organisms are given in the alignments. **(B)** Phylogenetic analysis of the hypothetical GCN5-related sequences from the different species. The phylogenetic tree is based on the ClustalW multiple sequence alignment of the various sequences (shown in A). GenBank accession numbers are shown next to the species prefix. *Mm*, *Mus musculus*; *Rn*, *Rattus novergus; Hs*, *Homo sapiens*; *At*, *Arabidopsis thaliana*; *Dm*, *Drosophila melanogaster*; *Ce*, *Caenorhabditis elegans, Sp, S. pombe; Nc, Neurospora crassa; Sc, S. cerevisiae.*

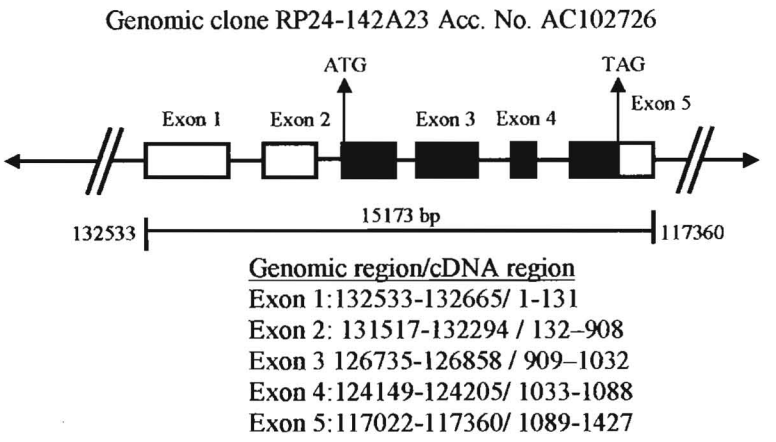

Figure 6.25 A schematic representation of the genomic organization of the mouse 23G1NAT. The exons are represented by the blocks with the lines joining blocks representing intronic sequences. The genomic and cDNA co-ordinates are shown. The positions of the start and stop codons are indicated, with coding regions in black blocks and the 5' and 3' UTR sequences in open blocks.

Tissue-specific distribution of the 23G1NAT mRNA was analyzed by RT-PCR using the primers fp433 and Rik621 (Table 2.2, Fig. 6.23). The RT-PCR demonstrated the presence of the gene in all the mouse tissues studied (Fig. 6.26). This is consistent with the vast collection of mouse ESTs from various tissues that matched 23G (UniGene Cluster Mm.275688, July 2004). This multi-tissue distribution pattern suggests that 23G has more of a generalized function rather than having a specific role in olfactory development.

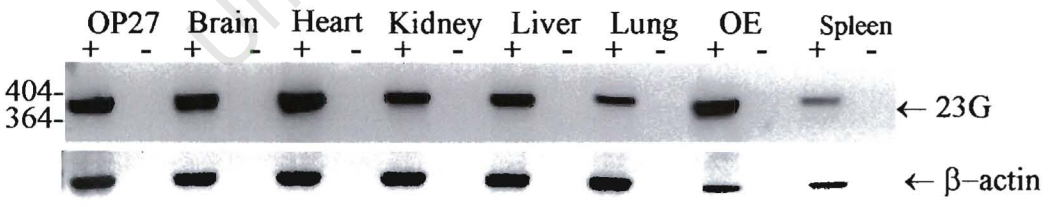

Figure 6.26 Expression of 23G1NAT in multiple tissues as detected by RT-PCR. Primers Rik621 and fp433 were used to amplify a 388 bp fragment from OP27 cells cultured at 33°C from various adult tissues. +, total RNA reverse transcribed in the presence of reverse transcriptase; -, RT reactions in which the reverse transcriptase was ommitted.

6.3 Discussion

In this study, FGF–2 induced differentiation of the OP27 cell line has presented a model system for the study of gene expression changes involved in olfactory neurogenesis. Differential display was used to identify genes that are differentially regulated by treatment with FGF-2. Twenty four primer combinations, comprising the 3 one-base anchored oligodT primers and eight arbitrary primers, were employed in this study. Both up- and down-regulated genes were identified. Sixteen of these genes were confirmed to be differentially regulated with FGF-2 treatment, with 15 up-regulated and one down-regulated.

Sequence analysis of the 16 clones revealed both previously characterized genes (8 clones) and those that have not been characterized (8 clones). Several genes identified in this study to be regulated by FGF-2 have been shown to be involved in neuronal differentiation. PP2A is the major serine/threonine phosphatase that has been implicated in various signal transduction pathways (such as the Wnt/β-catenin signalling pathway) and several cellular processes including regulation of cell cycle, transcription, differentiation and apoptosis (van Hoof and Goris, 2003; Zolnierowicz, 2000). The protein has been isolated as a heterotrimeric holoenzyme consisting of a catalytic subunit (C), a structural subunit (AR) and a third variable subunit known as the B regulatory subunit (BR) that influences substrate specificity and specific activity of PP2A. Three BR protein families have been identified. These are B55, B56, and PR72. B56, has 5 isoforms, viz. α, β, γ, δ, and ε (McCright *et al.*, 1996). The B56 γ subunit which is identical to the clone 17A1, up-regulated with FGF-2 treatment in OP27 cells, is highly expressed in the brain (Akiyama *et al.*, 1995). Transient transfection of the B56 γ has been shown to cause the PC12 cells to exit the cell cycle and differentiate into neuronal cells by activating the MAP kinase pathway (Strack, 2002). This suggests that the B56 γ subunit is a positive regulator of neuronal differentiation and its up-

regulation in the OP27 cells is consistent with this. The work presented here would therefore be the first report to show induction of this gene by FGF-2.

Collagen type IV, one of the major components of the extracellular matrix has also been implicated in the regulation of both proliferation and differentiation in various tissues. The expression of ColIVα2 was induced by the differentiation of the F9 teratocarcinoma cells upon induction with retinoic acid (Weigel and Nevins, 1990). FGF signalling has also been shown to activate Col IV gene expression leading to basement assembly and the induction of ectodermal differentiation (Li *et al.*, 2001a; 2001b). When added to E16 rat cortical cell cultures, ColIV inhibited their proliferation and promoted their differentiation towards a neuronal fate while inhibiting the astroglial fate (Ali *et al.*, 1998). In the rat olfactory system the protein has been hypothesized to contribute, along with other major ECM components, to axonal outgrowth from the OE and neurite guidance into the olfactory bulb (Julliard and Hartmann, 1998). FGF-2 is involved in the regulation of interactions between neuroepithelial cells and their immediate ECM during neurogenesis (Ali *et al.*, 1998). The identification of Col IV in differentiating OP27 cells is therefore in line with this. However, it is not clear why the expression of Col IV was first down-regulated in the first 6 hours and later induced.

ODAG, a novel gene recently identified in a cDNA array screen for genes that may have a role in eye development (Tsuruga *et al.*, 2002), is also up-regulated by FGF-2 in OP27 cells. ODAG is under temporal regulation during eye development, with mRNA levels high during the period E13-P6 and undetectable after P10. This gene has been proposed to play a role in transcriptional control, a hypothesis derived from analysis of the amino acid sequence (Tsuruga *et al.*, 2002).

Als2/Alsin is a putative cytoskeletal protein whose function is not known. It is thought to play a role in regulating cell membrane organization, trafficking of molecules in cells and cytoskeletal assembly. Its expression is highest in neurons throughout the brain, spinal cord and motoneurons and less in tissues outside of the CNS (Yang *et al.*, 2001).

Transgelin 2 (also called SM22β) is a actin-associated ctyoskeletal protein that is homologous to the 22KDa calponin-related smooth muscle specific protein SM22α and to the neuron-specific protein NP-25 (Zhang *et al.*, 2002). Although its function is known, SM22α is one of earliest markers of smooth muscle differentiation. Its expression is down-regulated in a variety of cell tumours, a consequence of the deregulation of the Ras signal transduction pathway (Shields *et al.*, 2002; Vasseur *et al.*, 2003). On the other hand, a 'transgelin-like protein' was identified in a SAGE analysis as one of substantially up-regulated transcripts in NGF-promoted neuronal differentiation of PC12 cells (Angelastro *et al.*, 2000). Transgelin 2 was also up-regulated in FGF-2 induced differentiation of OP27 cells but this regulation was transient, with transcript levels returning to basal levels. Whether this reflects what is happening *in vivo* is unknown. Both SM22α, SM22β and NP-25 bind cytoskeletal actin filaments. Scp1, the yeast homolog has also been found to bind, stabilize and organize the yeast actin cytoskeleton (Goodman *et al.*, 2003). These observations would therefore point to the significance of regulation of the actin cytoskeletal network during differentiation.

Cathepsin L, which is also up-regulated in differentiating OP27 cells, is a widely expressed lysosomal cysteine protease that has been reported to be involved in cellular growth and tumour invasion (Kirschke *et al.*, 2000). Increased cathepsin L activity has been shown to initiate or propagate the signal transduction pathway of apoptosis in certain neural diseases (Tsuchiya *et al.*, 1999). On the other hand, mutations in cathepsin L induce rapid loss of postnatal cerebral cortical

neurons thus suggesting an important role in the CNS (Felbor *et al.*, 2002)

MT-II is a small cystein-rich, metal binding protein that is induced in response to cellular stresses. Although abundantly expressed in a variety of tissues, a role for MT-II in promoting neuronal survival has been demonstrated (Trendelenburg *et al.*, 2002; Chung *et al.*, 2003). It has also been identified among potential targets of the transcription factor OTX2 (Zakin *et al.*, 2000).

I have also characterized, by bioinformatics, several novel genes identified in this study as being differentially regulated by FGF-2. The clone 23G encodes a protein, which has been termed 23G1NAT, with high homology to the yeast Mak3p acetyltransferase and shares consensus sequences with a group of N-acetyltransferases (NATs). Eighty five percent of eukaryotic proteins are subjected to N-terminal acetylation which is catalysed by NATs. These enzymes transfer an acetyl group from acetyl-CoA to the termini of α-amino groups of different proteins (Polevoda and Sherman, 2000). In yeast 3 different NATs: Nat A, Nat B, Nat C act on different substrates having different N-termini. Nat A is a complex of 2 genes NAT1 and ARD1. Mutations in both nat1 and ard1 are characterized by a lack of NAT activity, slower growth of the yeast strain, failure to sporulate and failure to enter the G_0 phase of the cell cycle. A mouse homolog of NAT1 (mNAT1) has been shown to be preferentially expressed in the developing brain, with high mRNA levels in proliferating undifferentiated regions. mNAT1 is then down-regulated as the cells differentiate into mature neuronal cells (Sugiura *et al.*, 2003). N-acetylation is a prerequisite for function for some proteins and can also regulate processes such as gene expression and nuclear import. Yeast Mak3, the catalytic subunit of NatC is involved in the N-acetylation of the L-A viral major coat protein gag, which is essential for viral assembly (Polevoda and Sherman, 2000). Lack of the N-terminal acetylation of gag in mak3 mutants prevents assembly of the viral particle.

In future it will be important to investigate whether 23G identified in this study has any NAT activity, and if it does, what are the specific targets of this translation modification. It will also be necessary to investigate whether the N-acetylation of these targets has any biological significance especially during neuronal differentiation. 23G1NAT is predicted to be a transmembrane protein, but it contains a putative NLS on its cytoplasmic domain that may target it to the nucleus. It is likely then that the activity of 23G1NAT may be regulated by a proteolytic cleavage of its intracellular domain (similarly to the processing of Notch-1) which then translocates to the nucleus to N-acetylate nuclear target proteins.

The conceptual protein sequence of the 20C3/Armet gene is characterized by the SAP/SAF-Box like domain, a bihelical DNA binding domain that binds to genomic scaffold attachment regions (SARs). SARs are AT rich regulatory elements observed close to transcriptional enhancers. They have been implicated in chromosomal organization and in regulation of gene expression. The SAF-Box was first identified in human scaffold attachment factor A (SAF-A) protein and has since been found in other non-orthologus proteins (Aravind and Koonin, 2000; Kipp *et al.*, 2000). The binding capacity of the SAF-Box to SARs has been shown experimentally (Kipp *et al.*, 2000). The functions of most SAR binding proteins are not known but they may be important for replication, gene transcription, proliferation or differentiation. Deletion of the SAF-Box of the SAF-A protein has been demonstrated to result in decrease in the proliferation of the MCF-7 cells (Kipp *et al.*, 2000). To determine whether Armet is also SAR binding protein we would need to conduct a series of studies to demonstrate the binding capacity of the predicted SAF-Box like domain to SAR.

In conclusion, differential display was used to characterize the gene expression patterns in OP27 cells in response to FGF-2 treatment. Among the genes identified in this study were transcripts that have been previously implicated in neuronal differentiation but shown here for the first time to be

regulated by FGF-2. Several other genes, whether up- or down-regulated have not been characterized before. These may represent useful markers to characterize the early stages of olfactory neuronal differentiation. The role of these transcripts could be explored by manipulating their patterns of expression in the OP27 cells.

Chapter 7

Conclusions

The main objective of this project was to study the effects of fibroblast growth factor-2 (FGF-2) on the olfactory epithelium using an olfactory neural precursor cell line, OP27 as a model system. FGF-2 is a signalling molecule that has been implicated in various cellular processes during development, including mitosis, migration, and differentiation of various cell types. The OP27 cell line was isolated by infection of primary cultures of olfactory epithelium from E10.5 mouse embryos with retrovirus carrying temperature sensitive allele of the SV40 large T antigen (Illing *et al.*, 2002). The retrovirus allows the cells to proliferate at the permissive temperature of 33°C, but the cells stop dividing when shifted to the non-permissive 39°C when the T antigen is inactivated. This cell line could thus be used as a *in vitro* model system to study neuronal differentiation in the olfactory epithelium.

I have shown that the OP27 cell line expresses only the main receptors for FGF-2, namely FGFR-1 and FGFR-2. When treated with FGF-2 and cultured at the non-permissive temperature, OP27 cells went through one round of cell division as assessed by thymidine incorporation. A gradual decrease in the rate of cell division then followed. This was accompanied by the appearance of cells that differentiate into cells with a bipolar morphology that was distinctly different from the cells at the permissive temperature. The number of the bipolar cells increased with time. In order to determine whether the OP27 cells were undergoing neuronal differentiation at the biochemical level, the expression of well-established markers that are consistent with differentiating neurons was studied in these cells using RT-PCR, western blots and immunocytochemistry. The mRNA levels of GAP-43 which is a marker for immature neurons are first up-regulated in OP27 during the first 2 days in culture and begin to decrease

with time, consistent with differentiating neurons *in vivo*. NCAM, also a marker for neurons downstream of GAP-43, was up-regulated in OP27 cells as they differentiate in the presence of FGF-2.

Olfactory neuronal cells are hypothesized to select only one of the possible 1500 OR genes to express as they begin to differentiate. The RT-PCR assay in combination with restriction enzyme digest analysis were carried out to establish whether FGF-2 induced OP27 cells could express any endogenous OR genes and to determine whether these cells are restricted to express only one or a limited set of ORs. OP27 cells were found to express OR genes at the immature stage, before they could express OMP, a marker for mature ORNs. It was also demonstrated that OP27 cells are not committed to express a single receptor. The choice of which OR genes to express was made each time the cells were induced to differentiate with FGF-2. The ORs identified in differentiating OP27 cells were found to be widely distributed in different chromosomes, an indication that these cells are not committed to express ORs that are clustered in the genome.

I have also studied the expression, in OP27 cells, of various transcription factors (FoxG1, O/E-1, OTX2, HES-1, NGN1 and NeuroD) and signalling molecules (Delta and Notch) that regulate cell fate choices at different stages in the differentiation of ORNs. While the expression of transcripts of some of these was not affected by FGF-2 treatment (viz. *Foxg1*, *Otx2*, *O/E-1*, and *Notch*1), others were differentially regulated. The mRNA transcripts of HES1, an effector of Notch signalling and a known inhibitor of neuronal differentiation, were up-regulated by FGF-2 treatment within 24 hours, the period when OP27 cells were still proliferating. *Hes1* levels were maintained high even when OP27 cells were observe to differentiate into a bipolar morphology. This therefore suggested that HES1 was required in a subpopulation of OP27 cells to inhibit neuronal differentiation. After 2 days following induction with FGF-2, OP27 cells up-regulated the expression *Delta1*. This was concomittant with the

both the emergence of cells with a bipolar morphology and the increase in these cells with time. *NeuroD*, a marker of postmitotic progenitor cells that are beginning to differentiate, is not expressed by OP27 cells at the non-differentiated state but when induced to differentiate, the cells are marked by a transient appearance of *NeuroD* mRNA transcripts downstream of both Ngn-1 and Delta-1. *NeuroD* appeared after 24 hours after treatment with FGF-2 and remained until after 4 days. This was a clear indication that these cells were indeed differentiating towards a neuronal phenotype. *Ngn1* which is transiently expressed by olfactory progenitors *in vivo* (Cau *et al.*, 1997) is also transient in differentiating OP27 cells. The transcription factor was expressed in OP27 cells at 33°C and until after 48 hours in culture.

The results summarized above therefore suggest that the behaviour of the OP27 cells in culture is characteristic of differentiating ORNs. The cell line could thus be used as an *in vitro* model system to study the mechanisms involved in the control of neuronal differentiation. Such mechamisms may be underscored by coordinated regulation of gene expression. The differential display RT-PCR technique has been used to identify differentially expressed genes in OP27 cells following FGF-2 induced differentiation. This was in an attempt to further increase our understanding of olfactory neuron development. I have identified genes that have been shown previously to be involved in neuronal development and genes that have not been characterized before. At present, it is difficult to correlate the function of the novel genes identified in this study to a role in neuronal differentiation.

The DD screen used in this study employed only 24 primer combinations. It has been proposed that a selection of 312 primer combinations would permit an almost complete analysis of the whole transcript pool. The number of primer combinations I have used here is considerably too low to allow for the identification of the genes that would be expected to be differentially regulated in differentiating

olfactory progenitor cells. The use of the microarray technology in the model system described in this work should facilitate the characterization of a more global gene expression pattern (Tloti and Illing, work in progress). Nevertheless, it is hoped that genes identified in this screen will throw light on the programme of gene activation that underlies neuronal differentiation and also the molecular mechanisms by which FGF-2 influences olfactory neurogenesis.

The characterization of the OP27 cell line in this thesis indicates that it is potentially a very useful *in vitro* model to study both extrinsic and intrinsic mechanisms that are involved in the regulation of olfactory neurogenesis. The cell line can be used to investigate which of the FGF receptors expressed in OP27 cells mediates the FGF-2 induced differentiation of these cells. The expression of the receptors in the OP27 cell line has been demonstrated using RT-PCR, we therefore do not know whether the 2 receptors are co-expressed in the same cell, or that a subpopulation of these cells express a single type of receptor and as a result acquire a distinct response to FGF-2. Immunocytochemistry with specific antibodies will be necessary to characterize the precise distribution of both receptors in the OP27 cell line, at the permissive temperature and in response to FGF-2 treatment at 39°C. Consequent to identifying the FGFR that is responsible for the FGF-2 induced neuronal differentiation, the cell line can be utilized to dissect out the signalling pathways that are activated in OP27 cells by that FGFR.

References

Abdel–Mageed, A.B, and Agrawal, K.C. 1997. Antisense down-regulation of metallothionein induces growth arrest and apoptosis in human breast carcinoma cells. *Cancer Gene Therapy* **4(3):**199-207.

Abdel–Mageed, A.B, and Agrawal, K.C. 1998. Activation of nuclear factor kappaB: potential role in metallothionein-mediated mitogenic response. *Cancer Research* **58(11):**2335-2338.

Akiyama, N., Shima, H., Hatano, Y., Osawa, Y., Sugimura, T., and Nagao, M. 1995. cDNA cloning of BRγ, a novel brain-specific isoform of the B regulatory subunit of type-2A protein phosphatase. *European Journal of Biochemistry* **230:**766-772.

Ali, S.A., Pappas, I.S., and Parnavelas, J.G. 1998. Collagen type IV promotes the differentiation of neuronal progeniors and inhibit astroglial differentiation in cortical cell cultures. *Developmental Brain Research* **110:**31-38.

Allen, B.L., and Rapraeger, A.C. 2003. Spatial and temporal expression of heparan sulfate in mouse development regulates FGF and FGF receptor assembly. *Journal of Cell Biology* **163(3):**637-648.

Altschul, S.F., Gish, W., Miller, W., Myers, E.W., and Lipman, D.J. 1990. Basic Local Alignment Search Tool. *Journal of Molecular Biology* **215:**402-410.

Amoureux, M., Cunningham, B.A., Edelman, G.M., and Crossin, K.L. 2000. N-CAM binding inhibits the proliferation of hippocampal progenitor cells and promotes their differentiation to a neuronal phenotype. *Journal of Neuroscience* **20(10)**:3631-3640.

Anderson, D.J. 1999. Lineages and transcription factors in the specification of vertebrate primary sensory neurons. *Current Opinion in Neurobiology* **9:**517-524.

Angelastro, J.M., Klimaschewski, L., Tang, S., Vitolo, O.V., Weissman, T.A., Donlin, L.T., Shelanski, M.L., and Greene, L.A. 2000. Identification of diverse nerve growth factor-regulated genes by serial analysis of gene expression (SAGE) profiling. *Proc. Natl. Acad. Sci. USA* **97(19):**10424-10429.

Appel, B., Givan, L.A., and Eisen, J.S. 2001. *Delta-Notch* signaling and lateral inhibition in zebrafish spinal cord development. *BMC Developmental Biology* **1:**13

Aravind, L., and Koonin, E.V. 2000. SAP- a putative DNA-binding motif involved in chromosomal organization. *TIBS* **25:**112-114.

Argo, S., Weth, F., and Korsching, S.I. 2003. Analysis of penetrance and expressivity during ontogenesis supports a stochastic choice of zebrafish odorant receptors from predetermined groups of receptor genes. *European Journal of Neuroscience* **17:**833-843.

Arnaud, E., Touriol, C., Boutonnet, C., Gensac, M., Vagner, S., Prats, H., and Prats, A. 1999. A new 34-Kilodalton isoform of human fibroblast growth factor 2 is CAP dependently synthesized by using a non-AUG start codon and behaves as a survival factor. *Molecular and Cellular Biology* **19:**505-514.

Averboukh, L., Douglas, S.A., Zhao, S., Lowe, K., Maher, J., and Pardee, A.B. 1996. Better gel resolution and longer cDNAs increase the precision of differential display. *Biotechniques* **20(5):**918-921.

Bae, S., Bessho, Y., Hojo, M., and Kageyama, R. 2000. The bHLH gene *Hes6*, an inhibitor of *Hes1*, promotes neuronal differentiation. *Development* **127:**2933-2943.

Bae, S.S., Perry, D.K., Oh, Y.S., Choi, J.H., Galadari, S.H., Ghayur, T., Ryu, S.H., Hannun, Y.A., and Suh, P-G. 2000. Proteolytic cleavage of phospholipase C-γ1 during apoptosis in Molt-4 cells. *Faseb J.* 14:1083-1092.

Bansal, R., Kumar, M., Murray, K., Morrison, R.S., and Pfeiffer, S.E. 1996. Regulation of FGF receptors in the oligodendrocyte lineage. *Molecular and Cellular Neuroscience* **7:**263-275.

Barber, R.D., Jaworsky, D.E., Yau, K., Ronnett, G.V. 2000. Isolation and in vitro differentiation of conditionally immortalized murine olfactory receptor neurons. *The Journal of Neuroscience* **20:**3695-3704.

Bassam, B.J., Caetano-Anollés, G., Gresshoff, P.M. 1991. Fast and sensitive silver staining of DNA in polyacrylamide gels. *Analytical Biochemistry* **196:**80-83.

Bauer, D., Müller, H., Reich, J., Riedel, H., Ahrenkiel, V., Warthoe, P. and Strauss, M. 1993. Identification of differentially expressed mRNA species by an improved display technique (DDTR-PCR). *Nucleic Acids Research* **21(18):**4272-4280.

Bellot, F., Crumble, G., Kaplow, J.M., Schlessinger, J., Jaye, M., and Dionne, C.A. 1991. Ligand-induced transphophorylation between different FGF receptors. *Embo J.* **10(10):**2849-2854.

Bernard, O., Li, M., and Reid, H.H. 1991. Expression of two different forms of fibroblast growth factor receptor 1 in different mouse tissues and cell lines. *Proc. Natl. Acad. Sci. USA* **88:**7625-7629.

Biffo, S., Verhaagen, J., Schrama, L.H., Schotman, P., Danho, W., and Margolis, F.L. 1990. B-50/GAP43 expression correlates with process outgrowth in the embryonic mouse nervous system. *European Journal Of Neuroscience* **2:**487-499.

Blader, P., Fischer, N., Gradwohl, G., Guillemot, F., and Strähle, U. 1997. The activity of Neurogenin 1 is controlled by local cues in the zebrafish embryo. *Development* **124:**4557-4569.

Bourguignon, C., Li, J., and Papalopulu, N. 1998. XBF-1, a winged helix transcription factor with dual activity, has a role positioning neurogenesis in *Xenopus* competent ectoderm. *Development* **125:**4889-4900.

Brickman, Y.G., Ford, M.D., Small, D.H., Bartlett, P.F., and Nurcombe, V. 1995. Heparan sulfates mediate the binding of basic fibroblast growth factor to a specific receptor on neural precursor cells. *Journal of Biological Chemistry* **270(42):**24941-24948.

Brown, A.J.H, Hutchings, C., Burke, J.F., and Mayne, L.V. 1999. Application of a rapid method (targeted display) for the identification of differentially expressed mRNAs following NGF-induced neuronal differentiation in PC12 cells. *Molecular and Cellular Neuroscience* **13:**119-130.

Brunet, A., Bonni, A., Zigmond, M.J., Lin, M.Z., Juo, P., Hu, L.S., Anderson, M.J., Arden, K.C., Blenis, J., and Greenberg, M.E. 1999. Akt promotes cell survival by phosphorylating and inhibiting a Forkhead transcription factor. *Cell* **96:**857-868.

Brunjes, P.C., and Greer, C.A. 2003. Progress and directions in olfactory development. *Neuron* **38:**371-374.

Buck, L., and Axel, R. 1991. A novel multigene family may encode odorant receptors: a molecular basis for odor recognition. *Cell* **65:**175-187.

Burgar, H.R., Burns, H.D., Elsden, J.L., Lalioti, M.D., and Heath, J.K. 2002. Association of the signalling adaptor FRS2 with fibroblast growth factor receptor 1 (Fgfr1) is mediated by alternative splicing of the juxtamembrane domain. *Journal of Biological Chemistry* **277(6):**4018-4023.

Cai, H., Howels, R., and Wagner, B.J. 1999. Identification of a novel gene product preferentially expressed in rat lens epithelial cells. *Molecular Vision* **5:**3.

Caldwell, M.A, and Svendsen, C.N. 1998. Heparin, but not other proteoglycans potentiates the mitogenic effects of FGF-2 on mesencephalic precursor cells. *Experimental Neurology* **152:**1-10.

Callard, D., Lescure, B., and Mazzolini, L. 1994. A method for the elimination of false positives generated by the mRNA differential display technique. *Biotechniques* **16(6):**1096-1103.

Calof, A.L., Lander, A.D., and Chikaraishi, D.M. 1991. Regulation of neurogenesis and neuronal differentiation in primary and immortalized cells from mouse olfactory epithelium. In *Regeneration of vertebrate sensory receptor cells.* Wiley, Chichester (Ciba Foundation Symposium 160):249-276.

Calof, A.L., Hagiwara, N., Holcomb, J.D., Mumm, J.S. and Shou, J. 1996. Neurogenesis and cell death in olfactory epithelium. *Journal of Neurobiology* **30(1):**67-81.

Calof, A.L., Bonnin, A., Crocker, C., Kawauchi, S., Murray, R.C., Shou, J., and Wu, H. 2002. Progenitor cells of the olfactory receptor neuron lineage. *Microscopy Research and Technique* **58:**176-188.

Carr, V.M., Walters, E., Margolis, F.L., and Farbman, A.I. 1998 An enhanced olfactory marker protein immunoreactivity in individual olfactory receptor neurons following olfactory bulbectomy may be related to increased neurogenesis. *Journal of Neurobiology* **34:**377-390.

Carter, L.A., and Roskams, A.J. 2002. Neurotrophins and their receptors in the primary olfactory neuraxis. *Microscopy Research and Technique* **58:**189-196.

Casarosa, Ş., Fode, C., and Guillemot, F. 1999. Mash-1 regulates neurogenesis in the ventral telencephalon. *Development* **126:** 525-534.

Castella, ., Wagner, J.A., and Caudy, M. 1999. Regulation of hippocampal neuronal differentiation by the basic helix-loop-helix transcription factors HES-1 and MASH-1. *Journal of Neuroscience Research* **56:**229-240.

Cau, E., Gradwohl, G., Fode, C., and Guillemot, F. 1997. *Mash-1* activates a cascade of bHLH regulators in olfactory neuron progenitors. *Development* **124:** 1611-1621.

Cau, E., Gradwohl, G., Fode, C., Casarosa, S., Kageyama, R., and Guillemot, F. 2000. *Hes* genes regulate sequential stages of neurogenesis in the olfactory epithelium. *Development* **127:**2323-2332.

Cau, E., Casarosa, S., and Guillemot, F. 2002. *Mash-1* and *Ngn1* control distinct steps of determination and differentiation in the olfactory sensory neuron lineage. *Development* **129:**1871-1880.

Chambers, C.B., Peng, Y., Nguyen, H., Gaiano, N., Fishell, G., and Nye, J.S. 2001. Spatiotemporal selectivity of response to Notch1 signals in mammalian forebrain precursors. *Development* **128:**689-702.

Chambers, D., Medhurst, A.D., Walsh, F.S., Price, J., and Mason, I. 2000. Differential display of genes expressed at the midbrain-hindbrain junction identifies sprouty2: an FGF8-inducible member of a family of intracellular FGF antagonists. *Molecular and Cellular Neuroscience* **15:**22-35.

Chauhan, B.K., Zhang, W., Cveklova, K., Kantorow, M., and Cvekl, A. 2002. Identification of differentially expressed genes in mouse Pax6 heterozygous lenses. *Investigative Ophthalmology and Visual Science* **43:**1884-1890.

Chen J.J.W. and Peck K. 1996. Non-radioisotopic differential display method to directly visualize and amplify differential bands on nylon membrane. *Nucleic Acids Research* **24**(4)**:**793-794.

Chen, H., Thiagalingam, A., Chopra, H., Borges, M.W., Feder, J.N., Nelkin, B.D., Baylin, S.B., and Ball, D.W. 1997. Conservation of the *Drosophila* lateral inhibition pathway in human lung cancer: A hairy-related protein (HES-1) directly represses achaete-scute homolog-1 expression. *Proc. Natl. Acad. Sci. USA* **94:**5355-5360.

Chen, S.L., Maroulakou, I.G, Green, J.E., Romano-Spica, V; Modi, W., Lautenberger, J., and Bhat, N.K. 1996. Isolation and characterisation of a novel gene expressed in multiple cancers. *Oncogene* **12:**741-751.

Chenchik A., Diachenko L., Moqadam F., Tarabykin V., Lukyanov S., Siebert P.D. 1996. Full-length cDNA cloning and determination of mRNA 5' and 3' ends by amplification of adaptor-ligated cDNA. *BioTechniques* **21**(3)**:**526-534.

Chitnis, A., and Kintner, C. 1996. Sensitivity of proneural genes to lateral inhibition affects the pattern of primary neurons in *Xenopus* embryos. *Development* **122:**2295-2301.

Choi, J-H., Jung, H-Y., Kim, H-S., Cho, H-G. 2000. PhyloDraw: a phylogenetic tree drawing system. *Bioinformatics Applications Note* **16(11):**1056-1058.

Chomczynski, P., and Sacchi, N. 1987. Single-step method of RNA isolation by acid guanidium thiocyanate-phenol-chloroform extraction. *Analytical Biochemistry* **162:**156-159.

Chuah, M.I., and Teague, R. 1999. Basic fibroblast growth factor in the primary olfactory pathway: mitogenic effect on eansheating cells. *Neuroscience* **88:**1043-1050.

Chung, K., Gomez, I., Wang, D., Lau, L.F., and Rosner, M.R. 1998. Raf and Fibroblast growth factor phosphorylate Elk1 and activate the serum response element of the immediate early gene *pip92* by mitogen-activated protein kinase-independent as well as –dependent signaling pathways. *Molecular and Cellular Biology* **18(4):**2272-2281.

Clinton M., and Scougall R.K. 1995. Detection and capture of ^{35}S-labelled gas released from reaction tubes during differential display PCR. *BioTechniques* **19**(5)**:**798-799.

Clyne, P.J., Warr, C.G., Freeman, M.R., Lessing, D., Kim, J., and Carlson, J.R. 1999. A novel family of divergent seven-transmembrane proteins: candidate odorant receptors in *Drosophila. Neuron* **22:**327-338.

Corbit, K.C., Foster, D.A., and Rosner, M.R. 1999. Protein kinase Cδ mediates neurogenic but not mitogenic activation of mitogen-activated protein kinase in neuron cells. *Molecular and Cellular Biology* **19(6):**4209-4218.

Cornell, R.A., and Eisen, J.S. 2002. Delta/Notch signalling promotes formation of zebrafish neural crest by repressing Neurogenin 1 function. *Development* **129:** 2639-2648.

Coronas, V., Féron, F., Hen, R., Sicard, G., Jourdan, F., and Moyse, E. 1997. In vitro induction of apoptosis or differentiation by dopamine in an immortalized olfactory neuronal cell line. *Journal of Neurochemistry* **69:**1870-1881.

Chung, R.S., Vickers, J.C., Chuah, M.I., and West, A.K. 2003. Metallothionein-IIA promotes initial neurite elongation and postinjury reactive neurite growth and facilitates healing after focal cortical brian injury. *Journal of Neurosience* **23(8):**3336-3342.

Cunningham, A.M., Manis, P.B., Reed, R.R., and Ronnett, G.V. 1999. Olfactory receptor neurons exist as distinct subclasses of immature and mature cells in primary culture. *Neuroscience* **93(4):**1301-1312.

Damon, D.H., D'Amore, P.A., and Wagner, J.A. 1988. Sulfated glycosaminoglycans modify growth factor-induced neurite outgrowth in PC12 cells. *Journal of Cell Physiology* **135:**293-300.

Dandoy-Dron, F., Guillo, F., Benboudjema, L., Deslys, J.-P., Lasmezas, C., Dormont, D., Tovey, M. G., and Dron, M. 1998. Gene Expression in Scrapie. Cloning of a new scrapie-responsive gene and the identification of increased levels of seven other mRNA transcripts. *Journal of Biological Chemistry* **273(13):**7691-7697.

Davis, J.A., and Reed, R.R. 1996. Role of Olf-1 and Pax-6 transcription factors in neurodevelopment. *Journal of Neuroscience* **16(16):**5082-5094.

de la Pompa, J.L., Wakeham, A., Correia, K.M., Samper, E., Brown, S., Aguilera, R.J., Nakano, T., Honjo, T., Mak, T.W., and Rossant, J. 1997. Conservation of the Notch signalling pathway in mammalian neurogenesis. *Development* **124:**139-1148.

DeHamer, M.K., Guevara, J.L., Hannon, K., Olwin, B.B., and Calof, A. 1994. Genesis of olfactory receptor neurons in vitro: Regulation of progenitor cell divisions by fibroblast growth factors. *Neuron* **13:**1083-1097.

Deng, C.X., Wynshaw-Borris, A., Shen, M.M., Daugherty, C., Ornitz, D.M., and Leder, P. 1994. Murine FGFR-1 is required for early postimplantation growth and axial organization. *Genes and Development* **8:**3045-3057.

Deng, C., Bedford, M., Li, C., Xu, X., Yang, X., Dunmore, J., and Leder, P. 1997. Fibroblast growth factor receptor-1 (FGFR-1) is essential for normal neural tube and limb development. *Developmental Biology* **185(1):**42-54.

Derrington, E.A., Dufay, N., Rudkin, B.B., and Belin, M-F. 1998. Human primitive neuroectodermal tumour cells behave as multipotent neural precursors in response to FGF2. *Oncogene* **17:**1663-1672.

Diancheko L.B., Ledesma J., Chenchik A.A. and Siebert P.D. 1996. Combining the technique of RNA fingerprinting and differential display to obtain differentially expressed mRNA. *Biochemical And Biophysical Research Communications* **219:**824-828.

Dilks, D.W., Ring, R.H., Khawaja, X.Z., Novak, T.J., Aston, C. 2003. High-throughput confirmation of differential display PCR results using reverse northern blotting. *Journal of Neuroscience Methods* **123:**47-54.

Dimitroulakos, J., Pienkowska, M., Sun, P., Farooq, S., Zielenska, M., Squire, J., and Yeger, H. 1999. Identification of a novel zinc finger gene, zf5-3, as a potential mediator of neuroblastoma differentiation. *International Journal of Cancer* **81:**970-978.

Dono, R., Texido G., Dussel R., Ehmke H., Zeller R. 1998. Impaired cerebral cortex development and blood pressure regulation in FGF-2 deficient mice. *Embo J.* **17:**4213-25.

Donohue, P., Alberts, G.F., Guo, Y., and Winkles, J.A. 1995. Identification by targeted differential display of an immediate early gene encoding a putative serine/threonine kinase. *Journal of Biological Chemistry* **270(17):**8604-8609.

Dryer, L., and Berghard, A. 1999. Odorant receptors: a plethora of G-protein-coupled receptors. *TiPS* **20:**413-417.

Dubois, L., Bally-Cuif, L., Crozatier, M., Moreau, J., Paquereau, L., and Vincent, A. 1998. Xcoe2, a transcription factor of the Col/Olf-1/EBF family involved in the specification of primary neurons in *Xenopus*. *Current Biology* **8:**199-209.

Eckstein, F.P. 1994. Fibroblast growth factors in the nervous system. *Journal of Neurobiology* **25(11):**1467-1480.

Edlund, T., and Jessel, T.M. 1999. Progression from extrinsic to intrinsic signaling in cell fate specification: A view from the nervous system. *Cell* **96:**211-224.

Eggan, K., Baldwin, K., Tackett, M., Osborne, J., Gogos, J., Chess, A., Axel, R., and Jaenisch, R. 2004. Mice cloned from olfactory sensory neurons. *Nature* **428:**44-49.

Emanuelsson, O., Nielsen, H., Brunak, S., and von Heijne, G. 2000. Predicting subcellular localization of proteins based on their N-terminal amino acid sequence. *Journal of Molecular Biology* **300:**1005-1016.

Ensoli, F., Fiorelli, V., Vanelli, B., Barni, T., De Cristofaro, M., Ensoli, B., and Thiele, C.J. 1998. Basic fibroblast growth factor supports human olfactory neurogenesis by autocrine/paracrine mechanisms. *Neuroscience* **86(3):**881-893.

Eves, E.M., Tucker, M.S., Roback, J.D., Dowen, M., Rosner, M.R., and Wainer, B.H. 1992. Immortal rat hippocampal cell lines exhibit neuronal and glial lineages and neurotrophin gene expression. *Proceedings of the National Academy of Sciences USA* **89:**4373-4377.

Eves, E.M., Xiong, W., Bellacosa, A., Kennedy, S.G., Tsichlis, P.N., Rosner, M.R., and Hay, N. 1998. Akt, a target of phosphatidylinositol 3-kinase, inhibits apoptosis in a differentiating neuronal cell line. *Molecular and Cellular Biology* **18(4):**2143-2152.

Eves, E.M., Skoczylas, C., Yoshida, K., Alnemri, E.S., and Rosner, M.R. 2001. FGF induces a switch in death receptor pathways in neuronal cells. *Journal of Neuroscience* **21(14):**4996-5006.

Fan, J., and Ngai, J. 2001. Onset of odorant receptor gene expression during olfactory sensory neuron regeneration. *Developmental Biology* **229(1):**119-127.

Farbman, A.I. 1994. Developmental biology of the olfactory sensory neurons. *Seminars in Cell Biology* **5:**3-10.

Faux, C.H., Turnley, A.M., Epa, R., Cappai, R., and Bartlett P. 2001. Interactions between fibroblast growth factors and *Notch* regulate neuronal differentiation. *Journal of Neuroscience* **21(15):**5587-5596.

Fishell, G. 3 June 2003 http://www.saturn.med.nyu.edu/groups/FishellLab

Foley, K.P., Leonard, M.W., and Engel, J.D. 1993. Quantitation of RNA using the polymerase chain reaction. *TIG* **9(11)**:380-385.

Ford-Perriş, M., Abud, H., and Murphy, M. 2001. Fibroblast growth factors in the derveloping central nervous system. *Clinical and Experimental Pharmacology and Physiology* **28:** 493-503.

Franz, O., Bruchhaus, I., and Roeder, T. 1999. Verification of differential gene transcription using virtual northern blotting. *Nucleic Acids Research* **27(11):**3e

Fujimoto, I., Bruses, J.L., and Rutishauser, U. 2001. Regulation of cell adhesion by polysialic acid. *Journal of Biological Chemistry* **276(34):**31745-31751.

Furukawa, T., Mukherjee, S., Bao, Z., Morrow, E.M., and Cepko, C.L. 2000. rax, Hes1, and notch1 promote the formation of Müller glia by postnatal retinal progenitor cells. *Neuron* **26:** 383-394.

Gaiano, N., Nye, J.S., and Fishell, G. 2000. Radial glial identity is promoted by Notch-1 signalling in the murine forebrain. *Neuron* **26:**395-404.

Garnier, M., Di Lorenzo, D., Albertini, A., and Maggi, A. 1997. Identification of estrogen-responsive genes in neuroblastoma SK-ER3 cells. *Journal of Neuroscience* **17(12):**4591-4599.

Gensburger, C., Labourdette G., Sensenbrenner M. 1987. Brain basic fibroblast growth factor stimulates the proliferation of rat neuronal precursor cells in vitro. *FEBS Lett.* **217:**1-5.

Gesemann, M., Litwack, E.D., Yee, K.T., Christen, U., and O'Leary, D.D.M. 2001. Identification of candidate genes for controlling development of the basilar pons by differential display PCR. *Molecular and Cellular Neuroscience* **18:**1-12.

Ghosh, A., and Greenberg, M.E. 1995. Distinct roles for bFGF and NT-3 in the regulation of cortical neurogenesis. *Neuron* **15:**89-103.

Gillespie, L.L, Chen, G., and Paterno, G.D. 1995. Cloning of a fibroblast growth factor receptor 1 splice variant from Xenopus embryos that lacks a protein kinase C site important for the regulation of receptor activity. *Journal of Biological Chemistry* **270(39):**22758-63.

Glusman, G., Sosinsky, A., Ben-Asher, E., Avidan, N., Sonkin, D., Bahar, A., Rosenthal, A., Clifton, S., Roe, B., Ferraz, C., Demaille, J., and Lancet, D. 2000. Sequence, structure, and evolution of a complete human olfactory receptor gene cluster. *Genomics* **63:**227-245.

Godfrey, P.A., Malnic, B., and Buck, L.B. 2004. The mouse olfactory receptor gene family. *Proceedings of the National Academy of Sciences* **101:**2156-2161.

Goldstein, B.J., Wolozin, B.L., and Schwob, J.E. 1997. FGF-2 suppresses neurogenesis of a cell line derived from rat olfactory epithelium. *Journal of Neurobioogy* **33:**411-428.

Gomez, G., Restrepo, D., Rawson, N., Lowry, L.D., Keane, W.M., and Rothstein, J.L. 1996. Induction of differentiation of human olfactory neuroblastoma cells into odorant – responsive cells. *Neuroscience* **74:**567-577.

Goodman, A., Goode, B.L., Matsudaira, P., and Fink, G.R. 2003. The *Saccharomyces cerevisiae* calponin/transgelin homolog Scp1 functions with fimbrin to regulate stability and organization of the actin cytoskeleton. *Molecular Biology of the Cell* **14:**2617-2629.

Götz, M., Hartfuss, E., and Malatesta, P. 2002. Radial glial cells as neuronal precursors: A new perspective on the correlation of morphology and lineage restriction in the developing cerebral cortex of mice. *Brain Research Bulletin* **57(6):**777-788.

Grandbarbe, L., Bouissac, J., Rand, M., de Angelis, M.H., Artavanis-Tsakonas, S., and Mohier, E. 2003. Delta-Notch signaling controls the generation of neurons/glia from neural stem cells in a stepwise process. *Development* **130:**1391-1402.

Green, C.D., Simons, J.F., Taillon, B.E., and Lewin, D.A. 2001. Open systems: panoramic views of gene expression. *Journal of Immunological Methods* **250:**67-79.

Guillemot, F., and Joyner, A. 1993. Dynamic expression of the murine *Achaete-scute* homologue *Mash-1* in the developing nervous system. *Mechanisms of Development* **42:**171-185.

Guillemot, F. 1999. Vertrbrate bHLH genes and the determination of neuronal fates. *Experimental Cell Research* **253:** 357-364.

Gupta, R., Thomas, P., Beddington, R.S.P., and Rigby, P.W.J. 1998. Isolation of developmentally regulated genes by differential display screening of cDNA libraries. *Nucleic Acids Research* **26(19)**:4538-4539.

Hadari, Y.R., Kouhara, H., Lax, L., and Schlessinger, J. 1998. Binding of Shp2 tyrosine phosphatase to FRS2 is essential for fibroblast growth factor-induced PC12 cell differentiation. *Molecular and Cell Biology* **18(7):** 3966-3973.

Hadari, Y.R., Gotoh, N., Kouhara, H., Lax, L., and Schlessinger, J. 2001. Critical role for the docking-protein FRS2 alpha in FGF receptor-mediated signal transduction pathways. *Proceedings of the National Academy of Sciences* **98:**8578-8583.

Hajihosseini, M.K., and Dickson, C. 1999. A subset of fibroblast growth factor (Fgfs) promote survival, but Fgf-8 specifically promotes astroglial differentiation of rat cortical precursor cells. *Molecular and Cellular Neuroscience* **14:**468-485.

Hanashima, C., Li, S.C., Shen, L., Lai, E., and Fishell, G. 2004. *Foxg1* suppresses early cortical cell fate. *Science* **303:**56-59.

Handler, M., Yang, X., and Shen, J. 2000. Presenilin-1 regulates neuronal differentiation during neurogenesis. *Development* **127:**2593-2606.

Hassan, B.A., and Bellen, H.J. 2000. Doing the MATH: is the mouse a good model for fly development? *Genes and Development* **14:**1852-1865.

Herzog, C., and Otto, T. 1999. Regeneration of olfactory receptor neurons following chemical lesion: time course and enhancement with growth factor administration. *Brain Research* **849:**155-161.

Higgins D., Thompson J., Gibson T., Thompson J.D., Higgins D.G., and Gibson T.J. 1994. CLUSTAL W: improving the sensitivity of progressivemultiple sequence alignment through sequence weighting,position-specific gap penalties and weight matrix choice. *Nucleic Acids Research* **22**:4673-4680.

Hitoshi, S., Alexson, T., Tropepe, V., Donoviel, D., Elia, A.J., Nye, J.S., Conlon, R.A., Bernstein, A., and van Der Kooy, D. 2002. Notch pathway molecules are essential for the maintenance, but not the generation, of mammalian neural stem cells. *Genes & Development* **16(7):**846-858.

Hofmann, K., Bucher, P., Falquet, L., Bairoch, A. 1999. The Prosite database, its status in 1999. *Nucleic Acids Research* **27:**215-219.

Holcomb, J.D., Mumm, J.S., and Calof, A.L. 1995. Apoptosis in the neuronal lineage of the mouse olfactory epithelium: Regulation in vivo and in vitro. *Developmental Biology* **172:**307-323.

Hoppe, R., Frank, H., Breer, H., and Strotmann, J. 2003. The clustered olfactory receptor gene family 262: Genomic organization, promoter elements, and interacting transcription factors. *Genome Research* **13:**2674-2685.

Hoppe, R., Weimer, M., Beck, A., Breer, H., and Strotmann, J. 2000. Sequence analysis of the olfactory receptor gene cluster mOR37 on mouse chromosome 4. *Genomics* **66:**284-295.

Horikawa, I., Miwa, T., Ishimaru, T., Furukawa, M., Kato, T., and Moriizumi, T. 1999. TrkA expression in olfactory epithelium and bulb during development. *NeuroReport* **10:**2205-2208.

Hsu, P.-e., Yu, F., Féron, F., Pickles, J.O., Sneesby, K., Mackay-Sim, A. 2001. Basic fibroblast growth factor and fibroblast growth factor receptors in adult olfactory epithelium. *Brain Research* **896:**188-197.

Illing, N., Boolay, S., Siwoski, J., Casper, D., Lucero, M., and Roskams, A.J. 2002. Conditionally immortalized clonal cell lines from the mouse olfactory placode differentiate into olfactory neurons. *Molecular and Cellular Neuroscience* **20:**225-243.

Inokuchi, K., Murayama,A., and Ozawa,F. 1996. mRNA differential display reveals *Krox-20* as a neural plasticityregulated gene in the rat hippocampus. *Biochemical and Biophysical Research Communications* **221:**430-436.

Ishibashi, M., Moriyoshi, K., Sasai, Y., Shiota, K., Nakanishi, S., and Kageyama, R. 1994. Persistant expression of helix-loop-helix factoe HES-1 prevents mammalian neural differentiation in the central nervous system. *EMBO J.* **13:**1799-1805.

Issel-Tarver, L. and Rine, J. 1996. Organization and expression of canine olfactory receptor genes. *Proceedings of the National Academy of Sciences* **93:**10897-10902.

Iwema, C.L., and Schwob, J.E. 2003. Odorant receptor expression as a function of neuronal maturity in the adult rodent olfactory system. *Journal of Comparative Neurology* **459:**209-222.

Jarriault, S., Bail, O., Hirsinger, E., Pourquié, O., Logeat, F., Strong, C.F., Brou, C., Siedah, N.G., and Israel, A. 1998. Delta-1 activation of Notch-1 signaling results in HES-1 transctivation. *Molecular and Cellular Biology* **18(12):** 7423-7431.

Jessel, T.M., and Sanes, J.R. 2000. The decade of the developing brain. *Current Opinion* **10:**599-611.

Johnson, D.E., and Williams L.T. 1993. Structural and functional diversity in the FGF receptor multigene family. *Advances in Cancer Research* **60:**1-41.

Johnson, S.W., Lissy, N.A., Miller, P.D., Testa, J.R., Ozols, R.F., and Hamilton, T.C. 1996. Identification of zinc finger mRNAs using domain-specific differential display. *Analytical Biochemistry* **236:**348-352.

Julliard, A.K., and Hartmann, D.J. 1998. Spatiotemporal patterns of expression of extracellular matrix molecules in the developing rat olfactory system. *Neuroscience* **84(4):**1135-1150.

Jung, M., Kim, S., Jeon, G.A., Kim, S., Kim, Y., Choi, K., Park, S., Joe, M., and Kimm, K. 2000. Identification of differentially expressed genes in normal and tumor human gastric tissue. *Genomics* **69:**281-286.

Jurecic, R., Nachtman, R.G., Colicos, S.M., and Belmont J.W. 1998. Identification and cloning of differentially expressed genes by long-distance differential display. *Analytical Biochemistry* **259:**235-244.

Justice, N.J., and Jan, Y.N. 2002. Variations on the Notch pathway in neural development. *Current Opinion in Neurobiology* **12:** 64-70.

Kageyama, R., Ishibashi, M., Takebayashi, K., and Tomita, K. 1997. bHLH transcription factors and mammalian neuronal differentiation. *Int. J. Biochem. Cell Biol.* **29(12):**1389-1399.

Kalyani, A.J., and Rao, M.S. 1998. Cell lineage in the developing neural tube. *Biochem. Cell Biol.* **76:**1051-1068.

Kalyani, A.J., Mujtaba, T., and Rao, M.S. 1999. Expression of EGF receptor and FGF receptor isoforms during neuropeithelial stem cell differentiation. *Journal of Neurobiology* **38:**207-224.

Katayama, M., Mizuta, I., Sakoyama, Y., Kohyama-Koganeya, A., Akagawa, K., Uyemura, K., and Ishii, K. Differential expression in primary cultures of cerebral cortical neurons. *Experimental Cell Research* **236:**412-417.

Kemp, B.E. and Pearson, R.B. 1990. Protein kinase recognition sequence motifs. *TIBS* **15:**342-346.

Kilkpatrick, T.J. and Bartlett, P.F. 1995. Cloned multipotential precursors from the mouse cerebrum require FGF-2, whereas glial restricted precursors are stimulated with either FGF-2 or EGF. *Journal of Neuroscience* **15(5):**3653-3661.

Kipp, M., Göhring, F., Ostendorp, T., van Drunen, C.M., van Driel, R., Przybylski, M., and Fackelmayer, F.O. 2000. SAF-Box, a conserved protein domain that specifically recognizes scaffold attachment region DNA. *Molecular and Cellular Biology* **20(20):**7480-7489.

Kirschke, H., Eerola, R., Hopsu-Havu, V.K., Brömme, D., and Vuorio, E. 2000. Antisense RNA inhibition of cathepsin L expression reduces tumorigenicity of malignant cells. *European Journal of Cancer* **36:**787-795.

Kito, K., Ito, T., and Sakaki, Y. 1997. Fluorescent differential display analysis of gene expression in differentiating neuroblastoma cells. *Gene* **184:**73-81.

Korada, S., Zheng, W., Basilico, C., Schwartz, M.L., and Vaccarino, F.M. 2002. Fibroblast growth factor 2 is necessary for the growth of glutamate projection neurons in the anterior neocortex. *Journal of Neuroscience* **22:**863-875.

Kouhara, H., Hadari, Y.R., Spivak-Kroizman, T., Schilling, J., Bar-Sagi, D., Lax, I., and Schlessinger, J. 1997. A lipid-anchored Grb2-binding protein that links FGF-receptor activation to the Ras/MAPK signaling pathway. *Cell* **89:**693-702.

Koyana-Nakagawa, N., Kim, J., Anderson, D., and Kintner, C. 2000. Hes6 acts in a positive feedback loop with the neurogenesis to promote neuronal differentiation. *Development* **127:**4203-4216.

Kratz, E., Dugas J.C., and Ngai, J. 2002. Odorant receptor gene regulation: implications from genomic organization. *Trends in Genetics* **18:**29-34.

Kretzler, M., Fan, G., Rose, D., Arend, L.J., Briggs, J.P., and Holzman, L.B. 1996. Novel mouse embryonic renal marker gene products differentially expressed during kidney developments. *American Journal of Physiology* **271:**F770-F777.

Kuhn, H.G., Winkler, J., Kempermann, G., Thal., L.J., and Gage, F.H. 1997. Epidermal growth factor and fibroblast growth factor-2 have different effects on neural progenitors in the adult rat brain. *Journal of Neuroscience* **17:**5820-5829.

Kuo, W., Abe, M., Rhee, J., Eves, E.M., McCarthy, S.A., Yan, M., Templeton, D.J., McMahon, M., and Rosner, M.R. 1996. Raf, but not MEK or ERK, is sufficient for differentiation of hippocampal neuronal cells. *Molecular and Cellular Biology* **16(4):**1458-1470.

Kuo, W., Chung, K., and Rosner, M.R. 1997. Differentiation of central nervous system neuronal cells by fibroblast-growth factor requires at least two signaling pathways: roles for Ras and Src. *Molecular and Cellular Biology* **17(8):**4633-4643.

Lee, J. 1997. Basic helix-loop-helix genes in neural development. *Current Opinion in Neurobiology* **7:**13-20.

Lee, J.E., Hollenberg, S.M., Snider, L., Turner, D.L., Lipnick, N., Weintraub, H. 1995. Conversion of Xenopus ectoderm into neurons by NeuroD, a basic helix-loop-helix protein. *Science* **268:**836-844.

Lee, J-K., Cho, J-H., Hwang, W-S., Lee, Y-D., Reu, D-S., and Suh-Kim, H. 2000. Expression of NeuroD/BETA2 in mitotic and postmitotic neuronal cells during the development of nervous system. *Developmental Dynamics* **217:**361-367.

Leibovici, M., Lapointe, F., Aletta, P., and Ayer-Le Lièvre, C. 1996. Avian olfactory receptors: differentiation of olfactory neurons under normal and experimental conditions. *Developmental Biology* **175:**118-131.

Lewcock, J.W. and Reed, R.R. 2004. A feedback mechanism regulates monoallelic odorant receptor expression. *Proceedings of the National Academy of Sciences USA* **101:**1069-1074.

Li, H., Schrick, J.J., Fewell, G.D., MacFarland, K.L., Witte, D.P., Bodenmiller, D.M., Hsieh-Li, H.-M., Su, C.-Y., and Potter, S.S. 1999. Novel strategy yields candidate Gsh-1 homeobox gene targets using hypothalamus progenitor cell lines. *Developmental Biology* **211:**64-76.

Li, J., Ishii, T., Feinstein, P., and Mombaerts, P. 2004. Odorant receptor gene choice is reset by nuclear transfer from mouse olfactory sensory neurons. *Nature* 428:393-399.

Li, X., Chen, Y., Schéele, S., Arman, E., Haffner-Krausz, R., Ekblom, P., and Lonai, P. 2001a. Fibroblast growth factor signaling and basement membrane assembly are connected during epithelial morphogenesis of the embryoid body. *Journal of Cell Biology* **153(4):**811-822.

Li, X., Talts, U., Talts, J.F., Arman, E., Ekblom, P., and Lonai, P. 2001b. Akt/PKB regulates laminin and collagen IV isotypes of the basement membrane. *Proceedings of the National Academy of Sciences USA* **98(25):**14416-14421.

Liang, P. 2002. A decade of differential display. *BioTechnique* **33:**338-346.

Liang, P., and Pardee, A. 1992. Differential display of eukaryotic messenger RNA by means of the polymerase chain reaction. *Science* **257:**967-971.

Lindsell, C.E., Boulter, J., diSibio, G., Gossler, A., and Weinmaster, G. 1996. Exression patterns of *Jagged, Delta1, Notch1, Notch2,* and *Notch3* genes indentify ligand-receptor pairs that may function in neural development. *Molecular and Cellular Neuroscience* **8:**14-27.

Lo, L., Dormand, E., Greenwood, A., and Anderson, D.J. 2002. Comparison of the generic neuronal differentiation and neuron subtype specification functions of mammalian *achaete-scute* and *atonal* homologs in cultured neural progenitor cells. *Development* **129:**15531567.

Lo, L.C., Sommer, L.C., and Anderson, D.J. 1997. MASH-1: maintains competence for BMP2-induced neuronal differentiation in post-migratory neural crest cells. *Current Biology* **7**:440-450.

Lukaszewicz, A., Savatier, P., Cortay, V., Kennedy, H., and Dehay, C. 2002. Contrasting effects of basic fibroblast growth factor and neurotrophin 3 on cell cycle kinetics of mouse cortical stem cells. *Journal of Neuroscience* **22(15)**:6610-6622.

Ma, Q., Kintner, C., and Anderson, D. 1996. Identification of *neurogenin*, a vertebrate neruronal determination gene. *Cell* **87**:43-52.

MacDonald, K.P.A., Murrel, W.G., Barlett, P.F., Bushell, G.R., and Mackay-Sim, A. 1996. FGF-2 promotes neuronal differentiation in explant cultures of adult and embryonic mouse olfactory epithelium. *Journal of Neuroscience Research* **44**:27-39.

Mackay-Sim, A., and Chuah, M.I. 2000. Neurotrophic factors in the primary olfactory pathway. *Progress in Neurobiology* **62**:527-559.

Mahanthappa, N.K., and Schwarting, G.A. 1993. Peptide growth factor control of olfactory neurogenesis and neuron survival in vitro: Roles of EGF and TGF-ßs. *Neuron* **10**:293-305.

Mallamaci, A., Di Blas, E., Briata, P., Boncinelli, E., and Corte, G. 1996. OTX2 homeoprotein in the developing central nervous sytem and migratory cells of the olfactory area. *Mechanisms of Development* **58**:165-178.

Malnic, B., Hirono, J., Sato, T., and Buck, L. 1999. Combinatorial receptor codes for odors. *Cell* **96**:713-723.

Marone, M., Mozzetti, S., De Ritis, D., Pierelli, L., and Scambia, G. 2001. Semiquantitative RT-PCR analysis to assess the expression levels of multiple transcripts from the same sample. *Biological Procedures Online* **3(1)**:19-25.

McCright, B., Rivers, A.M., Audlin, S., and Virshup, D.M. 1996. The B56 family of protein phosphatase 2A (PP2A) regulatory subunits encodes differentiation-induced phosphoproteins that target PP2A to both nucleus and cytoplasm. *Journal of Biological Chemistry* **271(36)**:22081-22089.

McEwen, D.G. and Ornitz, D.M. 1997. Determination of fibroblast growth factor receptor expression in mouse, rat and human samples using a single primer pair. *BioTechniques* **22**:1068-1070.

Miyasaka, N., and Matsuoka, I. 2000. Identification of basic fibroblast growth factor-responsive genes by mRNA-differential display in an immortalized neural stem cell line. *Biol. Pharm. Bull.* **23(3)**:349-351.

Mombaerts, P. 1999. Molecular biology of odorant receptors in vertebrates. *Annu. Rev. Neurosci.* **22**:487-509.

Morrison, S.J., Perz, S.E., Qiao, Z., Verdi, J.M., Hicks, C., Weinmaster, G., and Anderson, D.J. 2000. Transient *Notch* activation initiates an irreversible switch from neurogenesis to gliogenesis by neural crest stem cells. *Cell* **101:** 499-510.

Morrow, E.M., Furukawa, T., Lee, J.E., and Cepko, C. 1999. NeuroD regulates multiple functions in the developing neural retina in rodent. *Development* **126:** 23-36.

Mumm, J.S., Shou, J., and Calof, A.L. 1996. Colony-forming progenitors from mouse olfactory epithelium: Evidence for feedback regulation of neuron production. *Proceedings of the National Academy of Sciences USA* **93:**11167-11172.

Murphy, M., Drago, J. and Bartlett, P.F. 1990. Fibroblast growth factor stimulates the proliferation and differentiation of neural precursor cells in vitro. *J. Neurosci. Res.* **25:**463-75.

Murray, R.C., Navi., D., Fesenko, J., Lander, A.D., and Calof, A.L. 2003. Widespread defects in the primary olfactory pathway caused by loss of *Mash1* function. *The Journal of Neuroscience* **23(5):**1769-1780.

Murrell, J.R., and Hunter, D.D. 1999. An olfactory sensory neuron line, *Odora*, properly targets olfactory proteins and responds to odorants. *Journal of Neuroscience* **19(19)**:8260-8270.

Murrell, W., Bushell, G.R., Livesey, J., McGrath, J., MacDonald, K.P.A, Bates, P.R., and Mackay-Sim, A. 1996. Neurogenesis in adult human. *NeuroReport* **7:**1189-1194.

Nakai, K., and Horton, P. 1999. PSORT: a program for detecting sorting signals in proteins and predicting their subcellular localization. *Trends in Biochemical Sciences* **24:**34-35.

Nakamura, Y., Sakakibara, S., Miyata, T., Ogawa, M., Shimazaki, T., Weiss, S., Kageyama, R., and Okano, H. 2000. The bHLH gene *Hes1* as repressor of the neuronal commitment of CNS stem cells. *The Journal of Neuroscience* **20(1):** 283-293.

Nef, S., Allaman, I., Fiumelli, H., De Castro, E., Nef, P. 1996. Olfaction in birds: differential embryonic expression of nine putative odorant receptor in the avian olfactory system. *Mechanisms of Development* **55:**65-77.

Neuwald, A.F., and Landsman, D. 1997. GCN5-related histone N-acetyltransferases belong to a diverse superfamily that includes the yeast SPT10 protein. *TIBS* **22:** 154-155.

Newman, M.P., Féron, F., and Mackay-Sim, A. 2000. Growth factor regulation of neurogenesis in adult olfactory epithelium. *Neuroscience* **99:**343-350.

Ngai, J., Dowling, M.M., Buck, L., Axel, R., and Chess, A. 1993. The family of genes encoding odorant receptors in the channel catfish. *Cell* **72:**657-666.

Nibu, K., Li G., Kaga, K., and Rothstein, J. 2000. bFGF induces differentiation and death of olfactory neuroblastoma cells. *Biochemical and Biophysical Research Communications* **279:**172-180.

Nielsen, H., Engelbrecht, J., Brunak, S., and von Heijne, G. 1997. Identification of prokaryotic and eukaryotic signal peptides and prediction of their cleavage sites. *Protein Engineering* **10:**1-6.

Nieto, M.,Schuurmans, C., Britz, O., and Guillemot, F. 2001. Neural bHLH genes control the neuronal versus glial fate decision in cortical progenitors. *Neuron* **29:**401-413.

Nurcombe, V., Ford, M.D., Wildschut, J.A., and Bartlett, P.F. 1993. Developmental regulation of neural response to FGF-1 and FGF-2 by heparan sulfate proteoglycan. *Science* 260:103-106.

Nuthall, H.N., Husain, N., McLarren, K.W., and Stifani, S. 2002. Role for Hes1-induced phosphorylation in Groucho-mediated transcriptional repression. *Molecular and Cellular Biology* **22(2):**389-399.

Ohtsuka, T., Ishibashi, M., Gradwohl, G., Nakanishi, S., Guilemmot, F., and Kageyama, R. 1999. *Hes1* and *Hes5* as Notch effectors in mammalian neuronal differentiation. *EMBO J.* **18:**2196-2207.

Ohtsuka, T., Sakamoto, M., Guilemmot, F., and Kageyama, R. 2001. Roles of the basic helix-loop-helix genes *Hes1* and *Hes5* in expansion of neural stem cells of the developing brain. *Journal of Biological Chemistry* **276(32):**30467-30474.

Okada, M., Yamaga, S., Yasuda, S., Weissman, S.M., and Yasukochi, Y. 2002. Differential display of protein tyrosine kinase cDNAs from human fetal and adult brains. *BioTechniques* **32:**856-865.

Okamoto K. and Beach D. (1994). Cyclin G is a transcriptional target of the p53 tumor suppressor protein. *The EMBO Journal* **13**(19), 4186-4822.

Ornitz, D., Xu, J., Colvin, J., McEwen, D., MacArthur, C., Coulier, F., Gao, G., and Goldfarb, M. 1996. Receptor specificity of the fibroblast growth factor family. *Journal of Biological Chemistry* **271:**15292-15297.

Ornitz, D.M., and Itoh, N. 2001. Fibroblast growth factors. *Genome Biology* **2:** 3005.1-3005.12.

Ornitz, D.M., Xu, J., Colvin, J.S., McEwen, D.G., MacArthur, C.A., Coulier, F., Gao, G., and Goldfarb, M. 1996. Receptor specificity of the fibroblast growth factor family. *Journal of Biological Chemistry* **271:**15292-15297.

Orr-Urtreger, A., Bedford, M.T., Burakova, T., Arman, E., Zimmer, Y., Yayon, A., Givol, D., and Lonai, P. 1993. Developmental localization of the splicing alternatives of fibroblast growth factor receptor-2 (FGFR2). *Developmental Biology* **158:**475-486.

Ortega, S., Ittmann, M., Tsang, S.H., Ehrlich, M., and Basilico, C. 1998. Neuronal defects and delayed wound healing in mice lacking fibroblast growth factor 2. *Proceedings of the National Academy of Sciences USA* **95:**5672-5677.

Pascolo, S., Tsoukatou, D., and Mamalaki, C. 1999. Identification of thymus specific and developmentally regulated genes by an improved version of the mRNA differential display technique. *Developmental Immunology* **7(1):**1-7.

Pataky, D.M., Borisoff, J.F., Fernandez, K.J.L., Tetzlaff, W., and Steeves, J.D. 2000. Fibroblast growth factor treatment produces differential effects on survival and neurite outgrowth from identified bulbospinal neurons *in vitro*. *Experimental Neurology* **163:**357-372.

Pellier, V., Astic, L., Oestreicher, A.B., and Saucier, D. 1994. B-50/GAP-43 expression by the olfactory receptor cells and the neurons migrating from the olfactory placode in embryonic rats. *Developmental Brain Research* **80:**63-72.

Perez, S.E., Rebelo, S., and Anderson, D.J. 1999. Early specification of sensory neuron fate revealed by expression and function of neurogenins in the chick embryo. *Development* **126:**1715-1728.

Polevoda, B., and Sherman, F. 2000. N^{α}–terminal acetylation of eukaryotic proteins. *Journal of Biological Chemistry* **275(47):**36479-36482.

Polevoda, B., Norbeck, J., Takakura, H., Blomberg, A., and Sherman, F. 1999. Identification and specificities of N-terminal acetyltransferases from *Saccharomyces cerevisiae*. *The EMBO Journal* **18(21):**6155-6168.

Ponting, C.P., Schultz, J., Milpetz, F., Bork, P. 1999. SMART: identification and annotation of domains from signalling and extracellular protein sequences. *Nucleic Acids Research* **27:**229-232.

Powers, C.J., McLeskey, S.W., and Wellstein, A. 2000. Fibroblast growth factors, their receptors and signaling. *Endocrine-Related Cancer* **7:**165-197.

Pozzoli, O., Bosetti, A., Croci, L., Consalez, G.G., and Vetter, M.L. 2001. *Xebf3* is a regulator of neuronal differentiation during primary neurogenesis in *Xenopus*. *Developmental Biology* **233:**495-512.

Qasba, P., and Reed, R.R. 1998. Tissue and zonal-specific expression of an olfactory receptor transgene. *The Journal of Neuroscience* **18:**227-236.

Qian, X., Davis, A.A., Goderie, S.K., and Temple, S. 1997. FGF-2 concentration regulates the generation of neurons and glia from multipotent cortical stem cells. *Neuron* **18:**81-93.

Raballo, R., Rhee, J., Lyn-Cook, R., Leckman, J.F., Schwartz, M.L., and Vaccarino, F.M. 2000. Basic fibroblast growth factor is necessary for cell proliferation and neurogenesis in the developing cerebral cortex. *Journal of Neuroscience* **20:** 5012-5023.

Rawson, N.E., Eberwine, J., Dotson, R., Jackson, J., Ulrich, P., and Restrepo, D. 2000. Expression of Mrnas encoding for two different olfactory receptors in a subset of olfactory neurons. *Journal of Neurochemistry* **75:**185-195.

Reed, R.R. 2000. Regulating olfactory expression: controlling globally, acting locally. *Nature Neuroscience* **3(7):**638-639.

Reinhardt, A. and Hubbard, T. 1998. Using neural networks for prediction of the subcellular location of proteins. *Nucleic Acids Research* **26(9):**2230-2236.

Ressler, K.J., Sullivan, S.L, and Buck, L. 1993. A zonal organization of odorant receptor gene expression in the olfactory epithelium. *Cell* **73:**597-609.

Ressler, K.J., Sullivan, S.L, and Buck, L. 1994. Information coding in the olfactory system: evidence for a stereotyped and highly organized epitope map in the olfactory bulb. *Cell* **79:**1245-1255.

Robel, L., Ding, M., James, A., Lin, X., Simeone, A., Leckman, J.F., and Vaccarino, F.M. 1995. Fibroblast growth factor 2 increases Otx2 expression in precursor cells from mammalian telencephalon. *Journal of Neuroscience* **15(12):**7879-7891.

Rogers, K.E., Dasgupta, P., Gubler, U., Grillo, M., Khew-Goodall, Y.S., and Margolis, F.L. 1987. Molecular cloning and sequencing of a cDNA for olfactory marker protein. *Proceedings of the National Academy of Sciences USA* **84:**1704-1708.

Roskams, A.J.L, Bethel, M.A., Hurt, K.J., and Ronnett, G.V. 1996. Sequential expression of Trks A, B, and C in the regenerating olfactory neuroepithelium. *Journal of Neuroscience* **16:**1294-1307.

Roskams, A.J.I., Cai, X., and Ronnett, G.V. 1998. Expression of neuron-specific beta-III tubulin during olfactory neurogenesis in the embryonic and adult rat. *Neuroscience* **83:**191-200.

Santagati, S., Garnier, M., Carlo, P., Violani, E., Picotti, G.B., and Maggi, A. 1997. Quantitation of low abundance mRNAs in glial cells using different polymerase chain reaction (PCR)-based methods. *Brain Research Protocols* **1:**217-223.

Santhanam, R., and Naz, R.K. 2001. Novel human testis-specific cDNA: Molecular cloning, expression and immunobiological effects of the recombinant protein. *Molecular Reproduction and Development* **60:**1-12.

Satoh, M., and Yoshida, T. 1997. Promotion of neurogenesis in mouse olfactory neuronal progenitor cells by leukemia inhibitory factor in vitro. *Neuroscience Letters* **225:**165-168.

Schuurmans, C., and Guillemot, F. 2002. Molecular mechanisms underlying cell fate specification in the developing telencephalon. *Current Opinion in Neurobiology* **12:**26-34.

Schwab, M.H., Druffel-Augustin, S., Gass, P., Jung, M., Klugmann, M., Bartholomae, A., Rossner, M.J., and Nave, K-A. 1998. Neuronal basic helix-loop-helix proteins (NEX, neuroD, NDRF): spatiotemporal expression and targeted disruption of the NEX gene in transgenic mice. *Journal of Neuroscience* **18(4):**1408-1418.

Selbie, L.A., Townsend-Nicholson, A., Iismaa, T.P., and Shine, J. 1992. Novel G protein-coupled receptors: a gene family of putative human olfactory receptor sequences. *Molecular Brain Research* **13:**159-163.

Sengupta, P., Chou, J.H., and Bargmann, C.I. 1996. *odr-10* encodes a seven transmembrane domain olfactory receptor required for responses to the odorant diacetyl. *Cell* **84:**875-887.

Senju, S., and Nishimura, Y. 1997. Identification of human and mouse GP-1, a putative member of a novel G-protein family. *Biochemical and Biophysical Research Communications* **231:**360-364.

Serizawa, S., Ishii, T., Nakatani, H., Tsuboi, A., Nagawa, F., Asano, M., Sudo, K., Sakagami, J., Sakano, H., and Ijiri, T. 2000. Mutually exclusive expression of odorant receptor transgenes. *Nature Neuroscience* **3:**687-693.

Serizawa, S., Miyamichi, K., Nakatani, H., Suzuki, M., Saito, M., Yoshihara, Y. and Sakano, H. 2003. Negative feedback regulation ensures the one receptor-one olfactory neuron rule in mouse. *Science* **302:**2088-2094.

Shields J.M., Rogers-Graham, K., and Der, C.J. 2002. Loss of transgelin in breast and colon tumors and in RIE-1 cells by Ras deregulation of gene expression through Raf-independent pathways. *Journal of Biological Chemistry* **277(12):**9790-9799.

Shou, J., Murray, R.C., Rim, P.C., and Calof, A.L. 2000. Opposing effects of bone meorhogenetic proteins on neuron production and survival in the olfactory recetor neuron lineage. *Development* 127:5403-5413.

Shou, J., Rim, P.C., and Calof, A.L. 1999. BMPs inhibit neurogenesis by a mechanism involving degradation of a transcription factor. *Nature Neuroscience* **2(4):**339-345.

Shridhar, V., Rivard, S., Shridhar, R., Mullins, C., Bostick, L., Sakr, W., Grignon, D., Miller, O.J., and Smith, D.I. 1996. A gene from human chromosomal band 3p21.1 encodes a highly conserved arginine-rich protein and is mutated in renal cell carcinomas. *Oncogene* **12(9):**1931-1939.

Shridhar, V., Rivard, S., Wang, X., Shridhar, R., Paisley, C., Mullins, C., Beirnat, L., Dugan, M., Sakar, F., Miller, O.J., Vaitkevicius, V.K., and Smith, D.I. 1997. Mutations in the arginine-rich protein gene (ARP) in pancreatic cancer. *Oncogene* **14:**2213-2216.

Skaper, S.D, Kee, W.J., Facci, L., Macdonald, G., Doherty, P., and Walsh, F.S. 2000. The FGFR1 inhibitor PD 173074 selectively and potently anatagonizes FGF-2 neurotrophic and neurotropic effects. *Journal of Neurochemistry* **75:**1520-1527.

Sosinsky, A., Glusman, G., and Lancet, D. 2000. The genomic structure of human olfactory receptor genes. *Genomics* **70:**49-61.

Sriuranpong, V., Borges, M.W., Strock, C.L., Nakakura, E.K., Watkins, D.N., Blaumueller, C.M., Nelkin, B.D., and Ball, D.W. 2002. Notch signalling induces rapid degradation of Achaete-Scute homolog 1. *Molecular and Cellular Biology* **22(9):**3129-3139.

Strack, S. 2002. Overexpression of the protein phosphatase 2A regulatory subunit Bγ promotes neuronal differentiation by activating the MAP kinase (MAPK) cascade. *Journal of Biological Chemistry* **277(44):**41525-41532.

Ström, A., Castella, P., Rockwood, J., Wagner, J., and Caudy, M. 1997. Mediation of NGF signaling by post-translational inhibition of HES-1, a basic helix-loop-helix repressor of neuronal differentiation. *Genes and Development* **11:**3168-3181.

Strotmann, J., Wanner, I., Helfrich, T., Beck, A., Meinken, C., Kubick, S., and Breer, H. 1994. Olfactory neurons expressing distinct odorant receptor subtypes are spatially segregated in the nasal neuroepithelium. *Cell and Tissue Research* **276:**429-438.

Strotmann, J., Wanner, I., Helfrich, T., and Breer, H. 1995. Receptor expression in olfactory neurons during rat development. *In situ* hybridization studies. *European Journal of Neuroscience* **7:**492-500.

Strotmann, J., Hoppe, R., Conzelmann, S., Feinstein, P., Mombaerts, P., and Breer, H. 1999. Small subfamily of olfactory receptor genes: structural features, expression pattern and genomic organization. *Gene* **236:**281-291.

Sugiura, N., Adams, S.M., and Corriveau, R.A. 2003. An evolutionary conserved N-terminal acetyltransferase complex associated with neuronal development. *Journal of Biological Chemistry* **278(41):**40113-40120.

Sullivan, S.L., Bohm, S., Ressler, K.J., Horowitz, L.F., and Buck, L.B. 1995. Target-independent pattern of specification in the olfactory epithelium. *Neuron* **15:**779-789.

Sun, Y., Nadal-Vicens M., Misono, S., Lin, M.Z., Zubiaga, A., Hua, X., Fan, G., and Greenberg, M.E. 2001. Neurogenin promotes neurogenesis and inhibits glial differentiation by independent mechanisms. *Cell* **104:**365-376.

Sung, J.Y., Shin, S.W., Ahn, Y.S., and Chung, K.C. 2001. Basic fibroblast growth factor-induced activation of novel CREB kinase during the differentiation of immortalized hippocampal cells. *Journal of Biological Chemistry* **276(17):**13858-13866.

Szebenyi, G., and Fallon, J.F. 1999. Fibroblast growth factors as multifunctional signalling factors. *International Review of Cytology* **185:**45-106.

Takanori, T., Kanamoto, T., Kato, T., Yamashita, H., Miyagawa, K., and Mishima, H. 2002. Ocular development-associated gene (ODAG), a novel gene highly expressed in ocular development. *Gene* **290:**125-130.

Tanigaki, K., Nogaki, F., Takahashi, J., Tashiro, K., Kurooka, H., and Honjo, T. 2001. Notch1 and Notch3 instructively restrict bFGF-responsive multipotent neural progenitor cells to an astroglial fate. *Neuron* **29:**45-55.

Tao, W., and Lai, E. 1992. Telencephalon-restricted expression of BF-1, a new member of the HNF-3/fork gene family, in the developing rat brain. *Neuron* **8:**957-966.

Tao, Y., Black, B., and DiCicco-Bloom, E. 1997. In vivo neurogenesis is inhibited br neutralising antibodies to basic fibroblast growth factor. *Journal of Neurobiology* **33:**289-296.

Thelin, O., Zorzi, W., Lakaye, B., De Borman, B., Coumans, B., Hennen, G., Grisar, T., Igout, A., and Heinen, E. 1999. Housekeeping genes as internal standards: use and limits. *Journal of Biotechnology* **75:**291-295.

Thompson, J.D., Higgins, D.G., and Gibson, T.J. 1994. CLUSTAL W: improving the sensitivity of progressive multiple sequence alignments through sequence weighting, position-specific gap penalties and weight matrix choice. *Nucleic Acids Research* **22:**4673-4680.

Tomita, K., Moriyoshi, K., Nakanishi, S., Guillemot, F., and Kageyama, R. 2000. Mammalian achaete-scute and atonal homologs regulate neuronal versus glial fate determination in the central nervous system. 2000. *The EMBO Journal* **19(20):**5460-5472.

Torii, M., Matsuzaki, F., Osumi, N., Kaibuchi, K., Nakamura, S., Casarosa, S., Guillemot, F., and Nakafuku, M. 1999. Transcription factors Mash-1 and Prox-1 delineate early steps in differentiation of neural stem cells in the developing central nervous system. *Development* **126:**443-456.

Touhara, K., Sengoku, S., Inaki, K., Tsubo, A., Hirono, J., Sato, T., Sakano, H., and Haga, T. 1999. Functional identification and reconstitution of an odorant receptor in single olfactory neurons. *Proceedings of the National Academy of Sciences USA* **96:**4040-4045.

Treloar, H., Tomasiewicz, H., Magnuson, T., and Key, B. 1997. The central pathway of olfactory axons is abnormal in mice lacking the N-CAM-180 isoform. *Journal of Neurobiology* **32:**643-658.

Trendelenburg, G., Prass, K., Priller, J., Kapinya, K., Polley, A., Muselmann, C., Ruscher, K., Kannbley, U., Schmitt, A.O., Castell, S., Wiegand, F., Meisel, A., Rosenthal, A., and Dirnagl, U. 2002. Serial analysis of gene expression identifies metallothionein-II as major neuroprotective gene in mouse focal cerebral ischemia. *Journal of Neuroscience* **22(14):**5879-5888.

Tropepe, V., Sibilia, M., Ciruna, B.G., Rossant, J., Wagner, E.F., and van der Kooy, D. 1999. Distinct neural stem cells proliferate in response to EGF and FGF in the developing mouse telencephalon. *Developmental Biology* **208:**166-188.

Tsuchiya, K., Kohda, Y., Yoshida, M., Zhao, L., Ueno, T., Yamashita, J., Yoshioka, T., Kominami, E., and Yamashima, T. 1999. Postictal blockade of ischemic hippocampal neuronal death in primates using selective cathepsin inhibitors. *Experimental Neurology* **155:**187-194.

Tsuruga, T., Kanamoto, T., Kato, T., Yamashita, H., Miyagawa, K., and Mishima, H.K. 2002. Ocular development-associated gene (ODAG), a novel gene highly expressed in ocular development. *Gene* **290:**125-130.

Twigg, S.R., Burns, H.D., Oldridge, M., Heath, J.K., Wilkie, A.O. 1998. Conserved use of a non-canonical 5' splice site (/GA) in alternative splicing by fibroblast growth factor receptors 1, 2 and 3. *Human Molecular Genetics* **7(4):**685-91.

Vaccarino, F.M., Schwartz, M.L., Raballo, R., Nilsen, J., Rhee, J., Zhou, M., Doetschman, T., Coffin, J.D., Wyland, J.J., and Hung, Y.E. 1999. Changes in cerebral cortex size are governed by fibroblast growth factor during embryogenesis. *Nature Neuroscience* **2:**246-53.

Van Hoof, C., and Goris, J. 2003. Phosphatases in apoptosis: to be or not to be, PP2A is in the heart of the question. *Biochimica et Biophysica Acta* **1640:**97-104.

Vassar, R. Ngai, J., and Axel, R. 1993. Spatial segregation of odorant receptor expression in the mammalian olfactory epithelium. *Cell* **74:**309-318.

Vassar, R. Chao, S.K., Sitcheran, R., Nunez, J.M., Vosshal, L.B., and Axel, R. 1994. Topographic organization of sensory projections to the olfactory bulb. *Cell* **79:**981-991.

Vasseur S., Malicet, C., Calvo, E.L., Labrie, C., Berthezene, P., Dagorn, J.C., Iovanna, J.L. 2003. Gene expression profiling by DNA microarray analysis in mouse embryonic fibroblasts transformed by rasV12 mutated protein and the E1A oncogene. *Molecular Cancer* **2(1):**19.

Vaudry, D., Stork, P.J.S., Lazarovici, P., and Eiden, L.E. 2002. Signaling pathways for PC12 cell differentiation: making the right connections. *Science* **296:**1648-1649.

Vicario-Abejón, C., Johe, K.K., Hazel, T.G., Collazo, D., and McKay. R.D. 1995. Functions of basic fibroblast growth factor and neutrophins in the differentiation of hippocampal neurons. *Neuron* **15:**105-114.

Voyron, S., Giacobini, P., Tarozzo, G., Cappello, P., Perroteau, I., and Fasolo, A. 1999. Apoptosis in the development of the mouse olfactory epithelium. *Developmental Brain Research* **115:**49-55.

Wan, J.S., Sharp, S.J., Poirier, M.-C., Wagaman, P.C., Chambers, J., Pyati, J., Hom, Y., Galindo, J.E., Huvar, A., Peterson, P.A., Jackson, M.R., and Erlander, M.G. 1996. Cloning differentially expressed mRNAs. *Nature Biotechnology* **14:**1685-1691.

Wang, M.M., and Reed, R.R. 1993. Molecular cloning of the olfactory neuronal transcription factor Olf-1 by genetic selection in yeast. *Nature* **364:**121-126.

Wang, S.S., Lewcock, J.W., Feinstein, P., Mombaerts, P., and Reed, R.R. 2004. Genetic disruptions of *O/E2* and *O/E3* genes reveal involvement in olfactory receptor neuron projection. *Development* **131:**1377-1388.

Watson, M. and Flemming, T. 1994. Isolation of differentially expressed sequenced tags from human breast cancer. *Cancer Research* **54:**4598-4602.

Weigel, R.J., and Nevins, J.R. 1990. Adenovirus infection of differentiated F9 cells results in a global shut-off of differentiation-induced gene expression. *Nucleic Acids Research* **18(20):**6107-6112.

Wilson, S.W., and Rubenstein, J.L.R. 2000. Induction and dorsoventral patterning of the telencephalon. *Neuron* **28:**641-651.

Wolf, E., Vassilev, A., Makino, Y., Sali, A., Nakatani, Y., and Burley, S.K. 1998. Crystal structure of a GCN5-related N-acetyltransferase: Serratia marcescens aminoglycoside 3-N-acetyltransferase. *Cell* **94:**439-449.

Xu, J., Liu, Z., and Ornitz, D.M. 2000. Temporal and spatial gradients of Fgf8 and Fgf17 regulate proliferation and differentiation of midline cerebellar structures. *Development* **127:**1833-1843.

Xu, X., Li, C., Takahashi, K., Slavkin, H.C., Shum, L., and Deng, C-X. 1999. Murine fibroblast growth factor receptor 1α isoforms mediate node regression and are essential for posterior mesoderm development. *Developmental Biology* **208:**293-306.

Xuan, S., Baptista, C.A., Balas, G., Tao, W., Soares, V.C., and Lai, E. 1995. Winged helix transcription factor BF-1 is essential for the development of the cerebral hemispheres. *Neuron* **14:**1141-1152.

Yamada, M., Numakawa, T., Koshimizu, H., Tanabe, K., Wada, K., Koizumi, S., Hatanaka, H. 2002. Distinct usages of phospholipase Cγ and Shc in intracellular signaling stimulated by neurotrophins. *Brain Research* **955:**183-190.

Yamaguchi, F., Saya, H., Bruner, J.M., and Morrison, R.S. 1994. Differential expression of two fibroblast growth factor-receptor genes is associated with malignant progression in human astrocytomas. *Proceedings of the National Academy of Sciences USA* **91:**484-488.

Yang, Y., Hentati, A., Deng, H.X., Dabbagh, O., Sasaki, T., Hirano, M., Hung, W.Y., Ouahchi, K., Yan, J., Azim, A.C., Cole, N., Gascon, G., Yagmour, A., Ben-Hamida, M., Pericak-Vance, M., Hentati, F., and Siddique, T. 2001. The gene encoding alsin, a protein with three guanine-nucleotide exchange factor domains, is mutated in a form of recessive amyotrophic lateral sclerosis. *Nature Genetics* **29:**160-165.

Yang, E.J., Yoon, J., and Chung, K.C. 2004. Bruton's tyrosine kinase phosphorylates cAMP-responsive element binding protein at serine 133 during neuronal differentiation in immortalized hippocampal progenitor cells. *Journal of Biological Chemistry* **279(3):**1827-1837.

Yao, J., Lai, E., and Stifani, S. 2001. The winged-helix protein Brain Factor 1 interacts with Groucho and Hes proteins to repress transcription. *Molecular and Cellular Biology* **21(6):**1962-1972.

Yayon, A., Klagsbrun, M., Esko, J.D., Leder, P., and Ornitz, D.M. 1991. Cell surface, heparin-like molecules are required for binding of basic fibroblast growth factor to its high affinity receptor. *Cell* **64:**841-848.

Yeatman, T., and Mao, W. 1995. Identification of a differentially expressed message associated with colon cancer liver metastasis using an improved method of differential display. *Nucleic Acids Research* **23(19):** 4007-4008.

Zakin, L., Reversade, B., Virlon, B., Rusniok, C., Glaser, P., Elalouf, J., and Brûlet, P. 2000. Gene expression profiles in normal and *Otx2*$^{-/-}$ early gastrulating mouse embryos. *Proceedings of the National Academy of Sciences USA* **97:**14388-14393.

Zegzouti, H., Marty, C., Jones, B., Bouquin, T., Latché, A., Pech, J.C., and Bouzayen, M. 1997. Improved screening of cDNAs generated by mRNA differential display enables the selection of true positives and the isolation of weakly expressed messages. *Plant Molecular Biology Reporter* **15:**236-245.

Zhang, H., Zhang, R., and Liang, P. 1996. Differential screening of gene expression difference enriched by differential display. *Nucleic Acids Research* **24(12):**2454-2455.

Zhang, J.C.L., Helmke, B.P., Shum, A., Du, K., Yu, W.W., Lu, M., Davies, P.F., and Parmacek, M.S. 2002. SM22β encodes a lineage-restricted cytoskeletal protein with a unique developmentally regulated pattern of expression. *Mechanisms of Development* **115:**161-166.

Zhang, X., and Firestein, S. 2002. The olfactory receptor gene superfamily of the mouse. *Nature Neuroscience* **5(2):**124-133.

Zhang, Y., Pan, H., and Gao, S. 2001. Reverse transcription slippage over the mRNA secondary structure of the LIP1 gene. *BioTechniques* **31(6):**1286-1292.

Zimmerman, J. and Schultz, R. 1994. Analysis of gene expression in the preimplantation mouse embryo: use of mRNA differential display. *Proceedings of the National Academy of Sciences USA* **91:**5456-5460.

Zolnierowicz, S. 2000. Type 2A protein phosphatase, the complex regulator of numerous signaling pathways. *Biochemical Pharmacology* **60:**1225-1235.

Zuker, M. 2003. Mfold web server for nucleic acid folding and hybridization prediction. *Nucleic Acids Research* **31(13)**:3406-3415.

Appendix:

List of clones identified in the differential display screen as being differentially expressed in OP27 cells following FGF-2 induced neuronal differentiation. The cDNAs were identified as being up- (↑) or down-regulated (↓). PCR reamplifications of cDNAs that failed are indicated with a asterik while PCR reactions that resulted in the co-amplification of at least 2 PCR products in one tube are indicated by double asteriks. These were therefore not included in the reverse northern blot analysis.

DD clone	Banding pattern on DD gel
17A1	↑
17A2	↓
17C1**	↓
17C2**	↑
17C3**	↓
17C4**	↓
17C5	↓
17C6**	↓
17C7	↓
17G1	↓
17G2	↓
18A1*	↑
18C1	↑
18C2	↑
18C3*	↓
18C4	↓
18C5*	↑
18G1	↑
18G2	↓
18G3	↑
19A1	↓

DD clone	Banding pattern on DD gel
19A2	↓
19C1*	↓
19C2*	↓
19C3*	↓
19C4*	↓
19C5*	↓
19C6*	↓
19C7	↑
19G1*	↓
19G2	↓
19G3	↓
19G4	↓
19G5	↓
19G6	↓
19G7*	↑
19G8*	↑
19G9*	↓
19G10*	↓
19G11*	↓
19G12	↑
20A1*	↑
20A2*	↑
20A3*	↑
20A4	↓
20A5*	↑
20A6	↑
20A7	↑
20A8	↓
20A9	↑
20A10	↑
20A11*	↑
20A12	↑
20A13*	↓
20C1	↓
20C2	↓
20C3	↑
20G1	↓
20G2	↑
20G3	↓

DD clone	Banding pattern on DD gel
21C1	↑
22A1	↑
22A2	↓
22A3	↓
22C1	↑
22C2**	↓
23A1	↑
23A2	↑
23G1	↓
24C1	↑
24G1	↑